

Springer Series on
ATOMIC, OPTICAL, AND PLASMA PHYSICS 66

Springer Series on

ATOMIC, OPTICAL, AND PLASMA PHYSICS

The Springer Series on Atomic, Optical, and Plasma Physics covers in a comprehensive manner theory and experiment in the entire field of atoms and molecules and their interaction with electromagnetic radiation. Books in the series provide a rich source of new ideas and techniques with wide applications in fields such as chemistry, materials science, astrophysics, surface science, plasma technology, advanced optics, aeronomy, and engineering. Laser physics is a particular connecting theme that has provided much of the continuing impetus for new developments in the field. The purpose of the series is to cover the gap between standard undergraduate textbooks and the research literature with emphasis on the fundamental ideas, methods, techniques, and results in the field.

For further volumes:

<http://www.springer.com/series/411>

Mario Capitelli
Gianpiero Colonna
Antonio D'Angola

Fundamental Aspects of Plasma Chemical Physics

Thermodynamics

With 110 Figures



Springer

Mario Capitelli
Dipartimento di Chimica
Università di Bari
Via Omodeo, 4
70126 Bari
Italy
mario.capitelli@ba.imip.cnr.it

Antonio D'Angola
Dipartimento di Ingegneria
e Fisica dell'Ambiente (DIFA)
University of Basilicata
Viale dell'Ateneo Lucano 10
85100 Potenza
Italy
antonio.dangola@unibas.it

Gianpiero Colonna
Istituto di Metodologie Inorganiche
e dei Plasmi (IMIP)
Consiglio Nazionale delle Ricerche (CNR)
Via Amendola, 122/D
70126 Bari
Italy
gianpiero.colonna@ba.imip.cnr.it

ISSN 1615-5653
ISBN 978-1-4419-8181-3 e-ISBN 978-1-4419-8182-0
DOI 10.1007/978-1-4419-8182-0
Springer New York Dordrecht Heidelberg London

Library of Congress Control Number: 2011936387

© Springer Science+Business Media, LLC 2012

All rights reserved. This work may not be translated or copied in whole or in part without the written permission of the publisher (Springer Science+Business Media, LLC, 233 Spring Street, New York, NY 10013, USA), except for brief excerpts in connection with reviews or scholarly analysis. Use in connection with any form of information storage and retrieval, electronic adaptation, computer software, or by similar or dissimilar methodology now known or hereafter developed is forbidden.
The use in this publication of trade names, trademarks, service marks, and similar terms, even if they are not identified as such, is not to be taken as an expression of opinion as to whether or not they are subject to proprietary rights.

Printed on acid-free paper

Springer is part of Springer Science+Business Media (www.springer.com)

*I busied myself, from then on, that is,
from the day of its establishment,
with the task of elucidating a true physical
character for the formula, and this problem
led me automatically to a consideration of the
connection between entropy and probability,
that is, Boltzmann's trend of ideas;
until after some weeks of the most strenuous
work of my life, light came into the darkness,
and a new undreamed-of perspective
opened up before me.*

– Max Planck – Nobel Lecture

Preface

In this book, we develop basic and advanced concepts of plasma thermodynamics from both classical and statistical points of view. After a refreshment of classical thermodynamics applied to the dissociation and ionization regimes, the book introduces the reader, since the very beginning, to discover the role of electronic excitation in affecting the properties of plasmas, a topic often overlooked by the thermal (equilibrium) plasma community. This point is usually disregarded in the existing textbooks of statistical mechanics and thermodynamics mainly devoted to temperature ranges much lower than those covered in this book.

Concepts, such as translational and internal partition functions of atomic and molecular species, are introduced and discussed with different degrees of accuracy. Particular attention is paid to the problem of the divergence of partition function of atomic species as well as to the *state-to-state* approach for calculating the partition function of diatomic and polyatomic molecules, going beyond the well-known harmonic oscillator and rigid rotor approximations. The limit of the ideal gas approximation is then discussed by presenting non-ideal effects including Debye-Hückel and virial corrections. Plasma properties for one and multi-temperature situations are then discussed presenting in the last chapter tables of thermodynamic properties of high temperature planetary atmosphere (Earth, Mars, Jupiter) plasmas.

The book is intended as a graduate-level textbook as well as a monograph on high temperature statistical thermodynamics useful for thermal plasma researchers. The first four chapters are being used for undergraduate students of Physics and Chemistry of the University of Bari (Italy).

Bari

Mario Capitelli
Gianpiero Colonna
Antonio D'Angola

Acknowledgements

The book contains many results published by the authors in collaboration with friends and colleagues including Ettore Molinari, Claudine Gorse and Domenico Giordano as well as many other coworkers appearing in the references.

Many thanks to Annarita Laricchiuta for a careful review of the Appendix and for useful suggestions.

The authors dedicate this book to their wives Giuliana, Grazia and Marianna, the sons and daughters Paolo, Francesco and Cinzia, Mariachiara, Michelangelo, Gerardina, Maria Teresa and the grandsons Alberto and Stefano.

Contents

1	Classical Thermodynamics	1
1.1	Equilibrium Thermodynamics	1
1.2	Dissociation Equilibrium	5
1.3	Ionization Equilibrium	8
1.4	Dissociation and Ionization Equilibria: Coupled Solution	11
1.5	Ideal Gas Thermodynamics	13
1.5.1	Ideal Gas Mixture Enthalpy	14
1.5.2	Ideal Gas Mixture Heat Capacity	15
1.6	Single Species Enthalpy	16
1.6.1	Equipartition Theorem	17
1.7	Mixture Thermodynamics at Constant Pressure	19
1.7.1	Dissociation	19
1.7.2	Ionization	21
1.8	Mixture Thermodynamics at Constant Volume	22
1.9	The Isentropic Coefficient	26
1.9.1	Dissociation Regime.....	28
1.9.2	Ionization Regime	29
1.9.3	Hydrogen Plasma	31
1.10	Real Gas Thermodynamics	32
1.10.1	Virial Corrections to Thermodynamic Functions	34
1.10.2	Virial Corrections to Heat Capacity	36
2	Two and Three Level Systems: Toward the Understanding of the Thermodynamics of Multilevel Systems	39
2.1	Two-Level Systems	39
2.2	Three-Level Systems	42
2.3	Few-Level Model Accuracy	47
3	Statistical Thermodynamics	51
3.1	From Statistical Probability to Thermodynamic Functions	51
3.2	Statistical Mean	57
3.3	Multicomponent Ideal Systems	58

4 Atomic Partition Function	61
4.1 Atomic Structure	61
4.1.1 Nuclear Partition Function	62
4.1.2 Translational Partition Function	62
4.1.3 Internal Partition Function	65
4.2 Single Species Thermodynamics	65
4.2.1 Translational Contribution	65
4.2.2 Internal Contribution	68
4.2.3 The Atomic Hydrogen as a Case Study	70
4.3 The Saha Equation for Ionization Equilibrium	74
4.4 Plasma Thermodynamics	76
5 Molecular Partition Function: Vibrational, Rotational and Electronic Contributions	79
5.1 The Harmonic Oscillator	79
5.2 The Rigid Rotor	81
5.3 Molecular Partition Function: Beyond Closed Forms	86
5.3.1 Ro-Vibrational Energies	87
5.4 Polyatomic Molecular Partition Functions	95
6 Real Effects: I. Debye–Hückel	101
6.1 Debye–Hückel Theory	101
6.2 Debye–Hückel Corrections	103
6.2.1 Internal Energy	103
6.2.2 Helmholtz Free Energy	104
6.2.3 Pressure	105
6.2.4 Entropy, Enthalpy and Gibbs Free Energy	106
6.2.5 Heat Capacity	106
6.2.6 Chemical Potential and Equilibrium Constant	107
6.2.7 Lowering of the Ionization Potential	108
6.3 The Effects of Debye–Hückel Correction	109
6.4 Beyond Debye–Hückel Theory	113
7 Real Effects: II. Virial Corrections	117
7.1 Ensembles and Partition Functions	117
7.1.1 The Micro-Canonical Ensemble	118
7.1.2 The Canonical Ensemble	119
7.1.3 The Grand-Canonical Ensemble	119
7.2 Virial Expansion for Real Gases	120
7.2.1 The Virial Coefficient for Mixtures	126
7.3 Virial Coefficient Calculations	130
7.3.1 Phenomenological Potential	130
7.3.2 Open Shells Interactions	131
7.4 The REMC Method	132

8 Electronic Excitation and Thermodynamic Properties of Thermal Plasmas	141
8.1 Cutoff Criteria	141
8.1.1 The Ground State Method	142
8.1.2 Debye–Hückel Criteria	142
8.1.3 Fermi Criterion	143
8.2 Cutoff From the Schrödinger Equation	144
8.3 Case Study: Oxygen.....	147
8.4 Partition Function and Occupation Probability	158
8.5 Debye–Hückel Energy Levels	161
9 Multi-Temperature Thermodynamics: A Multiplicity of Saha Equations	163
9.1 General Considerations	163
9.1.1 Minimization of Gibbs Free Energy	166
9.1.2 Maximization of Entropy.....	167
9.2 Free Energy Minimization for Atomic Ionization	168
9.2.1 Case a: $T_h = T_{\text{int}} \neq T_e$	168
9.2.2 Case b: $T_h \neq T_{\text{int}} = T_e$	170
9.2.3 Case c: $T_h \neq T_{\text{int}} \neq T_e$	170
9.3 Entropy Maximization for Atomic Ionization	171
9.4 Multitemperature Dissociation	172
9.5 Diatom Two-Temperature Ionization	173
9.6 Two-Temperature Hydrogen Plasma	175
10 Thermodynamics of Planetary Plasmas.....	181
10.1 Basic Equations	181
10.2 Air Plasmas	184
10.3 Thermodynamic Properties of High-Temperature Mars-Atmosphere Species	202
10.4 Thermodynamic Properties of High-Temperature Jupiter-Atmosphere Species	217
A Spectral Terms for Atoms and Molecules	231
A.1 Atomic Electronic Terms	231
A.1.1 Calculation of L	232
A.1.2 Calculation of S	232
A.1.3 Calculation of J	233
A.2 Complete Sets of Electronic Levels	237
A.2.1 Helium	238
A.2.2 Oxygen	239
A.3 Beyond the Hydrogenoid Approximation	241
A.4 Electronic Terms of Diatomic Molecules	243
A.4.1 H_2 Molecule	244
A.4.2 N_2 Molecule	246
A.4.3 N_2^+ Molecule.....	249

B Tables of Partition Function of Atmospheric Species.....	251
B.1 Partition Functions Independent of the Pressure.....	251
B.2 Selfconsistent Partition Functions of Atomic Species in Air Atmosphere.....	261
B.3 Selfconsistent Partition Functions of Atomic Species in Mars Atmosphere.....	271
B.4 Selfconsistent Partition Functions of Atomic Species in Jupiter Atmosphere.....	290
C Constants	293
C.1 Conversion Factors	293
References.....	295
Index.....	303

Introduction

Plasma technology is an emerging multidisciplinary topics widely studied worldwide due to its relevance in many applications. The plasma, also called the fourth state of matter, is a mixture of molecules, atoms, ions and electrons, which can be described by the laws of classical and statistical mechanics.

Usually, plasma technology distinguishes between thermal and cold plasmas, the first characterized by the equilibrium between the different degrees of freedom including the chemical ones, and the second characterized by thermal and chemical non-equilibrium.

Thermal plasmas are usually characterized by a single temperature determining the distribution of internal states and the chemical composition through dissociation and ionization (Saha) equilibria. Boltzmann distributions hold for vibrationally, rotationally and electronically excited states of heavy particles, while Maxwell distributions characterize the velocity distribution of free electrons. On the contrary, thermal plasmas with different temperatures are still accepted in this kind of literature, the different temperatures being related to the corresponding reservoirs of energy. The internal distributions are still Boltzmann at a given (different) temperature. Also in this case chemical equilibrium characterizes the plasma properties even though caution must be exercised in using it. Typical conditions for thermal plasmas are temperatures in the range of 5,000–50,000 K, pressure in the range 10^{-2} – 10^{-3} bar and ionization degree larger than 10^{-3} .

In technological applications, thermal plasmas are considered as high enthalpy combustion flames, which can be used for cutting, welding, coating spray and waste removal. Thermal plasmas are also those faced by hypersonic flying objects (e.g. reentering shuttles or meteorites) impacting Earth or planetary atmospheres. Thermal plasma conditions are also generated in Laser Induced Breakdown Spectroscopy (LIBS) and Inductive Coupled Plasmas (ICP) plasmas, two analytical tools widely used to determine metal concentrations in complex matrices. For all these applications, the knowledge of high temperature thermodynamic properties becomes of paramount importance.

In this book, we develop the basic ideas for plasma thermodynamics trying to link the new arguments with the concepts that Science and Engineering students have already learned during physics and chemistry courses. Emphasis will be in particular given to the role of electronic excitation in affecting the thermodynamic properties, a topic often overlooked by the thermal plasma community.

Chapter 1 of the book is dedicated to the use of classical thermodynamics to derive the equations of a reacting mixture by using the equipartition energy theorem for translational, vibrational and rotational energies, the electronic term being inserted in parametric form. In this chapter are also presented the corrections of ideal equations due to real effects, in particular emphasizing the classical virial approach from Van der Waals equation.

Chapter 2 is dedicated to the development of two- or three-level models to estimate the electronic contribution for atoms and ions under plasma conditions. These models are based on grouping levels such to reproduce the thermodynamic behaviour of thousand and thousand electronic excited levels. As an example the nitrogen atom is reduced to a three-level system composed by the ground state (4S), a second level which coalesces with appropriate energy and multiplicity the two low lying excited states 2P and 2D and a third level which accounts for the huge number of electronically excited states coming from the interaction of the most important nitrogen core (3P) with the optical level jumping on the 3s, 3p, 3d, 4s, 4p, 4d, 4f, . . . electronic states. These first two chapters can be used to teach plasma thermodynamics to graduated students avoiding the massive use of statistical thermodynamics and quantum mechanics.

Chapter 3 presents statistical thermodynamics of the perfect gas by introducing the concept of partition function and its linking to the thermodynamic properties of single species and of mixture. The chapter uses the Boltzmann approach introducing molecule and system partition function approaches.

Chapter 4 deals with the calculation of the partition function of atomic species (translational and electronic) and its use in deriving plasma properties considering atomic hydrogen plasma as a case study. In this chapter, we also introduce the importance of imposing an upper limit of principal quantum number to avoid the divergence of partition function, a problem reconsidered in Chap. 8.

Chapters 5 introduces the reader to the partition function of molecular species by using closed forms and state-to-state approaches for the vibro-rotational partition functions of several electronic states. Results are presented and discussed to understand how the standard approach of harmonic oscillator and rigid rotor for a diatomic species deviates from the state-to-state approach emphasizing the role of electronic excitation in affecting the partition function and thermodynamic properties of diatomic molecules. This chapter also introduces the linking between the symmetry of rotational wavefunctions and nuclear spin discussing the ortho–para hydrogen case.

Chapter 6 develops Debye–Hückel equations for correcting the thermodynamic properties of an ideal mixture and for better understanding the problem of the divergence of partition function. In addition, developments to go beyond the Debye–Hückel approach are presented and quantified.

Chapter 7 discusses real gas effects on plasma thermodynamics either applying the virial approach or by using the Reaction Ensemble Monte Carlo (REMC) technique. In this chapter, the grand-partition function is introduced which is then used in the REMC. Problems associated with the calculations of virial coefficients of atom–atom open shell interactions are also presented.

Chapter 8 is dedicated to the study of the influence of the cutoff of partition functions on the thermodynamic properties of thermal plasmas. The most used cutoff criteria derived from Debye–Hückel and confined atom approaches are introduced. These approaches are rationalized on the basis of results obtained by solving the Schrödinger equation of atomic hydrogen in a box. Many results for high temperature-high pressure Oxygen plasmas are presented emphasizing the role of electronic excitation in affecting the frozen properties of a plasma as well as the total ones. The effects of electronic excitation on the global thermodynamic properties of a mixture is hidden, in some cases, by the onset of the reactive contributions due to the ionization reactions.

Chapter 9 describes plasma thermodynamics for multi-temperature systems describing the onset of a multitude of Saha equations coming from the maximization of the total entropy and by minimization of Gibbs potential taking into account different constraints. Results for hydrogen plasmas, again considered as a case study, are reported.

Chapter 10 finally discusses the thermodynamic properties of high temperature planetary atmospheres (Earth, Jupiter, Mars) either in graphical or in tabular form. The accuracy of the used data is discussed in the case of the air plasma by comparing with results existing in literature.

An useful appendix is dedicated to the calculation of energy levels and degeneracies of complex atoms/ions as well as of diatomic molecules.

Chapter 1

Classical Thermodynamics

In this chapter, we will discuss the equations describing the equilibrium composition of a system based on classical thermodynamics, limiting our presentation to the essential ingredients of the theory. The axiomatic approach (Callen 1985) will be used, leaving an alternative derivation in Chap. 3 in the framework of statistical thermodynamics.

We will introduce basic expressions for the thermodynamic functions, focusing on the enthalpy and the specific heats, of reacting ideal mixtures, describing dissociation and ionization regimes. In doing so, we will make use of the equipartition theorem for translational, rotational and vibrational degrees of freedom of molecules. The contribution of electronic energy, for both atoms and molecules, will be introduced parametrically. This last term, which is the heart of this book, will be widely discussed in Chaps. 2, 4, 5 and 8.

The axiomatic approach will be used also to estimate the correction to thermodynamic functions for a non-ideal gas starting from the Van der Waals equation, in the framework of virial expansion (Hirschfelder et al. 1966).

1.1 Equilibrium Thermodynamics

We start from the first and second laws of classical thermodynamics written in differential form (Callen 1985; Capitelli et al. 2010)

$$dU = dQ - dL \quad (1.1)$$

$$dS \geq \frac{dQ}{T}, \quad (1.2)$$

where U denotes the internal energy, Q and L the heat and the work exchanged between the system and the environment, S the system entropy and T the absolute

temperature. The differentials of Q and L are written using the symbol d to mean that they depend on the path of the transformation, i.e. they are not exact differentials.

The mechanical work in term of the pressure P and the volume V is given by the equation

$$dL = PdV. \quad (1.3)$$

The Clausius inequality in the entropy equation assesses that the heat exchanged reversibly (TdS) is larger than the heat exchanged irreversibly. Combining (1.1)–(1.3), we get

$$dU \leq TdS - PdV \quad (1.4)$$

$$dS \geq \frac{dU}{T} - \frac{PdV}{T}, \quad (1.5)$$

where the equality is valid for reversible transformations. The equilibrium is then obtained under the following conditions

$$(dU)_{V,S} = 0 \quad (1.6)$$

for constant volume and entropy and

$$(dS)_{V,U} = 0 \quad (1.7)$$

for constant volume and energy.

More familiar equilibrium conditions can be obtained by introducing the Helmholtz (A) and Gibbs (G) potentials defined as

$$A = U - TS \quad (1.8)$$

$$G = A + PV = H - TS, \quad (1.9)$$

where the new state function H , the enthalpy, is defined as

$$H = U + PV. \quad (1.10)$$

Differentiating (1.8), (1.9) and making use of (1.4), (1.5) we obtain

$$dA \leq -SdT - PdV \quad (1.11)$$

$$dG \leq VdP - SdT \quad (1.12)$$

which give the well-known equilibrium conditions for constant (V,T) or (P,T) constraints

$$(dA)_{V,T} = 0 \quad (1.13)$$

$$(dG)_{P,T} = 0. \quad (1.14)$$

Equilibrium conditions previously discussed apply to every thermodynamic system.

They, however, assume a different form for multi-component systems. In this case the Gibbs potential is commonly used to describe the equilibrium¹. From (1.12), we can deduce that the Gibbs potential can be written in implicit form as

$$G = G(P, T) \quad (1.15)$$

for a system with a constant number of particles. In the more general case of a system with a variable particle number, the Gibbs potential, which is an extensive quantity, can be written as

$$G = G(P, T, n) \quad (1.16)$$

where n is the number of moles in the system. Differentiating (1.16) we get

$$dG = \left(\frac{\partial G}{\partial T} \right)_{P,n} dT + \left(\frac{\partial G}{\partial P} \right)_{T,n} dP + \left(\frac{\partial G}{\partial n} \right)_{P,T} dn \quad (1.17)$$

and comparing (1.12) with (1.17)

$$\left(\frac{\partial G}{\partial T} \right)_{P,n} = -S \quad (1.18)$$

$$\left(\frac{\partial G}{\partial P} \right)_{T,n} = V. \quad (1.19)$$

We introduce the chemical potential μ , defined as

$$\mu = \left(\frac{\partial G}{\partial n} \right)_{P,T} \quad (1.20)$$

and then (1.17) can be written as

$$dG = -SdT + VdP + \mu dn. \quad (1.21)$$

Equation (1.21) can be generalized to a multi-component mixture: in this case, the Gibbs potential is a function of the number of moles n_i of each species

$$G = G(P, T, n_1, n_2, n_3, \dots) \quad (1.22)$$

¹See (Capitelli and Giordano 2002; Capitelli et al. 2005b) where the equivalence of the use of different potentials for describing chemical equilibrium is discussed.

and in differential form becomes

$$dG = -SdT + VdP + \sum_{i=1}^N \mu_i dn_i \quad (1.23)$$

being N the number of species. The chemical potentials μ_i are defined as

$$\mu_i = \left(\frac{\partial G}{\partial n_i} \right)_{P,T,n_j \neq i}. \quad (1.24)$$

The equilibrium condition for a reacting mixture at constant P, T is obtained combining (1.14), (1.23), giving

$$\sum_{i=1}^N \mu_i dn_i = 0. \quad (1.25)$$

Let us consider a generic reaction written as

$$\sum_{i=1}^N v_i X_i = 0, \quad (1.26)$$

where X_i 's are all the species in the reaction and v_i 's are the stoichiometric coefficients (positive for the products, negative for reactants). It is possible to define the advancement degree, $d\xi$, of the reaction as

$$d\xi = \frac{dn_i}{v_i} \quad (1.27)$$

independent of the species involved in the reaction². Using this new quantity, (1.25) can be rewritten as

$$\sum_{i=1}^N \mu_i v_i d\xi = d\xi \sum_{i=1}^N \mu_i v_i = 0 \Rightarrow \sum_{i=1}^N \mu_i v_i = 0 \quad (1.28)$$

which is the form commonly used to determine the equilibrium of a reaction.

To go on we introduce the chemical potential of the components of an ideal gas³

$$\mu_i(T, P_i) = \mu_i^0(T, P^0) + RT \ln P_i, \quad (1.29)$$

²This property is a direct consequence of the mass conservation law.

³The following results will be closely examined in Chap. 3.

where μ_i^0 is the chemical potential of the i -th species under standard conditions, P^0 is the standard pressure and P_i is the partial pressure of the i -th species. For the generic reaction in (1.26) in gas phase, we can define the variation of standard chemical potential as

$$\Delta\mu^0 = \sum_{i=1}^N v_i \mu_i^0 \quad (1.30)$$

and by means of the equilibrium condition given in (1.28) we have

$$\sum_{i=1}^N v_i \mu_i = \sum_{i=1}^N v_i \mu_i^0 + \sum_{i=1}^N v_i RT \ln P_i = \Delta\mu^0 + RT \ln \prod_{i=1}^N P_i^{v_i} = 0. \quad (1.31)$$

We introduce now the equilibrium constant K_p defined as

$$K_p = \prod_{i=1}^N P_i^{v_i}, \quad (1.32)$$

which can be also written as

$$K_p = \exp\left(-\frac{\Delta\mu^0}{RT}\right) \quad (1.33)$$

being

$$\Delta\mu^0 = \Delta\bar{H}^0 - T\Delta\bar{S}^0, \quad (1.34)$$

where $\Delta\bar{H}^0$ and $\Delta\bar{S}^0$, respectively, represent the molar reaction enthalpy and entropy under standard conditions i.e. $P_0 = 10^5$ Pa (Pauling 1988). Differentiation of (1.33) with respect to temperature yields the Van't Hoff equation

$$\frac{d\ln K_{eq}}{dT} \approx \frac{\Delta\bar{H}^0}{RT^2} \quad (1.35)$$

under the assumption of $\Delta\bar{H}^0$ and $\Delta\bar{S}^0$ independent of temperature.

1.2 Dissociation Equilibrium

Let us start with the dissociation process i.e. the simple chemical equation



We can write the equilibrium condition as

$$\mu_{A_2} = 2\mu_A, \quad (1.37)$$

which yields

$$K_p^d = \frac{P_A^2}{P_{A_2}} = \exp\left(-\frac{\Delta\mu_d^0}{RT}\right) \quad (1.38)$$

being in this case

$$\Delta\mu_d^0 = 2\mu_A^0 - \mu_{A_2}^0. \quad (1.39)$$

The equilibrium condition can be also expressed through the dissociation degree α_d

$$\alpha_d = \frac{n_d}{n_0} \quad (1.40)$$

i.e. the ratio of dissociated molecules⁴ (n_d) and the initial number of molecules (n_0). The moles and the molar fractions (χ) of the two species at the equilibrium can be expressed as

$$\begin{aligned} n_{A_2} &= n_0(1 - \alpha_d) & \chi_{A_2} &= \frac{1 - \alpha_d}{1 + \alpha_d} \\ n_A &= 2\alpha_d n_0 & \chi_A &= \frac{2\alpha_d}{1 + \alpha_d}. \end{aligned} \quad (1.41)$$

From (1.38) and (1.41), the equilibrium constant can be expressed through α_d and the total pressure P as

$$K_p^d = P \frac{4\alpha_d^2}{1 - \alpha_d^2}. \quad (1.42)$$

Now we have all the ingredients to understand the dependence of the dissociation degree α_d on pressure and temperature (see Figs. 1.1 and 1.2), we can directly use (1.42) in the form

$$\alpha_d = \sqrt{\frac{K_p^d}{4P + K_p^d}}. \quad (1.43)$$

From (1.43) it is possible to determine the two important limiting values of α_d as a function of P at constant temperature

$$\begin{aligned} P \rightarrow 0 &\Rightarrow \alpha_d \rightarrow 1 \\ P \rightarrow \infty &\Rightarrow \alpha_d \rightarrow 0. \end{aligned} \quad (1.44)$$

The dissociation degree α_d has a decreasing monotonic behavior with the pressure at constant temperature (see Fig. 1.1), reaching the limiting value of 1 for $P \rightarrow 0$, independently of the temperature.

⁴ It must be noted that in this example the advancement degree defined in (1.27) is related to the dissociation degree by the simple relation $\alpha_d = \frac{\xi}{n_0}$.

Fig. 1.1 Dependence of H_2 dissociation degree α_d on the gas pressure P for different values of the temperature

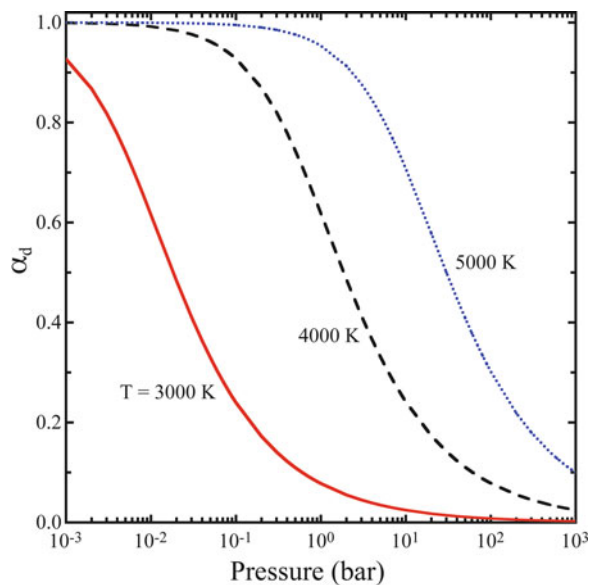
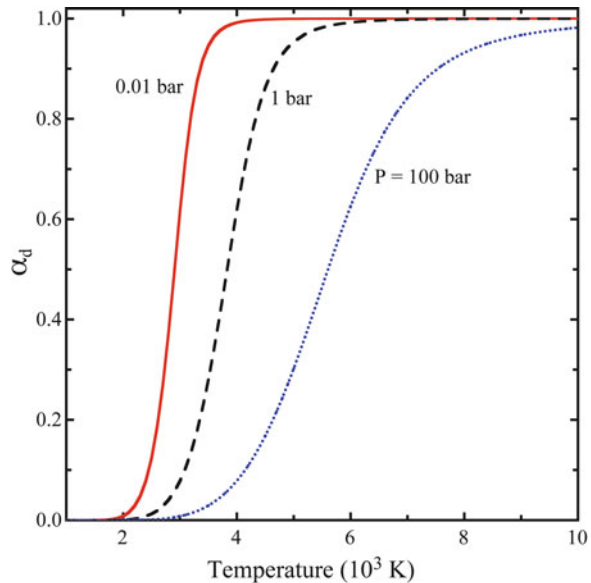


Fig. 1.2 Dependence of H_2 dissociation degree α_d on the gas temperature T for different values of the pressure



Let us now examine the behaviour of α_d as a function of T at constant pressure. We can still use (1.43); at low temperature we can assume that $4P \gg K_p^d$ so that (1.43) becomes

$$\alpha_d \approx \sqrt{\frac{K_p^d}{4P}} \quad (1.45)$$

We can consider K_p depending only on the temperature⁵ (see (1.33))

$$K_p^d = \exp\left(\frac{\Delta\bar{S}_d^0}{R}\right) \exp\left(-\frac{\Delta\bar{H}_d^0}{RT}\right). \quad (1.46)$$

As first approximation the standard entropy variation does not depend on temperature as well as the standard enthalpy that can be approximated by⁶ $\Delta\bar{H}^0 \approx D$, being D the dissociation energy. Therefore, we get the following expression for the equilibrium constant

$$K_p^d(T) \approx A \times \exp\left(-\frac{D}{RT}\right) \quad (1.47)$$

being $A = \exp(\Delta\bar{S}_d^0/R)$. Substituting in (1.45), we have

$$\alpha_d = \sqrt{\frac{A}{4P} \exp\left(-\frac{D}{RT}\right)} = \sqrt{\frac{A}{4P}} \exp\left(-\frac{D}{2RT}\right) \quad (1.48)$$

This equation shows that α_d increases exponentially with T (remember that $D > 0$) starting from $\alpha_d = 0$ for $T = 0$ K ($K_p^d(0) = 0$). At very high temperature, we can assume that $4P \ll K_p^d$ and neglecting $4P$ in (1.43) we have $\alpha_d = 1$, independently of the temperature. In the intermediate temperature range, α_d will present an inflection point (see Fig. 1.2). In the whole, the dissociation degree follows a sigmoid curve ranging from zero to one as the temperature increases. As a consequence of the previous discussion, we can deduce the following statement:

The dissociation degree increases with increasing gas temperature at constant pressure and decreases with increasing the pressure at constant temperature. This result satisfies the well known Le Chatelier principle.

1.3 Ionization Equilibrium

Another interesting example is the ionization process



⁵This assumption is valid only for ideal gases.

⁶This assumption, which will be eliminated in the next chapters, disregards the internal structure of atoms and molecules as well as differences in the translational energies of products and reactants.

which equilibrium condition can be written as (see (1.28))

$$\mu_{A+} + \mu_{e^-} = \mu_A \quad (1.50)$$

We can define the ionization equilibrium constant as

$$K_p^i = \frac{P_{A+} P_{e^-}}{P_A} = \exp\left(-\frac{\Delta\mu_i^0}{RT}\right) \quad (1.51)$$

where

$$\Delta\mu_i^0 = \mu_{A+}^0 + \mu_{e^-}^0 - \mu_A^0 = \Delta\bar{H}_i^0 - T\Delta\bar{S}_i^0 \quad (1.52)$$

being $\Delta\bar{H}_i^0$ and $\Delta\bar{S}_i^0$ respectively, the enthalpy and entropy variation in the ionization process and P_{A+} , P_{e^-} , P_A represent in the order the partial pressures of ions, electrons and atoms. This equation can be easily expressed through the ionization degree as⁷

$$\alpha_i = \frac{n_i}{n_0} \quad (1.53)$$

defined as the ratio of the moles of ionized atoms (n_i) and the initial atom moles (n_0). According to this definition, considering that the total number of moles is $n = n_A + n_{A+} + n_{e^-} = n_0(1 + \alpha_i)$, the moles and the molar fractions of the three species at the equilibrium can be expressed as

$$\begin{aligned} n_A &= n_0(1 - \alpha_i) & \chi_A &= \frac{1 - \alpha_i}{1 + \alpha_i} \\ n_{A+} &= \alpha_i n_0 & \chi_{A+} &= \frac{\alpha_i}{1 + \alpha_i} \\ n_{e^-} &= \alpha_i n_0 & \chi_{e^-} &= \frac{\alpha_i}{1 + \alpha_i} \end{aligned} \quad (1.54)$$

From (1.51) and (1.54), the equilibrium constant can be expressed through α_i and the total pressure P as

$$K_p^i = P \frac{\alpha_i^2}{1 - \alpha_i^2}, \quad (1.55)$$

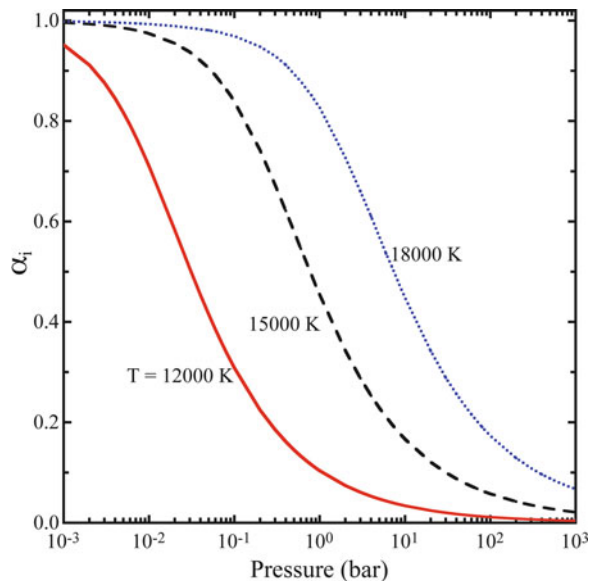
which is similar to the corresponding one (1.42) obtained for the dissociation.

The dependence of α_i on pressure can be written as

$$\alpha_i = \sqrt{\frac{K_p^i}{P + K_p^i}}, \quad (1.56)$$

⁷ As for the dissociation (see note 4), the advancement degree defined in (1.27) is related to the ionization degree by the simple relation $\alpha_i = \frac{\xi}{n_0}$.

Fig. 1.3 Dependence of atomic hydrogen ionization degree α_i on the gas pressure P for different values of the temperature



which differs from the corresponding expression for dissociation (1.43) by a factor 4 in the pressure term. As a consequence, the same limiting values reported in (1.44) for dissociation degree are valid for the ionization degree. The dependence of the ionization degree on pressure follows the same trend discussed for the dissociation process.

Following the same arguments used for the dissociation process (see (1.48)), we can consider $\Delta\bar{H}_i^0 \approx I$, being I the ionization energy⁸ we can write

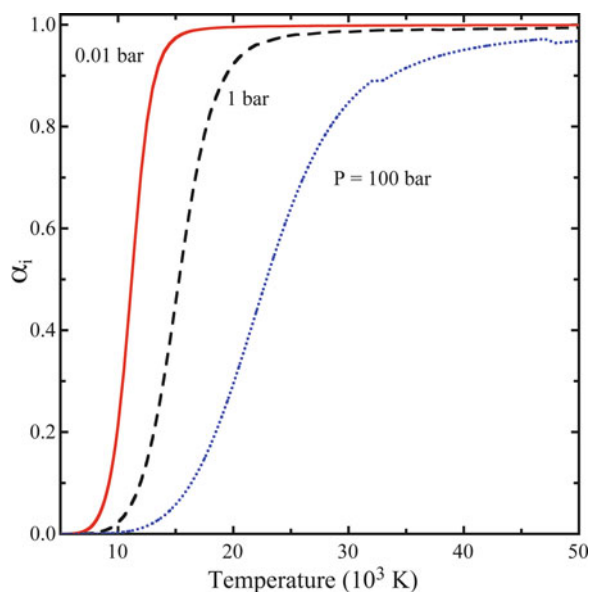
$$\alpha_i = \sqrt{AP \exp\left(-\frac{I}{RT}\right)} = \sqrt{\frac{A}{P}} \exp\left(-\frac{I}{2RT}\right), \quad (1.57)$$

where $A = \exp(\Delta S_i^0/R)$.

The dependence of the ionization degree on pressure and temperature is reported in Figs. 1.3 and 1.4: the results are very similar to those obtained for the dissociation case (Figs. 1.1 and 1.2), but shifted to higher values of temperature, because $I > D$.

⁸As for the case of dissociation, the assumption $\Delta\bar{H}^0 \approx I$ disregards the internal structure of atoms as well as differences in the translational energies of products and reactants. Debye–Hückel corrections, which introduces the lowering of ionization potential are also disregarded in (1.57).

Fig. 1.4 Dependence of atomic hydrogen ionization degree α_i on the gas temperature T for different values of the pressure

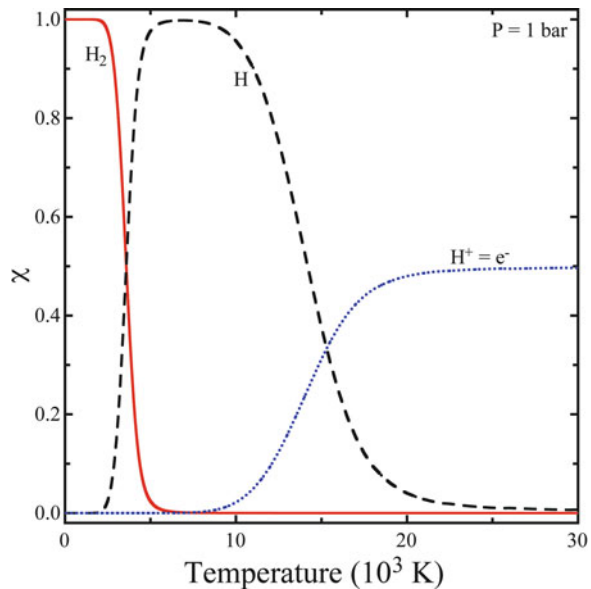


1.4 Dissociation and Ionization Equilibria: Coupled Solution

We have presented the dissociation and the ionization equilibrium as independent events. This is indeed an approximation since an overlapping temperature range in which the two reactions are mutually influenced does exist. In general, in a real system, many reactions act at the same time. As a consequence, all the equilibria must be considered simultaneously, writing a number of equations equal to the number of unknowns. In the case of a simple dissociating-ionizing system we have four unknowns (P_{A_2} , P_A , P_{A+} , P_{e^-}), linked by: (a) two equilibrium equations, (b) the conditions of constant total pressure and (c) the charge conservation i.e.

$$\left\{ \begin{array}{l} K_p^d = \frac{P_A^2}{P_{A_2}} \\ K_p^i = \frac{P_{A+} P_{e^-}}{P_A} \\ P = P_{A_2} + P_A + P_{A+} + P_{e^-} \\ P_{A+} = P_{e^-} \end{array} \right. \quad (1.58)$$

Fig. 1.5 Dependence of molar fractions χ on the gas temperature for $P = 1$ bar



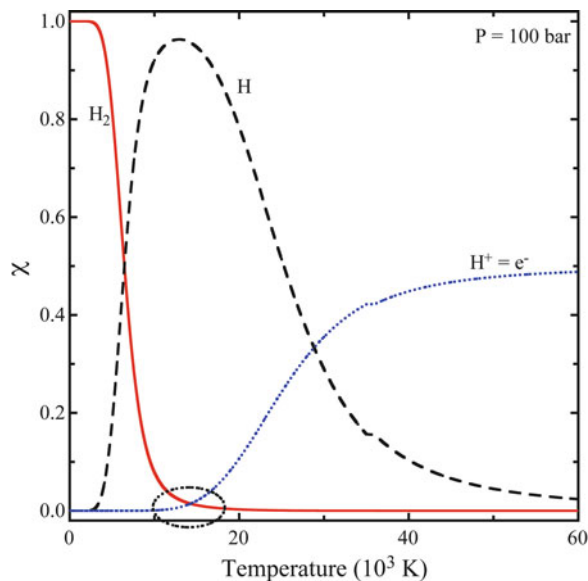
which form a non-linear system⁹. We can write all the pressures as a function of the partial pressure of electrons

$$\left\{ \begin{array}{l} P_{A+} = P_{e^-} \\ P_A = \frac{P_{e^-}^2}{K_p^i} \\ P_{A_2} = \frac{P_{e^-}^4}{(K_p^i)^2 K_p^d} \\ P = \frac{P_{e^-}^4}{(K_p^i)^2 K_p^d} + \frac{P_{e^-}^2}{K_p^i} + 2P_{e^-} \end{array} \right. \quad (1.59)$$

which reduces to the solution of a single non-linear equation in P_e , while the partial pressure of other species can be determined easily by the other relations. In Figs. 1.5 and 1.6, we have reported the molar fractions ($\chi_i = \frac{P_i}{P}$) of the species as a function of the temperature for $P = 1$ bar and $P = 100$ bar for an hydrogen plasma composed by H_2 , H , H^+ and e^- . It can be observed that at

⁹In general, the system of equilibrium equations is very complex and require computer programs to be solved.

Fig. 1.6 Dependence of molar fractions χ on the gas temperature for $P = 100$ bar



low pressure dissociation and ionization can be considered to a good approximation as independent events, this condition being not satisfied at high pressure (see Fig. 1.6).

1.5 Ideal Gas Thermodynamics

In the previous sections, we have shown how to calculate the equilibrium composition of a system in the dissociation and ionization regimes. The compositions enter in the thermodynamics of a reacting system modulating the properties of a single species. In this section, we will use concepts of classical thermodynamics¹⁰ to characterize the properties of the reacting mixture considered as an ideal gas, i.e. subjected to the following state equation

$$PV = nRT, \quad (1.60)$$

where R is the ideal gas constant and n the total number of moles.

An ideal gas is a system formed by classical¹¹ particles which interact between themselves only through collisions and which dimension is negligible with respect to the system volume. In few words, an ideal gas is a system formed by point

¹⁰Many of the quantities defined in this section will be recalculated in the Chap. 3 in the framework of statistical thermodynamics.

¹¹Following the Boltzmann statistical distribution.

particles with null interaction potential. As a consequence, the energy of the system is the sum of the energy of each particle. This property is reflected to all the extensive thermodynamic functions. In the following, we will focus on two quantities, the enthalpy and the specific heat.

1.5.1 Ideal Gas Mixture Enthalpy

For an ideal gas, the enthalpy of a mixture with N species is simply the sum of the enthalpies of its components

$$H = \sum_{i=1}^N n_i \bar{H}_i, \quad (1.61)$$

where \bar{H}_i is the molar enthalpy of the i -th species, that depends only on the temperature¹², and n_i the number of moles of the i -th species. The summation rule in (1.61) is valid for all the extensive thermodynamic functions of an ideal gas, such as U, S, G, A .

Starting from (1.61) we can define the molar enthalpy of the system, an intensive quantity, as

$$\bar{H} = \frac{H}{n} = \sum_{i=1}^N \frac{n_i}{n} \bar{H}_i = \sum_{i=1}^N \chi_i \bar{H}_i \quad (1.62)$$

being χ_i the molar fraction of the i -th species.

To calculate the enthalpy per unit mass h , we have to divide the total enthalpy by the mass of the mixture¹³

$$M = \sum_{i=1}^N n_i M_i, \quad (1.63)$$

where M_i is the molar mass of the i -th species. Defining the mean molar mass as

$$\bar{M} = \frac{M}{n} = \sum_{i=1}^N \frac{n_i}{n} M_i = \sum_{i=1}^N \chi_i M_i \quad (1.64)$$

we have

$$h = \frac{H}{M} = \frac{1}{M} \sum_{i=1}^N n_i \bar{H}_i = \frac{n}{M} \sum_{i=1}^N \frac{n_i}{n} \bar{H}_i = \frac{\bar{H}}{\bar{M}} \quad (1.65)$$

¹² This assumption is true only for an ideal gas, failing however when real effects are important.

¹³ It must be noted that the total mass of a reacting mixture is constant. This property can be demonstrated in general considering that the atomic constituents of the mixtures are rearranged during the chemical processes, remaining however in the system. A demonstration for the dissociation process is given in note 19.

Let us now introduce the single species enthalpy per unit mass as

$$h_i = \frac{\bar{H}_i}{M_i} \quad (1.66)$$

and the mass fraction of a given species as

$$c_i = \frac{n_i M_i}{\bar{M}} = \frac{\chi_i M_i}{\bar{M}}. \quad (1.67)$$

We can rearrange (1.66) multiplying and dividing by M_i obtaining

$$h = \sum_{i=1}^N n_i \frac{M_i}{\bar{M}} \frac{\bar{H}_i}{M_i} = \sum_{i=1}^N c_i h_i. \quad (1.68)$$

The properties described above are of general validity: the parallelism between (1.62), (1.68) can be extended to all the thermodynamic functions. Moreover to convert any molar quantity in mass unit is sufficient to divide by the mean molar mass as in (1.65).

1.5.2 Ideal Gas Mixture Heat Capacity

It is possible to define for a system the heat capacity as

$$C = \frac{\partial Q}{\partial T} \quad (1.69)$$

i.e. the quantity of heat necessary to increase the temperature of the system of one degree. This quantity depends on the path of the transformation, and usually it is defined for reversible transformations under constant volume or constant pressure constraints. It must be noted that in these cases, the heat exchanged is related to the variation of the relevant state functions, as

$$dQ = \begin{cases} dH & \text{at constant } P \\ dU & \text{at constant } V \end{cases} \quad (1.70)$$

giving

$$C_p = \left(\frac{\partial Q}{\partial T} \right)_P = \left(\frac{\partial H}{\partial T} \right)_P \quad (1.71)$$

and the constant volume heat capacity

$$C_v = \left(\frac{\partial Q}{\partial T} \right)_V = \left(\frac{\partial U}{\partial T} \right)_V. \quad (1.72)$$

Using the definitions in (1.61), (1.71), the heat capacity of an ideal gas mixture can be explicitly written as

$$C_p = \sum_{i=1}^N n_i \left(\frac{\partial \bar{H}_i}{\partial T} \right)_P + \sum_{i=1}^N \bar{H}_i \left(\frac{\partial n_i}{\partial T} \right)_P = C_{\text{pf}} + C_{\text{pr}} \quad (1.73)$$

the first term

$$C_{\text{pf}} = \sum_{i=1}^N n_i \frac{d\bar{H}_i}{dT} = \sum_{i=1}^N n_i \bar{C}_{\text{pi}} \quad (1.74)$$

is the so-called frozen heat capacity, where

$$\bar{C}_{\text{pi}} = \left(\frac{\partial \bar{H}_i}{\partial T} \right)_P \quad (1.75)$$

is the specific heat of the i -th species. The second term in (1.73) is called reactive heat capacity

$$C_{\text{pr}} = \sum_{i=1}^N \bar{H}_i \left(\frac{\partial n_i}{\partial T} \right)_P \quad (1.76)$$

To calculate the molar specific heat from the heat capacity, it is not sufficient to divide the heat capacity by the molar fraction. In fact the molar specific heat at constant pressure is given by

$$\bar{C}_p = \left(\frac{\partial \bar{H}}{\partial T} \right)_P = \frac{C_p}{n} - \frac{1}{n} \left(\frac{\partial n}{\partial T} \right)_P \bar{H} \neq \frac{C_p}{n}. \quad (1.77)$$

On the other hand, (1.65) can be extended to the heat capacity per unit mass, i.e. the specific heat is given by

$$c_p = \left(\frac{\partial h}{\partial T} \right)_P = \frac{C_p}{M} - \cancel{\frac{1}{M} \left(\frac{\partial M}{\partial T} \right)_P} \cancel{h} = \frac{C_p}{M} \quad (1.78)$$

because the total mass of the mixture, M , is constant.

1.6 Single Species Enthalpy

In this section, we will give an estimation of the single species enthalpy and specific heat. In general, the single species molar enthalpy, as well as the other thermodynamic functions, can be obtained as the sum of the translational (tr), internal (int) and formation (f) contributions

$$\bar{H}_i = \bar{H}_i^{\text{tr}} + \bar{H}_i^{\text{int}} + \bar{H}_i^f. \quad (1.79)$$

The molar energy is given by

$$\bar{U}_i = \bar{H}_i - RT. \quad (1.80)$$

For an ideal gas, the translational molar enthalpy does not depend on the considered species and is given by

$$\bar{H}_i^{\text{tr}} = \frac{5}{2}RT, \quad (1.81)$$

while the corresponding translational energy can be written as

$$\bar{U}_i^{\text{tr}} = \bar{H}_i^{\text{tr}} - RT = \frac{3}{2}RT. \quad (1.82)$$

The internal enthalpy depends on the species and in general is a function of the temperature only¹⁴. On the other hand, \bar{H}_i^f , a characteristic of each species, is a constant¹⁵.

The internal energy depends on the internal structure of the species considered, i.e. on the energy levels. For molecular species, a simple approach can be used, separating the different contributions coming from electronic (*el*), vibrational (*vib*) and rotational (*rot*) excitation

$$\bar{H}^{\text{int}} = \bar{U}^{\text{int}} = \bar{H}^{\text{el}} + \bar{H}^{\text{rot}} + \bar{H}^{\text{vib}}. \quad (1.83)$$

For atoms only the electronic contribution must be considered. An incorrect approach, often used in the literature, is to neglect \bar{H}^{el} , even if its contribution can be relevant, especially at high temperature. In this chapter, the electronic enthalpy will be considered as a parameter. The rotational and vibrational contributions can be estimated using the equipartition theorem.

1.6.1 Equipartition Theorem

Following the classical approach of statistical thermodynamics, the energy of a diatomic molecule can be obtained by the number of degrees of freedom characterizing the motion of the molecule considered as a two-point system. Each point is characterized by three cartesian coordinates so that the diatom will be characterized by six cartesian coordinates. The motion of the six-coordinate system can be transformed in three-translational, two-rotational and one-vibrational degrees

¹⁴ See note 12.

¹⁵ The value of the formation enthalpy depends on which species are considered as reference for energy.

of freedom. The equipartition theorem¹⁶ assigns to each degree of freedom an energy of $\frac{1}{2}RT$. Applying the equipartition theorem to diatomic molecules, we have¹⁷

$$\bar{U} = \bar{U}^{\text{tr}} + \bar{U}^{\text{rot}} + \bar{U}^{\text{vib}} + \bar{U}^{\text{el}} = \frac{3}{2}RT + RT + RT + \bar{U}^{\text{el}} = \frac{7}{2}RT + \bar{U}^{\text{el}} \quad (1.84)$$

and the enthalpy is given by

$$\bar{H} = \bar{U} + RT = \frac{7}{2}RT + \bar{H}^{\text{el}} + RT = \frac{9}{2}RT + \bar{H}^{\text{el}}, \quad (1.85)$$

where $\bar{U}^{\text{el}} = \bar{H}^{\text{el}}$ is the contribution of electronically excited states.

Considering the hypothesis in (1.83), the internal specific heat can be considered the sum of different contributions

$$\bar{C}_p = \bar{C}_p^{\text{rot}} + \bar{C}_p^{\text{vib}} + \bar{C}_p^{\text{el}} = \frac{9}{2}R + \bar{C}_p^{\text{el}}, \quad (1.86)$$

where

$$\bar{C}_p^{\text{el}} = \frac{d\bar{H}^{\text{el}}}{dT} \quad (1.87)$$

The equipartition theorem can be also applied to polyatomic molecules. In general, we must add $\frac{1}{2}RT$ for each rotational axis and RT for each vibrational mode. In particular, for linear molecule we have two rotational axes and $3N_{\text{atoms}} - 5$ vibrational modes, while for non-linear molecules there are three rotational axes and $3N_{\text{atoms}} - 6$ vibrational modes¹⁸, where N_{atoms} is the number of atoms in the molecule, giving

$$\begin{aligned} \bar{H} &= \left(3N_a - \frac{3}{2}\right)RT \\ \bar{C} &= \left(3N_a - \frac{3}{2}\right)R \end{aligned} \quad (1.88)$$

¹⁶The energy equipartition considers two conditions: each degree of freedom is independent from the others, the temperature is sufficiently high that the quantum behavior of internal levels is negligible. The use of the energy equipartition theorem, while correctly describing translational and rotational degrees of freedom, strongly overestimates the contribution of vibrational energy at low temperature, as discussed in Chap. 5.

¹⁷It should be noted that the vibrational degree of freedom gives to enthalpy a term RT due to kinetic and potential energy contribution.

¹⁸In general, the number of vibrational mode is given by $3N_{\text{atoms}} - r - 3$ being r the number of rotational axis.

for linear molecules, valid also for diatomic molecules, and

$$\begin{aligned}\bar{H} &= (3N_a - 2)RT \\ \bar{C}_p &= (3N_a - 2)R\end{aligned}\quad (1.89)$$

for non-linear molecules, neglecting the electronic contribution to enthalpy.

1.7 Mixture Thermodynamics at Constant Pressure

1.7.1 Dissociation

Let us consider again the dissociation reaction in (1.36), starting with a gas containing n_0 moles of A_2 molecules. The equilibrium composition is given in (1.41), being the dissociation degree α_d as in (1.43). Making use of the equipartition theorem, the molar enthalpy of atoms and molecules is given by

$$\begin{aligned}\bar{H}_{A_2} &= \frac{9}{2}RT + \bar{H}_{A_2}^{\text{el}} \\ \bar{H}_A &= \frac{5}{2}RT + \bar{H}_{A_2}^{\text{el}} + \frac{D}{2},\end{aligned}\quad (1.90)$$

where the enthalpy of molecules includes the contribution of translational, rotational, vibrational and electronic degrees of freedom. Atoms, on the other hand, include translational and electronic contributions plus the formation enthalpy ($\frac{D}{2}$). The total enthalpy is then written as

$$\begin{aligned}H &= n_0(1 - \alpha_d) \left(\frac{9}{2}RT + \bar{H}_{A_2}^{\text{el}} \right) + 2n_0\alpha_d \left(\frac{5}{2}RT + \frac{D}{2} + \bar{H}_A^{\text{el}} \right) \\ &= n_0 \left[\left(\frac{9}{2}RT + \bar{H}_{A_2}^{\text{el}} \right) + \alpha_d \left(\frac{1}{2}RT + D + 2\bar{H}_A^{\text{el}} - \bar{H}_{A_2}^{\text{el}} \right) \right].\end{aligned}\quad (1.91)$$

The enthalpy per unit mass (see (1.65), (1.68)) is obtained simply dividing both members of the equation by the total mass¹⁹ $M = n_0 M_{A_2}$ (which is constant)

$$h = \frac{1}{M_{A_2}} \left[\left(\frac{9}{2}RT + \bar{H}_{A_2}^{\text{el}} \right) + \alpha_d \left(\frac{1}{2}RT + D + 2\bar{H}_A^{\text{el}} - \bar{H}_{A_2}^{\text{el}} \right) \right].\quad (1.92)$$

¹⁹ The total mass as a function of the dissociation degree is given by

$M(\alpha_d) = n_0(1 - \alpha_d)M_{A_2} + 2\alpha_d n_0 M_A$.

Considering that

$M_A = M_{A_2}/2$

we have

$M(\alpha_d) = n_0(1 - \alpha_d + 2\alpha_d/2)M_{A_2} = n_0 M_{A_2}$.

To obtain the specific heat at constant pressure, we can calculate the derivative of (1.92) with respect to the temperature. Considering the frozen and reactive contributions to the specific heat as given in (1.71) for the dissociation we have

$$c_{\text{pf}} = \frac{1}{2M_{A_2}} \left[\frac{R}{2}(9 + \alpha_d) + (1 - \alpha_d)\bar{C}_{A_2}^{\text{el}} + 2\alpha_d\bar{C}_A^{\text{el}} \right]$$

$$c_{\text{pr}} = \frac{1}{M_{A_2}} \left(\frac{1}{2}RT + D + 2\bar{H}_A^{\text{el}} - \bar{H}_{A_2}^{\text{el}} \right) \left(\frac{\partial \alpha_d}{\partial T} \right)_P . \quad (1.93)$$

To calculate $\left(\frac{\partial \alpha_d}{\partial T} \right)_P$, we start determining the logarithm of the equilibrium constant as given in (1.42)

$$\ln K_p^d = 2 \ln \alpha_d - \ln(1 - \alpha_d^2) + \ln(4P)$$

and differentiating at constant pressure

$$\begin{aligned} \frac{d \ln K_p^d}{dT} &= 2 \left(\frac{\partial \ln \alpha_d}{\partial T} \right)_P - \left(\frac{\partial \ln(1 - \alpha_d^2)}{\partial T} \right)_P + \cancel{\left(\frac{\partial \ln(4P)}{\partial T} \right)_P} = \\ &= \left(\frac{2}{\alpha_d} + \frac{2\alpha_d}{1 - \alpha_d^2} \right) \left(\frac{\partial \alpha_d}{\partial T} \right)_P \end{aligned}$$

from which we get

$$\left(\frac{\partial \alpha_d}{\partial T} \right)_P = \frac{\alpha_d(1 - \alpha_d^2)}{2} \frac{d \ln K_p^d}{dT} \quad (1.94)$$

Using the Van't Hoff equation (see (1.35)), we have the approximate relation

$$\left(\frac{\partial \alpha_d}{\partial T} \right)_P \approx \frac{\alpha_d(1 - \alpha_d^2)}{2} \frac{\Delta \bar{H}_d^0}{RT^2} \quad (1.95)$$

The molar enthalpy of the dissociation is given by

$$\Delta \bar{H}_d^0 = \frac{1}{2}RT + D + 2\bar{H}_A^{\text{el}} - \bar{H}_{A_2}^{\text{el}} \quad (1.96)$$

and combining (1.93)–(1.96) we have

$$c_{\text{pr}} \approx \frac{R}{M_{A_2}} \Delta \bar{H}_d^0 \frac{\alpha_d(1 - \alpha_d^2)}{2} \frac{\Delta \bar{H}_d^0}{(RT)^2} = \frac{R}{2M_{A_2}} \alpha_d(1 - \alpha_d^2) \left(\frac{\Delta \bar{H}_d^0}{RT} \right)^2 \quad (1.97)$$

1.7.2 Ionization

Let us consider the ionization reaction as written in (1.49). In this section, we are considering the atomic species A coming from the dissociation of a diatomic molecule A_2 , which means that we are considering the energy bias of $\frac{D}{2}$ for both atomic and ionic species. Considering initially n_0 moles of atoms, the gas composition can be expressed as a function of the ionization degree α_i (see (1.53)), giving the composition reported in (1.54). Considering electronic contribution to atomic and ionic enthalpies, we have

$$\begin{aligned}\bar{H}_A &= \frac{5}{2}RT + \bar{H}_A^{\text{el}} + \frac{D}{2} \\ \bar{H}_{A^+} &= \frac{5}{2}RT + \bar{H}_{A^+}^{\text{el}} + \frac{D}{2} + I \\ \bar{H}_{e^-} &= \frac{5}{2}RT.\end{aligned}\quad (1.98)$$

The total enthalpy of the system is then given by

$$\begin{aligned}H &= n_0(1 - \alpha_i)\bar{H}_A + n_0\alpha_i\bar{H}_{A^+} + n_0\alpha_i\bar{H}_{e^-} \\ &= n_0 \left[(1 + \alpha_i)\frac{5}{2}RT + (1 - \alpha_i)\bar{H}_A^{\text{el}} + \alpha_i\bar{H}_{A^+}^{\text{el}} + D + \alpha_i I \right].\end{aligned}\quad (1.99)$$

The enthalpy per unit mass (see (1.65)) is obtained simply dividing both members of the equation by the total mass $M = n_0 M_A$

$$h = \frac{1}{M_A} \left[\frac{5}{2}RT + \bar{H}_A^{\text{el}} + D + \alpha_i \left(\frac{5}{2}RT - \bar{H}_A^{\text{el}} + \bar{H}_{A^+}^{\text{el}} + I \right) \right].\quad (1.100)$$

To obtain the specific heat at constant pressure, we can calculate the derivative of (1.100) with respect to the temperature. Following the same arguments previously used for the dissociation, we can write

$$\begin{aligned}c_{\text{pf}} &= \frac{1}{M_A} \left[\frac{5}{2}R(1 + \alpha_i) + (1 - \alpha_i)\bar{C}_{p,A}^{\text{el}} + \alpha_i\bar{C}_{p,A^+}^{\text{el}} \right] \\ c_{\text{pr}} &= \frac{1}{M_A} \left(\frac{5}{2}RT - \bar{H}_A^{\text{el}} + \bar{H}_{A^+}^{\text{el}} + I \right) \left(\frac{\partial \alpha_i}{\partial T} \right)_P\end{aligned}\quad (1.101)$$

in turn one can get

$$\left(\frac{\partial \alpha_i}{\partial T} \right)_P = \frac{\alpha_i(1 - \alpha_i^2)}{2} \frac{\Delta \bar{H}_i^0}{RT^2},\quad (1.102)$$

where the molar enthalpy of the ionization process is given by

$$\Delta \bar{H}_i^0 = \frac{5}{2}RT - H_A^{\text{el}} + H_{A^+}^{\text{el}} + I \quad (1.103)$$

and, combining (1.101)–(1.103), we have

$$c_{\text{pr}} \approx \frac{1}{M_A} \Delta \bar{H}_i^0 \frac{\alpha_d (1 - \alpha_i^2)}{2} \frac{\Delta \bar{H}_i^0}{(RT)^2} = \frac{R}{2M_A} \alpha_i (1 - \alpha_i^2) \left(\frac{\Delta \bar{H}_i^0}{RT} \right)^2 \quad (1.104)$$

that is the same result as the dissociation (compare with (1.97)) changing the index d with i .

To qualitatively understand the role of electronic excitation, on c_{pf} and c_{pr} we should take into account that usually the excitation of an ion occurs in a temperature range much higher than the corresponding one of the parent atom. We can therefore write (1.101) and (1.103)

$$\begin{aligned} c_{\text{pf}} &= \frac{1}{M_A} \left[\frac{5}{2} R (1 + \alpha_i) + (1 - \alpha_i) \bar{C}_{p,A}^{\text{el}} \right] \\ c_{\text{pr}} &= \frac{1}{M_A} \left(\frac{5}{2} RT - \bar{H}_A^{\text{el}} + I \right) \left(\frac{\partial \alpha_i}{\partial T} \right)_P \\ \Delta \bar{H}_i^0 &= \frac{5}{2} RT - H_A^{\text{el}} + I. \end{aligned} \quad (1.105)$$

These equations are exact for atomic hydrogen plasmas, due to the lack of electronic states in H^+ .

Inspection of the simplified (1.105) shows that the electronic contribution is a positive term in the frozen specific heat and a negative one, through $\Delta \bar{H}_i^0$, in the reactive term. As a consequence, a sort of compensation is to be expected for the total specific heat.

1.8 Mixture Thermodynamics at Constant Volume

In the previous section, we have considered a system working under constant pressure conditions. In this case, the thermodynamic potential that better characterize the system is the enthalpy²⁰ (see (1.71)). In this section, we will describe how to

²⁰This choice is done only on the basis of simplicity of the equations. Under global equilibrium, all the potentials are equivalent.

express the quantities under constant volume conditions, referring to the energy U (see (1.70), (1.72)).

For an ideal gas, enthalpy and energy are related by the simple equation

$$U = H - nRT \quad (1.106)$$

obtained by substituting the ideal gas state law (1.60) in the general definition of the enthalpy (1.10).

As a consequence, the energy of an ideal gas mixture is given by

$$U = \sum_{i=1}^N n_i \bar{U}_i = \sum_{i=1}^N n_i \bar{H}_i - nRT = \sum_{i=1}^N n_i \bar{H}_i - \sum_{i=1}^N n_i RT = \sum_{i=1}^N n_i (\bar{H}_i - RT) \quad (1.107)$$

for analogy with (1.61), and equating the arguments in the first and last summation, considering the properties in (1.79), (1.81), the single species molar energy is given by

$$\bar{U}_i = \bar{U}_i^{\text{tr}} + \bar{U}_i^{\text{int}} + \bar{U}_i^f = \frac{5}{2}RT + \bar{H}_i^{\text{int}} + \bar{H}_i^f - RT. \quad (1.108)$$

The last term RT can be grouped to any of the other terms, but clearly the more convenient choice is the translational part, giving

$$\begin{cases} \bar{U}_i^{\text{tr}} = \bar{H}_i^{\text{tr}} - RT = \frac{3}{2}RT \\ \bar{U}_i^{\text{int}} = \bar{H}_i^{\text{int}} \\ \bar{U}_i^f = \bar{H}_i^f. \end{cases} \quad (1.109)$$

Only the translational contribution is affected by (1.106), while the internal enthalpy and energy are exactly the same.

We can define the reaction molar energy $\Delta\bar{U}^0$ that can be related to the molar reaction enthalpy (referring to the generic reaction in (1.26)) by the equation

$$\Delta\bar{U}^0 = \sum_{i=1}^N v_i \bar{U}_i^0 = \sum_{i=1}^N v_i (\bar{H}_i^0 - RT) v_i = \Delta\bar{H}^0 - RT \sum_{i=1}^N v_i. \quad (1.110)$$

It is possible to extend the previous approach to the constant volume heat capacity (1.72) for an ideal gas mixture

$$C_v = \sum_{i=1}^N n_i \left(\frac{\partial \bar{U}_i}{\partial T} \right)_V + \sum_{i=1}^N \bar{U}_i \left(\frac{\partial n_i}{\partial T} \right)_V$$

$$\begin{aligned} C_{\text{vf}} &= \sum_{i=1}^N n_i \frac{d\bar{U}_i}{dT} \\ C_{\text{vr}} &= \sum_{i=1}^N \bar{U}_i \left(\frac{\partial n_i}{\partial T} \right)_V \end{aligned} \quad (1.111)$$

and for analogy with (1.74)–(1.75) we can write

$$\begin{aligned} C_{\text{vf}} &= \sum_{i=1}^N n_i \bar{C}_{\text{vi}} \\ \bar{C}_{\text{vi}} &= \bar{C}_{\text{vi}}^{\text{tr}} + \bar{C}_{\text{vi}}^{\text{int}} = \frac{3}{2}R + \frac{d\bar{U}_i^{\text{int}}}{dT} \end{aligned} \quad (1.112)$$

Being $\bar{U}_i^{\text{int}} = \bar{H}_i^{\text{int}}$ it follows that $\bar{C}_{\text{vi}}^{\text{int}} = \bar{C}_{\text{pi}}^{\text{int}}$. From now on, we will eliminate the specification v and p for the internal part and we will use the symbol \bar{C}_i^{int} for the internal contribution to the heat capacity.

Considering the dissociation process, the internal energy of the mixture at equilibrium is

$$U = H - (1 + \alpha_d)RT = \left(\frac{7}{2}RT + \bar{H}_{A_2}^{\text{el}} \right) + \alpha_d \left(D + 2\bar{H}_A^{\text{el}} - \bar{H}_{A_2}^{\text{el}} - \frac{1}{2}RT \right)$$

from which we recognize easily

$$\Delta\bar{U}_d^0 = \Delta\bar{H}_d^0 - RT = D + 2\bar{H}_A^{\text{el}} - \bar{H}_{A_2}^{\text{el}} - \frac{1}{2}RT.$$

The frozen specific heat is given by

$$C_{\text{vf}} = \left(\frac{\partial U}{\partial T} \right)_{V,\alpha_d} = \frac{R}{2}(7 - \alpha_d) + (1 - \alpha_d)\bar{C}_{A_2}^{\text{el}} + 2\alpha_d\bar{C}_A^{\text{el}}, \quad (1.113)$$

while the reactive specific heat is given by

$$C_{\text{vr}} = \left(\frac{\partial U}{\partial \alpha_d} \right)_{V,T} \left(\frac{\partial \alpha_d}{\partial T} \right)_V \quad (1.114)$$

where the first factor is $\Delta\bar{U}_d^0$ and the second one must be calculated as in Sect. 1.7.1 considering that $PV = nRT = (1 + \alpha_d)RT$ and calculating the logarithm of (1.42)

$$\ln K_p^d = 2 \ln \alpha_d - \ln(1 - \alpha_d^2) + \ln(4R/V) + \ln(T) + \ln(1 + \alpha_d).$$

The derivative at constant V ($\ln(4R/V)$ is constant) can be written as

$$\begin{aligned} \frac{d\ln K_p^d}{dT} &= 2 \left(\frac{\partial \ln \alpha_d}{\partial T} \right)_V - \left(\frac{\partial \ln(1 - \alpha_d^2)}{\partial T} \right)_V + \left(\frac{\partial \ln T}{\partial T} \right)_V + \left(\frac{\partial \ln(1 + \alpha_d)}{\partial T} \right)_V \\ &= \left(\frac{2}{\alpha_d} + \frac{2\alpha_d}{1 - \alpha_d^2} + \frac{1}{1 + \alpha_d} \right) \left(\frac{\partial \alpha_d}{\partial T} \right)_V + \frac{1}{T} \\ &= \frac{2 - \alpha_d}{\alpha_d(1 - \alpha_d)} \left(\frac{\partial \alpha_d}{\partial T} \right)_V + \frac{1}{T} \approx \frac{\Delta\bar{H}_d^0}{RT^2} \end{aligned}$$

Therefore,

$$\left(\frac{\partial \alpha_d}{\partial T} \right)_V \approx \frac{\alpha_d(1 - \alpha_d)}{2 - \alpha_d} \left(\frac{\Delta\bar{H}_d^0}{RT^2} - \frac{1}{T} \right) = \frac{\alpha_d(1 - \alpha_d)}{(2 - \alpha_d)RT^2} (\Delta\bar{H}_d^0 - RT)$$

giving as final result

$$\left(\frac{\partial \alpha_d}{\partial T} \right)_V \approx \frac{\alpha_d(1 - \alpha_d)}{(2 - \alpha_d)RT^2} \Delta\bar{U}_d^0 \quad (1.115)$$

and for the reactive heat capacity

$$C_{vr} = \Delta\bar{U}_d^0 \frac{\alpha_d(1 - \alpha_d)}{(2 - \alpha_d)RT^2} \Delta\bar{U}_d^0 = \frac{R\alpha_d(1 - \alpha_d)}{(2 - \alpha_d)} \left(\frac{\Delta\bar{U}_d^0}{RT} \right)^2. \quad (1.116)$$

The frozen and reactive specific heat for dissociation are given by

$$\begin{aligned} c_{vf} &= \frac{1}{M_{A_2}} \left[\frac{R}{2} (7 + \alpha_d) + (1 - \alpha_d) \bar{C}_{A_2}^{\text{el}} + 2\alpha_d \bar{C}_A^{\text{el}} \right] \\ c_{vr} &= \frac{1}{M_{A_2}} \left[R \frac{\alpha_d(1 - \alpha_d)}{(2 - \alpha_d)} \left(\frac{\Delta\bar{U}_d^0}{RT} \right)^2 \right] \end{aligned} \quad (1.117)$$

and for ionization, following the same procedure as for dissociation, we have

$$\begin{aligned} c_{\text{vf}} &= \frac{1}{M_A} \left[\frac{3R}{2}(1 + \alpha_i) + (1 - \alpha_i)\bar{C}_A^{\text{el}} + \alpha_i\bar{C}_{A+}^{\text{el}} \right] \\ c_{\text{vr}} &= \frac{1}{M_A} \left[R \frac{\alpha_i(1 - \alpha_i)}{(2 - \alpha_i)} \left(\frac{\Delta\bar{U}_i^0}{RT} \right)^2 \right] \end{aligned} \quad (1.118)$$

1.9 The Isentropic Coefficient

An important quantity, often used in fluid dynamics, is the isentropic coefficient γ . It enters in the equation of the sound speed (Anderson 2000)

$$c_{\text{sound}} = \sqrt{\frac{\gamma RT}{\bar{M}}} \quad (1.119)$$

and in the stationary shock tube or quasi-1D nozzle expansion relations (Anderson 2000), following from adiabatic transformations for an ideal gas. The isentropic coefficient is defined as

$$\gamma = \left(\frac{\partial \ln P}{\partial \ln \rho} \right)_S \quad (1.120)$$

being ρ the mass density. Equation (1.120) can be written as (Burm 2005; Burm et al. 1999; Henderson and Menart 2008)

$$\gamma = \frac{C_p \rho}{C_v P} \left(\frac{\partial P}{\partial \rho} \right)_T = \frac{c_p \rho}{c_v P} \left(\frac{\partial P}{\partial \rho} \right)_T. \quad (1.121)$$

We can write the isentropic coefficient as the product of two factors ($\gamma = \gamma_{\text{eq}} z_\gamma$)

$$\gamma_{\text{eq}} = \frac{c_p}{c_v} \quad (1.122)$$

and²¹

$$z_\gamma = \frac{\rho}{P} \left(\frac{\partial P}{\partial \rho} \right)_T. \quad (1.123)$$

²¹For an ideal, non-reacting gas, it is $z_\gamma = \frac{\rho}{P} \left(\frac{\partial P}{\partial \rho} \right)_T = 1$. In any case, it is $\lesssim 1$, therefore often the isentropic coefficient is written as $\gamma = \frac{c_p}{c_v}$ (Anderson 2000).

In some cases, it is very common to refer to the frozen isentropic coefficient²² defined as

$$\gamma_f = \frac{C_{\text{pf}}}{C_{\text{vf}}} = \frac{c_{\text{pf}}}{c_{\text{vf}}} \quad (1.124)$$

In this section, we will consider the equations describing frozen and total isentropic coefficients for the dissociation and ionization reactions considered as independent reactions. The discussion of the relevant equations will allow us to understand theoretical results when dissociation and ionization reaction are considered contemporaneously.

Let us evaluate the factor z_γ for the diatom dissociation (Sects. 1.2, 1.7.1) and for the atomic ionization (Sects. 1.3, 1.7.2). For the dissociation process, starting from one mole of molecules, the pressure as a function of the dissociation degree and temperature can be written as

$$P = (1 + \alpha_d) \frac{RT}{V} \quad (1.125)$$

and the mass density is

$$\rho = \frac{M_{A_2}}{V} = \frac{M_{A_2} P}{(1 + \alpha_d) RT}. \quad (1.126)$$

The derivative at constant temperature of the density with respect to the pressure

$$\begin{aligned} \left(\frac{\partial \rho}{\partial P} \right)_T &= \frac{M_{A_2}}{(1 + \alpha_d) RT} - \frac{M_{A_2} P}{(1 + \alpha_d)^2 RT} \left(\frac{\partial \alpha_d}{\partial P} \right)_T \\ &= \frac{M_{A_2}}{(1 + \alpha_d) RT} \left[1 - \frac{P}{(1 + \alpha_d)} \left(\frac{\partial \alpha_d}{\partial P} \right)_T \right]. \end{aligned} \quad (1.127)$$

To calculate the derivative $\left(\frac{\partial \alpha_d}{\partial P} \right)_T$, we start calculating the logarithm of the equilibrium condition in (1.42) and remembering that the equilibrium constant depends only on the temperature and therefore have null derivative i.e.

$$\left(\frac{\partial \ln K_p^d}{\partial P} \right)_T = \left(\frac{\partial \ln P}{\partial P} \right)_T + \ln 4 + 2 \ln \alpha_d - \ln(1 - \alpha_d^2) \Rightarrow$$

²²The frozen isentropic coefficient is used to calculate the frozen speed of sound (Anderson 2000), which is used for non-equilibrium flows, where the chemical composition is calculated solving a master equation (Colonna and Capitelli 2001a,b).

$$\begin{aligned}
0 &= \frac{1}{P} + 0 + \frac{2}{\alpha_d} \left(\frac{\partial \alpha_d}{\partial P} \right)_T + \frac{2\alpha_d}{1 - \alpha_d^2} \left(\frac{\partial \alpha_d}{\partial P} \right)_T \Rightarrow \\
\frac{1}{P} &= -\frac{2}{\alpha_d(1 - \alpha_d^2)} \left(\frac{\partial \alpha_d}{\partial P} \right)_T \Rightarrow \\
\left(\frac{\partial \alpha_d}{\partial P} \right)_T &= -\frac{\alpha_d(1 - \alpha_d)(1 + \alpha_d)}{2P}.
\end{aligned} \tag{1.128}$$

Substituting this result in (1.127), we have

$$\left(\frac{\partial \rho}{\partial P} \right)_T = \frac{M_{A_2}(2 + \alpha_d - \alpha_d^2)}{2(1 + \alpha_d)RT} = \frac{M_{A_2}(2 - \alpha_d)}{2RT} \tag{1.129}$$

and from (1.123) the coefficient z_γ for the dissociation process is then given by²³

$$z_{\gamma d} = \frac{2}{(1 + \alpha_d)(2 - \alpha_d)}. \tag{1.130}$$

For the ionization reaction, we should follow the same procedure as for dissociation. Noticing that, for both ionization and dissociation reactions, one particle of reactants produces two particles of products, we obtain for atomic ionization the same results as in (1.125)–(1.130) changing $M_{A_2} \rightarrow M_A$ and $\alpha_d \rightarrow \alpha_i$ i.e.

$$z_{\gamma i} = \frac{2}{(1 + \alpha_i)(2 - \alpha_i)}. \tag{1.131}$$

It should be noted that, in the considered cases, z_γ is the reverse of a parable, ranging from 1 (for $\alpha = 0$ and $\alpha = 1$) to 8/9 ($\alpha = 1/2$).

1.9.1 Dissociation Regime

In case of dissociation reaction, the frozen isentropic coefficient is

$$\gamma_{\text{df}} = \frac{\frac{R}{2}(9 + \alpha_d) + (1 - \alpha_d)\bar{C}_{A_2}^{\text{el}} + 2\alpha_d\bar{C}_A^{\text{el}}}{\frac{R}{2}(7 + \alpha_d) + (1 - \alpha_d)\bar{C}_{A_2}^{\text{el}} + 2\alpha_d\bar{C}_A^{\text{el}}} \tag{1.132}$$

²³From the theorem on derivatives $\left(\frac{\partial P}{\partial \rho} \right)_T = \left(\frac{\partial \rho}{\partial P} \right)_T^{-1}$.

while the total isentropic coefficient is given by

$$\gamma_d = z_\gamma \frac{\frac{R}{2}(9 + \alpha_d) + (1 - \alpha_d)C_{A_2}^{\text{el}} + 2\alpha_d\bar{C}_A^{\text{el}} + R\alpha_d(1 - \alpha_d^2)\left(\frac{\Delta\tilde{H}_d^0}{RT}\right)^2}{\frac{R}{2}(7 + \alpha_d) + (1 - \alpha_d)\bar{C}_{A_2}^{\text{el}} + 2\alpha_d\bar{C}_A^{\text{el}} + R\frac{\alpha_d(1 - \alpha_d)}{(2 - \alpha_d)}\left(\frac{\Delta\tilde{U}_d^0}{RT}\right)^2}. \quad (1.133)$$

For the pure molecular gas ($\alpha_d = 0$), or fully dissociated gas ($\alpha_d = 1$) the γ_{df} reduces to

$$\begin{aligned}\gamma_{\text{df}}(\alpha_d = 0) &= \frac{9R + 2\bar{C}_{A_2}^{\text{el}}}{7R + 2\bar{C}_{A_2}^{\text{el}}} \\ \gamma_{\text{df}}(\alpha_d = 1) &= \frac{5R + 2\bar{C}_{A_2}^{\text{el}}}{3R + 2\bar{C}_{A_2}^{\text{el}}}.\end{aligned}$$

Neglecting the internal contribution, the frozen isentropic coefficient becomes

$$\begin{aligned}\gamma_{\text{df}}(\alpha_d = 0) &= \frac{9}{7} = 1.29 \\ \gamma_{\text{df}}(\alpha_d = 1) &= \frac{5}{3} = 1.67.\end{aligned}$$

It should be also noted that the value 1.29 is the result obtained applying the classical equipartition theorem considering the excitation of the vibrational degree of freedom. However, at low temperature, the molecular vibration is not excited and only rotational and translational degrees of freedom should be included giving for the frozen isentropic coefficient

$$\gamma_{\text{df}}(\alpha_d = 0) = \frac{7}{5} = 1.40.$$

These considerations indicate that, in the absence of electronic excitation, the frozen isentropic coefficient in the dissociation regime changes with the temperature following the path $1.40 \rightarrow 1.29 \rightarrow 1.67$, this last value being valid for fully dissociated gas ($\alpha_d = 1$).

1.9.2 Ionization Regime

Let us now discuss the properties of the isentropic coefficient for an atomic plasma with a single ionization reaction. The frozen isentropic coefficient is given by

$$\gamma_{\text{if}} = \frac{5(1 + \alpha_i)R + 2(1 - \alpha_i)\bar{C}_A^{\text{el}} + 2\alpha_i\bar{C}_{A+}^{\text{el}}}{3(1 + \alpha_i)R + 2(1 - \alpha_i)\bar{C}_A^{\text{el}} + 2\alpha_i\bar{C}_{A+}^{\text{el}}}. \quad (1.134)$$

Neglecting the contribution of internal states leads to

$$\gamma_{\text{if}} = \frac{5(1 + \alpha_i)R}{3(1 + \alpha_i)R} = \frac{5}{3} \quad (1.135)$$

i.e. value for inert monoatomic gases with only translational degrees of freedom. However, this approximation can fail at high temperature, when electronic excitation is more important than the translational one. In this case, neglecting also the excitation of ions (see (1.105)), (1.134) can be written as

$$\gamma_{\text{if}} = \frac{\cancel{5(1+\alpha_i)R} + 2(1 - \alpha_i)\bar{C}_A^{\text{el}} + \cancel{2\alpha_i\bar{C}_{A+}^{\text{el}}}}{\cancel{3(1+\alpha_i)R} + 2(1 - \alpha_i)\bar{C}_A^{\text{el}} + \cancel{2\alpha_i\bar{C}_{A+}^{\text{el}}}} \approx 1. \quad (1.136)$$

This value is a lower theoretical limit, which can be approached only under particular conditions, depending also on the system under consideration.

The total isentropic coefficient is given by

$$\gamma_i = z_\gamma \frac{5(1 + \alpha_i)R + 2(1 - \alpha_i)\bar{C}_A^{\text{el}} + 2\alpha_i\bar{C}_{A+}^{\text{el}} + R\alpha_i(1 - \alpha_i^2) \left(\frac{\Delta\bar{H}_i^0}{RT}\right)^2}{3(1 + \alpha_i)R + 2(1 - \alpha_i)\bar{C}_A^{\text{el}} + 2R\alpha_i\bar{C}_{A+}^{\text{el}} + 2R\frac{\alpha_i(1-\alpha_i)}{(2-\alpha_i)} \left(\frac{\Delta\bar{U}_i^0}{RT}\right)^2}. \quad (1.137)$$

Let us consider the extreme case of pure atomic ($\alpha_i = 0, z_\gamma = 1$) system

$$\gamma_i = z_\gamma \frac{5R + 2\bar{C}_A^{\text{el}}}{3R + 2\bar{C}_A^{\text{el}}} = \frac{5R + 2\bar{C}_A^{\text{el}}}{3R + 2\bar{C}_A^{\text{el}}} \quad (1.138)$$

and of fully ionized ($\alpha_i = 1, z_\gamma = 1$) system

$$\gamma_i = z_\gamma \frac{5R + 2\bar{C}_{A+}^{\text{el}}}{3R + 2\bar{C}_{A+}^{\text{el}}} = \frac{5R + 2\bar{C}_{A+}^{\text{el}}}{3R + 2\bar{C}_{A+}^{\text{el}}}. \quad (1.139)$$

Note (1.138) and (1.139) show the same dependence of the γ ratio on the electronic excitation of atoms and ions.

If we neglect the electronic excitation, we obtain

$$\gamma_i = z_\gamma \frac{5(1 + \alpha_i)R + R\alpha_i(1 - \alpha_i^2) \left(\frac{5}{2} + \frac{I}{RT}\right)^2}{3(1 + \alpha_i)R + 2\frac{R\alpha_i(1-\alpha_i)}{(2-\alpha_i)} \left(\frac{3}{2} + \frac{I}{RT}\right)^2}. \quad (1.140)$$

It should be noted that the coefficient R is a common factor and can be simplified, and, expressing the ionization energy in temperature unit as $\theta = \frac{I}{R}$, we have

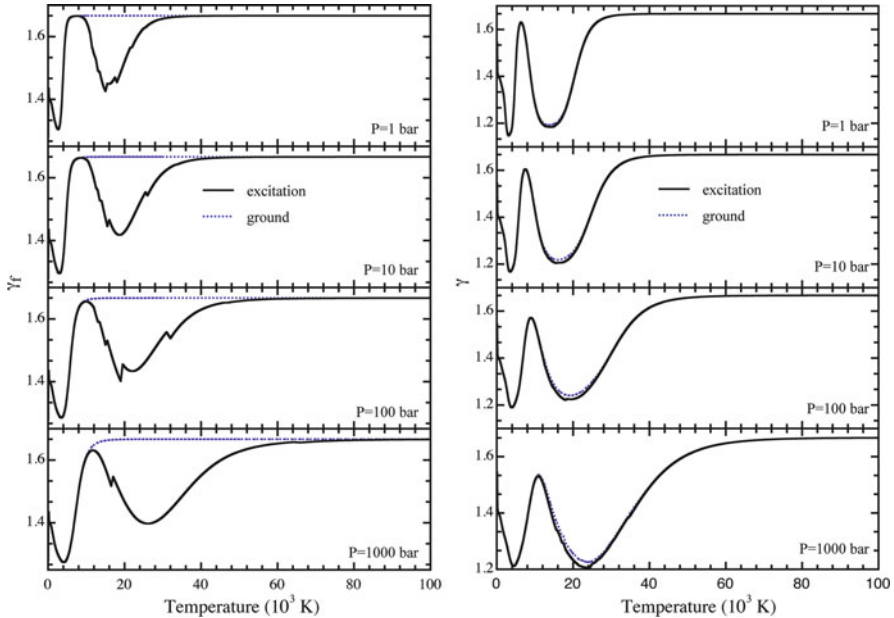


Fig. 1.7 γ_f (left) and $\gamma = \gamma_{\text{eq}} z_\gamma$ (right) for a multicomponent H_2 plasma, calculated considering (excitation) or neglecting (ground) electronic excitation

$$\gamma_i = z_\gamma \frac{5(1 + \alpha_i) + \alpha_i(1 - \alpha_i^2) \left(\frac{5}{2} + \frac{\theta}{T}\right)^2}{3(1 + \alpha_i) + 2\frac{\alpha_i(1 - \alpha_i)}{(2 - \alpha_i)} \left(\frac{3}{2} + \frac{\theta}{T}\right)^2} \quad (1.141)$$

an expression widely used in the literature (Burm et al. 1999; Burm 2005; Pierce 1968).

1.9.3 Hydrogen Plasma

As an example we consider the hydrogen plasma, formed by H_2 , H , H^+ and e^- , with dissociation and ionization processes. Figure 1.7 (left) reports the frozen isentropic coefficient for an hydrogen plasma as a function of temperature for different pressures, calculated considering (excitation) and neglecting (ground) the electronic excitation (important in this case only for atomic hydrogen) while Fig. 1.7 (right) reports the corresponding total isentropic coefficient. Inspection of the calculated frozen isentropic coefficients in the presence (excitation) and absence (ground) of electronic states confirms our simplified arguments. In particular, the approximate sequence $1.4 \rightarrow 1.29 \rightarrow 1.67$ appears in the frozen isentropic coefficient in the absence of electronic excitation. In these conditions, $\gamma_f = 1.67$ persists in the ionization regime. On the other hand, a deep minimum in the region of

partially ionized regime due to the excitation of electronic states of atomic hydrogen appears in γ_f . It should be also noted that at high pressure sudden variations of frozen isentropic coefficient in the partial ionization regime are due to the cutoff of electronic partition function (see Chap. 8). Note that the excitation of the electronic degree of freedom in the frozen isentropic coefficient assumes the role of a chemical reaction.

The behavior of the total isentropic coefficient, i.e. including the reactive contributions to the total specific heats, follows the trend of frozen isentropic coefficient in the presence of electronic excitation i.e. the electronic excitation behaves, as already pointed out, like a chemical reaction even though hidden by the ionization reaction in the total isentropic coefficient. As a consequence, the total isentropic coefficient calculated with and without electronic excitation presents a very similar trend, non-negligible differences appearing at high pressure.

Frozen and total isentropic coefficients coincide at low temperature when the dissociation and ionization degrees are zero. A deeper minimum in the frozen isentropic coefficient can be observed in other atomic plasmas such as oxygen, nitrogen and air (see Chap. 8).

1.10 Real Gas Thermodynamics

The ideal gas is only an approximate picture, considering atoms and molecules as dimensionless hard spheres. Obviously, this is not valid for a plasma or for high density systems, where particle interactions and size become effective. The equation of state of an ideal gas in (1.60) must be corrected to include non-real effects. Different equations of state have been introduced to describe real gases and the most famous is the Van der Waals equation

$$\left(P + a \frac{n^2}{V^2} \right) (V - nb) = nRT, \quad (1.142)$$

where a and b are coefficients depending on the given system²⁴.

A more general equation of state is obtained by the virial expansion (Hirschfelder et al. 1966) of $\frac{PV}{nRT}$ as

$$\frac{PV}{nRT} = 1 + B(T) \frac{n}{V} + C(T) \left(\frac{n}{V} \right)^2 + D(T) \left(\frac{n}{V} \right)^3 + \dots, \quad (1.143)$$

where B , C , D , etc. are known as virial coefficients. It should be noted that the Van der Waals equation can be derived from (1.143) expanding the parenthesis in (1.142)

$$\frac{PV}{nRT} = 1 - \frac{a}{RT} \frac{n}{V} + \frac{ab}{RT} \left(\frac{n}{V} \right)^2 + b \frac{P}{RT}. \quad (1.144)$$

²⁴The coefficients can be related to interaction potential between the particle in the mixture as will be discussed in the Chap. 7.

This equation is not closed because the last term contains the pressure. Therefore, we can substitute P with the whole expression in the same equation obtaining

$$\frac{PV}{nRT} = 1 - \frac{a}{RTV} n + \frac{ab}{RT} \left(\frac{n}{V} \right)^2 + b \frac{PV}{nRTV} n = 1 - \frac{a}{RTV} n + \frac{ab}{RT} \left(\frac{n}{V} \right)^2 + b \frac{PV}{nRTV} n \\ + b \frac{n}{V} \left[1 - \frac{a}{RTV} n + \frac{ab}{RT} \left(\frac{n}{V} \right)^2 + b \frac{PV}{nRTV} n \right]. \quad (1.145)$$

This procedure can be prosecuted to obtain the infinite series²⁵

$$\frac{PV}{nRT} = 1 - \frac{a}{RTV} n + b \frac{n}{V} + b^2 \left(\frac{n}{V} \right)^2 + b^3 \left(\frac{n}{V} \right)^3 + \dots \quad (1.146)$$

Comparing the coefficients in (1.143), (1.146), we have²⁶

$$B(T) = b - \frac{a}{RT} \\ C(T) = b^2 \\ D(T) = b^3 \\ \dots \quad (1.147)$$

and derivatives

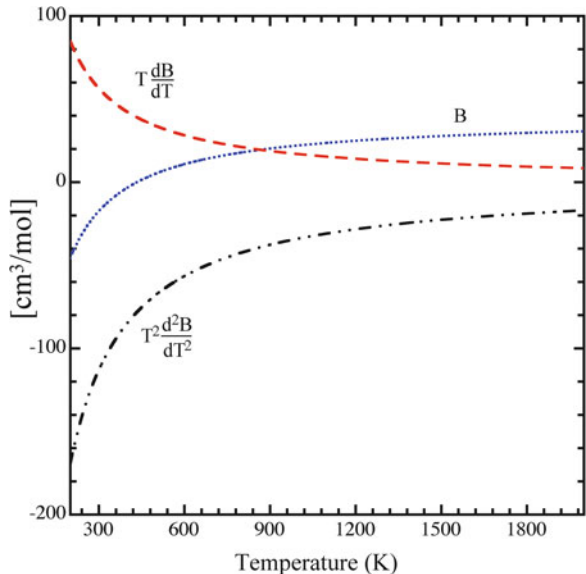
$$T \frac{dB(T)}{dT} = \frac{a}{RT} \\ T^2 \frac{d^2B(T)}{dT^2} = -2 \frac{a}{RT} \\ \frac{dC(T)}{dT} = \frac{d^2C(T)}{dT^2} = 0 \\ \dots \quad (1.148)$$

(see Fig. 1.8). Virial coefficients and the corresponding derivatives calculated by (1.147), (1.148) have been reported in Fig. 1.8 for $N_2 - N_2$ interaction. The second

²⁵It should be noted that the $\sum_{n=0}^{\infty} b^n = (1 - b)^{-1}$.

²⁶The parameter b is called co-volume and should be the minimum volume that can be occupied by one mole of molecules. Such coefficient is independent of the temperature. On the other hand, a is related to the attractive force and it depends on the temperature, with the asymptotic relation $\lim_{T \rightarrow \infty} a = 0$. From (1.147), we can say that the Van der Waals equation neglect the contribution of the attractive forces to higher order virial coefficients.

Fig. 1.8 Second virial coefficient and first and second derivatives from Van der Waals equation (see (1.147), $a = 1.37 \times 10^6$ bar cm⁶/mol² and $b = 39.1 \times 10^{-5}$ cm³/mol from (Pauling 1988))



virial coefficient presents a trend typical of neutral–neutral interaction showing a passage from negative (prevalence of attractive forces) to positive values (prevalence of repulsive forces).

1.10.1 Virial Corrections to Thermodynamic Functions

From (1.143) we can determine the virial correction to the pressure of a gas in the volume V as

$$\Delta P^{\text{vir}} = \frac{nRT}{V} \left(\frac{B}{\bar{V}} + \frac{C}{\bar{V}^2} + \frac{D}{\bar{V}^3} + \dots \right), \quad (1.149)$$

where $\bar{V} = \frac{V}{n}$. To calculate the corrections due to virial expansion to the thermodynamic functions, we should start from the general definition of equation of state (Landau and Lifshitz 1986)

$$P = - \left(\frac{\partial A}{\partial V} \right)_{T, n_i}. \quad (1.150)$$

Let us integrate (1.143) over $\bar{V} = \frac{V}{n}$ after writing P as a function of the other quantities, obtaining

$$A = - \int P dV = -nRT \int \left(\frac{1}{\bar{V}} + \frac{B}{\bar{V}^2} + \frac{C}{\bar{V}^3} + \frac{D}{\bar{V}^4} + \dots \right) d\bar{V}. \quad (1.151)$$

The first term in the integral is the ideal gas Helmholtz free energy. From this equation, we can deduce that the virial correction to any thermodynamic function F is an additive term i.e.

$$F = F^{\text{ideal}} + \Delta F^{\text{vir}}. \quad (1.152)$$

Combining (1.151), (1.152), we have

$$\Delta A^{\text{vir}} = nRT \left(\frac{B}{\bar{V}} + \frac{C}{2\bar{V}^2} + \frac{D}{3\bar{V}^3} + \dots \right). \quad (1.153)$$

From the ΔA^{vir} we can calculate the corrections to all the other thermodynamic functions as the Gibbs free energy, taking PV from (1.143),

$$\Delta G^{\text{vir}} = \Delta A^{\text{vir}} + V\Delta P^{\text{vir}} = nRT \left(\frac{2B}{\bar{V}} + \frac{3C}{2\bar{V}^2} + \frac{4D}{3\bar{V}^3} + \dots \right) \quad (1.154)$$

the entropy²⁷

$$\begin{aligned} \Delta S^{\text{vir}} = - \left(\frac{\partial \Delta A^{\text{vir}}}{\partial T} \right)_V &= -nRT \left[\left(\frac{B}{T} + \dot{B} \right) \frac{1}{\bar{V}} + \left(\frac{C}{T} + \dot{C} \right) \frac{1}{2\bar{V}^2} \right. \\ &\quad \left. + \left(\frac{D}{T} + \dot{D} \right) \frac{1}{3\bar{V}^3} + \dots \right] \end{aligned} \quad (1.155)$$

the internal energy

$$\Delta U^{\text{vir}} = \Delta A^{\text{vir}} + T\Delta S^{\text{vir}} = -nRT^2 \left(\frac{\dot{B}}{\bar{V}} + \frac{\dot{C}}{2\bar{V}^2} + \frac{\dot{D}}{3\bar{V}^3} + \dots \right) \quad (1.156)$$

and the enthalpy

$$\begin{aligned} \Delta H^{\text{vir}} = \Delta U^{\text{vir}} + V\Delta P^{\text{vir}} &= nRT^2 \left[\left(\frac{B}{T} - \dot{B} \right) \frac{1}{\bar{V}} + \left(\frac{2C}{T} - \dot{C} \right) \frac{1}{2\bar{V}^2} \right. \\ &\quad \left. + \left(\frac{3D}{T} - \dot{D} \right) \frac{1}{3\bar{V}^3} + \dots \right]. \end{aligned} \quad (1.157)$$

²⁷In this section, we consider $\dot{X} = \left(\frac{\partial X}{\partial T} \right)_{n_i}$.

1.10.2 Virial Corrections to Heat Capacity

Calculating the derivative at constant composition with respect to temperature of ΔU^{vir} , we have the correction to the frozen heat capacity at constant volume

$$\begin{aligned} \Delta C_{\text{vf}}^{\text{vir}} = \left(\frac{\partial \Delta U^{\text{vir}}}{\partial T} \right)_{V,n_i} &= -nRT^2 \left[\left(\frac{2\dot{B}}{T} + \ddot{B} \right) \frac{1}{\bar{V}} + \left(\frac{2\dot{C}}{T} + \ddot{C} \right) \frac{1}{2\bar{V}^2} \right. \\ &\quad \left. + \left(\frac{2\dot{D}}{T} + \ddot{D} \right) \frac{1}{3\bar{V}^3} + \dots \right]. \end{aligned} \quad (1.158)$$

The calculation of correction to frozen heat capacity at constant pressure is more complex because in (1.157), we have an explicit dependence on \bar{V} and not on P . Considering the properties of partial derivatives of composite functions²⁸, the correction to specific heat is given by

$$\Delta C_{\text{pf}}^{\text{vir}} = \left(\frac{\partial \Delta H^{\text{vir}}}{\partial T} \right)_{P,n_i} = \left(\frac{\partial \Delta H^{\text{vir}}}{\partial T} \right)_{\bar{V},n_i} + \left(\frac{\partial \Delta H^{\text{vir}}}{\partial \bar{V}} \right)_{T,n_i} \left(\frac{\partial \bar{V}}{\partial T} \right)_{P,n_i} \quad (1.159)$$

therefore

$$\begin{aligned} \left(\frac{\partial \Delta H^{\text{vir}}}{\partial T} \right)_{\bar{V},n_i} &= nRT^2 \left[\left(\frac{B}{T^2} - \frac{\dot{B}}{T} - \ddot{B} \right) \frac{1}{\bar{V}} + \left(\frac{2C}{T^2} - \ddot{C} \right) \times \right. \\ &\quad \left. \times \frac{1}{2\bar{V}^2} + \left(\frac{3D}{T^2} + \frac{\dot{D}}{T} - \ddot{D} \right) \frac{1}{3\bar{V}^3} + \dots \right] \end{aligned} \quad (1.160)$$

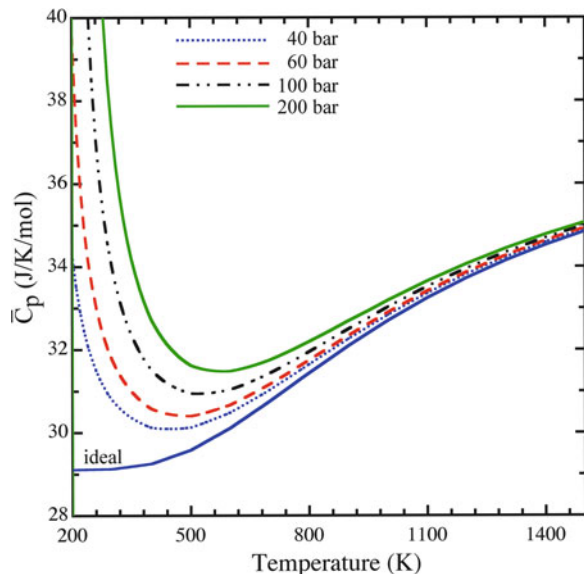
$$\begin{aligned} \left(\frac{\partial \Delta H^{\text{vir}}}{\partial \bar{V}} \right)_{T,n_i} &= -\frac{nRT^2}{\bar{V}} \left[\left(\frac{B}{T} - \dot{B} \right) \frac{1}{\bar{V}} + \left(\frac{2C}{T} - \dot{C} \right) \frac{1}{\bar{V}^2} + \right. \\ &\quad \left. + \left(\frac{3D}{T} - \dot{D} \right) \frac{1}{\bar{V}^3} + \dots \right] \end{aligned} \quad (1.161)$$

To calculate the derivative of the molar volume (\bar{V}) with respect to temperature we should consider (1.143) dividing both terms by \bar{V}

$$\frac{P}{RT} = \frac{1}{\bar{V}} + \frac{B}{\bar{V}^2} + \frac{C}{\bar{V}^3} + \frac{D}{\bar{V}^4} + \dots = f(T, \bar{V}). \quad (1.162)$$

²⁸For a general function $F[x, y(x)]$, the derivative $\frac{dF}{dx} = \left(\frac{\partial F}{\partial x} \right)_y + \left(\frac{\partial F}{\partial y} \right)_x \frac{dy}{dx}$.

Fig. 1.9 A comparison of the constant pressure specific heat in N_2 calculated using second and third virial coefficients from Van der Waals equation with *ideal* gas calculation (see Sect. 5.3)



Then the temperature derivative at constant pressure is given by

$$-\frac{P}{RT^2} = \left(\frac{\partial f}{\partial T} \right)_{\bar{V}, n_i} + \left(\frac{\partial f}{\partial \bar{V}} \right)_{T, n_i} \left(\frac{\partial \bar{V}}{\partial T} \right)_{P, n_i} \quad (1.163)$$

Now we can isolate the derivative of the volume and, substituting $P/RT = f$, we have

$$\left(\frac{\partial \bar{V}}{\partial T} \right)_{P, n_i} = -\frac{f + T \left(\frac{\partial f}{\partial T} \right)_{\bar{V}, n_i}}{T \left(\frac{\partial f}{\partial \bar{V}} \right)_{T, n_i}} = -\frac{\left(\frac{\partial P}{\partial T} \right)_{\bar{V}, n_i}}{\left(\frac{\partial P}{\partial \bar{V}} \right)_{T, n_i}}, \quad (1.164)$$

where

$$\left(\frac{\partial P}{\partial T} \right)_{\bar{V}, n_i} = nR \left[\frac{(B + T \dot{B})}{\bar{V}^2} + \frac{(C + T \dot{C})}{\bar{V}^3} + \frac{(D + T \dot{D})}{\bar{V}^4} + \dots \right] \quad (1.165)$$

$$\left(\frac{\partial P}{\partial \bar{V}} \right)_{T, n_i} = -\frac{nRT}{\bar{V}} \left[\frac{1}{\bar{V}} + \frac{2B}{\bar{V}^2} + \frac{3C}{\bar{V}^3} + \frac{4D}{\bar{V}^4} + \dots \right]. \quad (1.166)$$

Virial corrections are usually important at high pressure and low temperature regimes. This point can be appreciated (Fig. 1.9) by comparing the molar specific

heat of pure nitrogen calculated in the ideal approximation (see also Fig. 5.5) and the corresponding one obtained by (1.159) inserting in it the virial coefficient reported in Fig. 1.8. These data are in good agreement with more involved calculation reported in (Tournier and El-Genk 2008), thus indicating that Van der Waals approach can be used for a rapid estimation of the virial coefficients.

Chapter 2

Two and Three Level Systems: Toward the Understanding of the Thermodynamics of Multilevel Systems

In this chapter, we will introduce few level systems to analyze the contribution of excited states on thermodynamic properties of atomic species, using elementary concepts of statistical thermodynamics. The present formulation will be applied to enthalpy and energy, as well as to the specific heats.

Describing the properties of two- or three-level systems gives a general overview of the contribution of atomic internal states on the thermodynamic functions (Colonna and Capitelli 2009; D’Ammando et al. 2010; Maczek 1998). Nevertheless, the few-level approach goes over the simple qualitative description of the internal contribution, because level lumping in two or three groups approximates with a good accuracy the contribution of the whole ladder of electronic states for many systems.

2.1 Two-Level Systems

Let us model an atom as a two-level system, the ground state and one excited level having, respectively, degeneracies g_1 and g_2 and molar energies of $\varepsilon_1 = 0$ and $\varepsilon_2 > 0$. Denoting with n_1 , n_2 and n , respectively, the ground state, excited level and total number of moles, we can write the following balance equation

$$n_1 + n_2 = n. \quad (2.1)$$

The population n_1 and n_2 are linked by the Boltzmann distribution

$$\frac{n_2}{n_1} = \frac{g_2}{g_1} e^{-\frac{\theta_2}{T}} \quad (2.2)$$

$$\theta_2 = \frac{\varepsilon_2}{k}. \quad (2.3)$$

Solving the system of equations for n_1 and n_2 , we get the moles of atom in each state as

$$\begin{aligned} n_1 &= n \frac{g_1}{g_1 + g_2 e^{-\frac{\theta_2}{T}}} \\ n_2 &= n \frac{g_2 e^{-\frac{\theta_2}{RT}}}{g_1 + g_2 e^{-\frac{\theta_2}{T}}}. \end{aligned} \quad (2.4)$$

The denominator of the above expressions

$$\mathcal{Q} = g_1 + g_2 e^{-\frac{\theta_2}{T}} \quad (2.5)$$

is the partition function of the two-level system.

The populations in the low and high temperature limits are given by

$$\begin{aligned} T \ll \theta_2 \Rightarrow n_1 &= n & n_2 &= 0 \\ T \gg \theta_2 \Rightarrow n_1 &= n \frac{g_1}{g_1 + g_2} & n_2 &= n \frac{g_2}{g_1 + g_2} \end{aligned} \quad (2.6)$$

i.e., at low temperature, only the ground state is populated while at high temperature both levels are populated proportionally to the respective statistical weight.

The molar internal energy is given by

$$\bar{U}^{\text{int}} = \frac{R}{n} (\theta_1 n_1 + \theta_2 n_2) = R\theta_2 \frac{n_2}{n} = R\theta_2 \frac{g_2 e^{-\frac{\theta_2}{T}}}{g_1 + g_2 e^{-\frac{\theta_2}{T}}}, \quad (2.7)$$

where $\theta_1 = \varepsilon_1/k = 0$. The corresponding limiting values are

$$\begin{aligned} T \ll \theta_2 \Rightarrow \bar{U}^{\text{int}} &= 0 \\ T \gg \theta_2 \Rightarrow \bar{U}^{\text{int}} &= R\theta_2 \frac{g_2}{g_1 + g_2}. \end{aligned} \quad (2.8)$$

As a general behavior, we have $g_2 \gg g_1$ and $\theta_2 \approx I/k$, I being the ionization potential. As a consequence, at high temperature we have $\bar{U}^{\text{int}} \approx N_a I$. Finally, the internal specific heat \bar{C}^{int} is given by

$$\bar{C}^{\text{int}} = \frac{d\bar{U}^{\text{int}}}{dT} = \frac{R\theta_2}{n} \frac{dn_2}{dT} = R \left(\frac{\theta_2}{T} \right)^2 \frac{g_1 g_2 e^{-\frac{\theta_2}{T}}}{\left(g_1 + g_2 e^{-\frac{\theta_2}{T}} \right)^2}, \quad (2.9)$$

which goes to zero in both high temperature and low temperature limits.

Table 2.1 Degeneracy (g^*) and characteristic temperature (θ^*) for atomic hydrogen considered as a two-level system, for different values of the maximum principal quantum number included in the upper lumped level

	g^*	$\theta^* [\text{K}]$
$n = 1$	2	0
n_{\max}		
5	108	146,187
10	768	154,181
25	11,048	157,196
50	85,848	157,701
75	286,898	157,800
100	676,698	157,835

As case study, let us consider atomic hydrogen which levels have energy and multiplicity given by

$$g_{H,n} = 2n^2$$

$$\varepsilon_{H,n} = I_H \left(1 - \frac{1}{n^2}\right), \quad (2.10)$$

where n is the principal quantum number and I_H is the ionization potential of the hydrogen atom. We reduce the multiplicity of electronically excited states of the atomic hydrogen to a two-level system¹:

1. The ground state characterized by energy $\varepsilon_{H,1}^* = 0$, degeneracy $g_{H,1}^* = 2$.
2. One excited level having the degeneracy equal to the sum of degeneracies and the energy equal to the mean energy of all excited states from $n = 2$ up to a fixed n_{\max} .

$$g_{H,2}^* = \sum_{n=2}^{n_{\max}} g_{H,n} \quad (2.11)$$

$$\theta_{H,2}^* = \frac{1}{k g_{H,2}^*} \sum_{n=2}^{n_{\max}} g_{H,n} \varepsilon_{H,n}. \quad (2.12)$$

The energy of the excited state and its characteristic temperature, as well as the statistical weight depend on n_{\max} , as shown in Table 2.1, where total degeneracy and characteristic temperature are reported for some values of n_{\max} .

Inspection of the table shows the strong dependence of the upper level degeneracy on the number of states inserted in the lumped level, while its energy rapidly converges to I_H , spreading around 10,000 K passing from $n_{\max} = 5$ to $n_{\max} = 100$.

¹For the sake of clarity, the symbols of the reduced levels are distinguished by those of the real level by the superscript*.

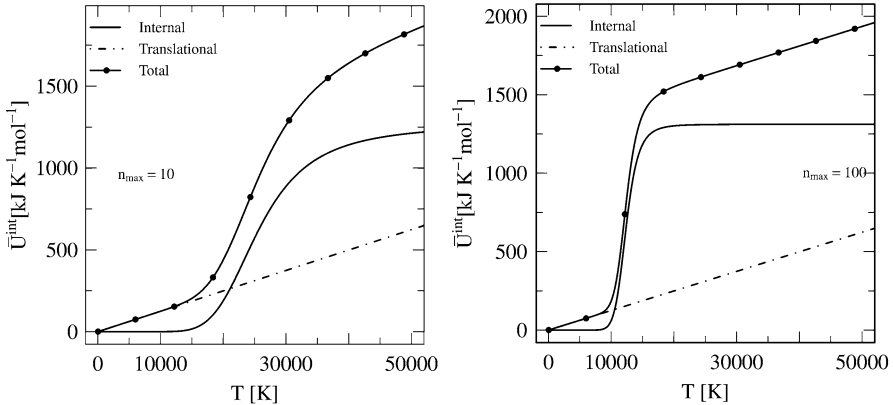


Fig. 2.1 Atomic hydrogen translational, internal and total molar energy as a function of the temperature for (a) $n_{\max} = 10$ and (b) $n_{\max} = 100$

In Fig. 2.1, one can observe the sensitivity of the molar internal energy on n_{\max} . For $n_{\max} = 100$, the internal energy grows rapidly with the temperature, reaching an asymptotic value equal to the ionization potential, while for $n_{\max} = 10$ the growth is much slower, and up to $T = 50,000$ K the asymptotic value of 1,282 kJ/mole has not been reached yet. The upper limit of the internal energy can be obtained from (2.7), considering that, in any case (see Table 2.1), $g_{H,2}^* \gg g_{H,1}^*$ and therefore in the denominator of (2.8) $g_{H,1}^* + g_{H,2}^* \approx g_{H,2}^*$ thus giving $\bar{U}_H^{\text{int}} \approx R\theta_2$. In both cases, the internal energy becomes much higher than the translational one if the temperature is sufficiently high.

Figure 2.2 shows the dimensionless constant volume specific heat for the same cases discussed in Fig. 2.1. The internal specific heat presents a maximum value, which is shifted at lower temperature as n_{\max} increases. It should be also noted that the internal specific heat, negligible at low and high temperatures, overcomes the translational contribution ($\frac{3}{2}$) for intermediate temperatures, as reported in Fig. 2.2.

2.2 Three-Level Systems

Many-electron atoms often possess low lying energy states corresponding to rearrangement of angular and spin momenta of the valence electrons. In this case, the two-level approximation must be improved introducing a new level which describes the low-lying excited states. To this end, we consider a three-level system composed by the ground state and two excited states, characterized by

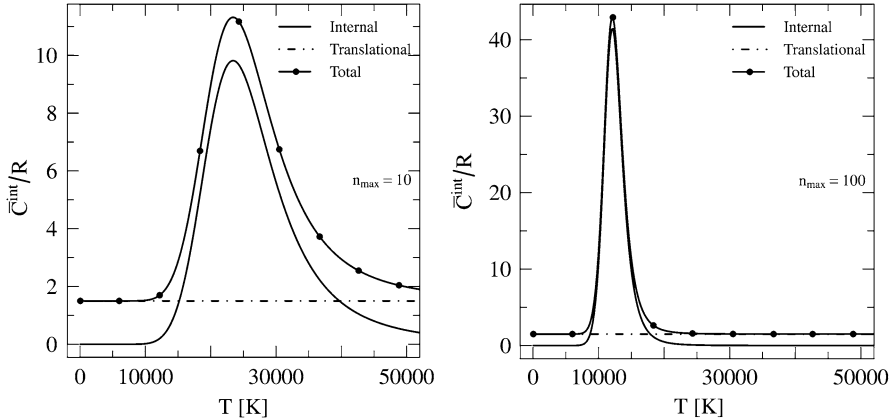


Fig. 2.2 Atomic hydrogen translational, internal and total reduced molar specific heat for (a) $n_{\max} = 10$ and (b) $n_{\max} = 100$

level degeneracies g_1 , g_2 , g_3 and energies $\varepsilon_1 = 0$ and $\varepsilon_1 < \varepsilon_2 \ll \varepsilon_3$. The balance equations read

$$n_1 + n_2 + n_3 = n$$

$$\begin{aligned} \frac{n_2}{n_1} &= \frac{g_2}{g_1} e^{-\frac{\theta_2}{T}} \\ \frac{n_3}{n_1} &= \frac{g_3}{g_1} e^{-\frac{\theta_3}{T}}, \end{aligned} \quad (2.13)$$

where the θ 's are the energies expressed in K as in (2.3). Solution of the above system leads to the following expressions for the molar fractions of levels

$$\begin{aligned} \frac{n_1}{n} &= \frac{g_1}{g_1 + g_2 e^{-\frac{\theta_2}{T}} + g_3 e^{-\frac{\theta_3}{T}}} \\ \frac{n_2}{n} &= \frac{g_2 e^{-\frac{\theta_2}{T}}}{g_1 + g_2 e^{-\frac{\theta_2}{T}} + g_3 e^{-\frac{\theta_3}{T}}} \\ \frac{n_3}{n} &= \frac{g_3 e^{-\frac{\theta_3}{T}}}{g_1 + g_2 e^{-\frac{\theta_2}{T}} + g_3 e^{-\frac{\theta_3}{T}}}. \end{aligned} \quad (2.14)$$

Likewise the two-level case, the denominator of the above expressions is the partition function of our three-level system

$$\mathcal{Q} = g_1 + g_2 e^{-\frac{\theta_2}{T}} + g_3 e^{-\frac{\theta_3}{T}} \quad (2.15)$$

Let us consider a temperature such that $\theta_2 \ll T \ll \theta_3$. In this case, we can drop the contribution of the last level and, being the first exponential very close to one, we have

$$\begin{aligned}\frac{n_1}{n} &\approx \frac{g_1}{g_1 + g_2} \\ \frac{n_2}{n} &\approx \frac{g_2}{g_1 + g_2} \\ \frac{n_3}{n} &\approx \frac{g_3 e^{-\frac{\theta_3}{T}}}{g_1 + g_2} \approx 0\end{aligned}\tag{2.16}$$

reproducing the same situation as a two level system. At very high temperature ($\theta_2 \ll \theta_3 \ll T$), the following asymptotic behavior is obtained

$$\begin{aligned}\frac{n_1}{n} &= \frac{g_1}{g_1 + g_2 + g_3} \\ \frac{n_2}{n} &= \frac{g_2}{g_1 + g_2 + g_3} \\ \frac{n_3}{n} &= \frac{g_3}{g_1 + g_2 + g_3}.\end{aligned}\tag{2.17}$$

The internal energy can be written as

$$\begin{aligned}\bar{U}^{\text{int}} &= \frac{R}{n} (\theta_1 n_1 + \theta_2 n_2 + \theta_3 n_3) \\ &= R \frac{g_2 \theta_2 e^{-\frac{\theta_2}{T}} + g_3 \theta_3 e^{-\frac{\theta_3}{T}}}{g_1 + g_2 e^{-\frac{\theta_2}{T}} + g_3 e^{-\frac{\theta_3}{T}}}\end{aligned}\tag{2.18}$$

and the internal specific heat as²

$$\begin{aligned}\bar{C}^{\text{int}} &= \frac{\ll U^2 \gg - (\bar{U}^{\text{int}})^2}{RT^2} \\ \ll U^2 \gg &= R^2 \frac{g_2 \theta_2^2 e^{-\frac{\theta_2}{T}} + g_3 \theta_3^2 e^{-\frac{\theta_3}{T}}}{g_1 + g_2 e^{-\frac{\theta_2}{T}} + g_3 e^{-\frac{\theta_3}{T}}}.\end{aligned}\tag{2.19}$$

²See Sect. 3.2 for a general definition of $\ll U^2 \gg$.

Table 2.2 Statistical weight and energy of low lying states of nitrogen atom

Configuration	g	ε [eV]
$^2D_{5/2,3/2}$	10	2.3838
$^2P_{3/2,1/2}$	6	3.5757

Table 2.3 Degeneracy and characteristic temperature for atomic nitrogen considered as a three-level system, ground state, low lying level and upper lumped level, in hydrogen-like approximation, for different values of the maximum principal quantum number

	g^*	θ^* [K]
Ground	4	0
Low lying	16	32849
n_{\max}		
5	900	158702
10	6840	165282
25	99360	168125
50	772560	168647
75	2582010	168752
100	6090210	168787

As a case study for the three-level system, let us consider the atomic nitrogen. The ground state configuration is ${}^4S_{3/2}$ having statistical weight $g_{N,1}^* = g_{N,1} = 4$. There are other two low-lying levels resulting from $2s^22p^3$ electronic configuration, one corresponding to ${}^2D_{5/2,3/2}$ and one to ${}^2P_{3/2,1/2}$ whose energy and statistical weight are reported in Table 2.2. These two levels are grouped together to give a single low lying state which statistical weight, given by

$$g_2^* = g({}^2D) + g({}^2P)$$

and characteristic temperature , calculated as

$$\theta^* = \frac{g({}^2D)\varepsilon({}^2D) + g({}^2P)\varepsilon({}^2P)}{k g_2^*}$$

are reported in Table 2.3.

The energy of the other levels are calculated by using an hydrogen-like approximation

$$\varepsilon_n = I_N - \frac{I_H}{n^2} \quad (2.20)$$

(I_N and I_H are, respectively, the ionization potential of nitrogen and hydrogen atoms) and a statistical weight

$$g_n = 2n^2 g_{\text{core}} \quad (2.21)$$

($g_{\text{core}} = 9$ represents the statistical weight of the ground state of the more stable nitrogen core (3P)). They are then grouped to form the third lumped level (see Table 2.3), limited to the maximum number n_{\max} . A more accurate approach to calculate electronically excited state energies consists in extending available (experimental or theoretical) data following the Ritz–Rydberg series (see Appendix A).

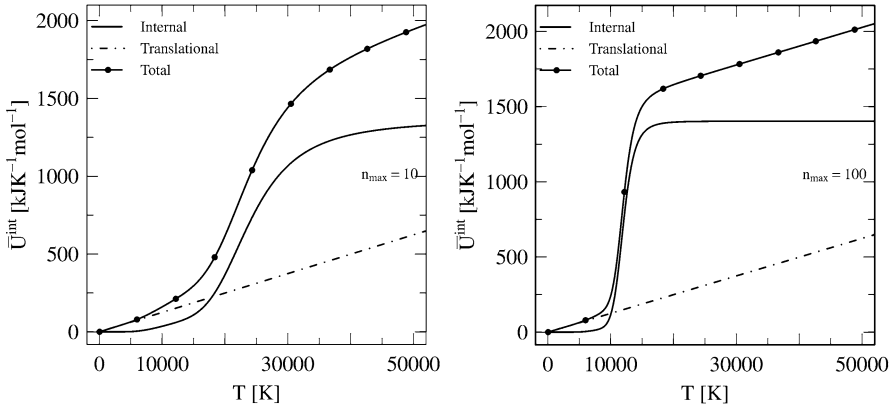


Fig. 2.3 Atomic nitrogen translationaly, internally and total molar energy as a function of the temperature for (a) $n_{\max} = 10$ and (b) $n_{\max} = 100$

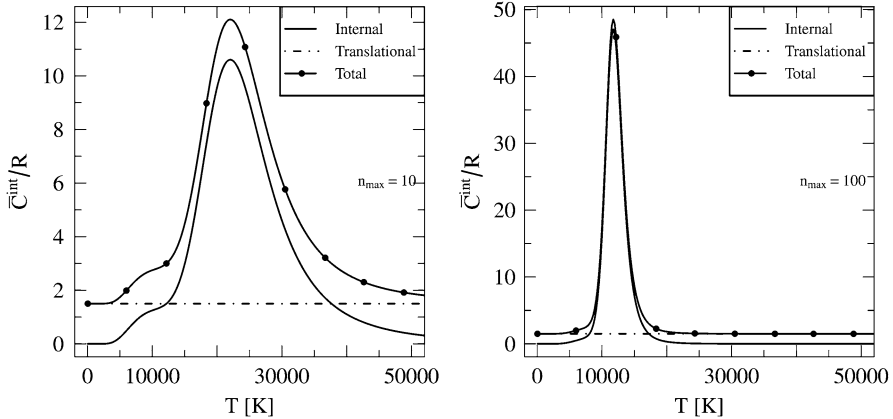
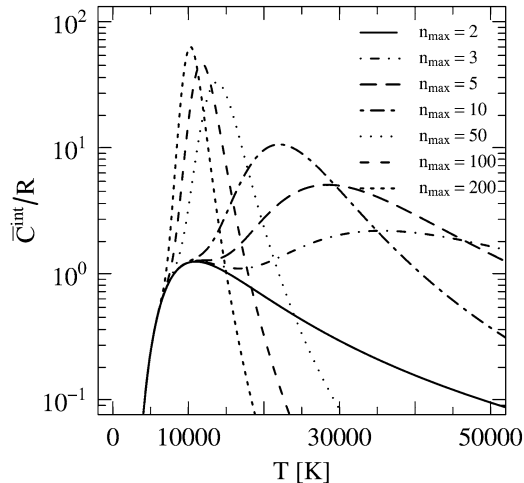


Fig. 2.4 Atomic nitrogen translational, internal and total reduced molar specific heat as a function of the temperature for (a) $n_{\max} = 10$ and (b) $n_{\max} = 100$

In Fig. 2.3, we report the internal energy of atomic nitrogen considered as a three level system. Inspection of this figure shows that, similar to the hydrogen atom case (see Fig. 2.1), the internal energy of the atomic nitrogen strongly increases with the temperature as well as with the number of excited states considered. In both cases, the internal energy is much higher than the translational one. This behavior is reflected on the specific heat (Fig. 2.4) showing similar behavior as the Hydrogen atom. It should be noted, for $n_{\max} = 10$, the presence of a shoulder in the internal contribution around $T = 10000$ K due to the low lying states. However, this effect disappears for $n_{\max} = 100$ hidden by highest lumped level. This point is evident in Fig. 2.5 where we report different \bar{C}^{int} curves corresponding to different n_{\max} values.

Fig. 2.5 Reduced internal specific heat of atomic nitrogen as a function of the temperature for different values of n_{\max} . Note that the case $n_{\max} = 2$ considers only the low-lying state



In particular, the curve labeled with $n_{\max} = 2$ does not consider the third level: in this case, the first maximum is well evident, disappearing as the degeneracy of the lumped level grows up.

The results reported in the different figures refers to atomic systems when the high level energies are lumped allowing their dependence on the principal quantum number.

2.3 Few-Level Model Accuracy

In previous sections, we have observed that a simplified atomic model, considering only two or three representative levels, gives a good qualitative description of the internal contribution to thermodynamic functions of atomic species. In a recent paper (Colonna and Capitelli 2009), it has been demonstrated that the few-level approach has a mathematical foundation, showing under what conditions the results obtained by detailed calculations are reproduced with good accuracy. The demonstration is based on the Taylor series expansion of the exponential function around the mean energy

$$\bar{\varepsilon} = \frac{1}{G} \sum_{n=2}^{n_{\max}} g_n \varepsilon_n$$

$$G = \sum_{n=2}^{n_{\max}} g_n \quad (2.22)$$

of the excited states, i.e.

$$\begin{aligned}
Q^{\text{exact}} &= \sum_{n=1}^{n_{\max}} g_n e^{-\frac{\varepsilon_n}{kT}} = g_1 + e^{-\frac{\bar{\varepsilon}}{kT}} \sum_{n=2}^{n_{\max}} g_n e^{-\frac{\varepsilon_n - \bar{\varepsilon}}{kT}} = \\
&= g_1 + e^{-\frac{\bar{\varepsilon}}{kT}} \sum_{n=2}^{n_{\max}} g_n \left[1 - \left(\frac{\varepsilon_n - \bar{\varepsilon}}{kT} \right) + \frac{1}{2} \left(\frac{\varepsilon_n - \bar{\varepsilon}}{kT} \right)^2 + \dots \right] \\
&= g_1 + Ge^{-\frac{\bar{\varepsilon}}{kT}} + e^{-\frac{\bar{\varepsilon}}{kT}} \sum_{n=2}^{n_{\max}} \frac{g_n}{2} \left(\frac{\varepsilon_n - \bar{\varepsilon}}{kT} \right)^2 + \dots
\end{aligned} \tag{2.23}$$

(2.5), (2.15) are obtained in the first order approximation³ i.e.

$$Q^1 = g_1 + Ge^{-\frac{\bar{\varepsilon}}{kT}}. \tag{2.24}$$

This approximation is obviously better as narrower the distribution of excited states around their mean value. To improve the results, higher order corrections can be used (see (Colonna and Capitelli 2009) for details) without losing the advantages of having coefficients that do not depend on the temperature. For example, the second order approximation is given by

$$Q^2 = g_1 + Ge^{-\frac{\bar{\varepsilon}}{kT}} + e^{-\frac{\bar{\varepsilon}}{kT}} \sum_{n=2}^{n_{\max}} \frac{g_n}{2} \left(\frac{\varepsilon_n - \bar{\varepsilon}}{kT} \right)^2 = Q^1 + \delta Q^*. \tag{2.25}$$

Moreover, it is possible to estimate the error calculating the successive term in expansion series. As an example, the first order approximate error (see Fig. 2.6 for atomic hydrogen) is given by the sum of the square terms in (2.23), i.e. the term δQ^* in (2.25). This value should be compared with the exact errors defined as the relative difference between the state-to-state calculation and the two-level value obtained in the i -th order approximation, i.e. retaining the i terms in the expansion. In our case we have as exact first order error $\delta Q^1 = Q^{\text{exact}} - Q^1$ and exact second order error $\delta Q^2 = Q^{\text{exact}} - Q^2$.

As an example, the hydrogen atom shows a good agreement between the two-level approximation and the exact calculation (see Fig. 2.6). The error is below 2% for the partition function and 3% for the specific heat when just 5 levels are considered, decreasing below 1% for 20 levels. It should be noted that the exact and approximate errors are quite similar and that the second order correction reduces the error below 0.5%.

To apply this model to nitrogen and oxygen atoms, we should consider the three-level approach, due to the presence of low-lying states. The results have been reported in Fig. 2.7 for a cutoff $\Delta I = 500 \text{ cm}^{-1}$, i.e. by considering levels with

³It should be noted that the first order term in (2.23) gives a null contribution.

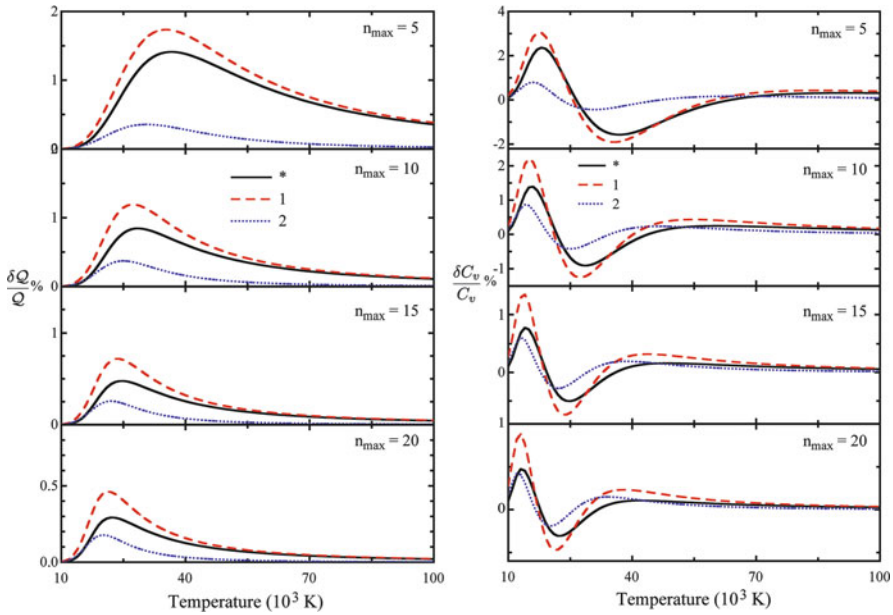


Fig. 2.6 Approximate first-order error (\star) and exact first (1) and second (2) order errors for the hydrogen atom partition function and total constant volume specific heat (internal plus translational) for different number of levels included in the calculation

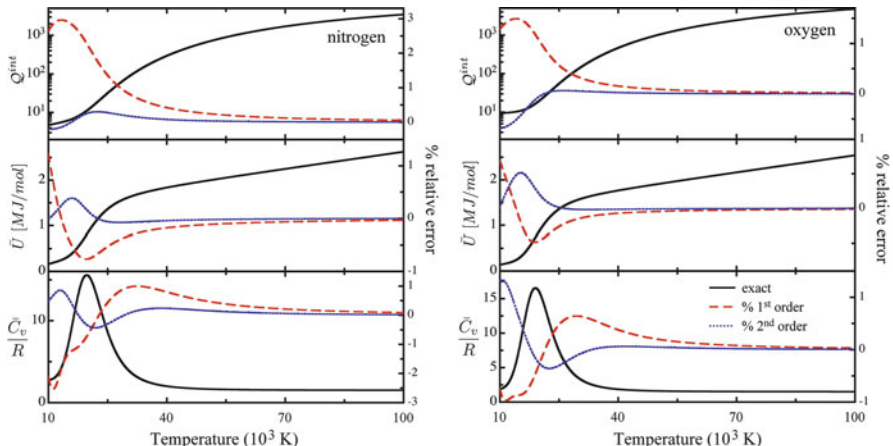


Fig. 2.7 Exact values and relative percentage errors (first and second order) of the partition function, internal energy (translational plus internal) and total constant volume specific heat (translational plus internal) of nitrogen and oxygen atom in the three-level approximation for cutoff $\Delta I = 500 \text{ cm}^{-1}$

energy lower than $I - \Delta I$ in the electronic partition function (see Chap. 8). Also in this case the first-order error is lower than 2% and the second order error is below 0.5% in the whole temperature range.

Chapter 3

Statistical Thermodynamics

In this chapter, the basic equations of statistical thermodynamics will be derived for an ideal gas on the basis of Boltzmann approach (Atkins 1986; Moelwin-Hughes 1947).

The method will be used to derive working equations for describing the thermodynamic properties of ideal gas mixtures. Other approaches, making use of more sophisticated statistical mechanic concepts, will be presented in Chap. 7.

3.1 From Statistical Probability to Thermodynamic Functions

Let us consider a system of \mathcal{N} (identical) particles subdivided by energies as

$$(\mathcal{N}_1, \varepsilon_1), (\mathcal{N}_2, \varepsilon_2), (\mathcal{N}_3, \varepsilon_3), \dots, (\mathcal{N}_i, \varepsilon_i), \dots, \quad (3.1)$$

where \mathcal{N}_i is the number of particles with energy ε_i . The total energy and the total number of particles can be written as

$$\begin{aligned} \mathcal{N} &= \sum_i \mathcal{N}_i \\ U &= \sum_i \mathcal{N}_i \varepsilon_i. \end{aligned} \quad (3.2)$$

Fixing U and \mathcal{N} , the statistical probability W of the existence of a given state is equal to the number of distinguishable ways realizing the given state i.e.

$$W = \mathcal{N}! \quad (3.3)$$

However, since the permutations in the i -th energy class are not distinguishable, the total permutations must be reduced by a factor $\mathcal{N}_i!$ for all the energy groups, and therefore

$$W = \frac{\mathcal{N}!}{\mathcal{N}_1!\mathcal{N}_2!\dots\mathcal{N}_i!\dots} = \frac{\mathcal{N}!}{\prod_i \mathcal{N}_i!}. \quad (3.4)$$

From the statistical point of view, the equilibrium is the state of maximum probability, while from the thermodynamic point of view is the state of the maximum entropy. Boltzmann first linked S and W writing the relation $S = S(W)$. In particular, considering two independent systems a and b , the entropies S_a and S_b , being extensive quantities, fulfill the additive property

$$S_{ab} = S_a + S_b. \quad (3.5)$$

On the other hand, given the probabilities W_a and W_b of the two independent systems, we have

$$W_{ab} = W_a W_b \quad (3.6)$$

and therefore

$$S(W_a W_b) = S(W_a) + S(W_b) \quad (3.7)$$

which is a property of the logarithm, i.e.

$$S(W) = k \ln(W), \quad (3.8)$$

where k is the Boltzmann constant. Taking into account the Stirling formula¹, (3.4), becomes

$$\frac{S}{k} = \ln W = \ln \mathcal{N}! - \sum_i \ln \mathcal{N}_i! = \mathcal{N} \ln \mathcal{N} - \sum_i \mathcal{N}_i \ln \mathcal{N}_i \quad (3.9)$$

We are considering an isolated system with the following constraints

$$\begin{aligned} d\mathcal{N} &= \sum_i d\mathcal{N}_i = 0 \\ dU &= \sum_i \varepsilon_i d\mathcal{N}_i = 0. \end{aligned} \quad (3.10)$$

The equilibrium state is at the maximum of the entropy

$$\frac{dS}{k} = (\ln \mathcal{N} + 1)d\mathcal{N} - \sum_i (\ln \mathcal{N}_i + 1)d\mathcal{N}_i = - \sum_i (\ln \mathcal{N}_i + 1)d\mathcal{N}_i = 0. \quad (3.11)$$

¹ $\ln x! = x \ln x - x = x \ln \frac{x}{e}$.

Using the Lagrange multipliers λ, β we can write (3.10) in the form

$$\begin{aligned}\lambda d\mathcal{N} &= \sum_i \lambda d\mathcal{N}_i = 0 \\ \beta dU &= \sum_i \beta \varepsilon_i d\mathcal{N}_i = 0.\end{aligned}\quad (3.12)$$

Adding these conservation equations in (3.11), we have

$$\begin{aligned}\frac{dS}{k} &= \frac{dS}{k} - \lambda d\mathcal{N} - \beta dU = - \sum_i (\ln \mathcal{N}_i + 1) d\mathcal{N}_i - \sum_i \lambda d\mathcal{N}_i + \\ &\quad - \sum_i \beta \varepsilon_i d\mathcal{N}_i = - \sum_i (\ln \mathcal{N}_i + 1 + \lambda + \beta \varepsilon_i) d\mathcal{N}_i = 0.\end{aligned}\quad (3.13)$$

This equation is valid for any value of $d\mathcal{N}_i$ and therefore we have for any subsystem

$$\ln \mathcal{N}_i + 1 + \lambda + \beta \varepsilon_i = 0 \quad (3.14)$$

which solution is

$$\begin{aligned}\mathcal{N}_i &= \mathcal{K} e^{-\beta \varepsilon_i} \\ \mathcal{K} &= e^{-(\lambda+1)}.\end{aligned}\quad (3.15)$$

Comparing (3.15) with (3.2) we have

$$\mathcal{N} = \sum_i \mathcal{N}_i = \mathcal{K} \sum_i e^{-\beta \varepsilon_i} \Rightarrow \mathcal{K} = \frac{\mathcal{N}}{\sum_i e^{-\beta \varepsilon_i}} \quad (3.16)$$

Calculating the logarithm of (3.15) and substituting the value of \mathcal{K} in (3.16) we have

$$\ln \mathcal{N}_i = \ln \mathcal{N} - \beta \varepsilon_i - \ln \sum_j e^{-\beta \varepsilon_j} \quad (3.17)$$

Multiplying both sides of this equation by \mathcal{N}_i and summing over i we have

$$\begin{aligned}\sum_i \mathcal{N}_i \ln \mathcal{N}_i &= \sum_i \mathcal{N}_i \ln \mathcal{N} - \sum_i \mathcal{N}_i \beta \varepsilon_i - \sum_i \mathcal{N}_i \ln \sum_j e^{-\beta \varepsilon_j} = \\ &= \mathcal{N} \ln \mathcal{N} - \beta U - \mathcal{N} \ln \sum_j e^{-\beta \varepsilon_j}.\end{aligned}\quad (3.18)$$

From the definition of entropy given in (3.9), we have

$$\frac{S}{k} = \mathcal{N} \ln \mathcal{N} - \sum_i \mathcal{N}_i \ln \mathcal{N}_i = \beta U + \mathcal{N} \ln \sum_j e^{-\beta \varepsilon_j} \quad (3.19)$$

Considering the first and second laws of thermodynamics (see Chap. 1) written as $dS = dU/T + PdV/T$, we get the following relation

$$\left(\frac{\partial S}{\partial U}\right)_{V,N} = \frac{1}{T}. \quad (3.20)$$

Comparing with the derivative calculated from (3.19)

$$\left(\frac{\partial S}{\partial U}\right)_{V,N} = k\beta \quad (3.21)$$

we have

$$\beta = \frac{1}{kT}. \quad (3.22)$$

The summation

$$\mathcal{Q} = \sum_i e^{-\beta \varepsilon_i} \quad (3.23)$$

is the partition function and from (3.15), (3.16) we have

$$\frac{\mathcal{N}_i}{\mathcal{N}} = \frac{e^{-\beta \varepsilon_i}}{\mathcal{Q}}. \quad (3.24)$$

The partition function gives a complete description of the thermodynamic state of the system at equilibrium and all the thermodynamic functions can be extracted from it. Let us start considering its first derivative²

$$\begin{aligned} \left(\frac{\partial \mathcal{Q}}{\partial T}\right)_V &= \sum_i \frac{d}{dT} e^{-\varepsilon_i/kT} = \frac{1}{kT^2} \sum_i \varepsilon_i e^{-\varepsilon_i/kT} \\ &= \frac{1}{kT^2} \sum_i \varepsilon_i \frac{\mathcal{N}_i \mathcal{Q}}{\mathcal{N}} = \frac{U \mathcal{Q}}{\mathcal{N} k T^2} \end{aligned} \quad (3.25)$$

dividing both sides by \mathcal{Q} we have³

$$U = \mathcal{N} k T^2 \left(\frac{\partial \ln \mathcal{Q}}{\partial T} \right)_V = \mathcal{N} k T \left(\frac{\partial \ln \mathcal{Q}}{\partial \ln T} \right)_V. \quad (3.26)$$

² The energy of a system is a function of its volume. As a consequence, the temperature derivatives is calculated at constant volume.

³ Remember that $\frac{1}{f} \frac{df}{dx} = \frac{d \ln f}{dx}$ and $x \frac{df}{dx} = \frac{df}{d \ln x}$.

The constant volume heat capacity (see (1.72)) is given by

$$\begin{aligned} C_v &= \left(\frac{\partial U}{\partial T} \right)_V = 2\mathcal{N}kT \left(\frac{\partial \ln \mathcal{Q}}{\partial T} \right)_V + \mathcal{N}kT^2 \left(\frac{\partial^2 \ln \mathcal{Q}}{\partial T^2} \right)_V \\ &= \mathcal{N}k \left[\left(\frac{\partial \ln \mathcal{Q}}{\partial \ln T} \right)_V + \left(\frac{\partial^2 \ln \mathcal{Q}}{\partial \ln T^2} \right)_V \right] \end{aligned} \quad (3.27)$$

For an ideal gas (see Sect. 1.5), the enthalpy is given by

$$H = \mathcal{N}kT \left(\frac{\partial \ln \mathcal{Q}}{\partial \ln T} \right)_V + \mathcal{N}kT = \mathcal{N}kT \left(\frac{\partial \ln(T\mathcal{Q})}{\partial \ln T} \right)_V. \quad (3.28)$$

We can separate the dependence on V and \mathcal{N}/P and T writing the partition function as

$$\mathcal{Q} = f(T)V = f'(T) \frac{\mathcal{N}}{P} \quad (3.29)$$

obtaining

$$\begin{aligned} \left(\frac{\partial \ln \mathcal{Q}}{\partial \ln T} \right)_P &= \frac{d \ln f'}{d \ln T} = \frac{d \ln f}{d \ln T} + \frac{d \ln T}{d \ln T} \\ &= \left(\frac{\partial \ln \mathcal{Q}}{\partial \ln T} \right)_V + 1 = \left(\frac{\partial \ln T \mathcal{Q}}{\partial \ln T} \right)_V \end{aligned} \quad (3.30)$$

as a consequence the enthalpy becomes

$$H = \mathcal{N}kT \left(\frac{\partial \ln(T\mathcal{Q})}{\partial \ln T} \right)_V = \mathcal{N}kT \left(\frac{\partial \ln \mathcal{Q}}{\partial \ln T} \right)_P \quad (3.31)$$

and the constant pressure heat capacity is given by

$$C_p = \left(\frac{\partial H}{\partial T} \right)_P = \mathcal{N}k \left(\frac{\partial \ln \mathcal{Q}}{\partial \ln T} \right)_P + \mathcal{N}k \left(\frac{\partial^2 \ln \mathcal{Q}}{\partial \ln T^2} \right)_P. \quad (3.32)$$

We have to generalize (3.23), (3.24) considering that different molecular states can have the same energy. We have to introduce the *statistical weight* g_i as the number of states with the same energy and therefore for a single molecule, the

equilibrium distribution ($\mathcal{N}_i/\mathcal{N}$), where \mathcal{N}_i are discriminated only by their energy independently of its molecular state, the partition function \mathcal{Q} and the energy become

$$\frac{\mathcal{N}_i}{\mathcal{N}} = \frac{1}{\mathcal{Q}} g_i e^{-\beta \varepsilon_i} \quad (3.33)$$

$$\mathcal{Q} = \sum_i g_i e^{-\beta \varepsilon_i} \quad (3.34)$$

$$U = \frac{\mathcal{N}}{\mathcal{Q}} \sum_i g_i \varepsilon_i e^{-\beta \varepsilon_i} \quad (3.35)$$

Extension of this approach to systems with variable number of particles \mathcal{N} yields to the partition function of the system in the form $\mathcal{Q}^{\mathcal{N}}$ that leads to the Gibbs paradox (Wannier 1966). This paradox can be solved by introducing the partition function of \mathcal{N} indistinguishable molecules in the form

$$\mathcal{Q}_{\mathcal{N}}^* = \frac{\mathcal{Q}^{\mathcal{N}}}{\mathcal{N}!}, \quad (3.36)$$

which is called *system partition function*. \mathcal{Q}^* is linked with the Helmholtz potential through the equation⁴

$$A = -kT \ln \mathcal{Q}_{\mathcal{N}}^* = -\mathcal{N}kT \ln \mathcal{Q} + kT \ln(\mathcal{N}!) = -\mathcal{N}kT \left(\ln \frac{\mathcal{Q}}{\mathcal{N}} + 1 \right). \quad (3.37)$$

The Gibbs function is obtained from (1.9)

$$G = A + PV = -\mathcal{N}kT \ln \left(\ln \frac{\mathcal{Q}}{\mathcal{N}} + 1 \right) + \mathcal{N}kT = -\mathcal{N}kT \ln \frac{\mathcal{Q}}{\mathcal{N}} \quad (3.38)$$

and the entropy from (1.8)

$$S = \frac{U - A}{T} = \mathcal{N}k \left[\ln \frac{\mathcal{Q}}{\mathcal{N}} + 1 + \left(\frac{\partial \ln \mathcal{Q}}{\partial \ln T} \right)_V \right]. \quad (3.39)$$

The entropy depends on the logarithm of partition function as well as on its first logarithmic derivative with respect to temperature.

Before defining the chemical potentials, we want to remember that \mathcal{Q} depends in general not only on the temperature but also on the volume V as will be discussed in Sect. 4.1.2. To get the chemical potential, we can equivalently calculate the derivative of the Helmholtz or Gibbs potentials with respect to \mathcal{N} , respectively, at

⁴ Applying the Stirling formula reported in note 1.

constant volume or at constant pressure. Using (3.29), we can write the chemical potential as

$$\mu = \left(\frac{\partial A}{\partial \mathcal{N}} \right)_{V,T} = kT \left(\ln \frac{\mathcal{Q}}{\mathcal{N}} + 1 \right) - \mathcal{N}kT \frac{\mathcal{N}}{\mathcal{Q}} \left(-\frac{\mathcal{Q}}{\mathcal{N}^2} \right) = -kT \ln \frac{\mathcal{Q}}{\mathcal{N}} \quad (3.40)$$

or using G (see (3.38), (3.29)) as

$$\left(\frac{\partial G}{\partial \mathcal{N}} \right)_{P,T} = \left(-\frac{\partial}{\partial \mathcal{N}} \mathcal{N}kT \ln \frac{\mathcal{Q}}{\mathcal{N}} \right)_{P,T} = -kT \ln \frac{f'(T)}{P} = -kT \ln \frac{\mathcal{Q}}{\mathcal{N}} \quad (3.41)$$

i.e.

$$\mu = \left(\frac{\partial G}{\partial \mathcal{N}} \right)_{P,T} = \left(\frac{\partial A}{\partial \mathcal{N}} \right)_{V,T}, \quad (3.42)$$

which can be obtained also in the framework of the classical thermodynamics presented in Chap. 1.

3.2 Statistical Mean

The thermodynamic functions of a system can be viewed as the statistical mean weighted by the distribution function, defined in general as $\mathcal{N}_i/\mathcal{N}$, that at the equilibrium is given by (3.33). Let us define the statistical thermodynamic mean over the distribution as

$$\ll x \gg = \frac{1}{\mathcal{Q}} \sum_i x_i g_i e^{-\frac{\varepsilon_i}{kT}} \quad (3.43)$$

Comparing with (3.35), we have

$$U = \mathcal{N} \ll \varepsilon \gg. \quad (3.44)$$

Similarly, starting from (3.27), we can express also the specific heat as a function of the statistical thermodynamic mean as

$$\begin{aligned} \frac{C_v}{\mathcal{N}k} &= 2T \left(\frac{\partial \ln \mathcal{Q}}{\partial T} \right)_V + T^2 \left[\frac{1}{\mathcal{Q}} \left(\frac{\partial^2 \mathcal{Q}}{\partial T^2} \right)_V - \left(\frac{1}{\mathcal{Q}} \left(\frac{\partial \mathcal{Q}}{\partial T} \right)_V \right)^2 \right] \\ &= \frac{1}{\mathcal{Q}} \left[2T \left(\frac{\partial \mathcal{Q}}{\partial T} \right)_V + T^2 \left(\frac{\partial^2 \mathcal{Q}}{\partial T^2} \right)_V \right] - \left(\frac{\ll \varepsilon \gg}{kT} \right)^2 \\ &= \frac{1}{\mathcal{Q}} \left[\frac{d}{dT} T^2 \left(\frac{\partial \mathcal{Q}}{\partial T} \right)_V \right] - \left(\frac{\ll \varepsilon \gg}{kT} \right)^2. \end{aligned} \quad (3.45)$$

From (3.25), the first term in the equation is given by

$$\begin{aligned} \left[\frac{d}{dT} T^2 \left(\frac{\partial Q}{\partial T} \right)_V \right]_V &= \frac{1}{k} \frac{d}{dT} \sum_i \varepsilon_i g_i e^{-\varepsilon_i/kT} \\ &= \frac{1}{(kT)^2} \sum_i \varepsilon_i^2 g_i e^{-\varepsilon_i/kT} = Q \frac{\ll \varepsilon^2 \gg}{(kT)^2} \end{aligned} \quad (3.46)$$

therefore we have

$$\frac{C_v}{Nk} = \frac{\ll \varepsilon^2 \gg - \ll \varepsilon \gg^2}{(kT)^2} = \frac{\sigma_\varepsilon^2}{(kT)^2}, \quad (3.47)$$

where σ_ε^2 the variance of the energy. These relations are important to compute the thermodynamic functions starting from energy levels, as discussed in the next chapters, avoiding to evaluate the numerical derivatives of the partition function, but calculating only the summations over the distribution function.

3.3 Multicomponent Ideal Systems

The thermodynamic properties of the N -component ideal gas mixture can be obtained operating on the total partition function of the system defined as

$$Q_{\text{tot}} = \prod_s^N \frac{Q_s^{\mathcal{N}_s}}{\mathcal{N}_s!} \exp \left(-\frac{\mathcal{N}_i \varepsilon_i^f}{kT} \right), \quad (3.48)$$

where Q_s and \mathcal{N}_s are the particle partition function and the number of particles of the s -th species. The quantity ε_s^f is the difference of energy of the s -th species and the common energy reference⁵. Applying the general definition in (3.22) and expressions for the case of variable particle number in (3.37), (3.38), the Helmholtz and Gibbs thermodynamic potentials are given by

$$\begin{aligned} A &= -kT \sum_s \mathcal{N}_s \left(\ln \frac{Q_s}{\mathcal{N}_s} + 1 + \frac{\varepsilon_s^f}{kT} \right) = \sum_s (A_s + \mathcal{N}_s \varepsilon_s^f) \\ G &= -kT \sum_s \mathcal{N}_s \left(\ln \frac{Q_s}{\mathcal{N}_s} + \frac{\varepsilon_s^f}{kT} \right) = \sum_s (G_s + \mathcal{N}_s \varepsilon_s^f) \end{aligned} \quad (3.49)$$

⁵ This quantity is related to the molar formation enthalpy in (1.79) by the equation $\bar{H}_s^f = N_a \varepsilon_s^f$ where N_a is the Avogadro number.

and the entropy is

$$\begin{aligned} S &= - \left(\frac{\partial A}{\partial T} \right)_{V, \mathcal{N}_s} = - \left(\frac{\partial G}{\partial T} \right)_{P, \mathcal{N}_s} = \\ &= k \sum_s \mathcal{N}_s \left[\ln \frac{\mathcal{Q}_s}{\mathcal{N}_s} + 1 + \left(\frac{\partial \ln \mathcal{Q}_s}{\partial \ln T} \right)_V \right] = \sum_s S_s \end{aligned} \quad (3.50)$$

showing the additive property that can be extended to all the thermodynamic functions

$$\begin{aligned} H &= \sum_s (H_s + \mathcal{N}_s \varepsilon_s^f) \\ U &= \sum_s (U_s + \mathcal{N}_s \varepsilon_s^f) \end{aligned} \quad (3.51)$$

Chapter 4

Atomic Partition Function

In this chapter, the statistical thermodynamic concepts described in the previous chapter will be applied to atomic species and to their plasma mixtures. Emphasis will be given to the translational and internal contributions to partition function, to their derivatives as well as to thermodynamic properties of single species. The mixture properties are then analyzed after the introduction of a simplified Saha equation for describing the equilibrium composition of an ionized system. Hydrogen is considered as a case study and the problem of the cutoff of the atomic partition function is introduced leaving to Chap. 8 a more detailed description.

4.1 Atomic Structure

Let us start our representation by describing an isolated atom with the appropriate Hamiltonian. The operator \hat{H} is the sum of three contributions

$$\hat{H} = \hat{H}^n + \hat{H}^{\text{tr}} + \hat{H}^{\text{int}} \quad (4.1)$$

describing the nuclear (*n*), the translational (*tr*) and the internal (*int*) degrees of freedom¹. The solution of the stationary Schrödinger equation

$$\hat{H}\Psi = \varepsilon\Psi \quad (4.2)$$

can be obtained by factorizing the wave function in nuclear, translational and internal contributions

$$\Psi = \Psi^n \Psi^{\text{tr}} \Psi^{\text{int}} \quad (4.3)$$

¹This result is the consequence of the independence of the nuclear degrees of freedom, atomic motion and the relative motion of the electrons with respect to the nucleus.

and solving separately an equation for each degree of freedom (Landau and Lifshitz 1981)

$$\begin{aligned}\hat{H}^n \Psi^n &= \varepsilon^n \Psi^n \\ \hat{H}^{\text{tr}} \Psi^{\text{tr}} &= \varepsilon^{\text{tr}} \Psi^{\text{tr}} \\ \hat{H}^{\text{int}} \Psi^{\text{int}} &= \varepsilon^{\text{int}} \Psi^{\text{int}},\end{aligned}\quad (4.4)$$

where the total energy is given as the sum of the eigenvalues

$$\varepsilon = \varepsilon^n + \varepsilon^{\text{tr}} + \varepsilon^{\text{int}}. \quad (4.5)$$

The corresponding partition function can be expressed as the product of three independent terms

$$Q = Q^n Q^{\text{tr}} Q^{\text{int}} \quad (4.6)$$

reflecting the separability property of the Schrödinger equation.

4.1.1 Nuclear Partition Function

The nuclear partition function can be considered equal to the degeneracy of the nuclear ground state ($\varepsilon^n = 0$)

$$Q^n = g_0^n \quad (4.7)$$

since nuclear excitation requires thousand eV. The nuclear partition function does not affect the internal energy of a species, as well as the specific heat, because its logarithmic derivative is zero in the temperature range ($T < 100,000$ K) examined in this book. It can affect those properties that depend on $\ln Q^n$ such as the entropy. We will further examine Q^n in different points of this book, with the particular regard to the interdependence of the nuclear spin and rotational partition function of homo-nuclear diatomic molecules (see Sect. 5.2).

4.1.2 Translational Partition Function

Energy levels corresponding to the translational degree of freedom of a free particle can be obtained by the so-called particle in the box quantum mechanical model. Consider a particle of mass m in a cubic box with length L . The classical Hamiltonian can be written as

$$\hat{H}^{\text{tr}} = -\frac{\hbar}{2m} \left(\frac{\partial^2}{\partial x^2} + \frac{\partial^2}{\partial y^2} + \frac{\partial^2}{\partial z^2} \right) \quad (4.8)$$

being \hbar the Planck constant. Being the box cubic and the three coordinates independent, the translational wave function can be factorized in three separated one-dimensional cases. For the x direction, we have

$$-\frac{\hbar}{2m} \frac{\partial^2}{\partial x^2} \Psi_x^{\text{tr}}(x) = \varepsilon_x^{\text{tr}} \Psi_x^{\text{tr}}(x) \quad (4.9)$$

and the same for y and z directions. The boundary conditions consist in null wave function at the box limits, $\Psi_x^{\text{tr}}(0) = \Psi_x^{\text{tr}}(L) = 0$. The solution of this problem can be found in text books of quantum mechanics (Pauling and Wilson 1985) and is given by

$$\varepsilon_{x,n_x}^{\text{tr}} = \frac{\hbar^2 \pi^2}{2mL^2} n_x^2 \quad (4.10)$$

$$\Psi_x^{\text{tr}}(x) = A_x \sin\left(\frac{n_x \pi x}{L}\right), \quad (4.11)$$

where $n_x \geq 1$ is a quantum number having an integer value.

The partition function along the x coordinate is given by

$$\mathcal{Q}_x^{\text{tr}} = \sum_{n_x=1}^{\infty} \exp\left(-\frac{\varepsilon_{x,n}^{\text{tr}}}{kT}\right) = \sum_{n_x=0}^{\infty} \exp\left(-\frac{\hbar^2 \pi^2}{2mL^2 kT} n_x^2\right) - 1. \quad (4.12)$$

The effect of quantized energy can be appreciated only at very low temperature, very close to the absolute zero. Ideal gas exists at high temperature, when a large number of states are populated. As a consequence, we can approximate the sum with an integral over n_x , neglecting also -1 in (4.12) obtaining²

$$\mathcal{Q}_x^{\text{tr}} \approx \int_0^{\infty} \exp\left(-\frac{\hbar^2 \pi^2}{2mL^2 kT} n_x^2\right) dn_x = \frac{1}{2} \sqrt{\frac{2mL^2 kT}{\pi \hbar^2}} = L \sqrt{\frac{mkT}{2\pi \hbar^2}}. \quad (4.13)$$

Due to the independence between the three coordinates, the translational partition function is the product of the x , y , z contribution that are all equals, giving

$$\begin{aligned} \mathcal{Q}^{\text{tr}} &= \mathcal{Q}_x^{\text{tr}} \mathcal{Q}_y^{\text{tr}} \mathcal{Q}_z^{\text{tr}} = (\mathcal{Q}_x^{\text{tr}})^3 = \left(\frac{mkT}{2\pi \hbar^2}\right)^{\frac{3}{2}} L^3 \\ &= \left(\frac{mkT}{2\pi \hbar^2}\right)^{\frac{3}{2}} V = \left(\frac{mkT}{2\pi \hbar^2}\right)^{\frac{3}{2}} \frac{\mathcal{N}kT}{P}, \end{aligned} \quad (4.14)$$

²This demonstration is based on the calculation of the integral $\mathcal{I} = \int_0^{\infty} \exp(-ax^2) dx$. It is calculated considering that $\mathcal{I} = \frac{1}{2} \sqrt{\int_{-\infty}^{\infty} \exp(-ax^2) dx \exp(-ay^2) dy}$. The integral inside the square root can be calculated in polar coordinates giving $\pi \int_0^{\infty} \exp(-ar^2) 2r dr = \frac{\pi}{a} \int_0^{\infty} \exp(-s) ds = \frac{\pi}{a}$ where $s = ar^2$. Going back to the original integral we have to divide by two the square root of this result obtaining $\mathcal{I} = \frac{1}{2} \sqrt{\frac{\pi}{a}}$.

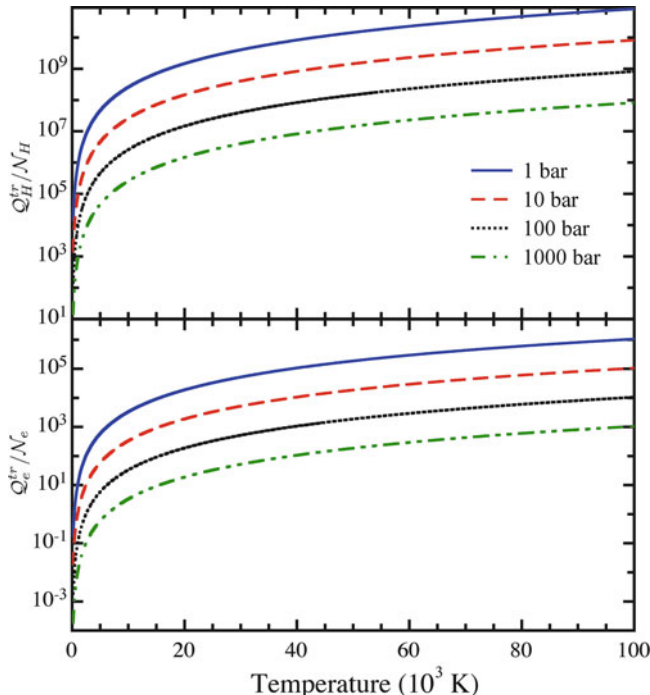


Fig. 4.1 Atomic hydrogen and free electron translational partition function, divided by the number of particles, as a function of temperature for different pressures

where V is the volume of the box. The fraction in the parenthesis is related to the thermal de Broglie length

$$\lambda_{\text{th}} = \sqrt{\frac{2\pi\hbar^2}{mkT}} \quad (4.15)$$

and the translational partition function can be written as

$$\mathcal{Q}^{\text{tr}} = \frac{V}{\lambda_{\text{th}}^3} = \frac{\mathcal{N}kT}{P\lambda_{\text{th}}^3}. \quad (4.16)$$

As an example, the reduced translational partition functions ($\mathcal{Q}^{\text{tr}}/\mathcal{N}$) of atomic hydrogen and free electrons are reported in Fig. 4.1.

For an ideal gas only the translational partition function depends directly on volume (and therefore inversely on pressure). On the other hand, non-ideal corrections introduce indirectly the dependence on volume also of the internal partition function.

4.1.3 Internal Partition Function

The internal partition function of atomic species is obtained as the sum over the quantum states of atoms. We have to consider that different states can have the same energy (degeneracy) that can be grouped together giving a single term, considering the statistical weight $g_{s,l}$ of the l -th level of the s -th species. Therefore, we should apply directly (3.33)–(3.35). We must point out that sum in the partition function is divergent, because the number of levels is infinite while the exponential goes to a finite value. This problem follows from considering an isolated atom in an infinite space. The presence of other particles and the confinement of the atom in a finite volume limits the number of bound states as will be discussed in Chap. 8. Therefore, we will change (3.34) as

$$\mathcal{Q}_s^{\text{int}} = \sum_{i=1}^{N_s^m} g_{s,i} e^{-\frac{\varepsilon_{s,i}}{kT}} \quad (4.17)$$

being N_s^m the maximum number of levels. The level energies are usually referred to the ground state of the species. For a multi-species system, we need a common reference of energy, therefore to the energy levels we should add what is called the *formation energy* ε_s^f and the level energy is written as $\varepsilon'_{s,i} = \varepsilon_{s,i} + \varepsilon_s^f$, where $\varepsilon_{s,1} = 0$. Defining as $\mathcal{Q}_s^{\text{int}}$ and $\mathcal{Q}'_s^{\text{int}}$ the partition function calculated, respectively, using $\varepsilon_{s,i}$ and $\varepsilon'_{s,i}$ we have

$$\mathcal{Q}'_s^{\text{int}} = e^{-\frac{\varepsilon_s^f}{kT}} \sum_{i=1}^{N_s^m} g_{s,i} e^{-\frac{\varepsilon'_{s,i}}{kT}} = e^{-\frac{\varepsilon_s^f}{kT}} \mathcal{Q}_s^{\text{int}} \quad (4.18)$$

4.2 Single Species Thermodynamics

In this section, we describe the contribution of the different degrees of freedom to the single atomic species thermodynamic properties, usually given per unit mole (see Sect. 1.5), considering an Avogadro number \mathcal{N}_a of particles. To obtain the molar quantity, it is sufficient to perform the substitution $\mathcal{N}_a k \rightarrow R$.

4.2.1 Translational Contribution

To determine the translational energy, let us consider (3.26) applied to the translational partition function as reported in (4.14)

$$U_s^{\text{tr}} = \mathcal{N}_s k T \left(\frac{\partial \ln \mathcal{Q}_s^{\text{tr}}}{\partial \ln T} \right)_V \quad (4.19)$$

the derivative is given by

$$\left(\frac{\partial \ln \mathcal{Q}_s^{\text{tr}}}{\partial \ln T} \right)_V = \cancel{\left(\frac{\partial \ln V}{\partial \ln T} \right)}_V + \frac{3}{2} \cancel{\left(\frac{\partial \ln m_s k}{\partial \ln T} \right)}_V + \frac{3}{2} \left(\frac{\partial \ln T}{\partial \ln T} \right)_V - \cancel{\frac{3}{2} \left(\frac{\partial \ln 2\pi\hbar^2}{\partial \ln T} \right)}_V = \frac{3}{2} \quad (4.20)$$

i.e. all the terms are null except that one containing the temperature, giving for the translational energy

$$U_s^{\text{tr}} = \frac{3}{2} \mathcal{N}_s k T = \frac{3}{2} n_s R T \quad (4.21)$$

$$\bar{U}_s^{\text{tr}} = \frac{U_s^{\text{tr}}}{n_s} = \frac{3}{2} R T. \quad (4.22)$$

For the enthalpy, we have

$$H_s^{\text{tr}} = U_s^{\text{tr}} + PV = \frac{5}{2} \mathcal{N}_s k T = \frac{5}{2} n_s R T \quad (4.23)$$

$$\bar{H}_s^{\text{tr}} = \frac{H_s^{\text{tr}}}{n_s} = \frac{5}{2} R T. \quad (4.24)$$

This result was already discussed in Sect. 1.6 reporting the translational contribution to specific heats.

Let us now complete the derivation of the thermodynamic potentials from the statistical mechanics determining the contribution of the atom translation on Helmholtz and Gibbs free energies. Applying the definitions reported in (3.37), (3.38), we have

$$A_s^{\text{tr}} = -\mathcal{N}_s k T \left(\ln \frac{\mathcal{Q}_s^{\text{tr}}}{\mathcal{N}_s} + 1 \right) = -\mathcal{N}_s k T \ln \left[\left(\frac{mkT}{2\pi\hbar^2} \right)^{\frac{3}{2}} \frac{V}{\mathcal{N}_s} \right] - \mathcal{N}_s k T \quad (4.25)$$

$$G_s^{\text{tr}} = -\mathcal{N}_s k T \ln \frac{\mathcal{Q}_s^{\text{tr}}}{\mathcal{N}_s} = -\mathcal{N}_s k T \ln \left[\left(\frac{mkT}{2\pi\hbar^2} \right)^{\frac{3}{2}} \frac{kT}{P_s} \right]. \quad (4.26)$$

The translational entropy is obtained from (3.39), (3.50) considering the derivative reported in (4.20)

$$S_s^{\text{tr}} = \mathcal{N}_s k \left[\ln \frac{\mathcal{Q}_s^{\text{tr}}}{\mathcal{N}_s} + 1 + \left(\frac{\partial \ln \mathcal{Q}_s^{\text{tr}}}{\partial \ln T} \right)_V \right] = -\frac{A_s^{\text{tr}}}{T} + \frac{3}{2} \mathcal{N}_s k. \quad (4.27)$$

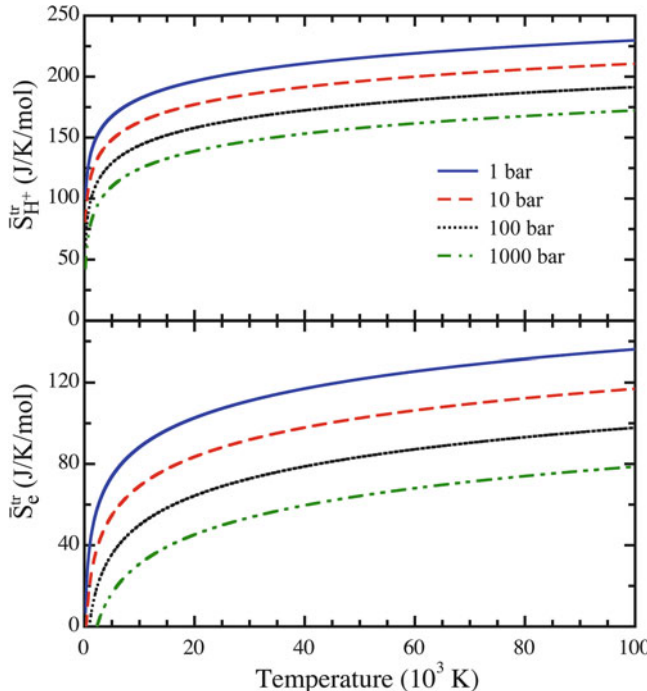


Fig. 4.2 Proton (H^+) and free electron translational molar entropy as a function of temperature for different pressures

A more familiar expression for the molar translational entropy is given by the Sackur–Tetrode equation

$$\bar{S}_s^{\text{tr}} = \frac{3}{2}R \ln M_s + \frac{5}{2}R \ln T - R \ln P_s + C, \quad (4.28)$$

where $C = 86.14857414$ if P_s is expressed in Pa, M_s in g/mole and T in K. As an example, the translational molar entropies of H^+ ($M_{H^+} = 1$ g/mol) and electron ($M_e = 5.485798959 \times 10^{-4}$ g/mol) are reported in Fig. 4.2.

The chemical potential, which expression has been anticipated in (1.29) can be calculated as the derivative with respect to the number of particles of A_s^{tr} or G_s^{tr} as given in (3.42) and explicitly written in (3.40) obtaining

$$\mu_s^{\text{tr}} = -kT \ln \frac{Q_s^{\text{tr}}}{\mathcal{N}} = -kT \ln \left[\left(\frac{mkT}{2\pi\hbar^2} \right)^{\frac{3}{2}} \frac{kT}{P_s} \right] = \mu_s^{0,\text{tr}} + kT \ln P_s, \quad (4.29)$$

where

$$\mu_s^{0,tr}(T) = -kT \ln \left[\left(\frac{mkT}{2\pi\hbar^2} \right)^{\frac{3}{2}} kT \right] \quad (4.30)$$

4.2.2 Internal Contribution

To determine the contribution of internal levels, we will start from (4.17), considering a finite number of levels. The internal contribution to energy is given by

$$U_s^{\text{int}} = \mathcal{N}_s kT \left(\frac{\partial \ln Q_s^{\text{int}}}{\partial \ln T} \right)_v = \frac{\mathcal{N}_s}{Q_s^{\text{int}}} \sum_{i=1}^{N_s^m} \varepsilon_{s,i} g_{s,i} e^{-\frac{\varepsilon_{s,i}}{kT}}, \quad (4.31)$$

where $\varepsilon_{s,i}$ and the Helmholtz free energy is

$$A_s^{\text{int}} = -\mathcal{N}_s kT \ln Q_s^{\text{int}}. \quad (4.32)$$

The internal contribution to enthalpy is the same as the energy ($H_s^{\text{int}} = U_s^{\text{int}}$). The same relation holds between Helmholtz and Gibbs free energies ($G_s^{\text{int}} = A_s^{\text{int}}$). As a consequence, $C_{p,s}^{\text{int}} = C_{v,s}^{\text{int}} = C^{\text{int}}$.

For a mixture, the formation energy must be considered, as already discussed in Sect. 3.3 for the general case. Starting from (4.18) and substituting in (4.31), the internal energy U'^{int} , that includes the formation energy, becomes

$$\begin{aligned} U_s'^{\text{int}} &= \mathcal{N}_s kT \frac{d \ln Q_s'^{\text{int}}}{d \ln T} = \mathcal{N}_s kT \left(\frac{d \ln Q_s^{\text{int}}}{d \ln T} - \frac{d}{d \ln T} \frac{\varepsilon_s^f}{kT} \right) = \\ &= U_s^{\text{int}} + \mathcal{N}_s kT^2 \varepsilon_s^f \frac{1}{kT^2} = U_s^{\text{int}} + \mathcal{N}_s \varepsilon_s^f. \end{aligned} \quad (4.33)$$

The same property hold for the Helmholtz free energy (see (3.49))

$$A_s'^{\text{int}} = -\mathcal{N}_s kT \ln Q_s'^{\text{int}} = \mathcal{N}_s kT \left(\ln Q_s^{\text{int}} - \frac{\varepsilon_s^f}{kT} \right) = A_s^{\text{int}} + \mathcal{N}_s \varepsilon_s^f \quad (4.34)$$

The energy functions U , H , A and G include the contribution of the formation energy simply by adding $\mathcal{N}_s \varepsilon_s^f$.

For the entropy things are different:

$$\begin{aligned} S_s'^{\text{int}} &= \frac{U_s^{\text{int}} - A_s^{\text{int}}}{T} = \frac{U_s^{\text{int}} + \mathcal{N}_s \varepsilon_s^f - A_s^{\text{int}} - \mathcal{N}_s \varepsilon_s^f}{T} \\ &= \frac{U_s^{\text{int}} - A_s^{\text{int}}}{T} = S_s^{\text{int}}. \end{aligned} \quad (4.35)$$

The same property is valid for the heat capacity³. Starting from (3.47)

$$C_s'^{\text{int}} = \frac{dU'^{\text{int}}}{dT} = \frac{dU^{\text{int}}}{dT} + \cancel{\frac{d\mathcal{N}_s \varepsilon_s^f}{dT}} = C_s^{\text{int}} \quad (4.36)$$

The internal entropy and the heat capacity are not affected by the energy reference.

The internal contribution to the chemical potential can be obtained deriving the Helmholtz free energy with respect to the number of particles

$$\mu_s^{\text{int}} = \left(\frac{\partial A_s^{\text{int}}}{\partial \mathcal{N}_s} \right)_{V,T,\mathcal{N}_i \neq s} = -kT \ln Q_s^{\text{int}} \quad (4.37)$$

and considering the formation energy

$$\mu_s'^{\text{int}} = \left(\frac{\partial A_s'^{\text{int}}}{\partial \mathcal{N}_s} \right)_{V,T,\mathcal{N}_i \neq s} = -kT \ln Q_s^{\text{int}} + \varepsilon_s^f = \mu_s^{\text{int}} + \varepsilon_s^f. \quad (4.38)$$

We have analyzed the contribution of the formation energy to all the thermodynamic functions. As for the internal energy, it contributes as an additional term with superscript *f* as

$$\begin{aligned} U_s^f &= H_s^f = A_s^f = G_s^f = \mathcal{N}_s \varepsilon_s^f \\ S_s^f &= 0 \\ \mu_s^f &= \varepsilon_s^f. \end{aligned} \quad (4.39)$$

The internal chemical potential does not depend on the pressure,⁴ therefore we can write for the total chemical potential

$$\mu_s = \mu_s^{\text{tr}} + \mu_s^{\text{int}} + \mu_s^f = \mu_s^{0,tr} + kT \ln P_s + \mu_s^{\text{int}} + \varepsilon_s^f \quad (4.40)$$

³This property is valid only for the single species heat capacity. For a mixture, the formation energy enters in the reactive contribution to the heat capacity (see Chap. 3).

⁴This assumption is valid only for an ideal gas. The level cutoff as well as higher order corrections, as Debye–Hückel, make μ^{int} a function of the pressure and of the plasma composition.

Table 4.1 Some energy states of the hydrogen atoms

n	$\varepsilon_n(cm^{-1})$	$\varepsilon_n(eV)$	$\varepsilon_n(K)$	g_n
1	0	0	0	2
2	82,041	10.20436	118,416	8
3	97,234	12.09406	140,345	18
4	102,552	12.75545	148,020	32
...
∞	109,388	13.605813	157,888	∞

and grouping the terms that depends only on the temperature in μ^0

$$\mu_s^0 = \mu_s^{0,tr} + \mu_s^{\text{int}} + \varepsilon_s^f \quad (4.41)$$

and the total chemical potential is

$$\mu_s(T, P) = \mu_s^0(T) + kT \ln P_s \quad (4.42)$$

as anticipated in (1.29).

The reported equations can be also used for taking into account the electronic energies of molecular species.

4.2.3 The Atomic Hydrogen as a Case Study

Let us start to describe the atomic hydrogen for which we know, from quantum mechanics, both level energies and degeneracies (see Table 4.1). The energy of electronic levels, referred to the ground state, is given by

$$\varepsilon_n = I_H \left(1 - \frac{1}{n^2} \right)$$

being

$$I_H = \frac{m_e e^4}{8h^2 \epsilon_0^2} = \frac{e^2}{8\pi \epsilon_0 a_0} = 13.60 \text{ eV} \quad (4.43)$$

the ionization energy, n the principal quantum number, ϵ_0 the vacuum dielectric constant and a_0 the Bohr radius. The level degeneracy is given by

$$g_n = 2n^2.$$

The internal partition function of atomic hydrogen is then written as

$$Q_H^{\text{int}} = 2 + 8 \exp\left(-\frac{118,416}{T}\right) + 18 \exp\left(-\frac{140,345}{T}\right) + 32 \exp\left(-\frac{148,020}{T}\right) + \dots$$

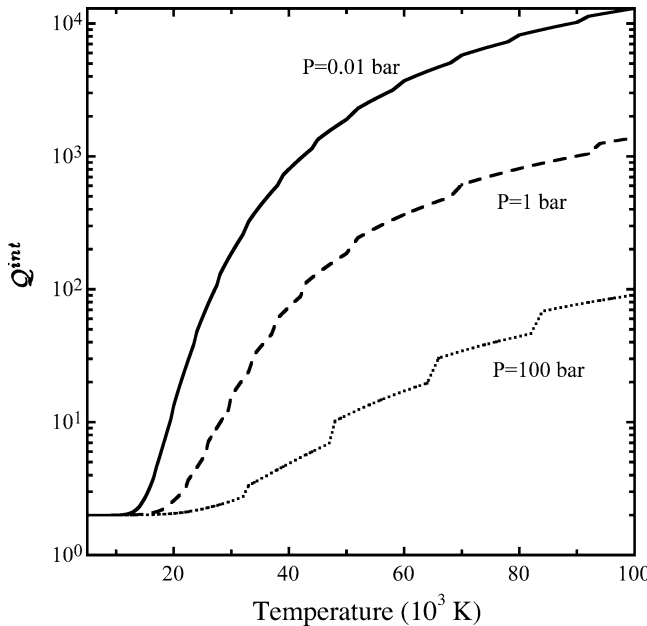


Fig. 4.3 Electronic partition function of atomic hydrogen in H , H^+ , e^- plasma as a function of temperature for different pressures

As anticipated in Sect. 4.1.3, the electronic partition function of an isolated atom diverges. In fact, the electronic energy converges to the ionization potential while the statistical weight diverges. We must therefore resort to some cutoff criterion to limit the number of levels in the electronic partition function (see Chap. 8). The effect of cutoff on the electronic partition function is higher as the temperature increases, since only at high temperature excited states start contributing. Indeed, at room temperature the partition function of atomic hydrogen is equal to the degeneracy of its ground state ($g_1=2$). Increasing the temperature, the number of levels entering in the calculation changes, making the partition function and its derivatives discontinuous with respect to the temperature. These effects are amplified by the pressure, due to the minor number of levels included in the partition function. This is true for the most used cutoff criteria used in the literature (see Chap. 8). Results reported in Figs. 4.3–4.9 have been obtained by using the Debye–Hückel cutoff criterion as implemented by Griem (1962; 1997).

Let us first examine the dependence of the electronic partition function on the temperature at different pressures (see Fig. 4.3). In all the reported cases, the electronic partition function of atomic hydrogen starts from the value of 2, showing a strong increase with the temperature. The onset and the magnitude of Q_H^{int} strongly depends on the pressure. As an example for $P=0.01$ bar the onset occurs at approximately $T=12,000$ K, while at $P=100$ bar, the electronic partition function starts increasing from $20,000$ K; however, in this case, the growth of the partition

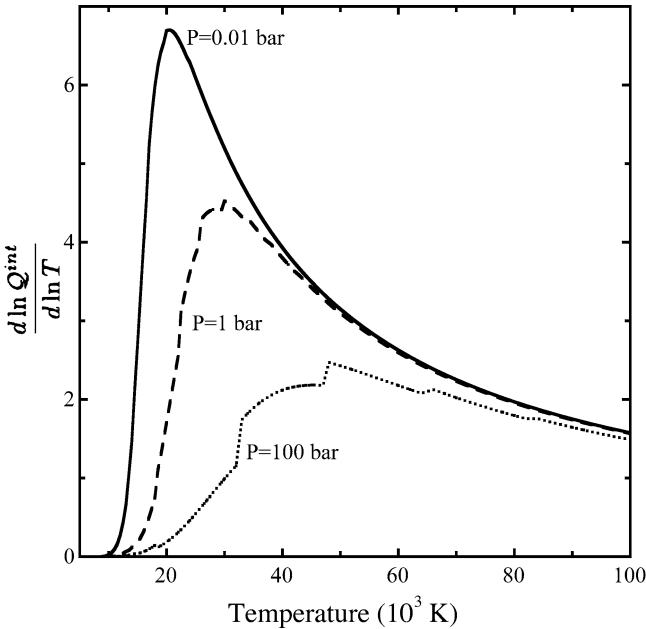


Fig. 4.4 First derivative of the electronic partition function of atomic hydrogen in H , H^+ , e^- plasmas a function of temperature for different pressures

function is much smaller. This behaviour is obviously due to the number of excited states entering in the electronic partition function at low pressure much larger than in the high pressure case.

The trend of the electronic partition function against temperature determines the shape of the first logarithmic derivative. We should expect a strong increase of the first derivative up to a maximum followed by a decline. This is indeed the case, as shown in Fig. 4.4. It should be also noted that the first logarithmic derivative reported in Fig. 4.4 starts from 0, being negligible the contribution of the internal energy. Remembering that (see (4.31)) the first derivative is equal to $\frac{U_H^{\text{int}}}{N_H kT}$, it must be compared with the reduced translational contribution ($\frac{U^{\text{tr}}}{N kT} = \frac{3}{2}$ and $\frac{H^{\text{tr}}}{N kT} = \frac{5}{2}$ as shown in (4.21)–(4.24)). We can observe that at low pressure ($P = 0.01$ bar) the ratio between the reduced internal energy and the reduced translational one at its maximum is about 4.7 decreasing at 1.5 at 100 bar. For $P = 1$ bar the normalized electronic energy reaches a maximum value of about 4, more than twice the translational reduced energy. A further contribution to the normalized energy is $\frac{\varepsilon^d}{2kT}$ coming from the dissociation energy of molecules $\varepsilon^d \approx 4.5$ eV. This term ranges from 26 to 0.26 in the temperature range $1,000 < T < 100,000$ K. As an example at $P = 0.01$ bar, this contribution at its maximum ($T = 20,000$ K) is 1.30 to be compared with the translational contribution of 1.5 and the electronic one of about 6.5. The trend of the first logarithmic derivative determines in turn

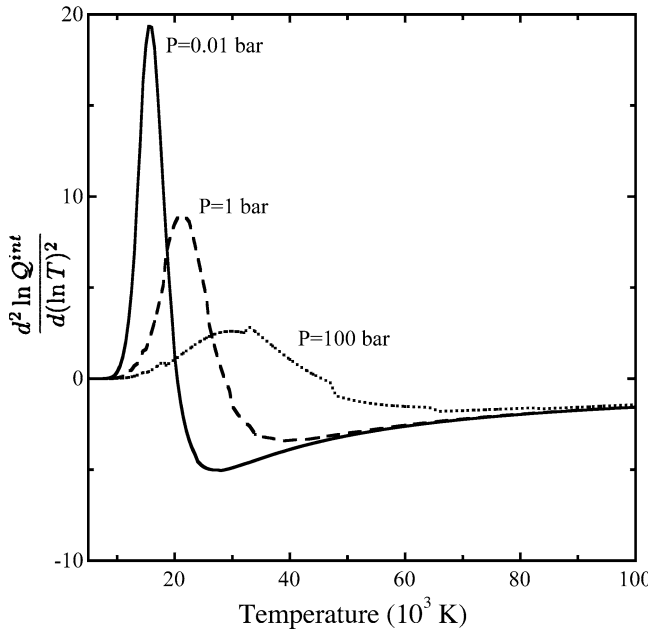


Fig. 4.5 Second derivative of the electronic partition function of atomic hydrogen in H , H^+ , e^- plasma as a function of temperature for different pressures

the behaviour of the second logarithmic derivative (see Fig. 4.5). This last in fact should increase with the temperature reaching a maximum, then should vanish in correspondence of the maximum of the first derivative and then becoming negative. The maximum and the minimum in the second derivative move to higher temperature as the pressure increases.

Finally, the normalized internal specific heat (\bar{C}_H^{int}/R) at different pressures (Fig. 4.6) reflects the trends of both first and second derivatives (see (3.27)). It presents a maximum after which the specific heat falls again to 0. Similar to the second derivative, the $C_{v,H}^{\text{int}}$ maximum moves towards higher temperatures as the pressure increases. Note also that, at low pressure ($P = 0.01$ bar), the contribution of the electronic specific heat is 10 times larger than the translation ($C_{v,H}^{\text{tr}}/R = \frac{3}{2}$). Moreover, we observe that, after exciting the electronic states, the specific heat reaches the maximum and then it starts decreasing until it vanishes. This behaviour can be reconducted to the case of the two-level systems as discussed in Chap. 2.

A comparison of the specific heat at $P = 1$ bar in Fig. 4.6 with the corresponding one in Fig. 2.2 for $n_{\max} = 10$ shows an excellent agreement emphasizing the good accuracy of the two-level approach in calculating the partition function. Note also that, as will be clarified in Chap. 8, $n_{\max} = 10$ is approximatively the value that the Debye–Hückel theory gives for an hydrogen plasma at atmospheric pressure in the temperature range 10,000–40,000 K.

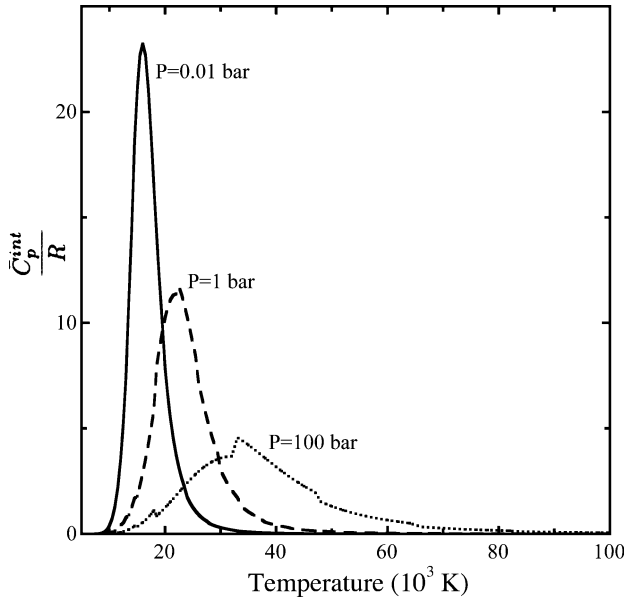


Fig. 4.6 Internal molar specific heat of the electronic partition function of atomic hydrogen in H , H^+ , e^- plasma as a function of temperature for different pressures

4.3 The Saha Equation for Ionization Equilibrium

Consider again the ionization reaction in (1.49) and the equilibrium condition in (1.50) given by

$$\mu_{A^+} + \mu_{e^-} - \mu_A = 0$$

Taking into account the expression of the atomic chemical potential reported in (3.40), the partition function in (4.6) and the different contributions to the chemical potentials presented in the previous chapter, we have for each species

$$\mu_s = \mu_s^{\text{tr}} + \mu_s^{\text{int}} + \mu_s^f = -kT \ln \left[\left(\frac{m_s kT}{2\pi \hbar^2} \right)^{\frac{3}{2}} \mathcal{Q}_s^{\text{int}} \exp \left(-\frac{\varepsilon_s^f}{kT} \right) \right] + kT \ln \frac{N_s}{V}.$$

Considering $N_s = \frac{N_s}{V}$ the particle density, grouping the terms depending on the temperature and those depending on the particle density, the equilibrium equation becomes

$$\begin{aligned} \ln \left(\frac{N_{A^+} N_{e^-}}{N_A} \right) &= \ln \left[\left(\frac{kT}{2\pi \hbar^2} \right)^{\frac{3}{2}} \left(\frac{m_{e^-} - m_{A^+}}{m_A} \right)^{\frac{3}{2}} \frac{\mathcal{Q}_{e^-}^{\text{int}} \mathcal{Q}_{A^+}^{\text{int}}}{\mathcal{Q}_A^{\text{int}}} \right. \\ &\quad \times \left. \exp \left(-\frac{\varepsilon_{e^-}^f + \varepsilon_{A^+}^f - \varepsilon_A^f}{kT} \right) \right]. \end{aligned} \quad (4.44)$$

The following relations must be considered⁵:

- (a) $m_A \approx m_{A^+}$
- (b) $\varepsilon_A^f = \frac{D}{2}$
- (c) $\varepsilon_{A^+}^f = \frac{D}{2} + I$
- (d) $\varepsilon_e^- = 0$
- (e) $\mathcal{Q}_e^-^{\text{int}} = 2$

and substituting in (4.44) we have

$$\ln \left(\frac{N_{A^+} N_{e^-}}{N_A} \right) = \ln \left[\left(\frac{kT}{2\pi\hbar^2} \right)^{\frac{3}{2}} (m_{e^-})^{\frac{3}{2}} \frac{2\mathcal{Q}_{A^+}^{\text{int}}}{\mathcal{Q}_A^{\text{int}}} \exp \left(-\frac{I}{kT} \right) \right] \quad (4.45)$$

resulting in the mass action law

$$\frac{N_{A^+} N_{e^-}}{N_A} = \left(\frac{kT m_{e^-}}{2\pi\hbar^2} \right)^{\frac{3}{2}} \frac{2\mathcal{Q}_{A^+}^{\text{int}}}{\mathcal{Q}_A^{\text{int}}} \exp \left(-\frac{I}{kT} \right) \quad (4.46)$$

and for partial pressures becomes

$$K_p^I = \frac{P_{A^+} P_{e^-}}{P_A} = \left(\frac{m_{e^-}}{2\pi\hbar^2} \right)^{\frac{3}{2}} (kT)^{\frac{5}{2}} \frac{2\mathcal{Q}_{A^+}^{\text{int}}}{\mathcal{Q}_A^{\text{int}}} \exp \left(-\frac{I}{kT} \right) \quad (4.47)$$

(4.47) together with the conditions of constant pressure and of electro-neutrality (see (1.58)) is used to calculate the partial pressure of the species in the system and therefore the ionization degree (see Figs. 1.3 and 1.4).

K_p^I depends not only on temperature but also on pressure through the corresponding dependence of the internal partition functions (see Fig. 4.3).

⁵Here, we are eliminating the nuclear partition functions of both atoms and ions. It must be pointed out that atomic and its parent ion nuclear partition functions are equal (see (4.7)) and therefore they are eliminated from the equation. This property is valid also for the dissociation process, even if the demonstration is not straightforward. Consider the nuclear contribution to the H_2 molecule. The nuclear spin is 1/2 and therefore $g_0^n = 2$ for the atom. In this case, the nuclear partition function of atomic hydrogen should appear as the product of two protons. From the same point of view, we should consider a nuclear partition function of H_2 molecule as a product of two independent protons obtaining the same result and therefore the cancelation in the equilibrium constant.

4.4 Plasma Thermodynamics

So far, we have shown the properties of single species as well as the ionization equilibrium. To simplify the problem, we consider an hydrogen plasma in a temperature range in which the dissociation process can be considered complete. We already discussed about the influence of electronic excitation on the thermodynamic properties of a single species, in particular for the specific heat of atomic hydrogen. Now we want to understand the impact of electronic excitation on the thermodynamic properties of the mixture, leaving in Chap. 8 a detailed analysis. Here, we present results for the specific heat of an ideal mixture in the framework of statistical thermodynamics, separating, as already discussed in Sects. 1.5, 1.7.2, the frozen and the reactive contributions.

Consider again the ionization reaction described in (1.49), the frozen specific heat at constant pressure of the system H , H^+ , electrons, is given by

$$c_{\text{pf}} = \frac{1}{M_H} \left[\frac{5}{2} R(1 + \alpha_i) + (1 - \alpha_i) \bar{C}_H^{\text{el}} \right] \quad (4.48)$$

as a function of the temperature and the ionization degree. The reactive contribution is given by

$$c_{\text{pr}} = \frac{1}{2M_H} R\alpha_i(1 - \alpha_i^2) \left(\frac{\Delta \bar{H}^0}{RT} \right)^2, \quad (4.49)$$

where the reaction enthalpy has been reported in (1.103). The total specific heat is given by $c_p = c_{\text{pf}} + c_{\text{pr}}$, while the internal contribution, already included in c_{pf} , is given by

$$c^{\text{int}} = \frac{1}{M_H} [(1 - \alpha_i) \bar{C}_H^{\text{el}}]. \quad (4.50)$$

Values of c_{pf} , c_{pr} , c_p and c^{int} have been reported in Fig. 4.7 as a function of the temperature for different pressures. In the temperature range where the ionization reaction is occurring, the reactive specific heat is much higher than the frozen one, this predominance decreasing with increasing of the pressure. However, the internal contribution plays a not negligible role reaching a maximum value of about 22% with respect to c_{pf} (Fig. 4.8), and a value of about 14% with respect to the total specific heat (see Fig. 4.9), at $P = 1$ bar. Note also that the trend of the internal specific heat reproduces the reactive one (see Chap. 2), being to some extent hidden in the total specific heat. We can anticipate that the use of other cutoff criteria i.e. the Fermi one, approximately increases by a factor 2 the ratios $c^{\text{int}}/c_{\text{pf}}$ and c^{int}/c_p (De Palma et al. 2006), as compared with results in Figs. 4.8, 4.9.

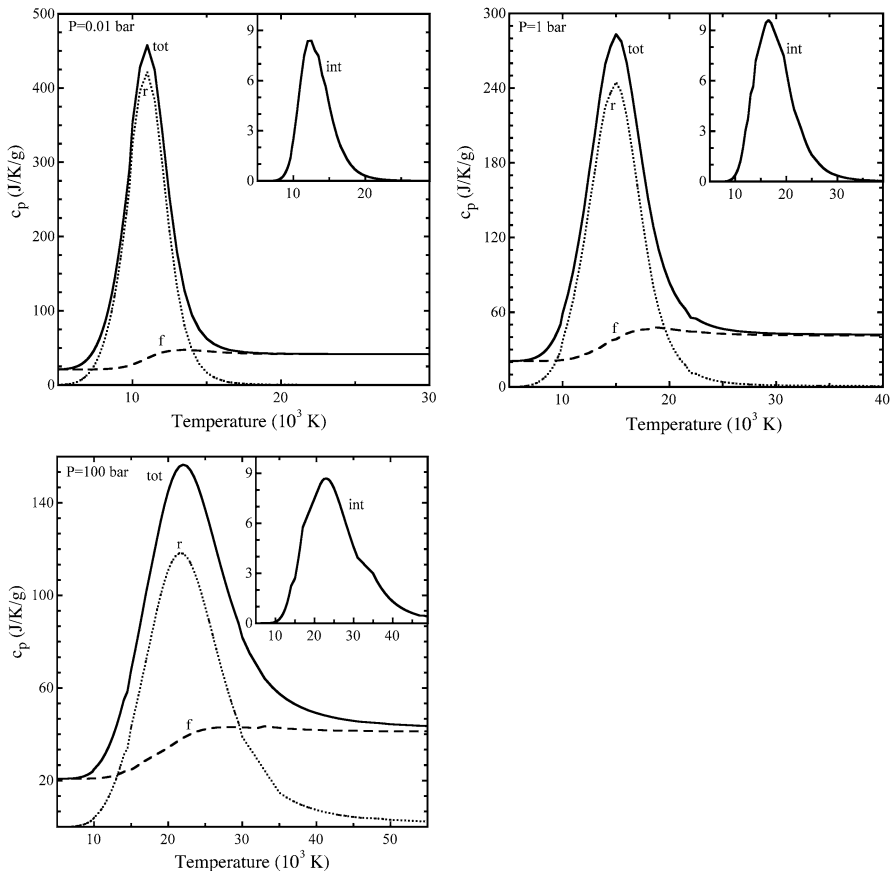


Fig. 4.7 Frozen (f), reactive (r) and total (tot) specific heat as a function of the temperature of (H , H^+ , e^-) mixture for $P = 0.01$, 1 , 100 bar. The internal (int) contribution has also been reported in the smaller box

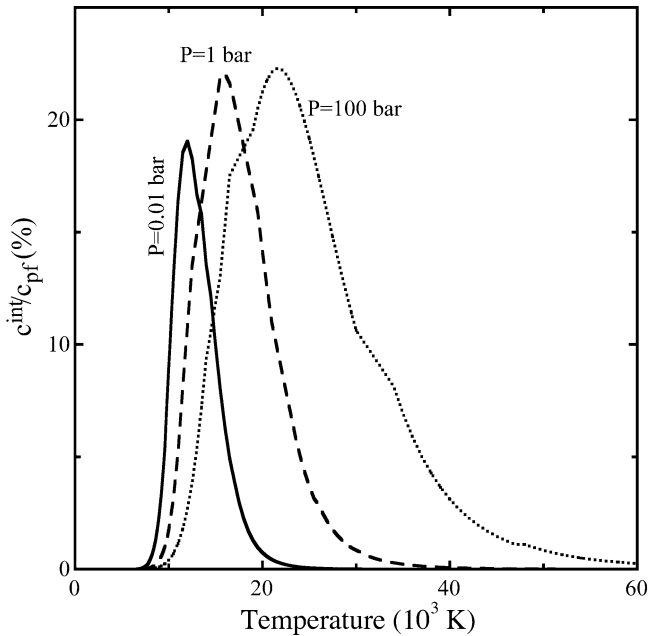


Fig. 4.8 Ratio (%) between the internal contribution and the frozen specific heat at constant pressure of (H , H^+ , e^-) for different pressures

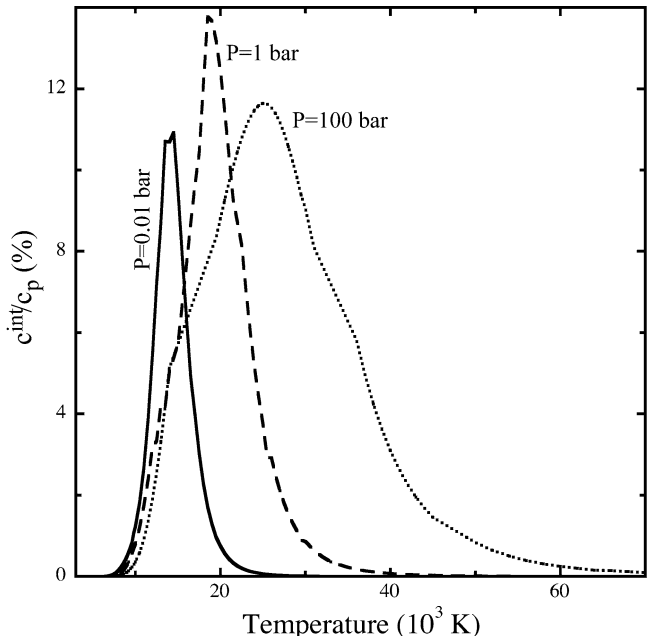


Fig. 4.9 Ratio (%) between the internal contribution and the total specific heat at constant pressure of (H , H^+ , e^-) for different pressures

Chapter 5

Molecular Partition Function: Vibrational, Rotational and Electronic Contributions

In this chapter, the working equations for the vibrational, rotational and electronic partition functions of the diatomic species and their contribution to the thermodynamic properties will be discussed. First, we present closed forms for the vibrational and rotational partition functions based on the harmonic oscillator and rigid rotor models. These approximations can be used for both diatomic and polyatomic molecules. This model considers the molecular partition function as the product of the contributions of four independent degrees of freedom, nuclear (n), vibration (vib), rotation (rot) and electronic (el):

$$Q^{\text{int}} = Q^n Q^{\text{vib}} Q^{\text{rot}} Q^{\text{el}}. \quad (5.1)$$

The energy is the sum of the three corresponding contributions

$$U = U^{\text{vib}} + U^{\text{rot}} + U^{\text{el}} \quad (5.2)$$

being the nuclear energy negligible in the temperature range examined in this book. The sum rule is valid for all the thermodynamic functions, as Gibbs free energy or the specific heat. The electronic partition function can be obtained by summing over electronic levels as for the atoms (see Sect. 4.1.3).

However, a real molecule is neither an harmonic oscillator nor a rigid rotor. Anharmonic, not-separable, ro-vibrational states must be considered and the general formalism will be presented. Moreover also the contribution of electronically excited states can have an important role, with their own ro-vibrational ladders.

5.1 The Harmonic Oscillator

We start examining the vibrational partition function of the so-called harmonic oscillator (HO). The classical Hamiltonian for this system is the sum of a kinetic contribution plus a potential term, which depends on the square of the displacement.

The Schrödinger equation can be exactly solved for this system, giving analytical eigenfunctions and eigenvalues. In particular, the energy levels are

$$\varepsilon_v^{\text{vib}} = \left(v + \frac{1}{2}\right) h\nu, \quad (5.3)$$

where v is the vibrational quantum number, ranging from 0 to ∞ and ν is the classical frequency of the harmonic oscillator. The relevant vibrational wave functions are not degenerate so that the statistical weight of each vibrational level is $g_v = 1$. The vibrational partition function of an harmonic oscillator is then calculated as

$$\mathcal{Q}^{\text{vib}} = \sum_{v=0}^{\infty} e^{-\varepsilon_v^{\text{vib}}/kT} = e^{-h\nu/2kT} \sum_{v=0}^{\infty} e^{-vh\nu/kT}. \quad (5.4)$$

In the harmonic approximation, the energy of levels monotonically grows with v , tending to infinity, so that the exponential Boltzmann factors entering in the partition function approaches zero very rapidly as v increases. In this case, no problem of divergence is present, differently from the electronic partition function of atoms.

Equation (5.4) can be written in term of the quantity $\chi = e^{-h\nu/kT}$ as

$$\mathcal{Q}^{\text{vib}} = \sqrt{\chi} \sum_{v=0}^{\infty} \chi^v. \quad (5.5)$$

The series in (5.5) is well known and converges, being $\chi < 1$, to the following expression

$$\mathcal{Q}^{\text{vib}} = \frac{\sqrt{\chi}}{1 - \chi} = (e^{h\nu/2kT} - e^{-h\nu/2kT})^{-1} \quad (5.6)$$

We can define the characteristic vibrational temperature as

$$\theta_v = \frac{h\nu}{k} \quad (5.7)$$

rewriting the partition function as

$$\mathcal{Q}^{\text{vib}} = (e^{\theta_v/2T} - e^{-\theta_v/2T})^{-1} = \frac{e^{-\theta_v/2T}}{1 - e^{-\theta_v/T}}. \quad (5.8)$$

For temperatures $T \gg \theta_v$, we can approximate the two exponentials in (5.8) as

$$e^{\pm\theta_v/2T} \approx 1 \pm \frac{\theta_v}{2T} \quad (5.9)$$

giving for the vibrational partition function at high temperature the following simple expression:

$$\mathcal{Q}^{\text{vib}} \approx \frac{T}{\theta_v} \quad (5.10)$$

and applying the general definitions of the internal energy (3.26) and constant volume specific heat (1.72) we have the well-known relation

$$U'^{\text{vib}} \approx \mathcal{N}kT \quad (5.11)$$

$$C'^{\text{vib}} \approx \mathcal{N}k \quad (5.12)$$

already obtained in Sect. 1.6.1 from the equipartition theorem.

However, we should remember that this result is valid only at high temperature. In general, the internal energy and the specific heat of the harmonic oscillator should be calculated applying (1.72), (3.26) to the partition function in (5.4)–(5.8), assuming the following forms

$$U'^{\text{vib}} = \frac{1}{2}\mathcal{N}hv + \frac{\mathcal{N}hv}{e^{hv/kT} - 1} \quad (5.13)$$

$$C'^{\text{vib}} = \mathcal{N} \left(\frac{hv}{kT} \right)^2 \frac{e^{hv/kT}}{(e^{hv/kT} - 1)^2}. \quad (5.14)$$

It should be noted that energy of vibrational levels included in the partition function are referred to the bottom of the potential curve. On the other hand, we can refer the level energy to the ground state ($v = 0$)

$$\varepsilon_v^{\text{vib}} = \varepsilon_v'^{\text{vib}} - \varepsilon_0'^{\text{vib}} = \left(v + \frac{1}{2} \right) hv - \frac{1}{2}hv = vhv \quad (5.15)$$

obtaining for the partition function and for the vibrational energy

$$\mathcal{Q}^{\text{vib}} = (1 - e^{-hv/kT})^{-1} \quad (5.16)$$

$$U^{\text{vib}} = \frac{\mathcal{N}hv}{e^{hv/kT} - 1} \quad (5.17)$$

while the vibrational heat capacity is independent of the energy reference. The choice of the reference level in the vibrational partition function, while giving different results, especially at low temperature, does not affect the equilibrium constant for the dissociation process, provided that also the dissociation energy is referred to the bottom of the potential energy (D_e) when using (5.8) or to the ground state (D_0) when using (5.16) (see Fig. 5.1).

5.2 The Rigid Rotor

As for the harmonic oscillator, the rigid rotor (RR) can be described exactly by the Schrödinger equation. The energy of rotational levels are given by

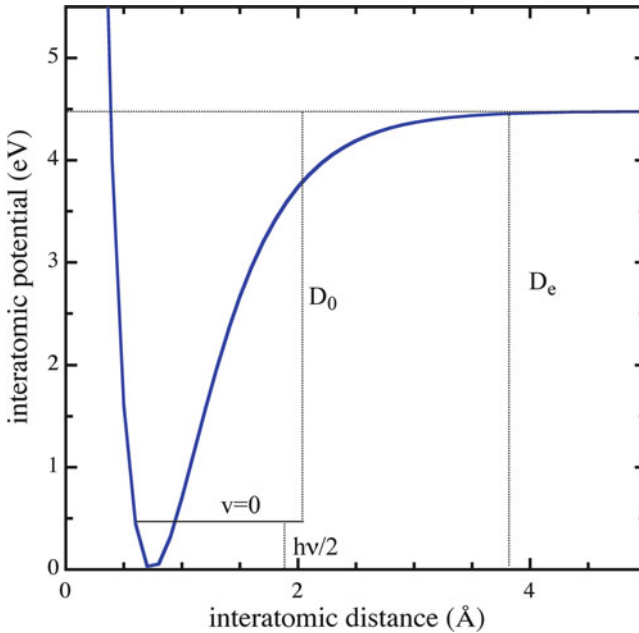


Fig. 5.1 Molecular potential, vibrational ground state and dissociation energies from the ground state (D_0) and from the minimum of the potential curve (D_e)

$$\varepsilon_J^{\text{rot}} = J(J + 1) \frac{\hbar^2}{8\pi^2 \mathcal{I}} = J(J + 1)k\theta_r, \quad (5.18)$$

where \mathcal{I} is the momentum of inertia of the rotor (considered as a constant) and

$$\theta_r = \frac{\hbar^2}{8\pi^2 \mathcal{I} k} \quad (5.19)$$

is the characteristic rotational temperature. The statistical weight (the degeneracy) of a rotational level is given by

$$g_J = 2J + 1. \quad (5.20)$$

As for the harmonic oscillator, we must note that the rotational partition function of the rigid rotor

$$\mathcal{Q}^{\text{rot}} = \sum_{J=0}^{\infty} (2J + 1) e^{-\varepsilon_J^{\text{rot}}/kT} = \sum_{J=0}^{\infty} (2J + 1) e^{-J(J+1)\theta_r/T} \quad (5.21)$$

converges since the exponential factor goes to zero, as J increases, faster than the statistical weight, that depends linearly on the rotational quantum number.

The rotational characteristic temperature of diatomic species is usually small¹, and therefore, for $T \gg \theta_r$, the sum in (5.21) can be approximated by the integral, giving

$$\mathcal{Q}^{\text{rot}} \approx \int_0^\infty (2J+1)e^{-J(J+1)\theta_r/T} dJ = \int_0^\infty \frac{T}{\theta_r} \frac{d}{dJ} e^{-J(J+1)\theta_r/T} dJ = \frac{T}{\theta_r} \quad (5.22)$$

For $T \ll \theta_r$ only the ground state contribution survive, while for $T \approx \theta_r$

$$\mathcal{Q}^{\text{rot}} \approx 1 + 3e^{-2\theta_r/T} + 5e^{-6\theta_r/T} + 7e^{-12\theta_r/T} + \dots, \quad (5.23)$$

which can be adequately approximated with the first two or three terms.

This approach cannot be applied to homo-nuclear diatomic molecules. Due to the Pauli's exclusion principle, the total wave function must be antisymmetric with respect to the exchange of the nuclei with semi-integer spin, like H_2 or symmetric for those with integer spin, as D_2 . The molecules with symmetric nuclear wave function are called *ortho*-, those with antisymmetric nuclear wave functions are called *para*-. As a consequence, the rotational wave function must be coupled with the proper nuclear wave function to have the global symmetry properties. It must be noted that J even and odd correspond respectively to a symmetric and antisymmetric rotational wave functions. As an example, $J = 0$ behaves like the $1s$ orbital of atomic hydrogen (i.e. symmetric), $J = 1$ behaves like $2p$ orbitals (i.e. anti-symmetric), $J = 2$ as $3d$ orbitals (i.e. symmetric) and so on.

A simple formula links the nuclear multiplicity to the symmetry:

$$\begin{cases} g^s = (s+1)(2s+1) \\ g^a = s(2s+1), \end{cases} \quad (5.24)$$

where g^s and g^a are the nuclear statistical weight of symmetric (ortho-) and antisymmetric (para-) states and s is the spin of a single nucleus.

Being g^e and g^o the statistical weight of the nuclear spin wave function corresponding to rotational states, respectively, with even and odd² J , they are related to the nuclear multiplicity depending on the spin of the nuclear particles: for s semi-integer

$$\begin{cases} g^e = \frac{g^a}{g^s + g^a} \\ g^o = \frac{g^s}{g^s + g^a} \end{cases} \quad (5.25)$$

¹Commonly $\theta_r \approx 10$ K, except for H_2 having $\theta_r \approx 90$ K.

²It must be noted that J even is coupled with the antisymmetric nuclear state if s is semi-integer and with the symmetric nuclear state if s is integer.

while for s integer we have the opposite

$$\begin{cases} g^e = \frac{g^s}{g^s + g^a} \\ g^o = \frac{g^a}{g^s + g^a}. \end{cases} \quad (5.26)$$

The rotational partition function must be written as

$$Q^{\text{rot}} = g^e \sum_{J \text{ even}} (2J+1)e^{-\varepsilon_J^{\text{rot}}/kT} + g^o \sum_{J \text{ odd}} (2J+1)e^{-\varepsilon_J^{\text{rot}}/kT}. \quad (5.27)$$

As an example, in the case of molecular hydrogen, taking into account that the protons are fermions, i.e. $s = 1/2$, we get $g^e = 3/4$ and $g^o = 1/4$ so that

$$Q_{H_2}^{\text{rot}} = 3/4 \sum_{J \text{ even}} (2J+1)e^{-\varepsilon_J^{\text{rot}}/kT} + 1/4 \sum_{J \text{ odd}} (2J+1)e^{-\varepsilon_J^{\text{rot}}/kT}. \quad (5.28)$$

In the high temperature limit, we have

$$\sum_{J \text{ even}} (2J+1)e^{-E_J/kT} \approx \sum_{J \text{ odd}} (2J+1)e^{-E_J/kT} \approx \frac{1}{2} \sum_{J=0}^{\infty} (2J+1)e^{-E_J/kT} \quad (5.29)$$

and therefore (5.28) becomes

$$Q^{\text{rot}} \approx \frac{T}{2\theta_r}. \quad (5.30)$$

In general, we can write the partition function of diatomic molecules as

$$Q^{\text{rot}} \approx \frac{T}{\sigma\theta_r}, \quad (5.31)$$

where σ is a symmetry factor = 1 for hetero-nuclear diatomic molecules and = 2 for homo-nuclear ones.

At low temperature, (5.28) cannot be used because the interchange between *ortho*- and *para*-hydrogen is practically forbidden. This means that the *ortho*-and *para*-configurations must be treated as independent, non-reacting species. As a consequence, also at $T = 0$ K both configurations are present in the ratio $g^s : g^a$. In this case, the partition functions of the *ortho*-and *para*-systems must be calculated separately, i.e.

$$\begin{aligned} Q_{\text{even}} &= \sum_{J \text{ even}} (2J+1)e^{-\varepsilon_J^{\text{rot}}/kT} \\ Q_{\text{odd}} &= \sum_{J \text{ odd}} (2J+1)e^{-\varepsilon_J^{\text{rot}}/kT} \end{aligned} \quad (5.32)$$

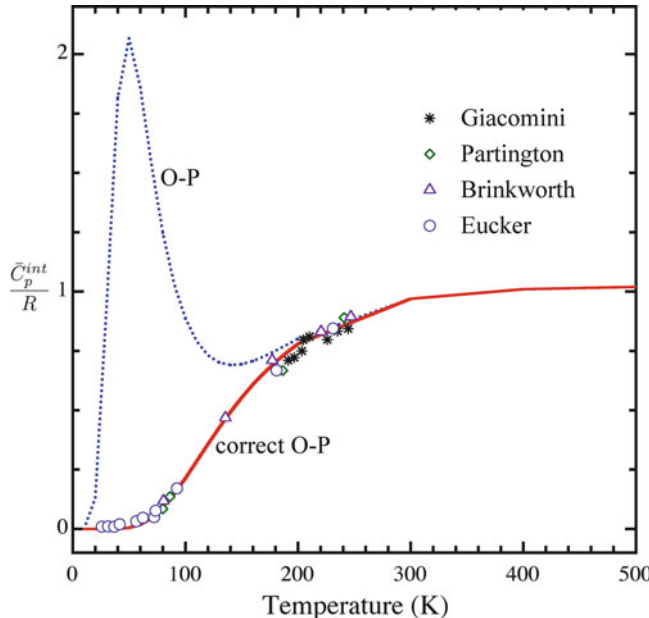


Fig. 5.2 Comparison between rotational specific heat of H_2 calculated from the partition function in (5.28) (*O-P*) and in (5.33) (*Correct O-P*). The marked data are experimental results taken from (Wannier 1966)

and the thermodynamic properties have to be summed weighted by the respective statistical weight, i.e.

$$\begin{aligned}\bar{U}^{\text{rot}} &= g^e \bar{U}_{\text{even}} + g^o \bar{U}_{\text{odd}} \\ \bar{C}^{\text{rot}} &= g^e \bar{C}_{\text{even}} + g^o \bar{C}_{\text{odd}},\end{aligned}\quad (5.33)$$

where the ortho- and para- contributions are calculated from the log derivatives of the relative partition function. This result can be obtained rigorously considering that the ortho-hydrogen and para-hydrogen are separate species, therefore the hydrogen partition function must be calculated using (3.48), i.e. the total partition function is given by³ (see (Wannier 1966))

$$Q^* = \frac{(Q^{\text{tr}} Q_{\text{even}})^{g^e N} (Q^{\text{tr}} Q_{\text{odd}})^{g^o N}}{(g^e N)! (g^o N)!} \quad (5.34)$$

which leads to (5.33) when applying the log derivatives to the partition function in (5.34). The rotational specific heat calculated in the two formulations (i.e (5.28), (5.33)) is given in Fig. 5.2. It should be noted that when considering the partition

³Note that ortho- and para-hydrogen have the same translational partition function, because it depends only on the mass of the species.

function in (5.28), a peak is observed at low temperature, corresponding to a reactive specific heat due to the interchange between ortho-hydrogen and para-hydrogen. This peak disappears when the partition function in (5.34) is considered. The *ortho–para* effect in any case disappears for $T > 400$ K.

5.3 Molecular Partition Function: Beyond Closed Forms

In the previous sections, closed forms for the vibrational and rotational partition functions have been obtained separating the different degrees of freedom. In doing so, we should be aware that, summing over the vibrational and rotational ladders, we are considering levels with energy exceeding the dissociation limit. In the most general case, each electronic state is described by its own potential energy curve that can be approximated by an harmonic oscillator only in a small region close to the minimum. As a consequence, the momentum of inertia depends on vibrational state. Moreover, the potential energy curve should be corrected by adding the contribution of the centrifugal force, which depends on the rotational state. In this way, the vibrational and rotational states are strictly related and we cannot consider them separately. For this reason, the relative motion of molecular nuclei is described by ro-vibrational levels. In this picture, the energy of internal levels of the s -th diatomic molecule depends on the electronic state n , vibrational v and rotational J quantum numbers, writing the partition function as⁴

$$\mathcal{Q}^{\text{int}} = \frac{1}{\sigma} \sum_{n=0}^{n_s^m} \sum_{v=0}^{v_s^m(n)} \sum_{J=0}^{J_s^m(nv)} g_{s,n}(2J+1) e^{-\frac{\epsilon_{s,nvJ}}{kT}}, \quad (5.35)$$

where we can understand that the vibrational energy depends not only on the vibrational quantum number but also on the electronic state, as well as the rotational energy depends also on the electronic and vibrational state. The relevant sums are extended on the available electronic states and the limiting values v_s^m , J_s^m represent the maximum vibrational and rotational quantum numbers such that the maximum total energy is below the dissociation limit of the corresponding electronic state⁵. Using this approach, it is not possible to obtain closed form for the partition function and thermodynamic quantities, and the sum over the energy levels must be calculated directly, as for the atomic species.

To calculate diatomic molecule energy levels, as well as their statistical weights, the Schrödinger equation must be considered. The Born–Oppenheimer approximation, which separates the motion of the electrons from that of the nuclei

⁴When considering *ortho–para* effects (5.34), must be extended considering the whole internal partition function, including the contribution of electronically excited states, of *ortho*-and *para*-configurations calculated separately.

⁵The centrifugal potential introduces a barrier in the energy curve, resulting in the existence of quasi-bound states above the dissociation limit. The inclusion of these states in the internal partition function is argument of a debate.

is commonly used to this end. The solution of the electronic Schrödinger equation yields the approximate wave functions of the infinite electronic states, expressing the energy as a function of the internuclear distance. In this way, the potential energy curve can be built up, so that the nuclear Schrödinger equation can be solved, including the centrifugal contribution, to describe the relative motion of the nuclei. The WKB (Wentzel–Kramers–Brillouin) approach is often used to this end (Patch and McBride 1969; Stancil 1994; Esposito 1999).

In principle dealing with the electronic partition function of diatomic species, one is faced with the same problems already encountered for atomic species. Also in this case, the partition function diverges due to the infinite levels existing for the isolated molecule so that one should use a cutoff criterion to avoid this kind of divergence. In general however one profits of the fact that the high-lying excited states of a diatomic molecule are characterized by excitation energies much higher than the corresponding dissociation energy so that, at high temperature, dissociation is favored with respect to electronic excitation. This is not anymore true for the so-called low-lying molecular excited states, originating either from the interaction of the ground state and the low-lying excited states of atoms or from the interaction of low-lying excited states with themselves (see Appendix A).

5.3.1 Ro-Vibrational Energies

The approach described above requires large computational efforts, and often the level of ro-vibrational states are calculated by semi-empirical formula, which coefficients are determined from molecular spectra (Herzberg 1963). The treatment for diatomic molecules follows the method developed by Drellishak (Drellishak et al. 1964, 1965) and by Stupochenko (Stupochenko et al. 1960) see also (Capitelli et al. 1994, 2005a; Giordano et al. 1994; Pagano et al. 2009; Babou et al. 2007). In this method, the energy of a molecular state is split into three contributions: the electronic excitation, the vibrational and the rotational energy

$$\varepsilon_{s,nvJ} = \varepsilon_{s,n}^{\text{el}} + \varepsilon_{s,nv}^{\text{vib}} + \varepsilon_{s,nvJ}^{\text{rot}}. \quad (5.36)$$

The vibrational energy associated with the v -th vibrational level of the n -th electronic state of a diatomic molecule is expressed in analytical form as⁶

$$\begin{aligned} \frac{\varepsilon'_{s,nv}^{\text{vib}}}{hc} &= \omega_e \left(v + \frac{1}{2} \right) - \omega_e x_e \left(v + \frac{1}{2} \right)^2 + \omega_e y_e \left(v + \frac{1}{2} \right)^3 \\ &\quad + \omega_e z_e \left(v + \frac{1}{2} \right)^4 + \omega_e k_e \left(v + \frac{1}{2} \right)^5 + \dots \end{aligned} \quad (5.37)$$

⁶The spectroscopic constants are usually expressed as wave numbers (the reverse of a length), therefore, to be converted in energy unit, the energy equations must be multiplied by the factor hc .

referring to the bottom of the potential energy curve (see Sect. 5.1). It is more practical to refer to the ground state ($v = 0$)

$$\frac{\varepsilon'_{s,n0}^{\text{vib}}}{hc} = \frac{1}{2}\omega_e - \frac{1}{4}\omega_ex_e + \frac{1}{8}\omega_ey_e + \frac{1}{16}\omega_ез_e + \frac{1}{32}\omega_ek_e \quad (5.38)$$

and the energy of excited levels can be expressed as

$$\frac{\varepsilon_{s,nv}^{\text{vib}}}{hc} = \frac{\varepsilon'_{s,nv}^{\text{vib}} - \varepsilon'_{s,n0}^{\text{vib}}}{hc} = \omega_0v + \omega_0x_0v^2 + \omega_0y_0v^3 + \omega_0z_0v^4 + \omega_0k_0v^5, \quad (5.39)$$

where the index 0 means that the constants refers to the ground state. The following relation holds:

$$\left\{ \begin{array}{l} \omega_0 = \omega_e - \omega_ex_e + \frac{3}{4}\omega_ey_e + \frac{1}{2}\omega_ез_e + \frac{3}{16}\omega_ek_e \\ \omega_0x_0 = \omega_ex_e - \frac{3}{2}\omega_ey_e - \frac{3}{2}\omega_ез_e - \frac{5}{4}\omega_ek_e \\ \omega_0y_0 = \omega_ey_e + 2\omega_ез_e + \frac{5}{2}\omega_ek_e \\ \omega_0z_0 = \omega_ез_e + \frac{5}{2}\omega_ek_e \\ \omega_0k_0 = \omega_ek_e. \end{array} \right. \quad (5.40)$$

Assuming that (5.37), (5.39) are valid for all the existing vibrational levels, we can determine the maximum permissible vibrational quantum number from the following condition

$$\left\{ \begin{array}{l} \varepsilon_{s,nv}^{\text{vib}} < D_0(n) \quad \forall v \leq v_s^m(n) \\ \varepsilon_{s,nv}^{\text{vib}} \geq D_0(n) \quad v = v_s^m(n) + 1, \end{array} \right. \quad (5.41)$$

where $D_0(n)$ (see Fig. 5.1) is the dissociation energy of the n -th electronic state referred to the ground state ($v = 0$).

The analytical expression of the vibrational energies implies that the potential energy curve is not an harmonic oscillator. A better approximation is given by the Morse potential

$$V(r) = D_e [1 - e^{-\beta(r-r_e)}]^2, \quad (5.42)$$

where D_e is the depth of the potential well and r_e is the equilibrium position. The Schrödinger equation can be solved exactly for the Morse potential, giving for the eigenvalue the expression in (5.37) truncated at the term ω_ex_e . In this way, it is possible to relate the potential coefficients to the first spectroscopic coefficients

$$\begin{cases} \omega_e = \frac{\beta}{2\pi} \sqrt{\frac{2D_e}{\mu}} \\ x_e = \beta r_e. \end{cases} \quad (5.43)$$

Also, the Morse potential is an approximation that cannot reproduce adequately the potential energy curve in the asymptotic region, and therefore the Morse potential eigenvalues are improved by adding higher order terms to the energy expression in (5.37).

The rotational energy for a non-non-rigid rotor is associated to each vibrational level in a given electronic states, and is given by

$$\frac{\varepsilon_{s,\text{nv}}^{\text{rot}}(J)}{hc} = \mathcal{B}_{s,\text{nv}} J(J+1) - \mathcal{D}_{s,\text{nv}} J^2(J+1)^2 + \dots, \quad (5.44)$$

where

$$\begin{cases} \mathcal{B}_{s,\text{nv}} = \mathcal{B}_e(s, n) - \alpha_e(s, n) \left(v + \frac{1}{2} \right) + \dots \\ \mathcal{D}_{s,\text{nv}} = \mathcal{D}_e(s, n) - \beta_e(s, n) \left(v + \frac{1}{2} \right) + \dots \end{cases} \quad (5.45)$$

The Morse potential describes a non-rotating molecule. In case of rotation, the centrifugal potential must be added obtaining

$$V'(J, r) = D_e [1 - e^{-\beta(r-r_e)}]^2 + \frac{h^2}{8\pi^2 c \mu r_e^2} J(J+1). \quad (5.46)$$

The constants in the rotational energy expression can be easily related to the modified potential constants, obtaining

$$\begin{cases} \mathcal{B}_e = \frac{h}{8\pi^2 c \mu r_e^2} \\ \mathcal{D}_e = \frac{4\mathcal{B}_e^3}{\omega_e^2} \\ \alpha_e = \frac{6}{\omega_e} \left(\sqrt{\omega_e x_e B_e^3} - B_e^2 \right) \\ \beta_e = \mathcal{D}_e \left(\frac{8\omega_e x_e}{\omega_e} - \frac{5\alpha_e}{\mathcal{B}_e} - \frac{\alpha_e^2 \omega_e}{24\mathcal{B}_e^3} \right). \end{cases} \quad (5.47)$$

The function in (5.46) describes a series of potential curves for consecutive J s (see Fig. 5.3), which shows a maximum, for $J > 0$, in a position $r_m(J)$ larger than the potential minimum $r_e(J)$. There exist a value J_m^* beyond which the maximum and the minimum coalesce and the potential becomes purely repulsive. This means that for $J = 0$ all vibrational states with energy lower than the dissociation limit are present and no stable state is present for $J > J_m^*$.

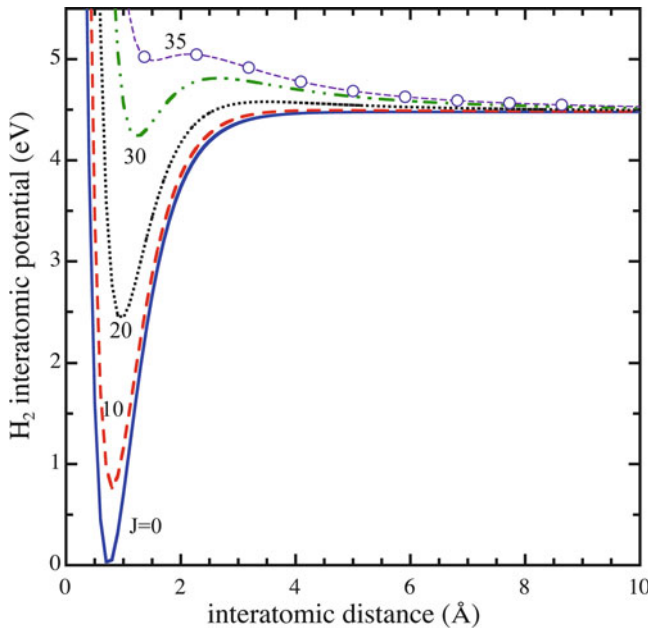


Fig. 5.3 Molecular potential for the H_2 molecule as a function of the interatomic distance for different values of the rotational quantum number

The centrifugal distortion of the potential energy determines the existence of “quasi-bound” states, which have energy between the dissociation limit and the maximum of the rotational barrier. The classical representation of ro-vibrational levels given by Herzberg (Herzberg 1963) considers all the rotational states for each vibrational quantum number, therefore the maximum rotational quantum number $J_m(v)$ for each v must be determined. In order to calculate $J_m(v)$, we differentiate (5.46) with respect to r

$$\frac{\partial V'(J, r)}{\partial r} = 2D_e\beta e^{-\beta(r-r_e)} [1 - e^{-\beta(r-r_e)}] - \frac{\hbar^2}{4\pi^2\mu r^3} J(J+1) \quad (5.48)$$

and the position of the maximum $r_m(J)$ is obtained setting this derivative equal to zero

$$\frac{\partial V'(J, r_m)}{\partial r} = 0 \quad (5.49)$$

for each J and for any electronic state of the molecule. Once the position of the maximum of the rotational barrier has been determined, we calculate the corresponding value of the potential

$$\varepsilon_{\max}(J) = V'(J, r_m) \quad (5.50)$$

Known $\varepsilon_{\max}(J)$ we can calculate the maximum value of the rotational quantum number $J_m(v)$ levels from the condition

$$\begin{aligned}\varepsilon_{s,\text{nv}}^{\text{rot}}(J_m) + \varepsilon_{s,\text{nv}}^{\text{vib}} &\leq \varepsilon_{\max}(J_m) \\ \varepsilon_{s,\text{nv}}^{\text{rot}}(J_m + 1) + \varepsilon_{s,\text{nv}}^{\text{vib}} &> \varepsilon_{\max}(J_m + 1)\end{aligned}\quad (5.51)$$

This procedure includes the contribution of bound and quasi-bound states in the calculation of the partition function.

This method has been extensively applied to many diatomic molecules. We start examining the H_2 molecule, and in particular the behaviour of the internal partition function Q^{int} , its first and the second log derivatives as well as the reduced internal specific heat. The first and second log derivatives are linked with the reduced internal energy U^{int}/RT and to the reduced specific heat \bar{C}^{int}/R through (3.26), (3.27).

All the quantities have been calculated according to the methods outlined in this chapter i.e. the curves refer to:

- All* Partition function calculated following (5.35) where the ro-vibrational energy is calculated following (5.36)–(5.45) including electronically excited states;
- Ground* As *All* but considering only the contribution of the ground electronic state;
- Closed* Partition function calculated considering only the ground electronic state and applying the closed form equations. i.e. the harmonic oscillator (see Sect. 5.1) and the rigid rotor (see Sect. 5.2);
- SE* Energy levels obtained from the solution of the Schrödinger equation for the effective potential curve of the ground state of H_2 ;

A comparison of the results obtained applying the four methods reported in Fig. 5.4 is instructive to understand the limits of harmonic oscillator and rigid rotor approximation and the role of electronic excitation in the partition function and related quantities of diatomic molecules. We start discussing the different quantities obtained by using the closed-form approach. In this case, the internal partition function presents an abrupt increase in the low and intermediate temperature range followed by a mild continuous increase of partition function due to the infinite number of considered vibro-rotational states. In the *Ground* case, Q^{int} follows the *Closed* values in the low and intermediate temperature range, approaching a plateau in the high temperature region due to the finite number of ro-vibrational levels inserted in the partition function. On the other hand, the *All* partition function closely follows the *Ground* values until the high temperature starts populating the electronically excited states.

More pronounced are the differences in the first log derivative (i.e. \bar{U}^{int}/RT) which starts from 1 (excitation of rotational degree of freedom) in the *Closed* form case, rapidly approaching the asymptotic value of 2 (excitation of rotational and vibrational degrees of freedom). Also in the *Ground* case Q^{int} reaches the maximum value of 2, decreasing soon after due to saturation effect. It must be noted

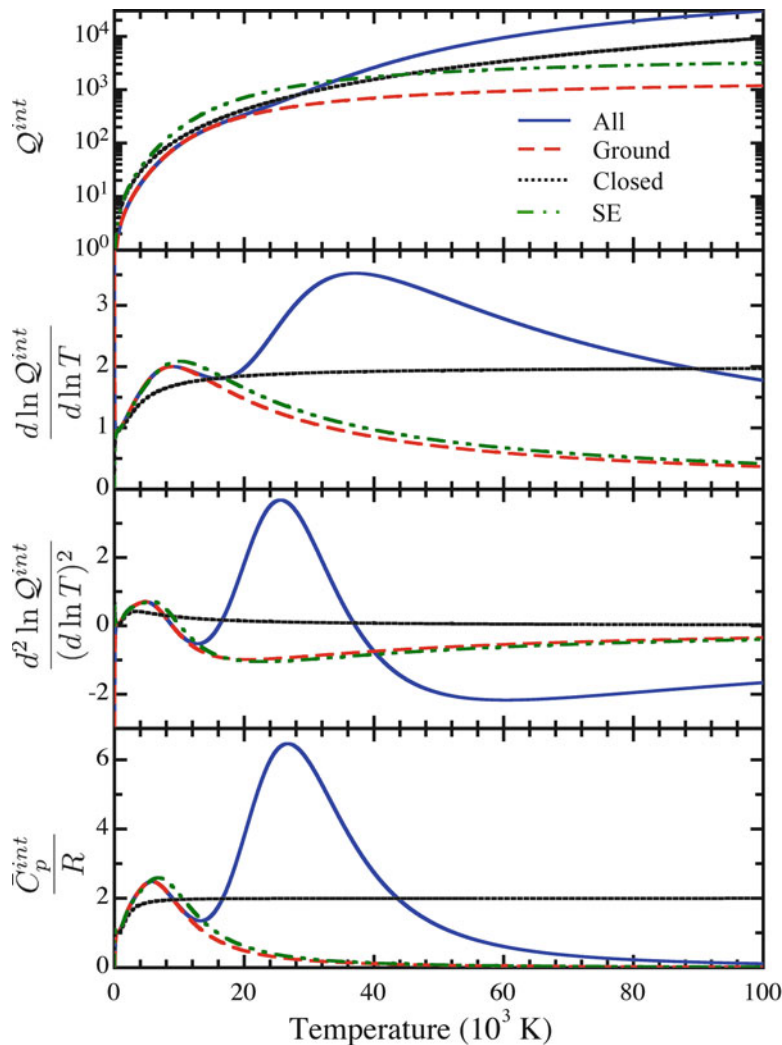


Fig. 5.4 Partition function, its first and second log derivatives and internal specific heat of H_2 molecule as a function of the temperature: comparison between calculation with inclusion of electronically excited states (All), only ground state (Ground), closed expression (Closed), and ro-vibrational levels from the solution of the Schrödinger equation considering the potential curve of the ground electronic state (SE)

that the *Ground* case reaches the value of 2 at lower temperature than the *Closed* calculation, because of anharmonicity of vibrational levels. The same occurs for the *All* values, which however presents a larger maximum at higher temperature due to the excitation of electronic states.

These behaviors are also reflected to the second log derivative that in the *Closed* case suddenly increases up to a small maximum and then asymptotically decreases to zero. This behaviour is completely different from that one obtained by the other methods. The *Ground* calculation presents a maximum and a minimum, vanishing very high temperatures, while the *All* values present two maxima and two minima, approaching the zero value after the second minimum.

Finally the reduced internal specific heat from *Closed* form method rapidly passes from a value of 1 (rotational excitation) to a value of 2 (rotational and vibrational excitation) keeping this last value in all the temperature range. On the contrary, the *Ground* specific heat rapidly reaches a value a little larger than 2, after which starts decreasing to zero. The electronic excitation, on the other hand, is responsible in the *All* calculation for the large maximum at $T \approx 30,000$ K after which it starts to decrease to zero. It is interesting to notice that the log derivatives and specific heat calculated in the *Ground* case are in good agreement with the values obtained with *SE* method, when accurate ro-vibrational states calculated solving the Schrödinger equation are included in the partition function. This result demonstrates the accuracy of the method described in this section.

The results presented in this figure are representative of many other diatomic systems. In particular, the internal specific heat calculated with the *All* method should present at least two maxima, one due to the ro-vibrational excitation of ground electronic state of the diatom and one to the electronic excitation. The magnitude and the temperature of the second maximum depends on the number and the energies of electronic states inserted in the partition function. In the case of H_2 , the two maxima are separated, because in addition to ground state, a series of excited states with a total multiplicity of 129 and energy ranging from 11.37 to 15.31 eV have been inserted in the partition function (Pagano et al. 2008; Pagano et al. 2009). Moreover, the difference in the energy between the last ro-vibrational levels of the ground electronic state of H_2 (i.e. approximately 4.50 eV) and the energy of inserted electronic states is high enough to clearly separate the influence, on the thermodynamic properties, of the electronic excitation and of the ground state.

Results for N_2 , N_2^+ and O_2 , O_2^+ calculated according to the *All* approach (including electronically excited states) have been reported in Fig. 5.5. These results present a similar qualitative trend for all the considered systems, while strong differences appearing in the maximum of internal energy and specific heat due to the different number of electronic states inserted in the relevant partition functions. Comparison with Fig. 5.4 shows that the electronic contribution to the specific heats is evident in the case of N_2 and O_2^+ molecules where the jump of the specific heat after the excitation of the vibrational degree of freedom clearly appears. This behaviour is a little hidden in the case of O_2 and N_2^+ molecules. The relevant differences, as already pointed out, are due to the number of bound states considered in different molecules (Capitelli et al. 2005a; Giordano et al. 1994). As an example, in the case of N_2 molecule, we consider, in addition to the ground state, 10 electronically excited states the energy of which ranges from 6.22 to 11.05 eV with a total multiplicity of 40, partially overlapping with the vibrational manyfold

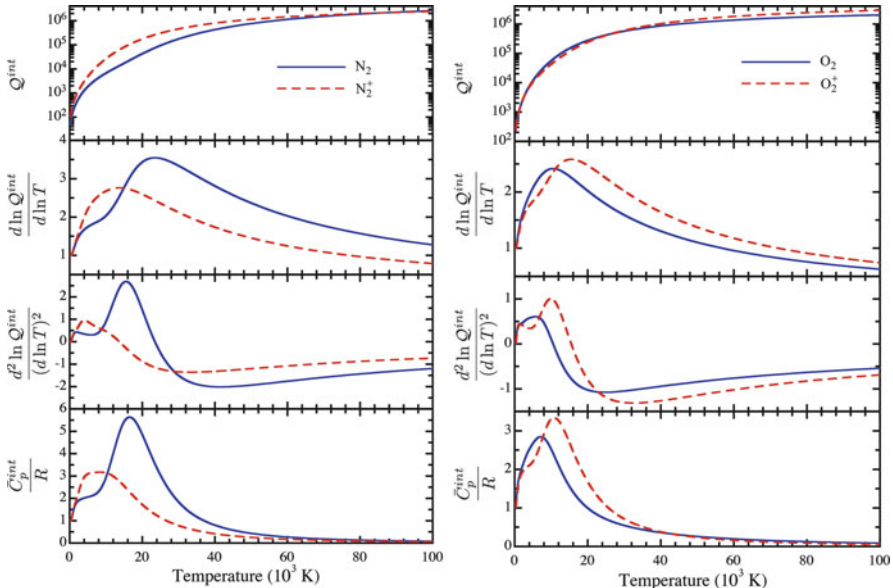


Fig. 5.5 Partition function, its log derivatives and reduced internal specific heat of N_2 , N_2^+ , O_2 and O_2^+ as a function of temperature

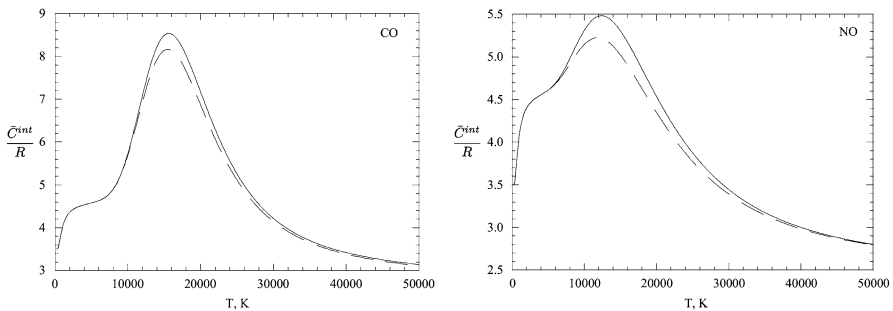


Fig. 5.6 Reduced specific heat of CO and NO molecules as a function of the temperature: comparison between calculation including (continuous line) and neglecting (dashed lines) quasi-bound states

of the ground state. On the other hand, for N_2^+ we consider, in addition to the ground state, 5 electronically excited states with energy ranging from 1.14 to 8.01 eV and a total multiplicity of 16. Details can be found in (Capitelli et al. 2005a; Giordano et al. 1994) where one can also appreciate the quality of the reported results by comparison with existing accurate calculations as well as other results for diatomic and polyatomic molecules for high temperature planetary atmospheres (Earth, Mars and Jupiter).

Note that our results have been obtained by considering both bound and quasi-bound rotational states. Inclusion of quasibound levels increases the specific heat in the zone of the excitation of electronic states, due to the fact the quasi-bound rotational energy levels merge with the corresponding electronic levels of the considered molecules (see Fig. 5.6 for *CO* and *NO* molecules).

5.4 Polyatomic Molecular Partition Functions

The calculation of the partition function of molecules containing more than two atoms is much more complex. The general picture of considering electronic, vibrational and rotational state contributions to energy levels, as in (5.36), maintains its validity, the nuclear motion involves many different degrees of freedom: there are two rotational axes for linear molecules and three for the others.

The number of vibrational modes n_m can be determined easily from the number of atoms n_a in the molecule, given by

$$n_m = 3n_a - 5 \quad (5.52)$$

for linear molecules and

$$n_m = 3n_a - 6 \quad (5.53)$$

for non-linear one⁷. Not all the vibrational modes are distinguishable in polyatomic molecules, therefore, differently from the diatomic molecules, a degeneracy factor (statistical weight) can appear. To simplify the notation, consider as $[v]$ the set $[v_1, v_2, \dots, v_m]$ of all the modes, being m the number of independent vibrational modes. The total partition function is then obtained generalizing (5.35), (5.36) (see (Herzberg 1966) for the general theory) giving

$$\mathcal{Q}^{\text{int}} = \frac{1}{\sigma} \sum_n g_n^{\text{el}} e^{-\frac{\epsilon_n^{\text{el}}}{kT}} \sum_{[v]} g_{n[v]}^{\text{vib}} e^{-\frac{\epsilon_{n[v]}^{\text{vib}}}{kT}} Q_{n[v]}^{\text{rot}}. \quad (5.54)$$

For polyatomic molecules, the harmonic oscillator approximation is usually considered, supposing also that different modes do not interact between each other⁸. Under these approximations, the vibrational energies and the statistical weights are

⁷This result can be obtained easily by considering that a system with n_a atoms has $3n_a$ degrees of freedom, three directions of motion (x, y, z) for each atom. However, three degrees of freedom, corresponding to the translational motion of the centre of mass, must be eliminated, together with the rotational motion of the molecule. In general a polyatomic molecule has three independent rotational axes, but for linear molecules, having only two axes, because the molecular axis is not a rotational one.

⁸The vibrational modes are calculated finding the eigenvalues and eigenvectors of the Hessian matrix of the potential. As a consequence, the hypothesis of independent modes is valid only for weakly excited molecules.

$$\begin{cases} \varepsilon_{n[v]}^{\text{vib}} = \sum_{i=1}^m \varepsilon_{ni}^{\text{vib}}(v_i) \\ g_{n[v]}^{\text{vib}} = \prod_{n=1}^m g_{ni}^{\text{vib}} v_i \end{cases} \quad (5.55)$$

$$\begin{cases} \varepsilon_{ni}^{\text{vib}}(v_i) = \omega_e \left(v_i + \frac{d_i}{v_i} \right) \\ g_{ni}^{\text{vib}}(v_i) = \frac{(v_i + d_i - 1)!}{v_i!(d_i - 1)!}, \end{cases} \quad (5.56)$$

where d_n is the degeneracy of the n -th vibrational mode. The energy includes the contribution of the ground state that must be subtracted. Higher order expansion can be also considered in this formalism, but available data are very scanty.

The symmetry properties can be extracted by comparing the moment of inertia with respect to the three axes: considering the constants $\mathcal{A}_e \geq \mathcal{B}_e \geq \mathcal{C}_e$ as

$$\begin{cases} \mathcal{A}_e = \frac{h}{8\pi^2 c I_A} \\ \mathcal{B}_e = \frac{h}{8\pi^2 c I_B} \\ \mathcal{C}_e = \frac{h}{8\pi^2 c I_C}, \end{cases} \quad (5.57)$$

where I_X is the momentum of inertia with respect to the relevant axis. We must distinguish three cases:

1 – spherical symmetric molecules

This case includes linear molecules or methane, for which $I_A = I_B = I_C$. The rotational partition function is given by

$$Q_{n[v]}^{\text{rot}} = \sum_J (2J + 1) e^{-\frac{\varepsilon_{i[v]J}^{\text{rot}}}{kT}}. \quad (5.58)$$

and the rotational energy is given by the relation

$$\varepsilon_{n[v]J}^{\text{rot}} = \mathcal{B}_{n[v]} J(J + 1) \quad (5.59)$$

2 – symmetric top molecules

This case includes H_2O , NH_3 , CO_2 , for which $I_A \neq I_B = I_C$. The expression of rotational partition function includes a further sum over the index l , the projection of the total angular momentum on the rotational axis,

$$Q_{n[v]}^{\text{rot}} = \sum_J (2J + 1) \sum_{k=-J}^J e^{-\frac{\varepsilon_{i[v]Jl}^{\text{rot}}}{kT}} \quad (5.60)$$

being the rotational levels non-degenerate because of the symmetry breaking resulting from rotation–vibration interaction. The energy of the levels is given by

$$\varepsilon_{n[v]J}^{\text{rot}} = \mathcal{B}_{n[v]} J(J + 1) + (\mathcal{A}_{n[v]} - \mathcal{B}_{n[v]})l^2 \quad (5.61)$$

3 – asymmetric top molecules

In this case, $I_A \neq I_B \neq I_C$. The rotational partition function is the same as for symmetric top molecules given in (5.60), and the energy of the levels is given by

$$\varepsilon_{n[v]J}^{\text{rot}} = \frac{1}{2}(\mathcal{B}_{n[v]} + \mathcal{C}_{n[v]})J(J + 1) + \left[\mathcal{A}_{n[v]} - \frac{1}{2}(\mathcal{B}_{n[v]} + \mathcal{C}_{n[v]}) \right] l^2. \quad (5.62)$$

The coefficients $\mathcal{A}_{n[v]}$, $\mathcal{B}_{n[v]}$, $\mathcal{C}_{n[v]}$ used in the energy equations (5.59)–(5.62) are calculated as

$$\begin{cases} \mathcal{A}_{n[v]} = \mathcal{A}_e(n) - \sum_i \alpha_{ni}^A \left(v_i + \frac{1}{2}d_i \right) \\ \mathcal{B}_{n[v]} = \mathcal{B}_e(n) - \sum_i \alpha_{ni}^B \left(v_i + \frac{1}{2}d_i \right) \\ \mathcal{C}_{n[v]} = \mathcal{C}_e(n) - \sum_i \alpha_{ni}^C \left(v_i + \frac{1}{2}d_i \right). \end{cases} \quad (5.63)$$

A sample of results for CO_2 and NO_2 are reported in Figs. 5.7, 5.8. These results have been taken from (Capitelli et al. 2005a) where one can also find the relevant spectroscopic data as well as complete tables for other molecules. Figure 5.7, in particular, shows the internal partition function and its logarithmic derivatives for both molecules as a function of temperature, these data being calculated with the state-to-state approach including electronically excited states. On the other hand, Fig. 5.8 reports the reduced internal specific heat calculated according to the state-to-state approach with and without electronically excited states and with the *Closed* model. The results can be understood on the same basis discussed for the diatomic molecules especially the well-defined role of electronically excited states in affecting the reduced internal specific heat. Note that *Closed* model behaves differently for the two reported molecules taking into account that CO_2 is linear and NO_2 is angular. As a consequence (remember also the equipartition theorem), the *Closed* reduced specific heat for CO_2 starts from 1 at very low temperatures (excitation of the two rotational degrees of freedom) rapidly reaching a plateau of 5 (excitation of 2 rotational and 4 vibrational degrees of freedom). On the other hand, the corresponding values of NO_2 are, respectively, 1.5 (three rotations) and 4.5 (three rotations and three vibrations). Note, however, that for this molecule the Born–Oppenheimer approximation is violated (Leonardi et al. 1996; Leonardi and Petronolo 1997).

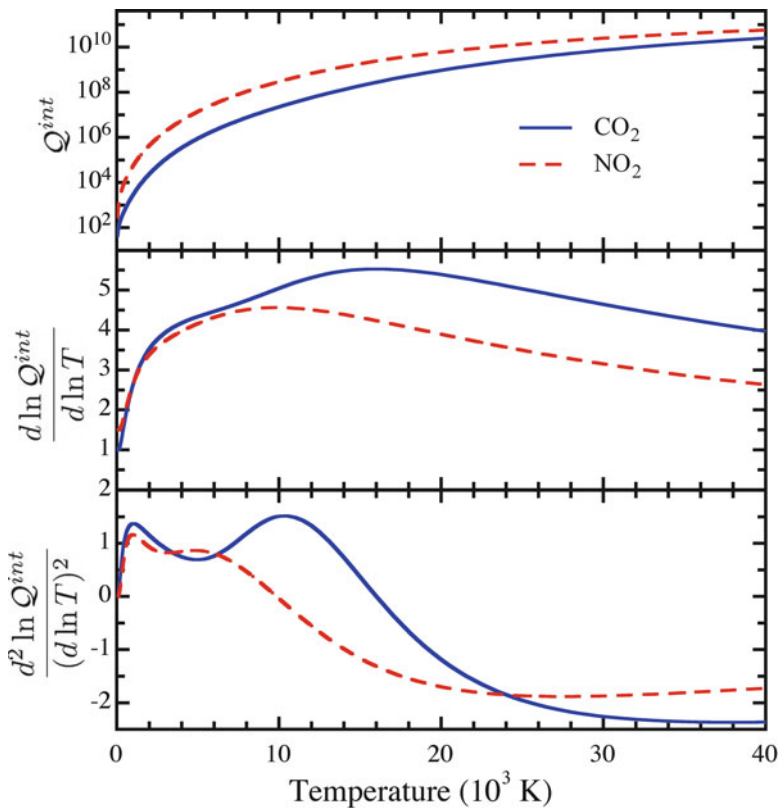


Fig. 5.7 Partition function and first and second log derivative of CO_2 and NO_2 as a function of temperature

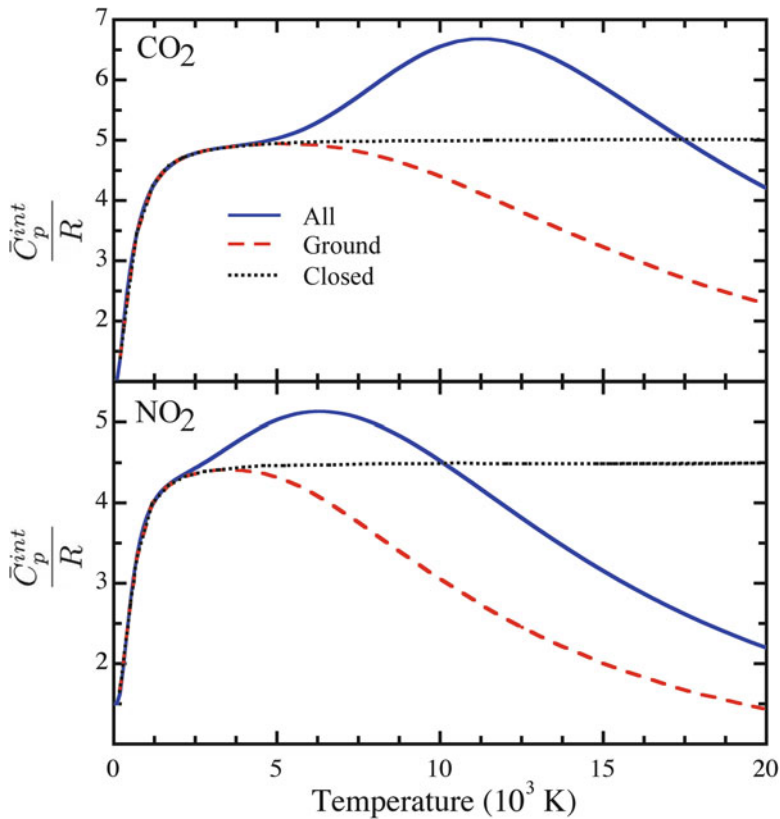


Fig. 5.8 Reduced internal specific heat of CO_2 and NO_2 as a function of temperature: direct sum (see (5.54)) including electronically excited states (*All*) or ground state only (*Ground*) compared with *Closed* form calculation, i.e. harmonic oscillator and rigid rotor

Chapter 6

Real Effects: I. Debye–Hückel

The thermodynamic model described in previous chapters is valid only for an ideal gas, formed by dimensionless particles colliding as hard spheres. However, a plasma contains also charged particles, interacting through electrostatic forces, which are effective also at long distance. If the density of charged particle is sufficiently high, the plasma must be considered as a Debye mixture and the thermodynamic functions must be consistently corrected (Fermi 1936; Griem 1962, 1997; Wannier 1966; Zaghloul 2005, 2004).

6.1 Debye–Hückel Theory

The corrections to thermodynamic properties of ideal plasmas can be obtained by using the Debye–Hückel theory, first developed to describe high concentration electrolyte solutions. The starting idea is that every ion tends to attract ions of opposite charge and to repel those with the same charge sign. Each positive ion feels a negative potential which modifies in the first place the internal energy of the system and thereafter all the other thermodynamic properties. We can write down an expression for the electrostatic energy ΔU_{DH} of a solution of ions as

$$\Delta U_{\text{DH}} = \frac{1}{2} q_e \sum_{s=1}^N \mathcal{N}_s z_s \Phi_s, \quad (6.1)$$

where q_e is the absolute value of the electron charge, \mathcal{N}_s is the number of particles of the s -th species having charge $z_s q_e$ and experiencing a mean electrostatic potential Φ_s due to the presence of other ions. To determine Φ_s , we consider an ion of the species s -th placed at the origin of the coordinates and investigate the behavior of the potential $\phi(\mathbf{r})$ as a function of the position \mathbf{r} relative to the reference ion. The number density $\hat{\mathcal{N}}_i$ of the other ions in such a potential is assumed to follow a spatial Boltzmann distribution

$$\widehat{\mathcal{N}}_i(\mathbf{r}) = \frac{\mathcal{N}_i}{V} \exp\left(-\frac{q_e z_i \phi(\mathbf{r})}{kT}\right). \quad (6.2)$$

The potential ϕ is the sum of the contribution of all the charged particles in the plasma. The Poisson equation¹ can be used

$$\nabla^2 \phi = -\frac{\rho_q}{\epsilon_0} = -\frac{q_e}{\epsilon_0} \sum_{i=1}^N \widehat{\mathcal{N}}_i z_i, \quad (6.3)$$

where ϵ_0 is the vacuum electric permittivity and ρ_q is the charge density. Combining (6.2), and (6.3), we obtain

$$\nabla^2 \phi = -\frac{q_e}{\epsilon_0 V} \sum_{i=1}^N \mathcal{N}_i z_i \exp\left(-\frac{q_e z_i \phi}{kT}\right). \quad (6.4)$$

Under the hypothesis that the thermal energy is larger than the electrostatic energy, i.e.

$$kT \gg |q_e z_i \phi| \quad (6.5)$$

for any i , we can expand the exponential in Taylor series², stopped at the second term, obtaining

$$\begin{aligned} \nabla^2 \phi &= -\frac{q_e}{\epsilon_0 V} \sum_{i=1}^N \mathcal{N}_i z_i \left(1 - \frac{q_e z_i \phi}{kT}\right) \\ &= -\frac{q_e}{\epsilon_0 V} \sum_{i=1}^N \mathcal{N}_i z_i + \frac{q_e^2 \phi}{\epsilon_0 V k T} \sum_{i=1}^N \mathcal{N}_i z_i^2. \end{aligned} \quad (6.6)$$

For the condition of global electro-neutrality, we have $\sum_{i=1}^N \mathcal{N}_i z_i = 0$ and defining the *Debye length* as

$$\frac{1}{\lambda_D^2} = \frac{q_e^2}{\epsilon_0 k T} \sum_{i=1}^N \frac{\mathcal{N}_i}{V} z_i^2 \Rightarrow \lambda_D = \sqrt{\frac{\epsilon_0 k T}{q_e^2 \sum_{i=1}^N \frac{\mathcal{N}_i}{V} z_i^2}} \quad (6.7)$$

the Poisson equation become

¹ $\nabla^2 = \frac{\partial^2}{\partial x^2} + \frac{\partial^2}{\partial y^2} + \frac{\partial^2}{\partial z^2}$

² $e^x = 1 + x + \frac{1}{2}x^2 + \frac{1}{6}x^3 + \dots$

$$\nabla^2 \phi - \frac{1}{\lambda_D^2} \phi = 0 \quad (6.8)$$

Looking for a spherical symmetric solution³ that vanishes for $r \rightarrow \infty$, we get the well-known Debye potential⁴

$$\phi = \frac{A}{r} e^{-\frac{r}{\lambda_D}}. \quad (6.9)$$

To determine the constant A , we should remember that we are considering the potential around an ion having charge $z_i q_e$, and noticing that at short range ($r \ll \lambda_D$) ϕ behaves like the coulomb potential we have $A = \frac{z_i q_e}{4\pi\epsilon_0}$ obtaining the Debye potential

$$\phi = \frac{z_i q_e}{4\pi\epsilon_0 r} e^{-\frac{r}{\lambda_D}}. \quad (6.10)$$

Now, the potential ϕ is the sum of the potential generated by the ion in the center of the reference system and that generated by all the other particles in the plasma. Obviously, this second contribution, considered as a mean field and therefore independent on the position (in the plasma bulk), is the potential Φ_s acting on our ion. From these assumptions, we can evaluate Φ_s for $r \gg \lambda_D$ expanding the exponential in (6.10) in Taylor series obtaining

$$\phi \approx \frac{z_i q_e}{4\pi\epsilon_0 r} \left(1 - \frac{r}{\lambda_D}\right) = \frac{z_i q_e}{4\pi\epsilon_0 r} - \frac{z_i q_e}{4\pi\epsilon_0 \lambda_D}. \quad (6.11)$$

It must be noted that the first term in (6.11) is the Coulomb potential generated by the reference ion; therefore, the potential Φ_s in (6.1) is given by

$$\Phi_s = -\frac{z_s q_e}{4\pi\epsilon_0 \lambda_D}. \quad (6.12)$$

6.2 Debye–Hückel Corrections

6.2.1 Internal Energy

The result obtained in the previous section allows us to calculate the contribution of the electrostatic interaction to the thermodynamic properties, starting from the internal energy. Combining (6.1), and (6.12), the internal energy is given by

³In this case, we have $\nabla^2 = \frac{\partial^2}{\partial r^2} + \frac{2}{r} \frac{\partial}{\partial r}$

⁴In nuclear physics, this is also known as Yukawa potential, to model the Strong interaction.

$$\Delta U_{\text{DH}} = -\frac{1}{2} q_e \sum_{s=1}^N \mathcal{N}_s z_s \frac{z_s q_e}{4\pi\epsilon_0\lambda_D} = -\frac{q_e^2}{8\pi\epsilon_0\lambda_D} \sum_{s=1}^N \mathcal{N}_s z_s^2. \quad (6.13)$$

From the definition of the Debye length (6.7), we have that the sum in the previous equation is given by

$$\sum_{s=1}^N \mathcal{N}_s z_s^2 = \frac{V k T \epsilon_0}{q_e^2 \lambda_D^2} \quad (6.14)$$

$$\Delta U_{\text{DH}} = -\frac{1}{8} k T \frac{V}{\pi \lambda_D^3}. \quad (6.15)$$

6.2.2 Helmholtz Free Energy

To determine the correction to the Helmholtz free energy, we have to consider the Massieu potential defined as

$$J = -\frac{A}{T} = k \ln \mathcal{Q}. \quad (6.16)$$

Its derivative with respect to temperature at constant volume is related to the internal energy as

$$\left(\frac{\partial J}{\partial T} \right)_V = k \left(\frac{\partial \ln \mathcal{Q}}{\partial T} \right)_V = \frac{U}{T^2}, \quad (6.17)$$

where the last equality follows directly from (3.26). Applying (6.16), (6.17) to the Debye-Hückel corrections of Helmholtz and internal energies, we have

$$-\left(\frac{\partial \frac{\Delta A_{\text{DH}}}{T}}{\partial T} \right)_V = \frac{\Delta U_{\text{DH}}}{T^2}. \quad (6.18)$$

Form (6.7), (6.13), we can assert that $\Delta U_{\text{DH}} \propto \frac{1}{\sqrt{T}}$ and integrating (6.18) we have

$$\Delta A_{\text{DH}} = -T \int \frac{\Delta U_{\text{DH}}}{T^2} dT = -\mathcal{K} T \int T^{-\frac{5}{2}} dT = \frac{2}{3} \frac{\mathcal{K}}{\sqrt{T}} = \frac{2}{3} \Delta U_{\text{DH}}. \quad (6.19)$$

6.2.3 Pressure

To determine the correction to pressure, we start from the general thermodynamic relation

$$\left(\frac{\partial A}{\partial V} \right)_T = -P. \quad (6.20)$$

Therefore, the correction to pressure is given by

$$\Delta P_{\text{DH}} = - \left(\frac{\partial \Delta A_{\text{DH}}}{\partial V} \right)_T = \frac{1}{12} kT \left[\frac{1}{\pi \lambda_D^3} - 3 \frac{V}{\pi \lambda_D^4} \left(\frac{\partial \lambda_D}{\partial V} \right)_T \right]. \quad (6.21)$$

From the definition in (6.7), we can say that $\lambda_D \propto \sqrt{V}$ and therefore

$$\left(\frac{\partial \lambda_D}{\partial V} \right)_T = \frac{d(\mathcal{K}\sqrt{V})}{dV} = \frac{1}{2} \frac{\mathcal{K}}{\sqrt{V}} = \frac{1}{2} \frac{\mathcal{K}\sqrt{V}}{V} = \frac{\lambda_D}{2V}. \quad (6.22)$$

Substituting this result in (6.21), we have

$$\Delta P_{\text{DH}} = \frac{1}{12} kT \left(\frac{1}{\pi \lambda_D^3} - \frac{3}{2} \frac{1}{\pi \lambda_D^3} \right) = -\frac{1}{24} \frac{kT}{\pi \lambda_D^3} = \frac{\Delta A_{\text{DH}}}{2V} = \frac{\Delta U_{\text{DH}}}{3V}. \quad (6.23)$$

The state equation follows directly from (6.20) giving

$$P = P_{\text{ideal}} + \Delta P_{\text{DH}} = \frac{\mathcal{N}kT}{V} + \Delta P_{\text{DH}} = kT \left(\frac{\mathcal{N}}{V} - \frac{1}{24\pi\lambda_D^3} \right). \quad (6.24)$$

We can use the state equation to derive V as a function of P and T ; noticing that ΔP_{DH} does not depend on the volume, being an extensive quantity, we have

$$V = \frac{\mathcal{N}kT}{P - \Delta P_{\text{DH}}}. \quad (6.25)$$

However, in general we have that $P \gg \Delta P_{\text{DH}}$ and therefore we can expand the equation in Taylor series⁵ that truncated at the first order gives

$$V \approx \frac{\mathcal{N}kT}{P} \left(1 + \frac{\Delta P_{\text{DH}}}{P} \right) \quad (6.26)$$

⁵It is $\frac{1}{a-x} = \frac{1}{a} + \frac{x}{a^2} + \frac{x^2}{a^3} + \dots$

from which we can calculate the corrections to the volume at constant pressure

$$\frac{\Delta V_{\text{DH}}}{V} = \frac{\Delta P_{\text{DH}}}{P}. \quad (6.27)$$

6.2.4 Entropy, Enthalpy and Gibbs Free Energy

The correction to the other thermodynamic functions can be obtained by using the fundamental relations between the thermodynamic functions. The entropy correction can be obtained by applying (1.8) to ΔU_{DH} (see (6.15)) and ΔA_{DH} (see (6.19))

$$\Delta S_{\text{DH}} = \frac{\Delta U_{\text{DH}} - \Delta A_{\text{DH}}}{T} = \frac{\Delta U_{\text{DH}}}{T} \left(1 - \frac{2}{3}\right) = \frac{\Delta U_{\text{DH}}}{3T} = -\frac{1}{24}k \frac{V}{\pi \lambda_D^3} \quad (6.28)$$

the enthalpy correction is given by (see (6.15), (6.23))

$$\Delta H_{\text{DH}} = \Delta U_{\text{DH}} + \Delta P_{\text{DH}}V = \Delta U_{\text{DH}} \left(1 + \frac{1}{3}\right) = \frac{4}{3} \Delta U_{\text{DH}} = -\frac{1}{6}kT \frac{V}{\pi \lambda_D^3} \quad (6.29)$$

and the Gibbs free energy correction is given by (see (6.19), (6.23))

$$\Delta G_{\text{DH}} = \Delta A_{\text{DH}} + \Delta P_{\text{DH}}V = \Delta U_{\text{DH}} \left(\frac{2}{3} + \frac{1}{3}\right) = \Delta U_{\text{DH}} = -\frac{1}{8}kT \frac{V}{\pi \lambda_D^3}. \quad (6.30)$$

6.2.5 Heat Capacity

Let us now calculate the correction to the frozen heat capacity. First, we focus on the constant volume heat capacity

$$\Delta C_{\text{vfDH}} = \left(\frac{\partial \Delta U_{\text{DH}}}{\partial T} \right)_{V, \mathcal{N}_i}. \quad (6.31)$$

Remembering that $\lambda_D \propto \sqrt{T}$ (see (6.7)), grouping all the constant quantities in a single constant we have $\Delta U_{\text{DH}} = \frac{\mathcal{K}}{\sqrt{T}}$; substituting this result in (6.31), we have

$$\Delta C_{\text{vfDH}} = \mathcal{K} \frac{d}{dT} \frac{1}{\sqrt{T}} = -\frac{\mathcal{K}}{2T\sqrt{T}} = -\frac{\Delta U_{\text{DH}}}{2T}. \quad (6.32)$$

For the constant pressure heat capacity, we refer to the equation

$$\Delta C_{\text{pfDH}} = \left(\frac{\partial \Delta H_{\text{DH}}}{\partial T} \right)_{P, \mathcal{N}_i} = \frac{4}{3} \left(\frac{\partial \Delta U_{\text{DH}}}{\partial T} \right)_{P, \mathcal{N}_i}. \quad (6.33)$$

In this case, considering (6.26), we have, at the zero-th order, that $\Delta U_{\text{DH}} \propto \frac{TV}{\lambda_D^3} \propto \frac{T^2}{\lambda_D^3}$, where $\lambda_D \propto \sqrt{TV} \propto T$. In this case, $\Delta U_{\text{DH}} \propto \frac{1}{T}$ and the heat capacity is then given by⁶

$$\Delta C_{\text{pfDH}} = \frac{4}{3} \mathcal{K} \frac{d}{dT} \frac{1}{T} = -\frac{4\mathcal{K}}{3T^2} = -\frac{4\Delta U_{\text{DH}}}{3T}. \quad (6.34)$$

6.2.6 Chemical Potential and Equilibrium Constant

Now we can calculate the Debye–Hückel correction to chemical potential using the general relation given in (3.42) extended to multicomponent system, i.e.,

$$\Delta \mu_s^{\text{DH}} = \left(\frac{\partial \Delta A_{\text{DH}}}{\partial n_s} \right)_{V, T, \mathcal{N}_i \neq s} = \frac{2}{3} \left(\frac{\partial \Delta U_{\text{DH}}}{\partial n_s} \right)_{V, T, \mathcal{N}_i \neq s}. \quad (6.35)$$

It should be noted that the dependence of ΔU_{DH} on the plasma composition is contained in the Debye length. Therefore, before proceeding in the calculation of the correction of the chemical potential, we have to determine the derivative of the Debye length with respect to the number of molecules of each species. Deriving both sides of (6.7), we have

$$\left(\frac{\partial \lambda_D^{-2}}{\partial \mathcal{N}_s} \right)_{V, T, \mathcal{N}_i \neq s} = -\frac{2}{\lambda_D^3} \left(\frac{\partial \lambda_D}{\partial \mathcal{N}_s} \right)_{V, T, \mathcal{N}_i \neq s} = \frac{q_e^2 z_s^2}{\epsilon_0 k T V} \quad (6.36)$$

from which we can obtain the desired derivative, i.e.,

$$\left(\frac{\partial \lambda_D}{\partial \mathcal{N}_s} \right)_{V, T, \mathcal{N}_i \neq s} = -\frac{\lambda_D^3 q_e^2 z_s^2}{2\epsilon_0 k T V} = \frac{1}{N_a} \left(\frac{\partial \lambda_D}{\partial n_s} \right)_{V, T, \mathcal{N}_i \neq s} \quad (6.37)$$

⁶This equation neglects the Debye–Hückel correction to volume. We can estimate easily this contribution considering that $\Delta U_{\text{DH}} \propto \frac{1}{\sqrt{TV}}$. Using the expression of V given in (6.25), we have $\Delta U_{\text{DH}} \propto \frac{\sqrt{P} - \Delta P_{\text{DH}}}{T} \approx \frac{\sqrt{P}}{PT}(P - \frac{1}{2}\Delta P_{\text{DH}})$. Calculating the derivatives we have that the contribution of volume variation in λ_D is proportional to $(\frac{\Delta U_{\text{DH}}}{T})^2$ which is a second-order correction.

remembering that $\mathcal{N}_s = n_s N_a$, being N_a the Avogadro number. Now that all the quantities have been determined, we substitute (6.15) in (6.35) obtaining

$$\Delta\mu_{s\text{DH}} = -\frac{kTV}{12\pi} \left(\frac{\partial\lambda_D^{-3}}{\partial n_s} \right)_{V,T,n_i \neq s} = \frac{kTV}{4\pi\lambda_D^4} \left(\frac{\partial\lambda_D}{\partial n_s} \right)_{V,T,n_i \neq s} \quad (6.38)$$

that combined with (6.37) it gives

$$\Delta\mu_{s\text{DH}} = -\frac{kTV}{4\pi\lambda_D^4} \frac{N_a\lambda_D^3 q_e^2 z_s^2}{2\epsilon_0 kTV} = -\frac{N_a q_e^2 z_s^2}{8\pi\epsilon_0 \lambda_D}. \quad (6.39)$$

The Debye–Hückel correction to the chemical potential of a given species is null for neutrals and negative for all charged particle

The chemical potential of a species inside a plasma is then the sum of the ideal contribution (see (1.29)) and the Debye–Hückel correction in (6.39), i.e.,

$$\mu_{is} = \mu_s^0 + RT \ln P_s + \Delta\mu_{s\text{DH}} = \mu_i^0 + RT \ln P_s - \frac{N_a q_e^2 z_s^2}{8\pi\epsilon_0 \lambda_D}. \quad (6.40)$$

Considering the generic reaction reported in (1.26), grouping the first and the last terms, the equilibrium constant in a plasma is given by

$$K_p = \exp\left(-\frac{\Delta\mu^0}{RT} - \frac{\Delta\mu_{\text{DH}}}{RT}\right) = \exp\left(-\frac{\Delta\mu^0}{RT}\right) \cdot \exp\left(-\frac{\Delta\mu_{\text{DH}}}{RT}\right). \quad (6.41)$$

The first exponential correspond to the equilibrium constant calculated in an ideal gas, the second exponential is the correction, where

$$\Delta\mu_{\text{DH}} = \sum_{i=1}^{N_s} v_i \Delta\mu_{i\text{DH}} = -\frac{N_a q_e^2}{8\pi\epsilon_0 \lambda_D} \sum_{s=1}^N v_s z_s^2. \quad (6.42)$$

6.2.7 Lowering of the Ionization Potential

The Debye–Hückel theory gives also the possibility to calculate the lowering of the ionization potential to be inserted in the Saha equation. Let us start from the definition of the chemical potential for an atomic species in an ideal gas mixture reported in (4.40)–(4.42): to this term we should add the Debye–Hückel corrections in (6.39) giving

$$\mu_s = \mu_s^{\text{tr}} + \mu_s^{\text{int}} + \mu_s^f + \Delta\mu_{s\text{DH}} = \mu'_s + \varepsilon_s^f - \frac{q_e^2 z_i^2}{8\pi\epsilon_0\lambda_D}, \quad (6.43)$$

where μ'_s combine the translational and the internal contributions⁷. From this equation, we can affirm that, in a plasma, due to the electrostatic energy (see (6.1)), the atoms need less energy to ionize, because the electron in the atom become free not when it can reach the infinity, but if it can move freely in the plasma. Therefore, the formation energy of an atom in a plasma can be considered as

$$\varepsilon_s^{f*} = \varepsilon_s^f - \frac{q_e^2 z_s^2}{8\pi\epsilon_0\lambda_D} = \varepsilon_s^f - K_{\text{DH}} z_s^2, \quad (6.44)$$

where the upscript * refers to quantity corrected by the Debye–Hückel and

$$K_{\text{DH}} = \frac{q_e^2}{8\pi\epsilon_0\lambda_D}. \quad (6.45)$$

To calculate the lowering of the ionization potential let us consider the reaction



The reaction energy, which correspond to the ionization energy of the A^{+q} species, is given by

$$I_{A^{+q}}^* = \Delta\varepsilon^* = \sum v_i \varepsilon_i^{f*} = \varepsilon_{A^{+(q+1)}}^f - K_{\text{DH}}(q+1)^2 - K_{\text{DH}} - \varepsilon_{A^{+q}}^f + K_{\text{DH}}q^2, \quad (6.47)$$

where the for electron it is $z_e = -1$ and $\varepsilon_e^f = 0$. Noticing that $I_{A^{+q}} = \varepsilon_{A^{+(q+1)}}^f - \varepsilon_{A^{+q}}^f$, with a simple algebra we have

$$I_{A^{+q}}^* = I_{A^{+q}} - K_{\text{DH}} [(q+1)^2 + 1 - q^2] \quad (6.48)$$

and the lowering of ionization potential becomes

$$\Delta I_{A^{+q}} = I_{A^{+q}} - I_{A^{+q}}^* = K_{\text{DH}}(q^2 + 2q + 1 + 1 - q^2) = 2K_{\text{DH}}(q+1). \quad (6.49)$$

6.3 The Effects of Debye–Hückel Correction

We now discuss the differences in thermodynamic properties of a reacting mixture by comparing results obtained by including or neglecting the Debye–Hückel (D–H) corrections. The differences are not simply given by the Debye–Hückel corrections

⁷Here we are neglecting the effect of the ionization lowering on the internal partition function of atomic species, that will be discussed in Chap. 8.

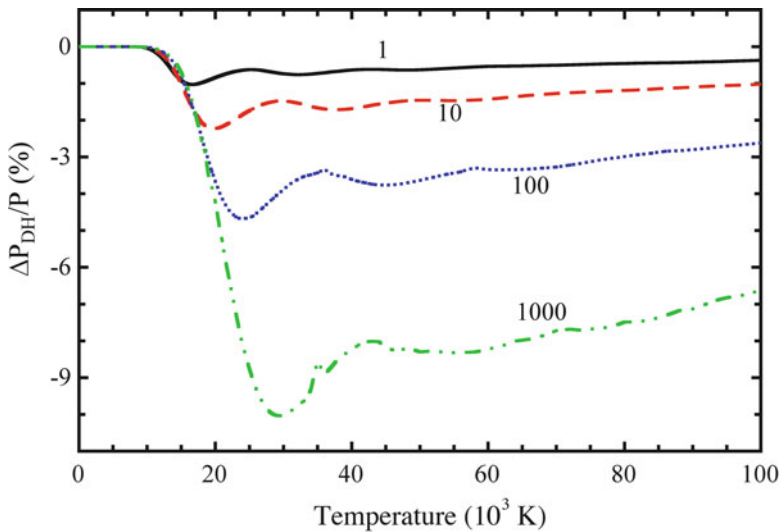


Fig. 6.1 Relative Debye–Hückel pressure correction as a function of the temperature for different values of the total pressure (bar)

described in the previous section. The equilibrium constant becomes a function of λ_D , so that the composition of the plasma changes. Moreover, for transformation at constant pressure, a further correction to composition follows from the nonideal equation of state in (6.24). As an example, we report results for air plasmas, obtained by the self-consistent approach described in (D’Angola et al. 2008)⁸.

To better enucleate the importance of Debye–Hückel corrections on the different plasma properties, we report the ratio of these corrections to the given thermodynamic properties as well as a comparison between D–H calculations and ideal quantities. In this last case, no D–H corrections are inserted in the relevant equations, in particular the lowering of the ionization potential in the different equilibria is absent. On the other hand, in the ideal case the lowering of ionization potential is used to truncate the partition function of the different atomic species. Let us first consider the D–H correction to the pressure, i.e., the quantity $\Delta P_{\text{DH}}/P$ as a function of temperature for different pressures for an air plasma (Fig. 6.1). Inspection of this figure shows that the negative corrections, while negligible at low pressure, can reach a value of 10% at $P = 1,000$ bar. For $P > 1,000$ bar, this ratio is expected to strongly increase (Zaghoul 2004, 2005).

Figure 6.2 (top) reports the correction to the enthalpy in the form $\Delta H_{\text{DH}}/H$, which closely follows the corresponding trend for the pressure with a maximum negative deviation of about 7%. In Fig. 6.2 (bottom), on the other hand, we report

⁸This paper updates self-consistently the cutoff of the electronic partition function of atoms using the lowering of the ionization potential (see (6.49)) that will be discussed in Chap. 8.

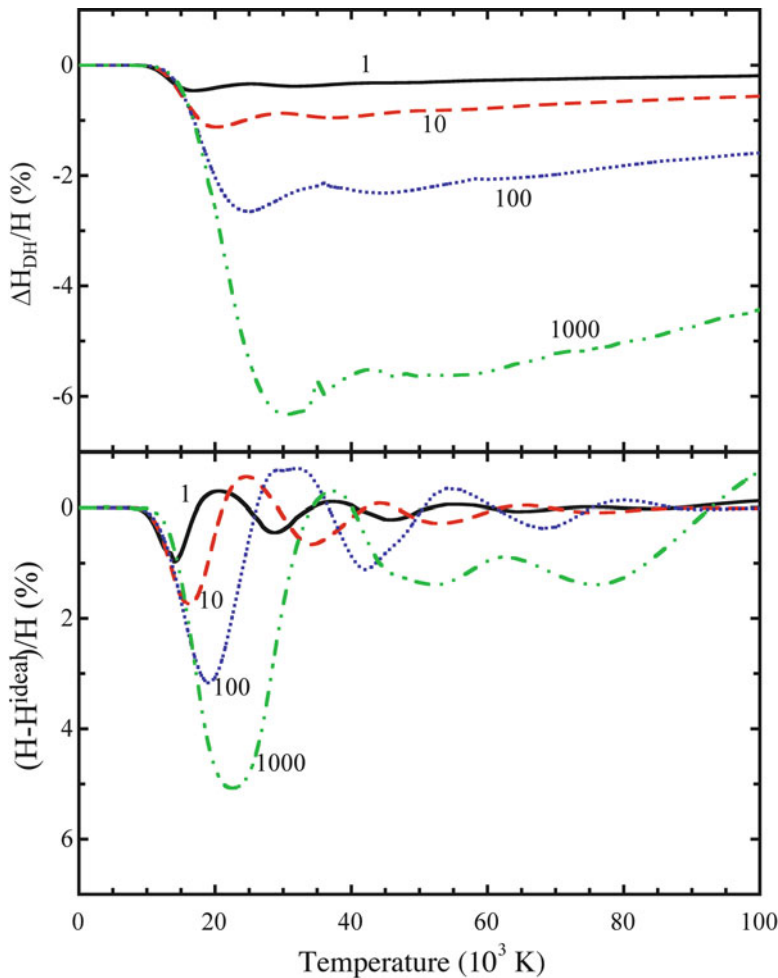


Fig. 6.2 Relative Debye–Hückel enthalpy correction (top) and the relative difference between Debye–Hückel and ideal calculations (bottom) as a function of the temperature for different values of the total pressure (bar)

the quantity $(H - H^{ideal})/H$, i.e., the relative difference between corrected (ideal + Debye–Hückel) and ideal enthalpy. The maximum deviation is similar to the results of the previous plot even though there is a continuous change of sign in this ratio.

Figure 6.3(top) reports the calculated total specific heat for the air plasma in the D–H approximation, while Fig. 6.3(bottom) reports the quantity $(c_p - c_p^{ideal})/c_p$, which presents alternance of sign as the enthalpy reaching however differences up to 15% for the higher examined pressure.

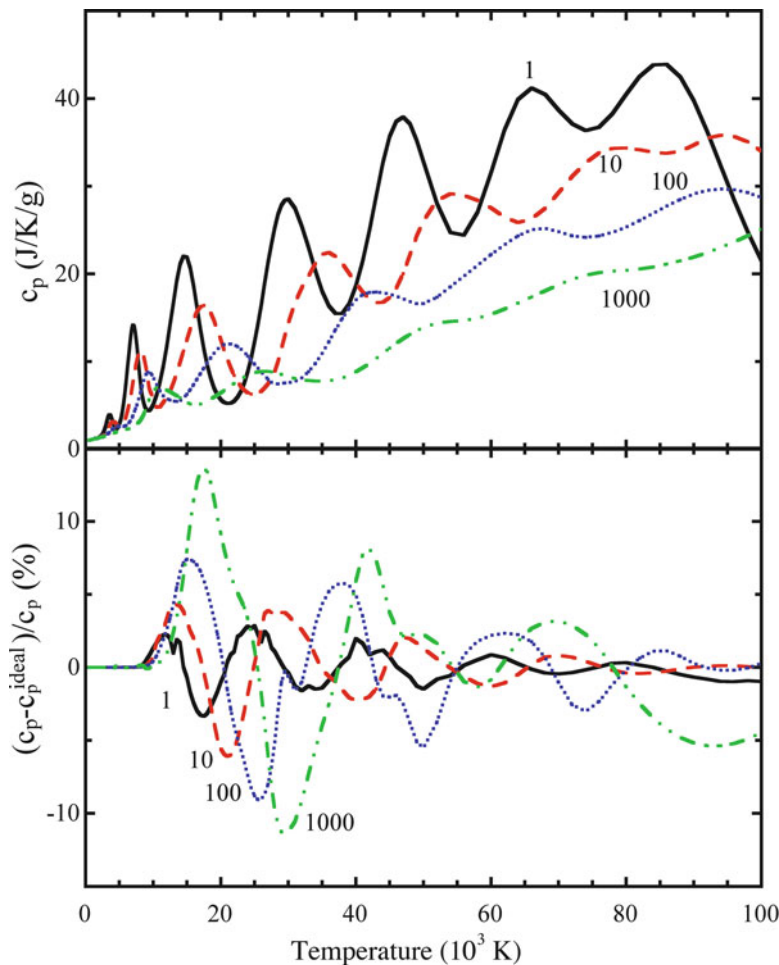


Fig. 6.3 Specific heat (top) and the relative difference between Debye–Hückel and ideal calculations (bottom) as a function of the temperature for different values of the total pressure (bar)

Finally, Fig. 6.4(top) reports the electron density for the air plasma as a function of temperature for the different pressure, while Fig. 6.4(bottom) reports the ratio N_e/N_e^{ideal} in the same conditions as Fig. 6.4(top). We can appreciate that at $P = 1,000$ bar this ratio reaches a value of approximately 1.5, probably due to the lack of the lowering of ionization potential in the ideal equilibrium constants. Similar results have been reported in (Patch 1969) for hydrogen plasma.

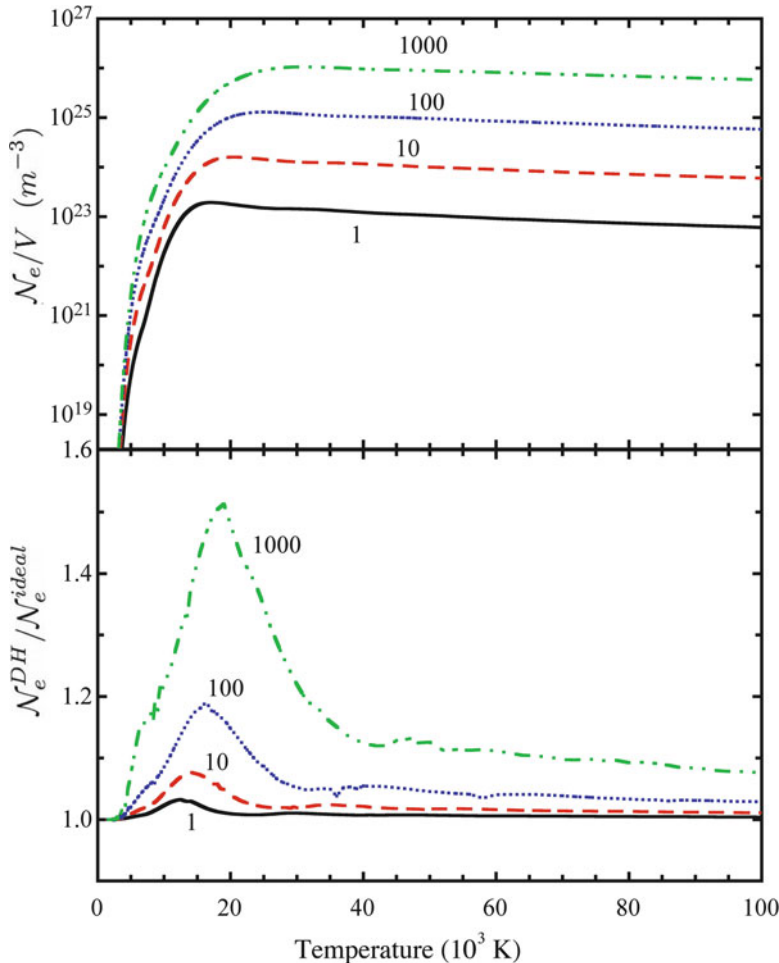


Fig. 6.4 Electron density (*top*) and ratio N_e/N_e^{ideal} (*bottom*) as a function of the temperature for different values of the total pressure (*bar*)

6.4 Beyond Debye–Hückel Theory

The results we have presented in the previous section can be considered representative of classical corrections of the ideal plasmas through the Debye–Hückel theory. The results, however, can be affected by two factors:

- the use of the classical Boltzmann statistics;
- Debye-Hückel theory considers electrons and ions as punctual charges.

Classical statistical physics can be considered a good approximation to quantum physics (Kremp et al. 2005; Fortov and Khrapak 2006) when the following

inequality between the thermal de Broglie wavelength ($\lambda_{\text{th},s}$) and the inter-particle mean distance (d_s) holds

$$\frac{\lambda_{\text{th},s}}{d_s} < 1. \quad (6.50)$$

The thermal de Broglie wavelength is given by

$$\lambda_{\text{th},s} = \sqrt{\frac{2\pi\hbar^2}{m_s k T}} = \frac{1.75 \times 10^{-9}}{\sqrt{M_s T}} \text{ m} \quad (6.51)$$

when M_s is the molar mass [g/mole] and T is expressed in (K). In turn, the inter-particle mean distance is given by

$$d_s = \frac{1}{\sqrt[3]{\hat{\mathcal{N}}_s}}, \quad (6.52)$$

where $\hat{\mathcal{N}}_s$ is the particle density of the species s .

Electrons, due to their mass, are the component which can suffer by the use of the classical Boltzmann statistics. To understand whether the inequality in (6.50) is satisfied for the limit conditions reported in this book, we consider an atomic hydrogen plasma in the following equilibrium cases (Capitelli et al. 1972).

- case (a) $P = 1,000 \text{ bar}, T = 15,000 \text{ K}$ and $\hat{\mathcal{N}}_e = 9.56 \times 10^{23} \text{ m}^{-3}$
- case (b) $P = 1,000 \text{ bar}, T = 35,000 \text{ K}$ and $\hat{\mathcal{N}}_e = 9.22 \times 10^{25} \text{ m}^{-3}$.

Use of (6.50)–(6.52) yields the following values for $\lambda_{\text{th},e}$, d_s and the ratio $\lambda_{\text{th},e}/d_e$ for the electrons in the plasma

- case (a) $\lambda_{\text{th},e} = 6.08 \times 10^{-10} \text{ m}, d_e = 1.01 \times 10^{-8} \text{ m}, \frac{\lambda_{\text{th},e}}{d_e} = 0.060$
- case (b) $\lambda_{\text{th},e} = 3.98 \times 10^{-10} \text{ m}, d_e = 2.21 \times 10^{-9} \text{ m}, \frac{\lambda_{\text{th},e}}{d_e} = 0.18$

indicating a fair amount of confidence in the use of Boltzmann statistics for the extreme conditions reported in this book.

Let us now consider the modification of the Debye–Hückel corrections allowing finite dimensions of the charged particles. The simplest model is to describe the plasma particles as hard spheres with a mean contact distance d_c . According to Ebeling (1976), this quantity is given by

$$d_c \approx \frac{\lambda_{\text{th},e}}{8}. \quad (6.53)$$

The chemical potential of a given charged species is then modified as follows (see (6.39))

$$\mu_s = \mu_s^{\text{id}} - \frac{q_e^2}{8\pi\epsilon_0\lambda_D} \left(\frac{\lambda_D}{\lambda_D + d_c} \right). \quad (6.54)$$

Inspection of (6.54) shows that the ideal chemical potential is corrected by the usual Debye–Hückel term (see (6.39)) with the additional factor $f_E = \left(\frac{\lambda_D}{\lambda_D + d_c} \right)$. Applying these corrections for the considered cases, we obtain

- case (a) $d_c = 4.98 \times 10^{-11}$ m, $\lambda_D = 8.64 \times 10^{-9}$ m, $f_E = 0.991$
 case (b) $d_c = 7.61 \times 10^{-11}$ m, $\lambda_D = 1.34 \times 10^{-9}$ m, $f_E = 0.964$.

The same conclusions can be reached by comparing the chemical potential of the electron component calculated in the ideal gas approximation with the corresponding values obtained by taking into account electron–electron interactions. Use of the results reported by Kremp et al. (2005) (see Fig. 2.1 in the reference) show that nonideality effects start contributing for $\mathcal{N}_e \geq 10^{28}$ m⁻³ ($T = 12,000$ K), an electron density range largely exceeding that one investigated in this book. Finally, we want to report that very recently corrections to the Debye–Hückel approximation have reported (Živný 2009) for calculating the constant volume thermodynamic properties of SF₆ plasma starting from different initial conditions by using essentially (6.54). The largest deviations occur for an initial concentration of SF₆ equal to 10 mole/m³, which generates a total pressure in the range 1–10,000 bar in the corresponding temperature range 1,000–50,000 K. The corresponding $\Delta P_{\text{DH}}/P$ increase from zero ($T = 1,000$ K, $P = 1$ bar) to 7.81×10^{-2} ($T = 50,000$ K, $P = 1,000$ bar). In the same temperature and pressure ranges $\Delta c_p^{\text{DH}}/c_p$ and $\Delta c_{\text{pf}}^{\text{DH}}/c_p$ values, respectively, increase from zero to 0.05 and 0.04. All corrections basically confirm the corresponding ones calculated in this chapter with first-order Debye–Hückel theory.

Chapter 7

Real Effects: II. Virial Corrections

This chapter starts defining statistical ensembles and the relative partition functions which are the starting point to completely characterize the thermodynamic properties of a system. It must be noted that the partition functions can be determined in the framework of the classical or quantum theory, considering the proper statistics. In this book, we consider mainly nondegenerate plasmas, where the effects of Pauli exclusion principle (Bose/Einstein or Fermi/Dirac distributions) are not relevant¹, and the Boltzmann statistics can be used.

7.1 Ensembles and Partition Functions

The statistical description of a system formed by a large number of particles \mathcal{N} need the definition of the phase space \mathcal{E} , having \mathcal{N}^6 dimensions, where each point is determined by the position \mathbf{r} and momentum $\mathbf{p} = m\mathbf{v}$ of each particle $[\mathbf{r}_1, \mathbf{p}_1, \mathbf{r}_2, \mathbf{p}_2, \dots, \mathbf{r}_{\mathcal{N}}, \mathbf{p}_{\mathcal{N}}] \equiv [r^{3\mathcal{N}}, p^{3\mathcal{N}}]$, where the particle position ranges in the volume of the system².

A system is also limited by constraints which define a subspace of \mathcal{E} . In the framework of statistical physics, three cases are considered, the micro-canonical (\mathcal{E}_{μ}), the canonical (\mathcal{E}_c), and grand-canonical (\mathcal{E}_G) ensembles. Each ensemble is characterized by the density of states, called also distribution function f_z , and

¹ An exception to this assumption can be found in Chap. 5 for the ortho–para effect in the rotation of light diatomic molecules.

² If the particles have internal structure, as excited states or angular momentum, variables to consider internal states must be added.

defined as the number of states in a small volume of the phase space, so that the volume of a given subsystem z , called partition function \mathcal{Q}_z is given by

$$\mathcal{Q}_z = \int_{\mathcal{E}_z} f_z(r^{3N}, p^{3N}) dr^{3N} dp^{3N} = \int_{\mathcal{E}} f_z(r^{3N}, p^{3N}) dr^{3N} dp^{3N} \quad (7.1)$$

being $f_z(r^{3N}, p^{3N}) = 0$ for $[r^{3N}, p^{3N}] \notin \mathcal{E}_z$. A physical quantity F associated with the system is then given as the mean over the given ensemble of the quantity \mathcal{F} assumed in each point of the space phase

$$F_z = \frac{1}{\mathcal{Q}_z} \int_{\mathcal{E}} \mathcal{F}(r^{3N}, p^{3N}) f_z(r^{3N}, p^{3N}) dr^{3N} dp^{3N}. \quad (7.2)$$

Nevertheless, the ensemble description is a mathematical picture and must be related to experimental operations. For a thermodynamic system, we measure the mean value of a quantity over a large interval of time over the trajectory of the system in the phase space $[r(t)^{3N}, p(t)^{3N}]$, i.e.,

$$F_z = \lim_{t \rightarrow \infty} \frac{1}{t} \int_0^t \mathcal{F}[r(\tau)^{3N}, p(\tau)^{3N}] d\tau. \quad (7.3)$$

The values calculated by the two expression in (7.2)–(7.3) must be equivalent and this is true only if for $t \rightarrow \infty$ the trajectory passes from all the points in the ensemble \mathcal{E}_z (ergodic hypothesis). Obviously, the distribution function completely defines the corresponding ensemble.

7.1.1 The Micro-Canonical Ensemble

The micro-canonical ensemble corresponds to an isolated system, defined by the constant energy constraint given by

$$E(r^{3N}, p^{3N}) = E_0. \quad (7.4)$$

Under the ergodic hypothesis, all the points of \mathcal{E} verifying (7.4) are equiprobable. Moreover, to account that in the Boltzmann statistics the exchange between particles will give no results, the factor $1/N!$ must be considered. Under these conditions, the micro-canonical distribution function is

$$f_\mu(r^{3N}, p^{3N}) = \frac{1}{N!} \delta[E(r^{3N}, p^{3N}) - E_0] \quad (7.5)$$

and the micro-canonical partition function (\check{Q}), which is the volume of the phase space occupied by the system states, is given by

$$\check{Q}_{N,E_0} = \frac{1}{N!} \int_{\mathcal{E}} \delta [E(r^{3N}, p^{3N}) - E_0] dP^{3N} dr^{3N}, \quad (7.6)$$

where δ is the Dirac function³.

7.1.2 The Canonical Ensemble

The canonical ensemble (\mathcal{E}_c) corresponds to a system, defined by the constant number of particle constraint exchanging energy with a reservoir, corresponding to a closed system in classical thermodynamics. The environment, having energy E_{res} and the system, having energy E , together must be described by a micro-canonical ensemble with the further conditions that the particles are not exchanged between the two systems, i.e.,

$$E_{\text{res}} + E(r^{3N}, p^{3N}) = E_0, \quad (7.7)$$

where E_{res} and E are calculated considering the summation in (7.4), considering the particles in its own subsystem. The canonical ensemble describes only the state of the system and the distribution function depends on the state of the environment. Considering that the environment is larger than the system and its thermal state is determined by the temperature, the distribution function is then given by (see Sect. 3.1)

$$f_c(r^{3N}, p^{3N}) = \frac{1}{N!} \delta [E_{\text{res}} + E(r^{3N}, p^{3N}) - E_0] e^{-\frac{E}{kT}} \quad (7.8)$$

and the canonical partition function (\mathcal{Q}_N^*) is defined by

$$\mathcal{Q}_N^*(T) = \int_{\mathcal{E}} \check{Q}_{N,E} e^{-\frac{E}{kT}} dE. \quad (7.9)$$

7.1.3 The Grand-Canonical Ensemble

The grand-canonical ensemble (\mathcal{E}_G) corresponds to a system exchanging energy and particles with the reservoir, i.e. an open system in classical thermodynamics. As for the canonical ensemble, the environment, having energy E_{res} and number of

³ The Dirac function can be calculated as the limit for $d \rightarrow 0$ of a square function of unitary surface and width d , i.e., $\delta(x) = \begin{cases} 0 & x \neq 0 \\ \infty & x = 0 \end{cases}$

particles \mathcal{N}_{res} , and the system, having energy E and number of particles \mathcal{N} , together must be described by a micro-canonical ensemble, i.e.,

$$\begin{aligned} E_{\text{res}} + E &= E_0 \\ \mathcal{N}_{\text{res}} + \mathcal{N} &= \mathcal{N}_0. \end{aligned} \quad (7.10)$$

The distribution function is given by

$$f_\mu(r^{3\mathcal{N}}, p^{3\mathcal{N}}) = \frac{1}{\mathcal{N}!} \delta[E_{\text{res}} + E - E_0] \delta(\mathcal{N} + \mathcal{N}_{\text{res}} - \mathcal{N}_0) e^{\frac{\mathcal{N}\mu - E}{kT}} \quad (7.11)$$

and the grand-canonical partition function ($\widehat{\mathcal{Q}}$) is calculated according the following equation

$$\widehat{\mathcal{Q}}(T) = \sum_{\mathcal{N}=0}^{\infty} \mathcal{Q}_{\mathcal{N}}^*(T) z^{\mathcal{N}}, \quad (7.12)$$

where

$$z = e^{\frac{\mu}{kT}} \quad (7.13)$$

is the fugacity (μ is the chemical potential). The summation in (7.12) has been extended to infinity because $\mathcal{N}_0 \approx \mathcal{N}_{\text{res}} \gg \mathcal{N}$.

7.2 Virial Expansion for Real Gases

The ideal gas represents the simplest model to describe a collection of \mathcal{N} mass points enclosed in a volume. Particles can interact with the boundaries of the volume by means of elastic collisions and the Hamiltonian for this system takes the form

$$\mathcal{H} = \sum_{i=1}^{\mathcal{N}} \frac{p_i^2}{2m_i}, \quad (7.14)$$

where the kinetic (or total) energies of individual particles are \mathcal{N} identified constants of the motion. This limit is valid for dilute gas, where the interactions between the particles and the interaction potential vanish over most of phase space. In this section, interactions between particles are introduced but the system will be considered sufficiently dilute so that an expansion of the pressure in a power series of the density quickly converges. This procedure, called *virial expansion*, was introduced in Sect. 1.10 in the framework of classical thermodynamics and in this chapter will be discussed from the statistical point of view. The virial expansion for a classical gas will be obtained developing the power series for the partition function $\widehat{\mathcal{Q}}$ in the grand-canonical ensemble. In the case of a real gas, the classical Hamiltonian is

$$\mathcal{H} = \sum_{i=1}^{\mathcal{N}} \frac{p_i^2}{2m_i} + \Phi(\{\mathbf{r}_i\}), \quad (7.15)$$

where $\Phi\{\mathbf{r}_i\}$ is the potential energy, function of the position of all the particles. The range of inter-particle interactions is considerably smaller than the size of the system; therefore, only pairwise interactions will be considered here, even if higher order terms can be important at high pressure.

The state of a system is characterized by the couple (E, \mathcal{N}) , whose probability is given by

$$W(E, \mathcal{N}) = \frac{1}{\bar{Q}} e^{-\frac{E-\mu\mathcal{N}}{kT}}. \quad (7.16)$$

The entropy of the system can be written as

$$\begin{aligned} S &= -k \sum_{E, \mathcal{N}} W(E, \mathcal{N}) \log W(E, \mathcal{N}) \\ &= -k \sum W \left(-\frac{E - \mu\mathcal{N}}{kT} - \log \hat{Q} \right) \\ &= \frac{U}{T} - \frac{\mu\bar{\mathcal{N}}}{T} + k \log \hat{Q} \end{aligned} \quad (7.17)$$

being

$$\begin{aligned} U &= \sum_{\mathcal{N}} E W(E, \mathcal{N}) \\ \bar{\mathcal{N}} &= \sum_{\mathcal{N}} \mathcal{N} W(E, \mathcal{N}), \end{aligned}$$

respectively, the average energy and the average number of particles. By introducing the following thermodynamic potential Ω ,

$$\Omega = -kT \log \hat{Q} \quad (7.18)$$

and by using (7.17), the Gibbs potential, introduced in Sect. 1.1, can be written as

$$G = \mu\bar{\mathcal{N}} = U - TS - \Omega = U - TS + PV \quad (7.19)$$

and the following general equation of state for a collection of $\bar{\mathcal{N}}$ indistinguishable mass points holds

$$PV = -\Omega = kT \log \hat{Q}. \quad (7.20)$$

The grand-canonical partition function is related to the canonical partition function through (7.12). In the continuos limit, the canonical partition function $\mathcal{Q}_{\mathcal{N}}^*$ can be calculated as

$$\mathcal{Q}_{\mathcal{N}}^* = \frac{1}{\mathcal{N}!} \int_{\mathcal{E}_c} d\omega e^{-\frac{\mathcal{H}(\{\mathbf{r}_i, \mathbf{p}_i\})}{kT}}, \quad (7.21)$$

where

$$d\omega = \prod_{i=1}^N d\mathbf{r}_i d\mathbf{p}_i \quad (7.22)$$

represents the volume element in the phase space \mathcal{E}_c .

For an ideal gas, the partition function (see Sect. 4.1.2 for details) is given by

$$\mathcal{Q}_N^* = \frac{1}{N!} \left(\frac{V}{\lambda_{\text{th}}^3} \right)^N, \quad (7.23)$$

where λ_{th} is the de Broglie thermal wavelength (see (4.15)). By recalling (7.12), (7.23), the grand-partition function becomes⁴

$$\widehat{\mathcal{Q}} = \sum_N \frac{1}{N!} \left(\frac{V}{\lambda_{\text{th}}^3} \right)^N z^N = \sum_N \frac{1}{N!} \left(\frac{zV}{\lambda_{\text{th}}^3} \right)^N = e^{\frac{zV}{\lambda_{\text{th}}^3}}. \quad (7.24)$$

The equation of state of ideal gas (1.60) becomes

$$\frac{PV}{kT} = \log \widehat{\mathcal{Q}} = \frac{z(\mu)V}{\lambda_{\text{th}}^3}. \quad (7.25)$$

Considering (7.19) and by recurring to thermodynamic principles

$$dU - TdS - \mu d\bar{N} = -PdV \quad (7.26)$$

the following expression holds

$$d\Omega = -SdT - \bar{N}d\mu - PdV. \quad (7.27)$$

From (7.27), the pressure P and the mean number of particles \bar{N} can be obtained, respectively, as follows

$$P = - \left(\frac{\partial \Omega}{\partial V} \right)_{T,\mu} \quad (7.28)$$

and

$$\bar{N} = - \left(\frac{\partial \Omega}{\partial \mu} \right)_{T,V}. \quad (7.29)$$

By using (7.24), the potential Ω is

$$\Omega = -kT \log \widehat{\mathcal{Q}} = -\frac{kTV}{\lambda_{\text{th}}^3} z(\mu) = -\frac{kTV}{\lambda_{\text{th}}^3} e^{\frac{\mu}{kT}} \quad (7.30)$$

⁴ $\sum_{n=0}^{\infty} \frac{x^n}{n!} = e^x$.

the mean number of particles becomes

$$\bar{\mathcal{N}} = \frac{z(\mu)V}{\lambda_{\text{th}}^3} \quad (7.31)$$

and the equation of state for an ideal gas is

$$\frac{PV}{kT} = \bar{\mathcal{N}}. \quad (7.32)$$

For real gases, the derivation of the equation of state is much more complicated due to the presence of the interaction potential in the Hamiltonian and as a consequence in the grand partition function. In fact, (7.21), considering also (7.23), becomes

$$\mathcal{Q}_{\mathcal{N}}^* = \frac{1}{\lambda_{\text{th}}^{3\mathcal{N}} \mathcal{N}!} \Theta_{\mathcal{N}}, \quad (7.33)$$

where $\Theta_{\mathcal{N}}$ are the configuration integrals⁵

$$\Theta_{\mathcal{N}} = \int \cdots \int \prod_{i=1}^{\mathcal{N}} d\mathbf{r}_i e^{-\frac{\phi(\{\mathbf{r}_i\})}{kT}} \quad (7.34)$$

and the grand-canonical partition function is

$$\hat{\mathcal{Q}} = \sum_{\mathcal{N}} \frac{1}{\lambda_{\text{th}}^{3\mathcal{N}} \mathcal{N}!} \Theta_{\mathcal{N}} z^{\mathcal{N}} \quad (7.35)$$

If the gas is sufficiently rarefied, pairwise interactions could be considered⁶ and the potential can be written as

$$\Phi(\{\mathbf{r}_i\}) = \sum_{i=1}^{\mathcal{N}} \sum_{j < i}^{\mathcal{N}} \Phi_{ij}(|\mathbf{r}_i - \mathbf{r}_j|). \quad (7.36)$$

As first step, the equation of state for a real gas is calculated in the framework of the canonical ensemble. From (7.28), considering that the partition function in the canonical ensemble is given by (7.21), the configuration integral in (7.34) becomes

$$\Theta_{\mathcal{N}} = \int \cdots \int \prod_{i=1}^{\mathcal{N}} d\mathbf{r}_i e^{-\sum_{i,j < i} \frac{\phi_{ij}}{kT}} = \int \cdots \int \prod_{i=1}^{\mathcal{N}} d\mathbf{r}_i \prod_{i,j < i} (1 + f_{ij}), \quad (7.37)$$

⁵ In this theory, interaction potentials depend only on positions $\{\mathbf{r}_i\}$ and not on the velocities $\{\mathbf{p}_i\}$ as it can happen in the presence of magnetic fields.

⁶ Considering forces which involve multi-particle interactions is possible but the theory becomes much more complicated.

where

$$f_{ij} = e^{-\frac{\phi_{ij}}{kT}} - 1 \quad (7.38)$$

are the Meyer's functions. Even considering only pairwise interactions, configuration integrals are extremely complex to evaluate. The first few terms in such an arrangement of the integrand have the form

$$\prod_{i,j < i} (1 + f_{ij}) = 1 + \sum_{j < i} f_{ij} + \sum_{j < i} \sum_{k < m} f_{ij} f_{km} + \dots, \quad (7.39)$$

where the third term must satisfy the conditions that $j \neq k$ if $i = m$ and $i \neq m$ if $j = k$. To deal systematically with such a series, it will be useful to adopt a diagrammatic notation (cluster expansion). For a dilute system, the first contribution of the series given in (7.39) is dominant and configuration integrals can be rearranged as

$$\Theta_N = V^N + \int \dots \int \sum_{j < i} f_{ij} \prod_{k=1}^N d\mathbf{r}_k. \quad (7.40)$$

Obviously, each f_{ij} depends only on the coordinates of two particles, and, for each interaction we can change the variables from single particle position to center of mass $\mathbf{R}_{ij} = (\mathbf{r}_i m_i + \mathbf{r}_j m_j)/(m_i + m_j)$ and to relative position $\mathbf{r}_{ij} = \mathbf{r}_i - \mathbf{r}_j$ ⁷ obtaining

$$\begin{aligned} \int \dots \int f_{ij} \prod_{k=1}^N d\mathbf{r}_k &= \int \dots \int \prod_{k \neq i,j} d\mathbf{r}_k \int d\mathbf{R}_{ij} \int f_{ij}(\mathbf{r}_{ij}) d\mathbf{r}_{ij} = \\ &= V^{N-1} \int f_{ij}(\mathbf{r}_{ij}) d\mathbf{r}_{ij} \end{aligned} \quad (7.41)$$

because the first integrals, as well as the one over \mathbf{R}_{ij} , are equal to the volume, and therefore we have

$$\Theta_N = V^N + V^{N-1} \sum_{j < i} \int f_{ij}(\mathbf{r}_{ij}) d\mathbf{r}_{ij}. \quad (7.42)$$

If the gas is formed by a single species, all the integrals are equal. In this case, the summation can be substituted by the factor $\frac{N(N-1)}{2} \approx \frac{N^2}{2}$ giving

$$\Theta_N = V^N + \frac{1}{2} V^{N-1} N^2 \int f_{ij}(\mathbf{r}_{ij}) d\mathbf{r}_{ij} = V^N \left(1 - \frac{N^2}{V} B_2 \right), \quad (7.43)$$

⁷ The potential here is considered spherical symmetric. The theory must be extended to consider potentials depending on the relative orientation of molecules. These effects can be important for large molecules.

where

$$B_2(T) = \frac{1}{2} \int d\mathbf{r} \left(1 - e^{-\frac{\phi(r)}{kT}} \right) = 2\pi \int_0^\infty r^2 \left(1 - e^{-\frac{\phi(r)}{kT}} \right) dr \quad (7.44)$$

represents the second coefficient of the virial expansion.

From (3.37), (7.33), in the framework of the canonical ensemble, the Helmholtz free energy A can be written as

$$\begin{aligned} A &= -kT \log Q_N^* = -kT \log \left[\frac{1}{N! \lambda_{\text{th}}^{3N}} V^N \left(1 - \frac{N^2}{V} B_2(T) \right) \right] = \\ &= -kT \left\{ N \log V - \log (N! \lambda_{\text{th}}^{3N}) + \log \left(1 - \frac{N^2}{V} B_2(T) \right) \right\} \simeq \\ &\simeq -kT \left\{ N \log V - \log (N! \lambda_{\text{th}}^{3N}) - \frac{N^2}{V} B_2(T) \right\}, \end{aligned} \quad (7.45)$$

where $\log(1+x) \approx x$ if $|x| \ll 1$. From (7.28), the equation of state can be written as

$$P = - \left(\frac{\partial A}{\partial V} \right)_T = kT \left[\frac{N}{V} + \left(\frac{N}{V} \right)^2 B_2(T) \right]. \quad (7.46)$$

Equation (7.46) contains only the first two terms of the more general virial expansion respect to $\bar{V} = V/N$ (compare with (1.143))

$$\frac{P}{kT} = \sum_{n=1}^{\infty} B_n \left(\frac{1}{\bar{V}} \right)^n, \quad (7.47)$$

which can be derived considering the full series given in (7.39) more generally in the framework of the grand-canonical ensemble.

The result in (7.47) has been derived for monoatomic gases, but it can be shown (Landau and Lifshitz 1986) that it is still valid for polyatomic gases, where the interaction potential depends on the mutual distance and on mutual orientation of the molecules. The rigorous and complete derivation of the virial expansion can be obtained in the framework of the grand-canonical ensemble, by adopting a diagrammatic notation (Hirschfelder et al. 1966; Huang 1987; Landau and Lifshitz 1986). As an example, the third and fourth virial coefficients are written as (Hirschfelder et al. 1966)

$$C = B_3 = \frac{1}{3} \iiint f_{ij} f_{jk} f_{ik} d\mathbf{r}_i d\mathbf{r}_j d\mathbf{r}_k \quad (7.48)$$

$$\begin{aligned} D = B_4 &= \frac{1}{8} \iiint \left(3f_{ij} f_{jk} f_{ks} f_{is} + 6f_{ij} f_{ik} f_{is} f_{jk} f_{ks} \right. \\ &\quad \left. + f_{ik} f_{is} f_{jk} f_{js} f_{ks} \right) d\mathbf{r}_i d\mathbf{r}_j d\mathbf{r}_k d\mathbf{r}_s. \end{aligned} \quad (7.49)$$

7.2.1 The Virial Coefficient for Mixtures

The theory presented in the previous section considers a gas formed by a single species. For mixtures, such approach needs to be extended. Being the interaction energy a global property of the gas, the expression of the thermodynamic properties does not change in the form, and it is reasonable to suppose that the differences between pure gases and mixtures are limited to the value of the virial coefficients. An important aspect of the virial expansion is that the multi-particle interaction potential is approximated as the combination of pairwise potentials⁸. To determine the dependence of the virial coefficients on the composition, we have to start from (7.42). Let us consider the particle i -th and let us group the second particle by species. Because the potential does not depend on the chosen particle, but only on the species, we can substitute the second sum over particles with the sum over species, multiplying by the number of particles

$$\Theta_N - V^N = V^{N-1} \sum_i \sum_{s_j} N_s \int f_{is_j} d\mathbf{r}_{is_j} = V^{N-1} \sum_{s_j} N_{s_j} \sum_i \int f_{is_j} d\mathbf{r}_{is_j}. \quad (7.50)$$

Now we can sum over the first index, grouping particles of the same species. However, we need to divide by 2 to account for particle exchange obtaining

$$\Theta_N - V^N = \frac{1}{2} V^{N-1} \sum_{s_i} \sum_{s_j} N_{s_i} N_{s_j} \int f_{s_i s_j} d\mathbf{r}_{s_i s_j}. \quad (7.51)$$

We can define now the second virial coefficient for the a couple of species

$$B_{s_i s_j} = \frac{1}{2} \int f_{s_i s_j} d\mathbf{r}_{s_i s_j} \quad (7.52)$$

transforming (7.51) in

$$\Theta_N = V^N \left(1 + \frac{N^2}{V} \sum_{s_i} \sum_{s_j} \chi_{s_i} \chi_{s_j} B_{s_i s_j} \right). \quad (7.53)$$

Comparing (7.43), and (7.53), we can obtain the virial coefficient for a mixture

$$B_2 = \sum_{s_i} \sum_{s_j} \chi_{s_i} \chi_{s_j} B_{2,s_i s_j}. \quad (7.54)$$

⁸ Even if the virial expansion can be applied for a generic multi-particle potential (Landau and Lifshitz 1986), a closed expression that relates the virial coefficients to the gas composition can be obtained only under the approximation of binary collisions.

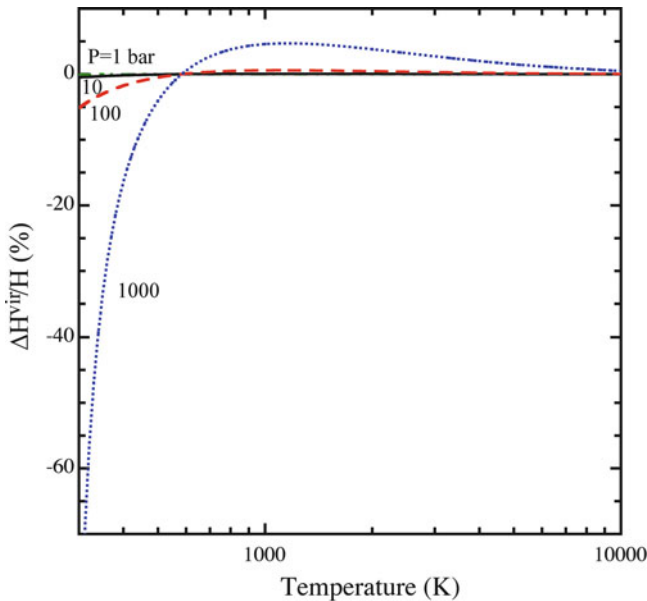


Fig. 7.1 Virial correction to air mixture enthalpy as a function of the temperature for different pressures

Similar procedure can be followed for higher approximation giving for the third coefficient

$$B_3 = \sum_{s_i} \sum_{s_j} \sum_{s_k} \chi_{s_i} \chi_{s_j} \chi_{s_k} B_{3,s_i s_j s_k}, \quad (7.55)$$

where $B_{3,s_i s_j s_k}$ is calculated following (7.48).

Virial corrections for an air mixture in the dissociation–ionization regime have been obtained by inserting (7.54), (7.55) in the relevant equations reported in Sect. 1.10. The relevant $B_{2,s_i s_j}$ and $B_{3,s_i s_j s_k}$ coefficients have been taken from the pioneeristic work of Hinselrath et al. (Hilsenrath and Klein 1965) who used phenomenological potentials for describing neutral–neutral and neutral–ion interactions. Ion–ion interactions are, on the other hand, considered in the framework of Debye–Hückel theory. It should be noted that second and third virial coefficients calculated by Hinselrath span a temperature range from 2,000 to 15,000 K so that a fitting procedure has been used to get information about their values for $T < 2,000$ K and $T > 15,000$ K.

Figures 7.1–7.4 report the virial corrections for an air plasma in a wide temperature range and for different total pressures. Inspection of the different figures shows that the virial corrections to the enthalpy, frozen specific heat, pressure and entropy

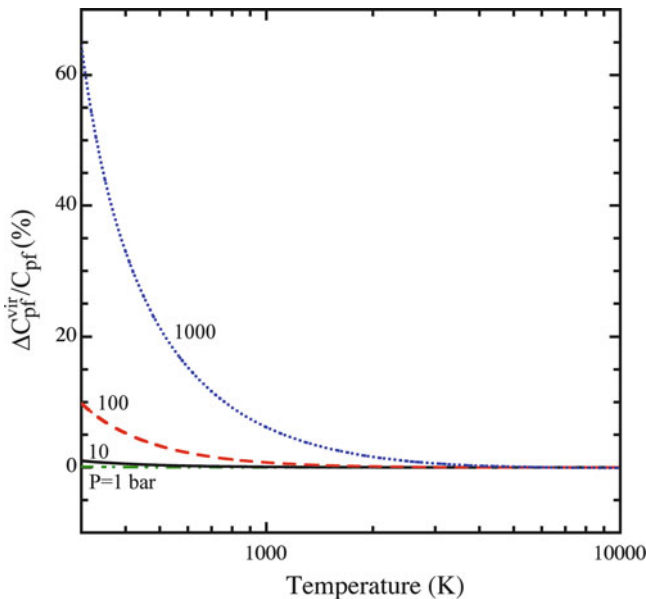


Fig. 7.2 Virial correction to air mixture frozen specific heat as a function of the temperature for different pressures

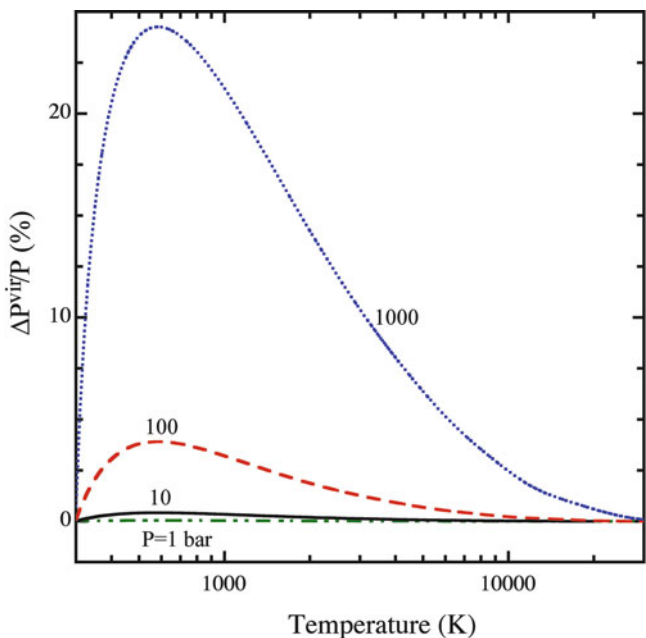


Fig. 7.3 Virial correction to air mixture pressure as a function of the temperature for different pressures

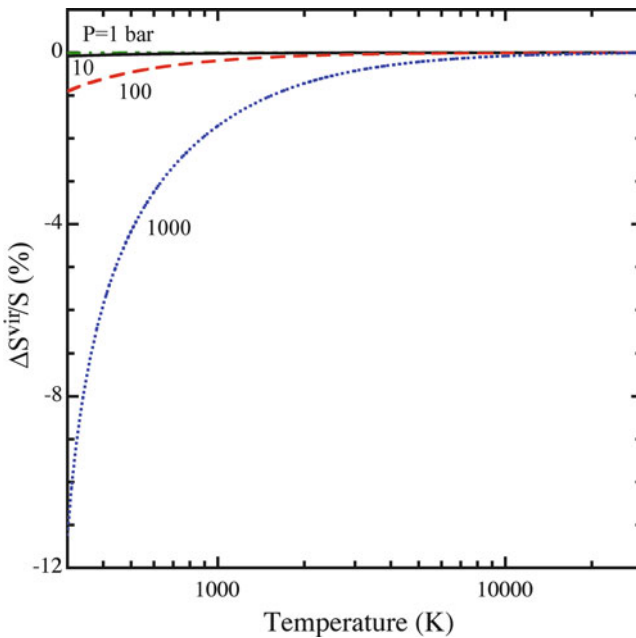


Fig. 7.4 Virial correction to air mixture entropy as a function of the temperature for different pressures

start being important from $P > 100$ bar becoming very important at $P = 1,000$ bar and $T < 2,000$ K. The entropy corrections are also in line with the estimation made in (Capitelli and Ficocelli 1977) for pure H_2 and pure Ar systems ($T = 2,000$ K, $P = 1,000$ bar). In this case, $\Delta S_{\text{vir}}/S$ are, respectively, of 0.5% and 1% against of a value of 2% for the air mixture at $P = 1,000$ bar and $T = 2,000$ K.

The results reported in Figs. 7.1–7.4 can be considered representative of the importance of virial corrections in affecting the thermodynamic properties of air plasmas in the low temperature-high pressure regime. An improvement of the input data should be made specially for correctly taking into account the atom–atom and atom–ion interactions occurring on several potential curves (see below). On the other hand, our calculations have been done by disregarding the effect of the virial corrections on the relevant equilibrium constants describing the different equilibria (see (Fisher 1966)).

Finally, it is worth noting that the results reported in Figs. 7.1–7.4 have been obtained neglecting the Debye–Hückel corrections to avoid possible compensation effects.

7.3 Virial Coefficient Calculations

The second virial coefficient can be obtained directly by experiments or by integrating (7.44) with suitable potentials. In addition to the considerations made in Sect. 1.10 on the linking between the virial coefficients and the parameters a and b in the Van der Waals equation, we want to discuss the following points:

1. The direct calculation of second virial coefficient from phenomenological potentials.
2. The calculation of second virial coefficient for atom–atom and atom–ion interactions occurring on bound and repulsive potential curves.

7.3.1 Phenomenological Potential

The calculation of $B(T)$ for neutral–neutral interaction is usually performed by using a phenomenological potential which contains a finite-sized hard core with a weak attractive well following at larger distances. These phenomenological potentials derive from improvement of Lennard-Jones (Hirschfelder et al. 1966) type potential (see also (Pirani et al. 2004, 2006)). Under many case, a Buckingham EXP6 potential (Hirschfelder et al. 1966) is used.

Second virial coefficients as a function of the temperature are reported in Fig. 7.5 (left) for $N_2 - N_2$, $N - N_2$ and $N - N$ interactions (Hilsenrath and Klein 1965) and in Fig. 7.5 (right) for $H_2 - H_2$, $H - H_2$ and $H - H$ (Fisher 1966). Note that the phenomenological $N - N$ virial coefficients (Hilsenrath and Klein 1965)

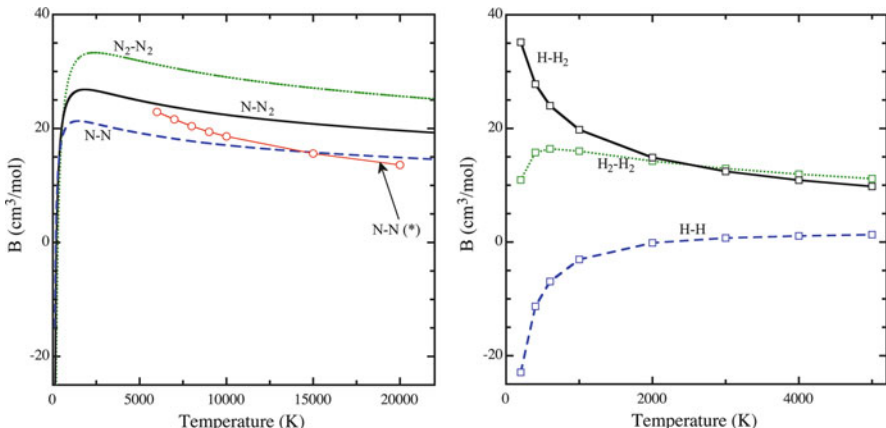


Fig. 7.5 Second virial coefficient for interactions in $N_2 - N$ (Hilsenrath and Klein 1965) and $H_2 - H$ (Fisher 1966) systems. Comparison with $N - N (*)$ (Guidotti et al. 1976) calculated for the pure repulsive potential ${}^7\Sigma_u$

is very close for $T > 2,000$ K to the corresponding values calculated considering only the repulsive septet state of the $N(^4S) + N(^4S)$ interaction (Guidotti et al. 1976), implying that the phenomenological potential overestimates the repulsive contribution.

7.3.2 Open Shells Interactions

In the case of atom–atom as well as atom–ion interactions with incomplete shells, the second virial coefficient is given by an average between all contributions arising in the collision (Capitelli and Lamanna 1976; Guidotti et al. 1976). As an example, two oxygen atoms in the ground state (3P) can interact along 18 potential curves (12 repulsive and 6 bound), while the same atoms in the electronic state 1S interact along one repulsive potential. The second virial coefficient in the case of multipotential interaction is given by

$$B(T) = \langle B \rangle = \frac{\sum_k g_k B_k}{\sum_k g_k}, \quad (7.56)$$

where g_k and B_k are, respectively, the statistical weight factor and the second virial coefficient for k -th potential curve. The sum is carried out over all potentials which correlate at large distances with the same electronic states (i.e., $n = 18$ for $^3P + ^3P$; $n = 1$ for $^1S + ^1S$).

The calculation of (7.44) for repulsive states⁹ is straightforward while some caution must be used for attractive potentials. In this last case, the virial coefficient can be split, to a good accuracy, into two contributions

$$B = B_f + B_b, \quad (7.57)$$

where B_f is the contribution due to the atoms which collide, but remain separated (positive energy states), and B_b is the contribution related to molecule formation in a bound state (negative energy). In many circumstances, one must calculate only B_f , because B_b is generally taken into account in the equilibrium constant of the dissociation reaction and internal partition function (Biolsi and Holland 1996, 2010). The coefficient B_f can be calculated by considering an effective potential following the Hill procedure (Hill 1955) or subtracting the bound and quasi-bound contributions from the total second virial coefficient following Rainwater (Rainwater 1984).

Figure 7.6 reports the second virial coefficients calculated by (7.57), (7.56) (only B_f for bound states) for $N - N$ (Guidotti et al. 1976) and $O - O$ (Capitelli and Lamanna 1976) interactions with the corresponding values obtained by Hilsenrath

⁹ In principle, no completely repulsive state exists due to the presence of very small depth due to Van der Waals forces.

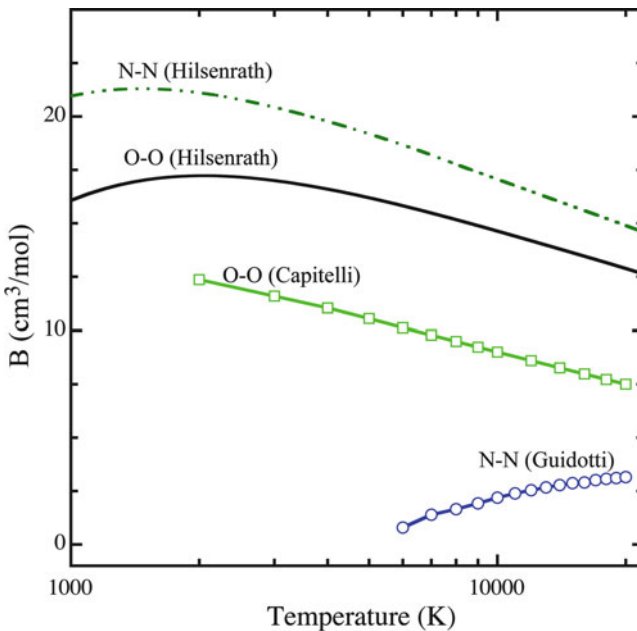


Fig. 7.6 Second virial coefficient of $O - O$ and $N - N$ interactions. Comparison between (Hilsenrath and Klein 1965; Capitelli and Lamanna 1976) and (Guidotti et al. 1976)

(Hilsenrath and Klein 1965). We can see that the differences between the two sets of results are very important, the phenomenological values being much larger than the corresponding ones, which consider the B_f in the calculation of the bound potential.

This contribution presents negative values decreasing the positive one from the completely repulsive states. In the case of $N - N$ interaction, the first two bound potentials (${}^1\Sigma_g^+$, ${}^3\Sigma_u^+$) states present B_f negative values which decrease the positive contribution from the septet state, the quintet state being in intermediate position. This explains the large differences reported in Fig. 7.6. In the case of $O - O$ interaction, the differences between values from (Hilsenrath and Klein 1965) and from (Capitelli and Lamanna 1976) are lower due to the fact that only six potentials over eighteen are bound. It should be noted that also B_{H-H} values reported in Fig. 7.5 have been calculated, in addition to the triplet repulsive state, taking into account the B_f contribution from the singlet bound $H - H$ potential.

7.4 The REMC Method

The Reaction Ensemble Monte Carlo method (REMC) is a molecular-level computer simulation technique for predicting the equilibrium behavior of reactions under nonideal conditions. The REMC method was independently developed and

published by two different groups in 1994 (Johnson et al. 1994; Smith and Triska 1994). REMC provides a computational tool for the exact¹⁰ calculation of macroscopic plasma properties, such as equilibrium concentration for each species, and relevant thermodynamic quantities, such as density, pressure and energy, considering simultaneously multiple reactions and multiphase transitions. The only required information for molecular-level computer simulation techniques is a description of the intermolecular forces among the particles and internal chemical potentials for the reacting components.

REMC is based on the grand-canonical ensemble for a multicomponent plasma, since it involves molecular and atomic production and loss due to chemical reactions and to particle movement in and out the computational volume.

REMC can be adopted considering different constraints, i.e., fixing two relevant quantities between internal energy, enthalpy, entropy, temperature, pressure, and volume (Smith and Lísal 2002; Smith et al. 2006). The resulting methods enable, for example, the direct solution of isoentropic or adiabatic problems.

In the following some details of REMC calculations under constant pressure and temperature conditions, for a single-phase system, will be given. Reaction equilibria in plasmas at specified temperature and pressure are attained when the Gibbs free energy of the system is minimized, subjected to mass conservation and charge neutrality conditions. Adding to the total partition function, the internal term $\mathcal{Q}_i^{\text{int}}$ for a molecule i which includes rotational, vibrational, electronic, and nuclear contributions, the grand-canonical partition function for a mixture of N reacting components can be written, from (7.33), as

$$\begin{aligned} \hat{\mathcal{Q}} &= \prod_{i=1}^N \sum_{\mathcal{N}_i=0}^{\infty} (\mathcal{Q}_i^{\text{int}})^{\mathcal{N}_i} \mathcal{Q}_{\mathcal{N}_i}^* z_i^{\mathcal{N}_i} = \\ &= \sum_{\mathcal{N}_1=0}^{\infty} \cdots \sum_{\mathcal{N}_s=0}^{\infty} \exp \left(\beta \sum_{i=1}^N \mathcal{N}_i \mu_i \right) \prod_{i=1}^N \frac{\mathcal{Q}_i^{\text{int}} \Theta_{\mathcal{N}_i}}{\lambda_{\text{th}}^{3\mathcal{N}_i} \mathcal{N}_i!} = \\ &= \sum_{\mathcal{N}_1=0}^{\infty} \cdots \sum_{\mathcal{N}_s=0}^{\infty} \exp(\Upsilon) \prod_{i=1}^N \frac{\Theta_{\mathcal{N}_i}}{V^{\mathcal{N}_i}}, \end{aligned} \quad (7.58)$$

where

$$\Upsilon = \sum_{i=1}^N \left[\beta \mathcal{N}_i \mu_i - \log(\mathcal{N}_i!) + \mathcal{N}_i \log \left(\frac{V \mathcal{Q}_i^{\text{int}}}{\lambda_{\text{th}}^3} \right) \right]. \quad (7.59)$$

Starting from the definition given in (7.34), configuration integrals $\Theta_{\mathcal{N}_i}$ can be written as

$$\Theta_{\mathcal{N}_i} = V^{\mathcal{N}_i} \int \cdots \int dx^{\mathcal{N}_i} d\omega^{\mathcal{N}_i} e^{-\beta\Phi(\{V, x_1, \dots, x_{\mathcal{N}_i}\})}, \quad (7.60)$$

¹⁰ Here, *exact* means that all the terms in the Debye–Hückel theory and infinite virial expansions are considered.

where $x = r/V^{1/3}$ is a set of scaled coordinates, and ω is a set of orientations and the grand canonical partition function given in (7.58) becomes

$$\hat{Q} = \sum_{N_1=0}^{\infty} \cdots \sum_{N_s=0}^{\infty} \int \cdots \int dx^{N_1} d\omega^{N_1} \cdots dx^{N_s} d\omega^{N_s} \exp [\Upsilon - \beta \Phi (\{V, x_{N_i}\})]. \quad (7.61)$$

Deviation from nonideality in plasmas arises from long-range Coulombic interaction between charged particles and from short-ranged neutral–neutral and neutral–charge interactions. Debye–Hückel theory, described in Chap. 6, takes into account the first source of nonideality¹¹. The contribution of Coulombic interaction can be accounted for into the REMC method using (6.23), (6.49) which are, respectively, the ionization potential lowering, entering in the Saha equation, and the correction to the system pressure.

Computer simulations are usually performed by using a small number N of particles and the size of the box is limited by the available storage and by the speed of execution of the program. The computational time taken for evaluating the potential energy is proportional to N^2 . When a particle moves crossing the boundary of the box, the problem of surface effects can be overcome by implementing periodic boundary conditions. The cubic box is replicated throughout space to form an infinite lattice. In the course of the simulation, as a particle moves in the original box, its periodic image in each of the neighboring boxes moves in exactly the same way. Thus, as a particle leaves the central box, one of its images will enter through the opposite face. There are no walls at the boundary of the central box, and no surface particle. This box simply forms a convenient axis system for measuring the coordinates of the N particles. When periodic boundary condition is adopted an infinite number of terms is requested in order to evaluate the total energy. For a short-range potential energy function, the summation to evaluate total energy can be restricted considering the particle at the center of a region which has the same size and shape as the basic simulation box, so that it interacts with all the particles whose centers lie within this region. This method is called the minimum image convention and involves $N(N-1)/2$ terms for the calculation of the potential energy due to pairwise-additive interactions.

The REMC method generates a Markov chain to simulate the properties of the system governed by (7.61); the chain consists of a combination of three main types of Monte Carlo steps or state transitions:

- D* Particle displacements.
- R* Reaction moves.
- V* Volume changes fixing the pressure.

¹¹ The Debye–Hückel theory introduces the lowering of ionization potential and the correction to pressure and to all the thermodynamic functions. It results in a correlation between the configuration integral and the internal partition function.

Particle displacements and volume changes are implemented and obtained as in traditional molecular dynamic simulations (Allen and Tildesley 1989; Frenkel and Smit 2002). Particles are initially placed in a simulation box and the total energy of the system is evaluated considering that only pairwise interactions are relevant. Initial configuration may correspond to a regular crystalline lattice or to a random configuration but with no hardcore overlaps. A particle is randomly selected and a random displacement is given by

$$\mathbf{r}^l = \mathbf{r}^k + \Delta (\varsigma - 0.5), \quad (7.62)$$

where k and l are, respectively, the initial and the final state of the system, Δ are small displacements properly selected and ς are random numbers uniformly distributed between 0 and 1. The reverse trial move is equally probable. The particle displacement is accepted with a transition probability $k \rightarrow l$ given by

$$W_{kl}^D = \min [1, \exp(-\beta \Delta \Phi_{kl})] \quad (7.63)$$

while old configuration is considered if the transition is not accepted, i.e. the generated random number is higher than W_{kl} .

In REMC simulations at pressure and temperature fixed, the volume is simply treated as an additional coordinate, and trial moves in the volume must satisfy the same rules as trial moves in positions. A volume trial move consists of an attempted change of the volume from V_k to V_l (Allen and Tildesley 1989; Frenkel and Smit 2002)

$$V_l = V_k + \Delta V (\varsigma - 0.5) \quad (7.64)$$

and such a random, volume-changing move will be accepted with the probability

$$W_{kl}^V = \min \left\{ 1, \exp \left[-\beta \Delta \Phi_{kl} - \beta (V_l - V_k) P + \mathcal{N} \log \frac{V_l}{V_k} \right] \right\}. \quad (7.65)$$

When a volume change is accepted, the size of the box and the relative position of the particles change. In order to calculate W_{kl}^V the new configuration energy must be recalculated considering the new distances between particles.

In the case of one phase, chemically reacting system with one reaction at constant temperature and volume (Lisal et al. 2000, 2002), changes in the number of particles \mathcal{N}_i due to the reaction steps satisfy the law of conservation of mass for the system, which may be expressed as

$$\mathcal{N}_i = \mathcal{N}_i^0 + \xi v_i \quad i = 1, 2, \dots, s, \quad (7.66)$$

where ξ is the extent of reaction (generally an integer equal to 1 for a forward reaction and -1 for a reverse reaction), \mathcal{N}_i^0 the number of particles of species i in the state prior to a reaction step, and v_i the stoichiometric number of species i . In

the following, reaction events are attempted in the forward and the reverse directions with equal probability and the reaction considered can be expressed as

$$\sum_{i=1}^N \nu_i X_i = 0, \quad (7.67)$$

where X_i denotes the chemical symbol of species i . Starting from the grand-canonical partition function 7.61, the probability that a system is in a state k is

$$W_k = \frac{1}{\mathcal{Q}} \exp \left[\beta \sum_{i=1}^N \mathcal{N}_i \mu_i - \sum_{i=1}^N \log (\mathcal{N}_i!) + \sum_{i=1}^N \mathcal{N}_i \log \left(\frac{V \mathcal{Q}_i^{\text{int}}}{\lambda_{\text{th}}^3} \right) - \beta \Phi_k \right], \quad (7.68)$$

where Φ_k is the configurational energy of state k . If the reaction proceeds in the forward direction the probability of the state l is

$$W_l = \frac{1}{\mathcal{Q}} \exp \left\{ \begin{aligned} & \beta \sum_{i=1}^N (\mathcal{N}_i + \nu_i) \mu_i - \sum_{i=1}^N \log [(\mathcal{N}_i + \nu_i)!] + \\ & + \sum_{i=1}^N (\mathcal{N}_i + \nu_i) \log \left(\frac{V \mathcal{Q}_i^{\text{int}}}{\lambda_{\text{th}}^3} \right) - \beta \Phi_l \end{aligned} \right\} \quad (7.69)$$

and the transition probability for the reaction in the forward direction $W_{kl}^{\xi=+1}$ is given by

$$W_{kl}^{\xi=+1} = \min \left\{ 1, V^{\bar{\nu}} \prod_{i=1}^N \left(\frac{\mathcal{Q}_i^{\text{int}}}{\lambda_{\text{th}}^3} \right)^{\nu_i} \prod_{i=1}^N \left[\frac{(\mathcal{N}_i^0)!}{(\mathcal{N}_i^0 + \nu_i)!} \right] \exp (-\beta \Delta \Phi_{kl}) \right\}, \quad (7.70)$$

where $\bar{\nu} = \sum_i \nu_i$ is the net change in the total number of particles for the reaction considered. Recalling that the ideal gas equilibrium constant is given by

$$K_p = \exp \left(-\frac{\Delta \mu^0}{RT} \right) = (\beta P)^{-\bar{\nu}} \prod_{i=1}^N \left(\frac{\mathcal{Q}_i^{\text{int}}}{\lambda_{\text{th}}^3} \right)^{\nu_i} \quad (7.71)$$

while the contribution of ionization lowering is not included in the equilibrium constant but as a further pressure correction (Lisal et al. 2000). The transition probability for a reaction move can be written as

$$W_{kl}^{\xi} = \min \left\{ 1, (\beta P V)^{\xi \bar{\nu}} K_p^{\xi} \prod_{i=1}^N \left[\frac{(\mathcal{N}_i^0)!}{(\mathcal{N}_i^0 + \xi \nu_i)!} \right] \exp (-\beta \Delta \Phi_{kl}) \right\}. \quad (7.72)$$

To simulate a chemically reacting system at specified temperature and pressure rather than at constant temperature and volume, a trial volume change as in (7.65) must be considered.

In the case of multiple reactions, the REMC approach outlined above for a single chemical reaction can be straightforwardly generalized (Turner et al. 2008). For any linearly independent set of n_R chemical reactions given by

$$\sum_{i=1}^N v_{ij} X_i = 0 \quad j = 1, 2, \dots, n_R \quad (7.73)$$

and considering that

$$\mathcal{N}_i = \mathcal{N}_i^0 + \sum_{j=1}^{n_R} v_{ij} \xi_j \quad i = 1, \dots, s; j = 1, \dots, n_R \quad (7.74)$$

the transition probability for a step ξ_j is

$$W_{kl}^{\xi_j} = \min \left\{ 1, (\beta P V)^{\xi_j \bar{v}_j} K_{p,j}^{\xi_j} \prod_{i=1}^{s_j} \left[\frac{(\mathcal{N}_i^0)!}{(\mathcal{N}_i^0 + \xi_j v_{ij})!} \right] \exp(-\beta \Delta \Phi_{kl}) \right\}, \quad (7.75)$$

where $\bar{v}_j = \sum_{i=1}^{s_j} v_{ij}$ is the net change in the total number of particles for the reaction j .

The procedure for a reaction move is the following:

- A reaction is randomly selected.
- The reaction direction, forward or reverse, is randomly selected.
- A set of reactants and products according to the stoichiometry of the reaction considered is randomly selected.
- The reaction move is accepted by evaluating the probability associated with performing changes of particle identities, together with particle insertions and deletions, if the total number of particles changes during the selected reaction.

If \mathcal{N} is the total number of particles, the optimal choice to speed up the convergence of the method is to consider steps (D) , (R) and (V) with the relative frequency $\mathcal{N} : \mathcal{N} : \alpha \mathcal{N}$ with α in the range 1–10.

REMC approach is particularly suitable for plasmas especially at high pressure. This method has been successfully applied to Helium (Smith and Triska 1994), Argon and air plasmas (Lisal et al. 2002), respectively, consisting of 2, 7 and 26 ionization reactions. The interactions between charged particles in these calculations were described by Deutsch potentials (Smith and Triska 1994; Lisal et al. 2002) while both the neutral–neutral particle interactions and the neutral–ion particle interactions were approximated by EXP6 potentials (Ree 1983).

Figures 7.7, 7.8 show the comparison of the molar specific heat and of the molar enthalpy of Helium at 4,000 bar obtained by REMC simulation with

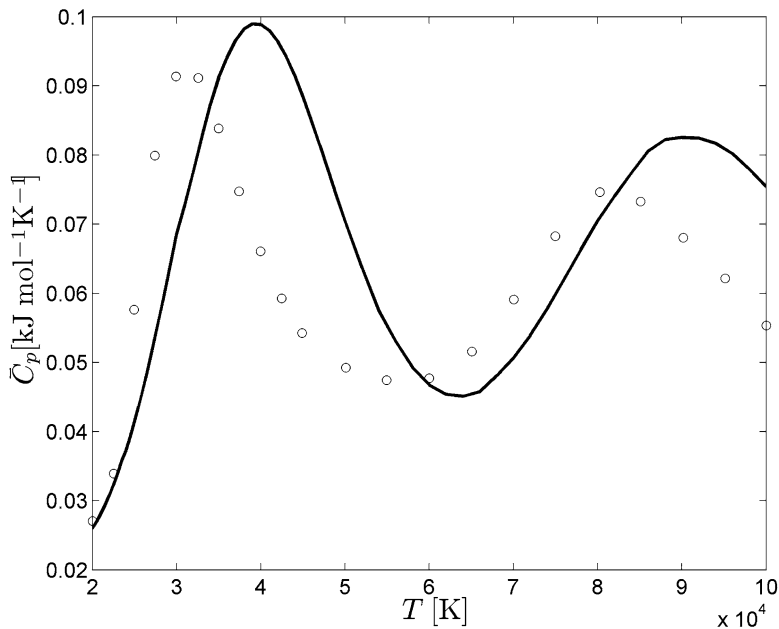


Fig. 7.7 Molar heat capacity of the helium plasma at 4,000 bar. Circles denote the REMC simulation results (Smith and Triska 1994), with solid curve corresponding to the results obtained using the Debye–Hückel approximation

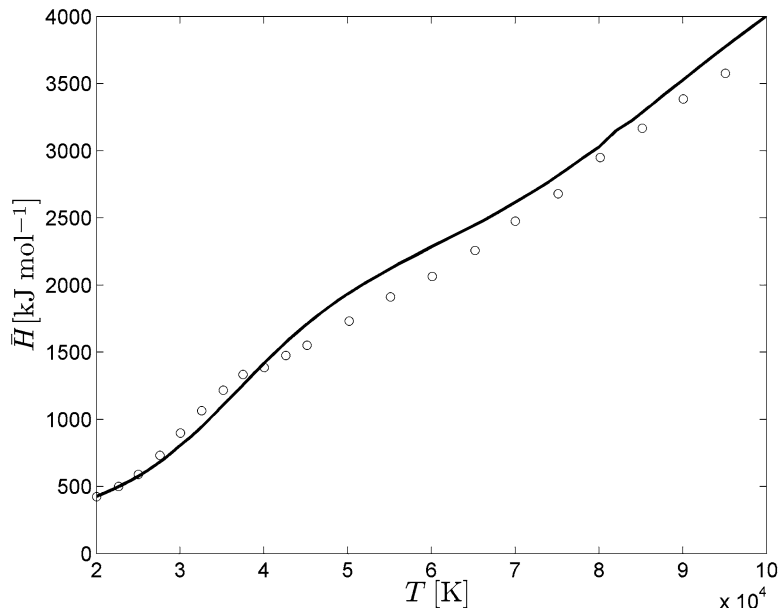


Fig. 7.8 Molar enthalpy of the helium plasma at 4,000 bar. Circles denote the REMC simulation results (Smith and Triska 1994), with solid curve corresponding to the results obtained using the Debye–Hückel approximation

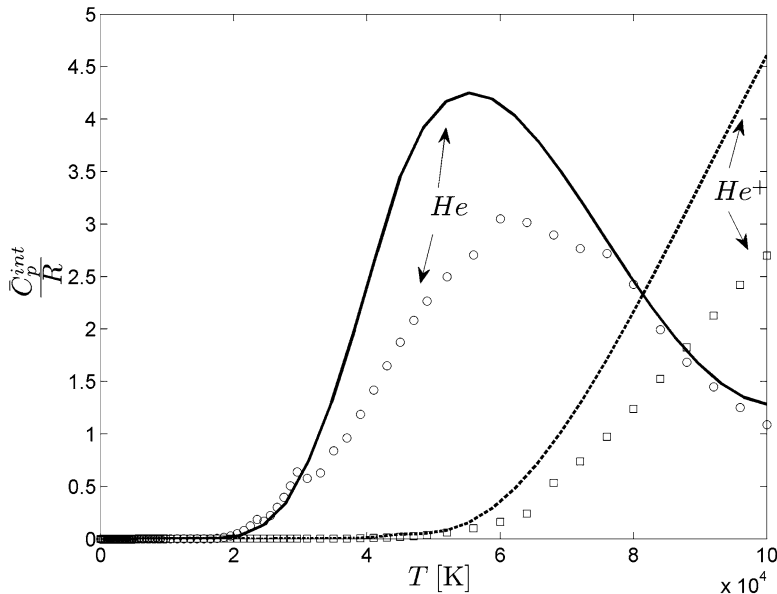


Fig. 7.9 Internal molar heat capacity of He and He^+ at 4,000 bar. Circles and squares denote results obtained using Debye–Hückel approximations, with dashed and solid curves corresponding to the data used by Lisal in REMC simulations (Smith and Triska 1994)

those obtained by statistical thermodynamic approach, including Debye–Hückel corrections (D’Angola et al. 2008) (see also Chap. 10). However, different data have been used in REMC (NIST 2009) and in statistical thermodynamic calculations (Pagano et al. 2008; Pagano et al. 2009), in order to estimate the internal contribution of atomic species to the thermodynamic properties and equilibrium constants. In particular, Fig. 7.9 shows internal molar heat capacity of He and He^+ adopted for REMC and our self-consistent calculations. It should be noted that the REMC data use only observed levels without any cutoff criteria, while the Debye–Hückel calculations consider extension of levels using Ritz–Rydberg approach (see Sect. A.3) with a proper cutoff criterion (see Chap. 8), which introduces in the internal contribution the dependence on the pressure. As a result, in the present case at very high pressure, the used self-consistent cutoff introduces less electronic levels in both He and He^+ partition functions with respect to the REMC method, having strong consequence on the internal specific heat. This point can partially explain the differences observed in Figs. 7.7, 7.8 in addition to the different methods to treat non-ideal effects.

Chapter 8

Electronic Excitation and Thermodynamic Properties of Thermal Plasmas

In this chapter, we will show the importance of electronic excitation in deriving partition functions, their first and second derivatives, as well as the thermodynamic properties of single atomic species and of plasma mixture. Recent results obtained by using different cutoff criteria are discussed and compared with the so-called *ground state method*, i.e., by inserting in the electronic partition function only the ground electronic state of the atomic species. The results obtained by a self-consistent calculation of partition function, equilibrium composition and thermodynamic properties will be rationalized taking into account the qualitative considerations reported in Chap. 1.

A rich literature (Capitelli and Molinari 1970; Capitelli and Ficocelli 1970, 1971; Capitelli et al. 1971, 2009) does exist on the subject indicating the existence of compensation effects in the calculation of the thermodynamic properties of thermal plasmas which hide in some cases the role of electronic excitation of atomic species in affecting the global thermodynamic properties of the plasmas. Results for the case study of an oxygen plasma in a wide range of temperature (500–100,000 K) and pressure (1–1,000 bar) are reported and can be considered representative of many other systems.

As a matter of fact, the atomic levels entering in the partition function are calculated or measured considering an isolated atom, such that the energy of the levels is not perturbed by the environment. On the other hand, we present some results obtained considering the influence of the plasma on the energy levels by solving the Schrödinger equation for the atomic hydrogen in the presence of the Debye potential.

8.1 Cutoff Criteria

We have already anticipated in Chap. 4 the necessity to introduce a suitable cutoff criterion to prevent the divergence of electronic partition functions of atomic

hydrogen. We extend these results to multi-electron atoms by using different cutoff criteria including:

- (a) The ground state method.
- (b) The Debye Hückel cutoff criteria.
- (c) The Fermi criterion.

Strong differences are expected especially when a complete set (observed and missing) of electronic levels is used in the calculation.

8.1.1 The Ground State Method

In this case, the internal partition function includes only the ground state

$$\mathcal{Q}^{\text{int}} = g_1 \quad (8.1)$$

resulting in null derivatives

$$\frac{d\mathcal{Q}^{\text{int}}}{dT} = \frac{d^2\mathcal{Q}^{\text{int}}}{dT^2} = 0 \quad (8.2)$$

completely disregarding the contribution of internal states.

8.1.2 Debye–Hückel Criteria

In this case, we have two types of approach, one due to Griem (Griem 1962, 1997) and one due to Margenau and Lewis (M&L) (Margenau and Lewis 1959).

According to Griem, we write the electronic partition function of a given atomic species as

$$\mathcal{Q}^{\text{int}} = \sum_{n=1}^{\varepsilon_{\max}} g_n e^{-\frac{\varepsilon_n}{kT}},$$

where ε_n and g_n represent in the order the energy and the statistical weight of the n -th level. The sum includes all levels with energy up to a maximum value given by

$$\varepsilon_{\max} = I_s - \Delta I_s.$$

In turn, the lowering of the ionization potential ΔI_s is given by

$$\Delta I_s = \frac{q_e^2}{4\pi\epsilon_0} \sqrt{\frac{q_e^2 \sum_{s=1}^N \frac{\mathcal{N}_s}{V} z_s^2}{\epsilon_0 k T}} (z_s + 1) = \frac{q_e^2 (z_s + 1)}{4\pi\epsilon_0 \lambda_D}. \quad (8.3)$$

Following M&L, the electronic partition function for atomic hydrogen is written as

$$\mathcal{Q}^{\text{int}} = \sum_{n=1}^{n_{\max}} g_n e^{-\frac{\varepsilon_n}{kT}},$$

where n_{\max} is the maximum principal quantum number to be inserted in the partition function. In turn, n_{\max} is obtained by assuming that the classical Bohr radius of hydrogenoid atoms does not exceed the Debye length λ_D i.e.

$$\frac{n_{\max}^2 a_0}{Z_{\text{eff}}} = \lambda_D,$$

where $Z_{\text{eff}} = z_s + 1$ is the effective charge seen by the electronic excited state being z_s the charge of the species¹ and a_0 is the Bohr radius. Keeping in mind the expression

$$\lambda_D [\text{m}] = 69.0 \sqrt{\frac{TV}{\sum_s N_s z_s^2}},$$

where V is the volume in [m^3], we get

$$n_{\max} = 1.14 \times 10^6 \sqrt[4]{\frac{Z_{\text{eff}}^2 TV}{\sum_s N_s z_s^2}}. \quad (8.4)$$

The two formulations coincide when use is made of hydrogen-like levels presenting, however, large differences when the dependence of energy on the angular and spin momenta is considered. In this last case, the partition functions and related properties calculated according to M&L method exceed the corresponding *Griem* values (Capitelli and Ficocelli 1971; Capitelli and Ferraro 1976). This point should be taken into account when comparing the well-known Drellishak et al. (1963a; 1963b; 1964; 1965) partition functions based on the M&L theory and the corresponding values obtained by the Griem method (see (Capitelli et al. 1970b)).

8.1.3 Fermi Criterion

The Fermi criterion considers an electronic state bound (and then to be included in the partition function) if its classical Bohr radius does not exceed the inter-particle distance. One can write

$$n_{\max}^2 \frac{a_0}{Z_{\text{eff}}} = \sqrt[3]{\frac{V}{N}}$$

¹ $z_s = 0$ for neutrals, $z_e = -1$ for electrons, $z_s = 1$ for single ionized atoms and so on.

$$n_{\max} = \sqrt{\frac{1}{a_0 \sqrt[3]{\frac{N}{V}}}}$$

$$PV = NkT. \quad (8.5)$$

It should be noted that, following the Fermi criterion, the electronic partition function depends on the pressure, n_{\max} decreasing as the pressure increases.

8.2 Cutoff From the Schrödinger Equation

The results reported in the previous sections can be rationalized by solving the radial Schrödinger equation for atomic hydrogen

$$-\frac{\hbar^2}{2m_e r^2} \frac{\partial}{\partial r} \left(r^2 \frac{\partial \mathcal{R}}{\partial r} \right) + \left[-q_e \phi(r) + \frac{\hbar^2 \ell(\ell+1)}{2m_e r^2} \right] = \varepsilon \mathcal{R}, \quad (8.6)$$

where $\mathcal{R}(r)$ is the radial wave function, ε is the energy eigenvalue, \hbar is the reduced Planck constant, ℓ (0,1,2,3) is the azimuthal quantum number, r is the radial coordinate, $\phi(r)$ is the potential energy and μ the reduced mass for the electron-proton system. Analytical solution of the equation with a Coulomb potential

$$\phi_c = \frac{q_e}{4\pi\epsilon_0 r} \quad (8.7)$$

provides the energy levels of the hydrogen atom

$$\varepsilon_n = -\frac{I_H}{n^2} \quad (8.8)$$

with degeneracy

$$g_n = 2n^2. \quad (8.9)$$

As already pointed out, (8.8), (8.9) inserted in the partition function determines its divergence implying the necessity of using a cutoff criterion for terminating it. In this section, we reexamine the problem by considering an hydrogen atom confined in a spherical box of radius δ . The radial Schrödinger equation has been solved numerically with the boundary condition (Capitelli and Giordano 2009)²

$$\mathcal{R}(r = \delta) = 0. \quad (8.10)$$

²This boundary condition is completely different from that one considered for the not confined atom, i.e., $\mathcal{R}(r = \infty) = 0$.

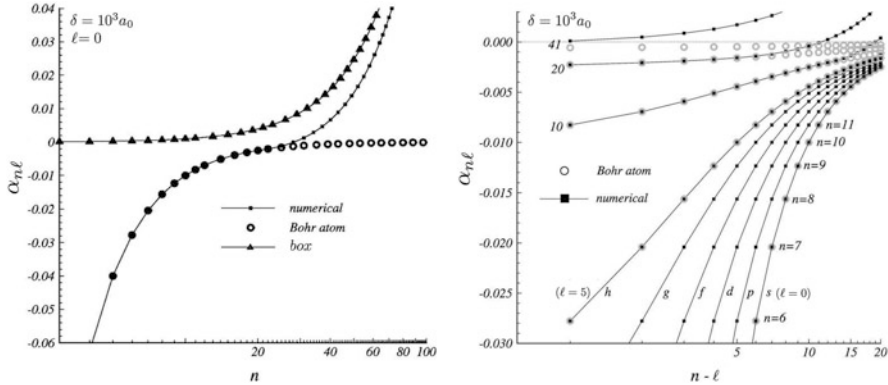


Fig. 8.1 Level energies of the hydrogen atom in a box (Capitelli and Giordano 2009) for $\ell = 0$ (left) and $\ell > 0$ (right) compared with the Bohr atom and the particle in a box

In (Capitelli and Giordano 2009), we report results for $\frac{\delta}{a_0} = 10^3$ and $\frac{\delta}{a_0} = 10^4$ values by imposing $\ell = 0$ in the radial part of the Schrödinger equation. Figure 8.1 (left) reports the adimensional level energy values

$$\alpha_n = \frac{\varepsilon_n}{I_H}$$

obtained with $\delta/a_0 = 10^3$ as a function of the principal quantum number n . In the same figure, we have also reported the analytical reduced level energies, i.e.,

$$\alpha_n^{\text{Bohr}} = -\frac{1}{n^2}$$

(labeled *Bohr atom*), which show the well-known asymptotic trend of level energies $\alpha_n^{\text{Bohr}} \xrightarrow{n \rightarrow \infty} 0$. The confined atom presents levels that closely follow α_n^{Bohr} for low n , becoming positive for $n > 28$, asymptotically approaching the values obtained for the electron in a box in absence of the interaction potential, given by the equation

$$\varepsilon_n^{\text{box}} = \frac{\pi \hbar^2}{2m_e \delta^2} n^2 \quad (8.11)$$

$$\alpha_n^{\text{box}} = \left(\frac{\pi n}{\delta/a_0} \right)^2, \quad (8.12)$$

where m_e is the electron mass (see Fig. 8.1). The same behavior has been obtained for $\delta/a_0 = 10^4$, the energy becoming positive for $n > 89$. Comparison between the results calculated with $\delta/a_0 = 10^3$ and $\delta/a_0 = 10^4$ shows that the increase of δ/a_0 shifts the onset of the positive levels to higher n . On the other hand, the bound

states disappear for $\delta/a_0 \rightarrow 0$. It is worth noticing that the values of n (for $\ell = 0$) corresponding to the transition to positive energies can be roughly approximated by $0.9\sqrt{\delta/a_0}$.

Different interesting points can be derived from these calculations. The first one is linked with the fact that the partition function of atomic hydrogen including bound and positive levels converges since the positive levels present energies increasing with n^2 . Thus, the solution of the Schrödinger equation for an hydrogen atom confined in a box introduces a natural cutoff criterion for the partition function. Moreover, the principal quantum number at which occurs the onset of the positive level energies is in satisfactory agreement with the corresponding values obtained by applying the Fermi cutoff, which gives for the conditions above studied the values of $n_{\max} = 40$ and 120 (see (Capitelli and Giordano 2009) for details). Finally, we want to mention that the equilibrium between bound and continuum levels can be used in the so-called physical picture to recover the well-known Saha equation in the chemical picture. All these effects have been obtained by using ns levels. Going beyond this approximation can be done by calculating the energy levels with different l values. Figure 8.1 (right), on the other hand, reports the level energies as a function of the azimuthal quantum number for the $\delta/a_0 = 10^3$ case. We can see that the quantum number ℓ starts affecting the results only for $n > 15$, the dependence on ℓ becoming dramatic when we consider very small δ/a_0 values.

So far we have presented results of the Schrödinger equation in the box considering a Coulomb potential. Now we consider the same problem accounting for a Debye potential (Capitelli et al. 2011a; Ecker and Weizel 1956, 1957; Smith 1964; Roussel and O'Connell 1974) i.e.

$$\phi_D = \frac{q_e}{4\pi\epsilon_0 r} e^{-r/\lambda_D}. \quad (8.13)$$

Figure 8.2 reports the energy levels for two Debye lengths $\lambda_D/a_0 = 10^2$ and $\lambda_D/a_0 = 10^8$ for a box $\delta/a_0 = 10^3$ (Capitelli et al. 2011a). In the same figure, we also report the Bohr levels as well as those of the particle in the box. Inspection of the figure again shows the transition from bound to continuum levels occurring, respectively, at $n_{\max} = 11$ for $\lambda_D/a_0 = 10^2$ and $n_{\max} = 29$ for $\lambda_D/a_0 = 10^8$. The last value coincides with the corresponding value in the presence of Coulomb potential, i.e., the Debye length is too high for affecting the results. In both cases, the positive levels asymptotically go toward the particle in the box, while the bound levels closely follow the Bohr results. On the other hand, the energy levels are strongly affected by the Debye length for $\lambda_D/a_0 < 10^2$ (see below). As an example, the transition between negative and positive energy values at $\lambda_D/a_0 = 10$ occurs at $n_{\max} = 3$, i.e., the Debye potential dominates the action of box confinement.

It should be noted that the Margenau and Lewis cutoff criterion for the reported three conditions give, respectively, n_{\max} values of 3, 10, and 104 compared to 3, 11, and 29 from numerical results. The excellent agreement between Margenau and Lewis results and numerical ones for the first two cases is not surprising because the Margenau and Lewis results were based on the energy levels calculated by Ecker

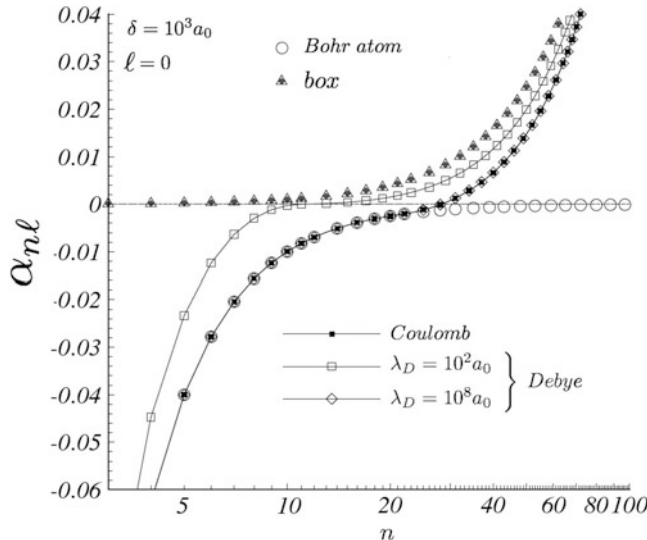


Fig. 8.2 energy levels for different values of the Debye length λ_D compared with the Coulomb levels and the particle in the box

and Weizel (Ecker and Weizel 1956, 1957) solving the Schrödinger equation in the presence of the Debye potential. The disagreement for the third case, i.e., for $\lambda_D/a_0 = 10^8$ is the consequence of the inefficiency of the Debye potential in affecting the energy levels for such large value of Debye length, as already pointed out.

8.3 Case Study: Oxygen

We consider a pure oxygen plasma composed mainly by O_2 , O , O^+ , O^{+2} , O^{+3} , O^{+4} , O^{+5} and electrons, and including also the minority species O_2^+ , O_2^- , O^- . We write a set of equilibrium constants as well as the condition of electroneutrality and the Dalton law for the total pressure. The equilibrium constants are calculated, following the statistical thermodynamics, from the relevant partition functions (Capitelli et al. 2005a; Giordano et al. 1994) which, in the case of atomic species, depend on electron and ionic species densities and temperature (Griem criterion) and on the pressure and temperature (Fermi criterion). On the other hand, the internal partition functions, calculated using the ground state method, are constant, having $Q^{\text{int}} = g_1$. Note also that in the case of atomic species we use a complete set of energy levels, including observed and missing ones, these last obtained by using semiempirical methods based on Ritz and Ritz–Rydberg equations (see Sect. A.3).

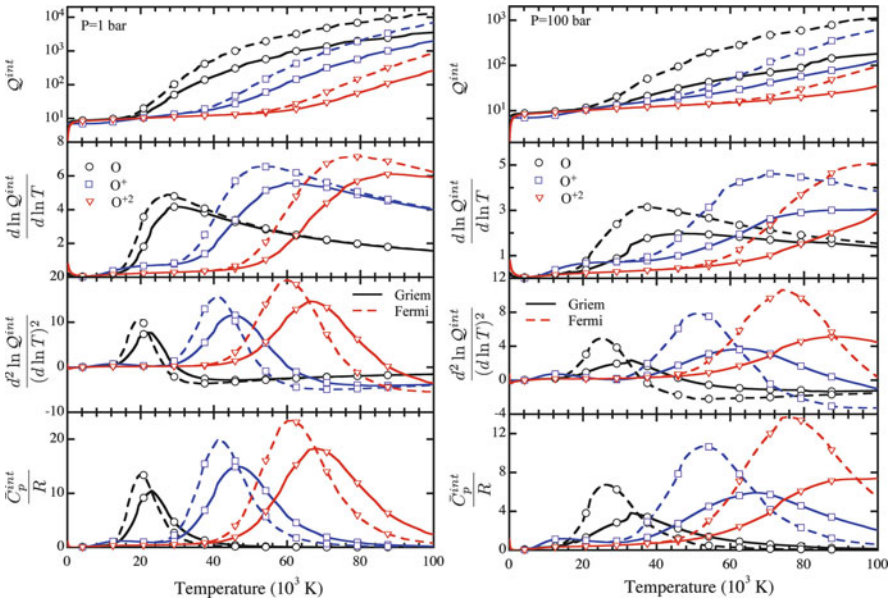


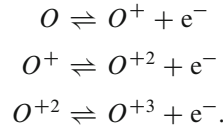
Fig. 8.3 Self-consistent atomic partition function, its temperature derivatives and internal specific heat as a function of the temperature for O , O^+ , O^{+2} for $P = 1 \text{ bar}$ (left) and $P = 100 \text{ bar}$ (right): comparison between *Griem* and *Fermi* cutoff

We start examining the properties of selected atomic species obtained by using the *Griem* and *Fermi* cutoff criteria. These data should be compared with the ground state values that for the O , O^+ and O^{+2} assume for $T > 2,000 \text{ K}$ the values $Q^{\text{int}}[O(^3P)] = 9$, $Q^{\text{int}}[O^+(^4S)] = 4$, $Q^{\text{int}}[O^{+2}(^2P)] = 6$, first and second derivatives being null (see Sect. 8.1.1).

Electronic partition functions, their first and second logarithmic derivatives and internal specific heats are reported as a function of temperature for the three species O , O^+ , and O^{+2} in Fig. 8.3 at 1 bar (left) and at 100 bar (right). In both cases, the two cutoff criteria give different values of partition function, these differences propagating on the first and second logarithmic derivatives as well as in the specific heats. In particular, the *Fermi* criterion includes in the calculation more levels than the *Griem* criterion, with the consequence of larger partition functions. Note also that, due to the energy range of electronic levels, the partition function of the different species increases in well-defined temperature ranges, without significant overlapping between each other. This aspect is better evidenced in the first and second logarithmic derivatives which present well distinct maxima. The values of the second logarithmic derivative calculated according to Fermi criterion overcome the corresponding *Griem* values up to the maximum, the opposite occurring in the decreasing region. This behavior is reflected on the specific heat of the single species which in any case presents the trend characteristic of a system containing a finite number of excited levels, i.e., the internal specific heat after the

maximum asymptotically reaches a zero value (see Chap. 1). The large influence of electronic excitation on the specific heat can be understood by reminding that the corresponding values for the ground state are null, independently of temperature, and the reduced translational contribution is 5/2 (Capitelli et al. 1970a).

Let us now examine the behavior of the enthalpy variation for the processes



We can write, respectively,

$$\begin{aligned} \Delta\bar{H}_1 &= \frac{5}{2}RT + \bar{U}_{O^+}^{\text{int}} - \bar{U}_O^{\text{int}} + I_O \\ \Delta\bar{H}_2 &= \frac{5}{2}RT + \bar{U}_{O^{+2}}^{\text{int}} - \bar{U}_{O^+}^{\text{int}} + I_{O^+} \\ \Delta\bar{H}_3 &= \frac{5}{2}RT + \bar{U}_{O^{+3}}^{\text{int}} - \bar{U}_{O^{+2}}^{\text{int}} + I_{O^{+2}}, \end{aligned}$$

where I_s represents, respectively, the first, second and third ionization potentials of oxygen. Values of $\Delta\bar{H}_i$ for the ionization reactions calculated at different pressures according to the three cutoff criteria have been plotted as a function of temperature in Fig. 8.4.

While $\Delta\bar{H}_i$ calculated in the ground state approach linearly increases as a function of temperature, results obtained according to *Griem* and *Fermi* cutoff criteria initially increases, as in the ground state case, but, as the temperature grows, $\Delta\bar{H}_i$ starts decreasing up to a minimum value, after which it increases again. Note that in all the cases the $\Delta\bar{H}_i$ calculated inserting the electronic excitation asymptotically converge at very high temperature to the $\Delta\bar{H}_{i+1}$ calculated without considering the electronic excitation, i.e.,

$$\Delta\bar{H}_1 = \frac{5}{2}RT + \bar{U}_{O^+}^{\text{int}} - \bar{U}_O^{\text{int}} + I_O \xrightarrow{\text{high T}} \frac{5}{2}RT + I_{O^+} = \Delta\bar{H}_2(\text{ground}). \quad (8.14)$$

As a matter of fact, at very high temperature we have that $\bar{U}_O^{\text{int}} \approx I_O$ and $\bar{U}_{O^+}^{\text{int}} \approx I_{O^+}$, because the level energies approach the ionization, therefore

$$I_O + \bar{U}_{O^+}^{\text{int}} - \bar{U}_O^{\text{int}} \xrightarrow{\text{high T}} I_{O^+}$$

justifying the asymptotic behavior previously discussed (see also Chap. 2). This is the consequence of taking into account the excitation of both O and O^+ which occurs in different temperature ranges. Beyond the minimum of $\Delta\bar{H}_1$, the electronic excitation of the ionized species $\bar{U}_{O^+}^{\text{int}}$ begins to contribute to $\Delta\bar{H}$ while

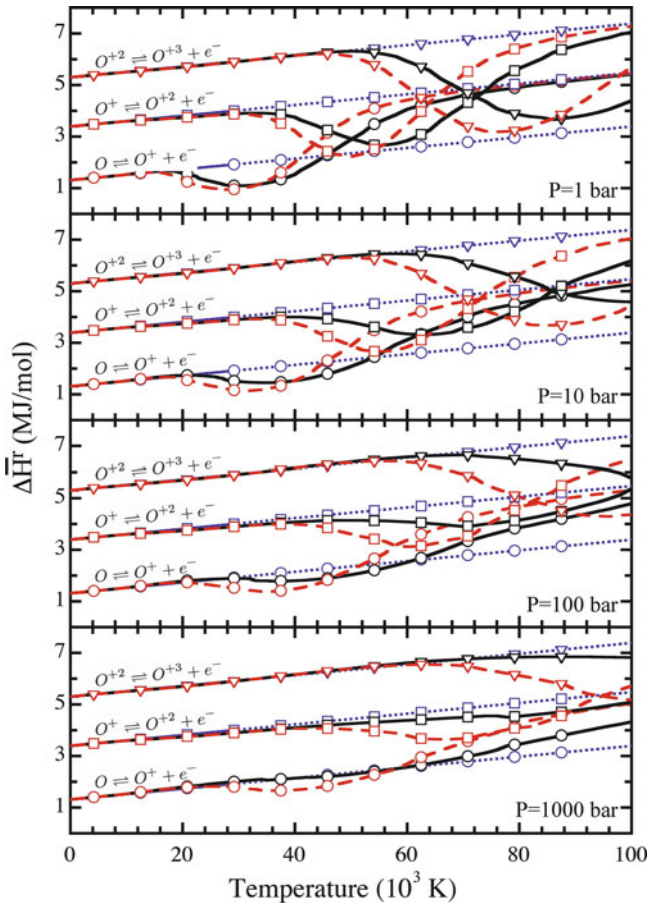


Fig. 8.4 Reaction enthalpy of the ionization processes of oxygen and its first and second ions calculated for $P = 1, 10, 100, 1,000$ bar. Comparison between *Griem* and *Fermi* cutoff and ground state model

the term \bar{U}_O^{int} is now decreasing with increasing temperature (compare Fig. 8.3). A similar behavior is found for the other ionization reactions, although shifted on the temperature axis.

Figures 8.5–8.7 report the entropy of the O , O^+ , and O^{+2} species as a function of temperature at different pressures calculated according to the ground state method and to *Griem* and *Fermi* cutoff criteria. The differences between the three methods reflect the trend of the corresponding electronic partition function and of its first logarithmic derivative. The contribution of the electronic states is well evident in the different plots when *Griem* and *Fermi* start deviating from the corresponding values calculated using the *Ground state* method. In any case, the trend of the entropy for

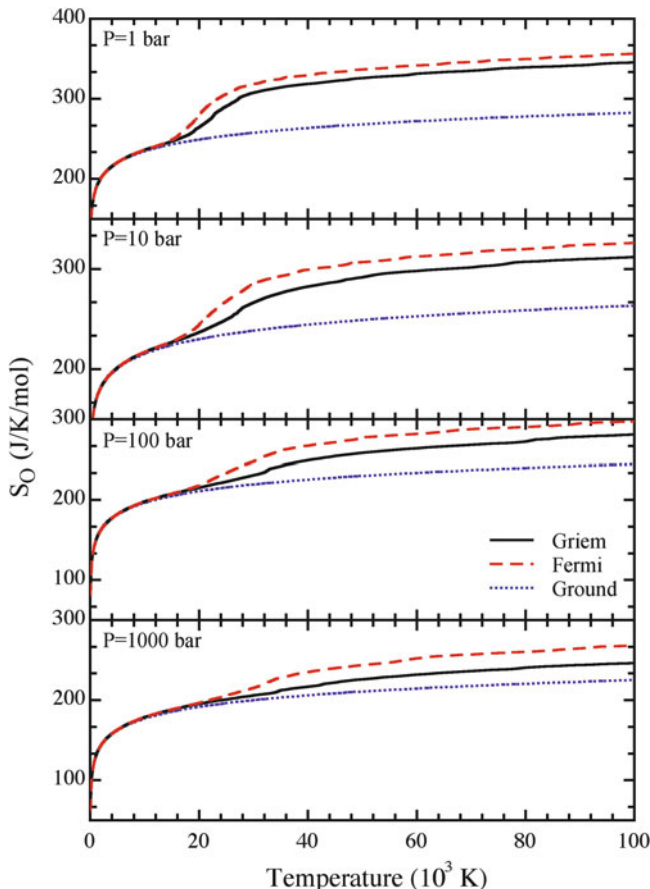


Fig. 8.5 Molar entropy of oxygen atom for different pressures and for different cutoff criteria

the different species monotonically increases, passing from ground to *Griem* and *Fermi* methods following the corresponding increase of the electronic contribution.

The dependence of the total thermodynamic quantities on cutoff criterion results from the combination of the single species properties and plasma composition. To analyze this contribution, we report the dependence of the molar fractions of the majority species of the oxygen plasma. Figure 8.8 reports the molar fractions of majority species (left) and their derivatives for O and O^{+2} (right) as a function of temperature at different pressures comparing the different cutoff criteria. The selected derivatives are representative of the dissociation and first ionization processes, corresponding, respectively, to the maximum and the minimum in O derivative, and the second and third ionizations (maximum and minimum in O^{+2} derivative). We can observe that the dissociation weakly depends on the chosen cutoff, while the three ionization processes are strongly influenced, showing large

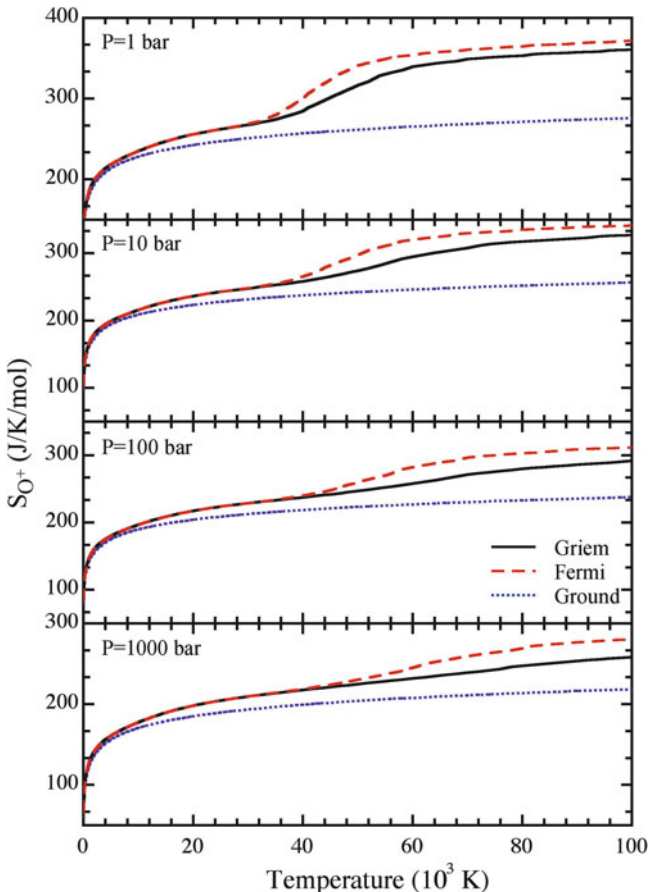


Fig. 8.6 Molar entropy of O^+ for different pressures and for different cutoff criteria

differences between the *Ground* and *Fermi/Griem* results. This behavior can be used to understand the trend of reactive contribution to the total specific heat.

Let us now examine the thermodynamic properties of plasma mixture. We start with the behavior of the total entropy (Fig. 8.9) of oxygen plasma as a function of temperature at different pressures calculated with the different methods. In general, the *Fermi* criterion presents larger entropy values compared to *Griem* and ground state methods, the differences not exceeding 10%.

The behavior of the different contributions (c_{pf} , c_{pr}) of the specific heat as well as the total specific heat (c_p) are reported in Figs. 8.10 and 8.11. In particular, Fig. 8.11 (left) reports the frozen specific heat as a function of temperature for the different pressures. In this case, the differences between the three methods can reach at high pressure a factor larger than 2, the values calculated by using the *Fermi* criterion overcoming in any case the values obtained by *Griem* and *Ground* state methods.

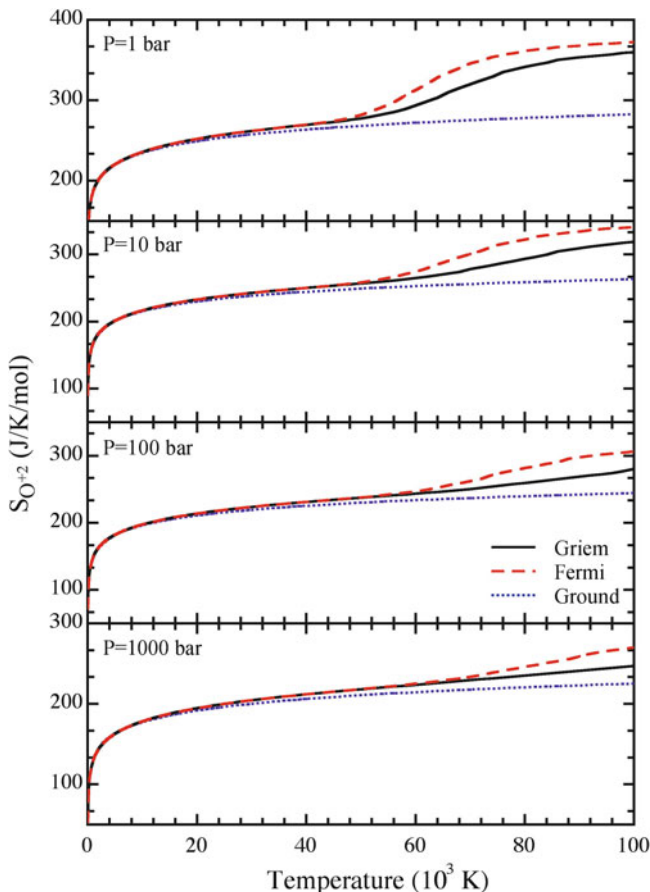


Fig. 8.7 Molar entropy of O^{+2} for different pressures and for different cutoff criteria

More complicated is the situation for the reactive contribution as reported in Fig. 8.11 (right), which however can be understood by using the derivatives of the molar fractions reported in Fig. 8.8. The dissociation regime is not affected by the cutoff of electronic partition function as confirmed by the results of Fig. 8.11 (right). The ionization regimes are strongly affected by the chosen cutoff criterion. In particular, the second ionization peak follows the history of the derivative of O^{+2} species. The compensation between *Fermi*, *Griem*, and *Ground* state methods occurs only in the dissociation and first ionization regimes while large differences are observed for the second, third, and fourth ionization reactions, these differences increasing at high pressure. At 1,000 bar, we observe the largest deviations between the three methods.

The differences between *Griem* and *Fermi* values are reduced in the total specific heat due to the partial compensation between frozen and reactive specific heats (see

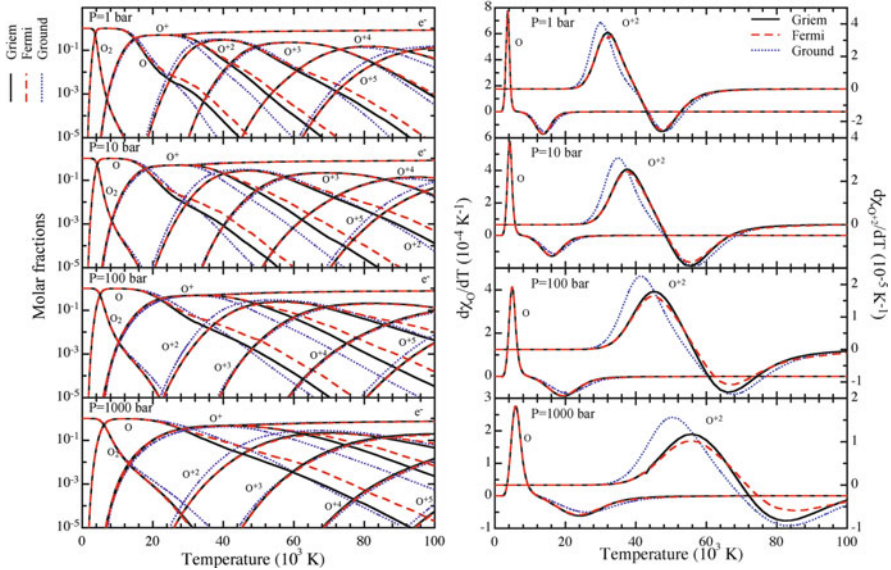


Fig. 8.8 Molar fractions of the majority species in the oxygen plasma (left) and its derivative (right), for O and O^{+2} , as a function of the temperature: comparison between *Griem* and *Fermi* cutoff criteria and *Ground* state method

Figs. 8.10–8.11). On the other hand, this compensation tends to disappear when comparing these values with the corresponding ground state values. Only at $P=1$ bar, the ground state values are in good agreement with the other two methods, while the differences strongly increase at high pressure.

To farther emphasize the role of electronic excitation in affecting the thermodynamic properties of thermal plasmas we plot, as an example, the ratio between the internal contribution

$$c^{\text{int}} = \frac{1}{M} \sum_{s=1}^N n_s \bar{C}_s^{\text{int}} \quad (8.15)$$

and the frozen and total specific heat, being n_s the number of moles of the s -th species and M the total mass. Figure 8.12 reports $c^{\text{int}}/c_{\text{pf}}$ and c^{int}/c_p calculated according to *Fermi* and *Griem* methods. From this figure, we can appreciate that the ratio $c^{\text{int}}/c_{\text{pf}}$ calculated with the *Fermi* criterion can exceed by more than a factor of 2 the corresponding ratio obtained by the *Griem* criterion, being in any case a large fraction of the frozen specific heat. On the other hand, the ratio c^{int}/c_p is less affected by the presence of electronic states, still representing however a large fraction of the total specific heat. In any case, the importance of electronic excitation is emphasized taking into account that c^{int} for the ground state method is zero in the ionization regimes. These results are confirmed by the corresponding ones recently reported in (Singh et al. 2010) for argon and argon–hydrogen plasmas.

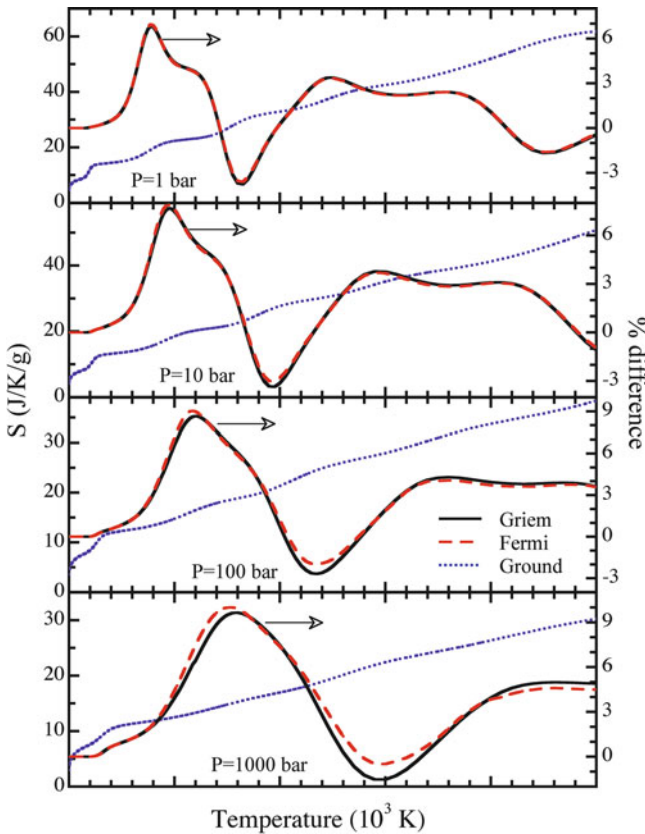


Fig. 8.9 Entropy, calculated using the *Ground* state method, and its relative difference with respect to calculations using *Griem* and *Fermi* cutoff criteria

Finally Fig. 8.13 report the frozen and the total isentropic coefficients for the oxygen plasmas calculated according to the three methods. Once more the effects of the electronic excitation is well evident on the frozen coefficient being in any case appreciable for the total isentropic coefficient. The low-temperature and high-temperature behaviors of the isentropic coefficient have been widely discussed in Sect. 1.9.

The results reported in this section do not exhaust the numerous methods used in the literature for the calculation of the electronic partition functions of atomic (neutral and ionized) species. It is worth noting that many researchers calculate the partition function inserting in it only the observed levels (Moore 1949) (see also the website (NIST 2009)) avoiding in this case any cutoff criterion (Capitelli and Ficocelli 1977). Of course, this method or other similar methods (Capitelli and Molinari 1970) which insert in the partition function only few levels above the ground state dramatically underestimate the electronic contribution to the

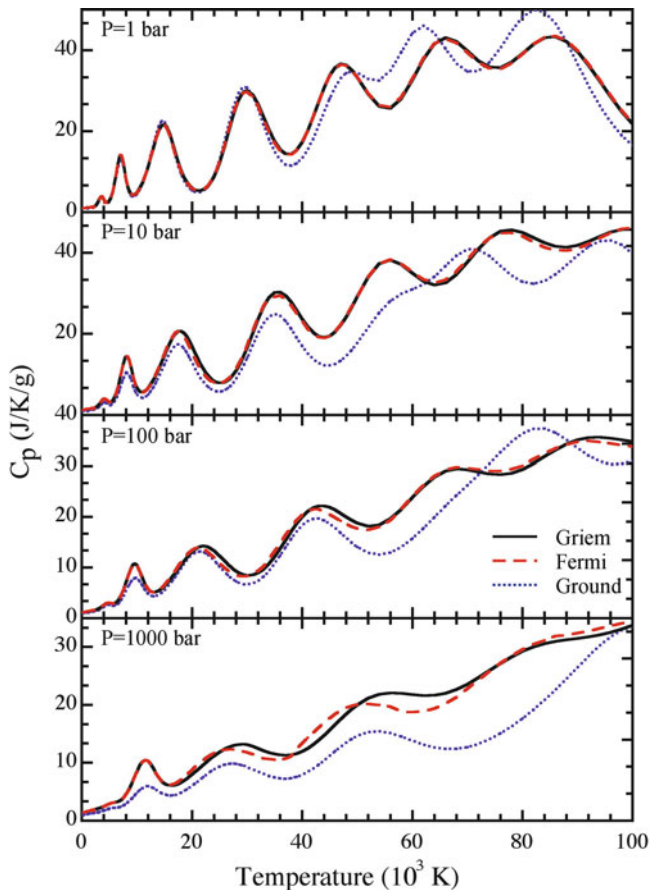


Fig. 8.10 Constant pressure specific heat calculated with different cutoff criteria

thermodynamic properties of thermal plasmas being not so far from the corresponding values obtained with the ground state method. Note that the famous Gurvich's tables (Gurvich and Veys 1989) insert in the partition function only the electronic levels coming from the rearrangement of valence electrons, i.e., only the low lying excited states are considered. As an example, the partition function of an oxygen atom is obtained by inserting the ground state 3P and the 1D and 1S metastable excited states. On the other hand, the well-known JANAF tables (Chase Jr. 1998) as well as the pioneeristic calculations of Gordon and McBride (Gordon and McBride 1994) consider levels which energy is lower than $(I - kT)$ where I is the ionization potential of the species. Also, in this case the electronic partition functions are underestimated.

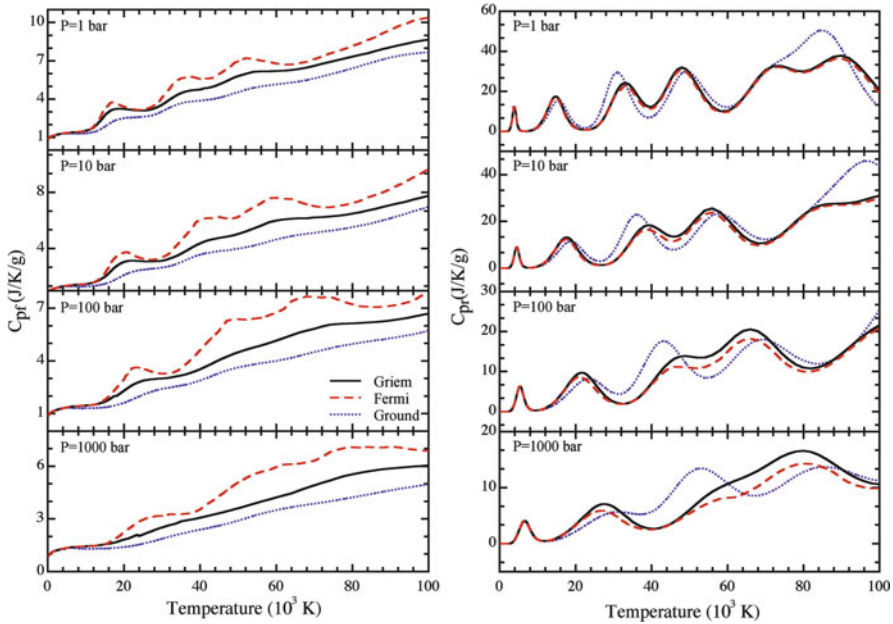


Fig. 8.11 Constant pressure specific heat calculated with different cutoff criteria: frozen (left) and reactive (right) contributions

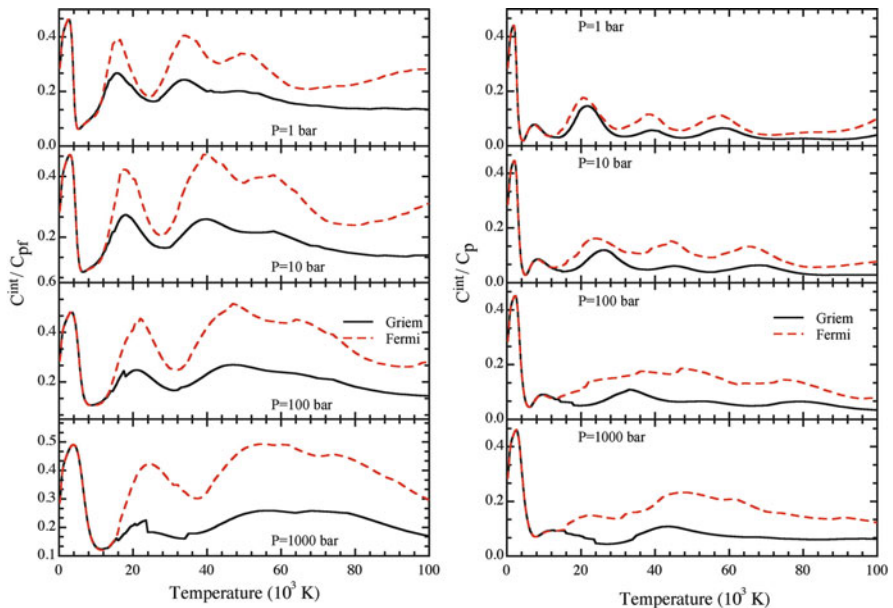


Fig. 8.12 c^{int}/c_{pf} (left) and c^{int}/c_p (right) as a function of the temperature for different pressures and calculated with different cutoff criteria

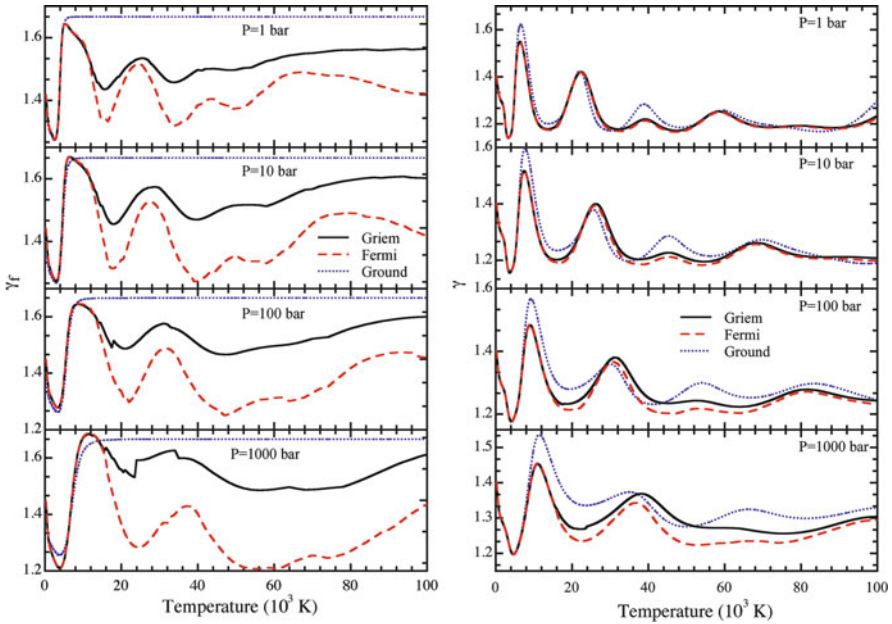


Fig. 8.13 γ_f (left) and γ (right) as a function of the temperature for different pressures and calculated with different cutoff criteria

8.4 Partition Function and Occupation Probability

In the astrophysical community as well as in dense plasma physics, other formulations of electronic partition functions are used. In particular, the Plank–Larkin (PL) partition function is widely used in the characterization of high pressure-high temperature non ideal plasmas. In this case, the partition function for the atomic hydrogen is given by the following equation³

$$\mathcal{Q}_H^{\text{PL}} = e^{-I_H/kT} \sum_{n=1}^{\infty} g_n \left(e^{\varepsilon'_n/kT} - 1 - \frac{\varepsilon'_n}{kT} \right), \quad (8.16)$$

where $\varepsilon'_n = I_H - \varepsilon_n = I_H/n^2$ and $g_n = 2n^2$. This equation is well known in the astrophysical literature as well as in the formulation of Equation of State (EOS) for high-temperature high-pressure plasmas because (Kremp et al. 2005):

1. It is convergent in the limit $N \rightarrow 0$.
2. It is continuous at the Mott densities.

³Note that the preexponential term reports the calculated electron partition function to the counting of electronic levels from the ground state

3. It is a good approximation, at low temperature, for the two-particle sum of states.
4. It depends only on the temperature.

However this partition function gives incorrect population of highly excited states. In fact, it does not include the contribution of states with binding energies less than kT . To overcome this point, Vorobeev et al. (2000) (see also (Hummer and Mihalas 1988)) introduces the following partition function (always for atomic hydrogen)

$$\mathcal{Q}_s^V = e^{-I_s/kT} \sum_{n=1}^{\infty} w_{sn} e^{\varepsilon'_{sn}/kT}, \quad (8.17)$$

where w_n is the occupation probability of the n -th quantum state which in the grand-canonical ensemble assumes the form

$$w_{sn} = \exp \left[-\frac{4\pi}{3} (f_e + f_i) r_n^3 \right], \quad (8.18)$$

where f_e and f_i are the fugacities of electrons and protons and r_n is the Bohr radius of the n -th quantum state. Moreover, Vorobeev et al. (2000) rewrite the equation as

$$\mathcal{Q}_s^V = e^{-I_s/kT} \sum_{n=1}^{\infty} w_{sn} \left(e^{\varepsilon'_{sn}/kT} - 1 - \frac{\varepsilon'_{sn}}{kT} \right) + e^{-I_s/kT} \sum_{n=1}^{\infty} w_{sn} \frac{\varepsilon'_{sn}}{kT}, \quad (8.19)$$

where $w_n = 1$ for the first term of (8.19) and w_n in the second term of (8.19) is derived from (8.18). Note that $w_n = 1$ is justified because the main contribution of this component is made by bound states with orbit dimension less than the Landau length $L_n = q_e^2/(4\pi\epsilon_0 kT)$. Values of partition function of atomic hydrogen obtained by the Vorobeev et al. (2000) approach as a function of temperature for different electron densities \mathcal{N}_e shows a qualitative and quantitative trend very similar to those calculated by using the *Griem* approach for the same electron densities.

A similar approach has been recently presented by Zaghoul (2010) who used (8.17) in combination with the occupation probability

$$w_{sn} = \exp \left[- \left(\frac{\Delta I_H}{I_H - \varepsilon_n} \right)^3 \right], \quad (8.20)$$

where ΔI_H is the lowering of the ionization potential of the hydrogen atom and ε_n is the energy of the n -th level. In turn, ΔI_H is expressed according the neighbor approximation, i.e.,

$$\Delta I_H = -C \frac{(z+1)q_e^2}{4\pi\epsilon_0 R_0}, \quad (8.21)$$

where C is a constant and $R_0 = \sqrt[3]{3\pi\mathcal{N}^*/4}$ with $\mathcal{N}^* = \mathcal{N}_H + \mathcal{N}_{H^+}$. This approach as well as that one reported in (Vorob'ev et al. 2000) can be reduced to the

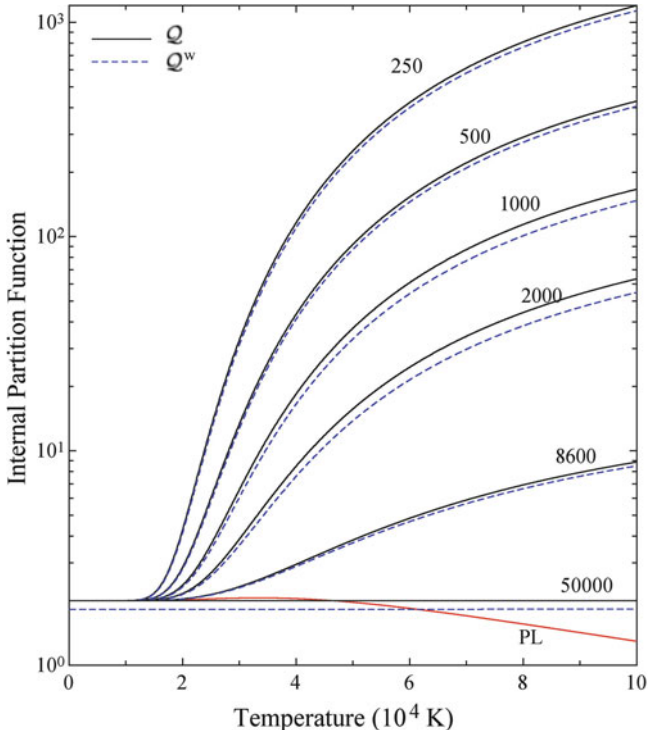


Fig. 8.14 Comparison between occupation probability method (Q^w) and traditional cutoff (Q). Plank–Larkin (PL) result is also reported

results, which can be obtained by a cutoff criterion. This point can be understood by looking at the results reported in Fig. 8.14, where we compare the partition function obtained by using (8.17) with the occupation numbers given by (8.18) and the corresponding values obtained by cutting the partition function of the atomic hydrogen to an n_{\max} consistent with a given lowering of the ionization potential taken, in this case, as a parameter. We can see that the two methods give essentially the same results in a wide range of temperature as well as for different lowering of the ionization potential. To a first approximation, the lowering of 500 cm^{-1} approximately mimics an atomic hydrogen plasma at atmospheric pressure of about 10^{23} m^{-3} , while $\Delta I_H = 8,600 \text{ cm}^{-1}$ is typical of an hydrogen plasma at 1,000 bar and $N_e = 10^{26} \text{ m}^{-3}$. The corresponding partition functions are in satisfactory agreement with those reported in (Vorob'ev et al. 2000).

Two other interesting aspects can be deduced from Fig. 8.14. The first one is that the value of the partition function for a lowering of $50,000 \text{ cm}^{-1} \approx 5 \text{ eV}$ calculated according to n_{\max} gives a constant value 2, i.e., the degeneracy of the ground state of atomic hydrogen, while the use of (8.17), (8.20) gives a constant value a

little smaller than 2. In the same figure, we have also reported the Plank–Larking partition function which strongly underestimates the partition function as underlined by Vorobeev et al (2000). Apparently, the PL can be used only for very dense plasmas when the excited states are practically disappearing. The results based on the occupation probabilities, while being in good agreement with the corresponding values derived from the use of a given cutoff criterion, could be used to eliminate the discontinuities in the partition functions occurring when the cutoff criterion is used specially when the complete set of energy levels is reduced to two or three levels.

8.5 Debye–Hückel Energy Levels

The results in Sect. 8.4 have been obtained by using in the relevant partition functions complete sets of electronic levels derived by using semiempirical methods and experimental results. In both cases, the energy values can be rationalized by solving an appropriate Schrödinger equation inserting in it a Coulomb potential. At high electron density, however, electron–ion interactions are better described by a Debye potential, which can change, as reported in Chap. 6, the thermodynamic properties of the plasma. In addition, the Debye potential, when inserted in the Schrödinger equation, can also change the magnitude of energy levels with further consequences on partition functions and thermodynamic properties of the mixture (see Sect. 8.2). A complete set of Debye energy levels up to $n = 9$ has been obtained in (Roussel and O’Connell 1974) (see also (Capitelli and Giordano 2009; Capitelli et al. 2011a) as a function of the Debye length λ_D for different (n, l) levels. The partition function in this case must be calculated allowing the (n, l) structure with the appropriate statistical weights, this structure disappearing for Coulomb levels.

We compare results obtained by using energy levels corresponding to the Debye (*Debye*) in the relevant figures and the Coulomb (*Coulomb*) potentials as well as with the ground state method (*Ground*) (Capitelli et al. 2008). From a qualitative point of view, it can be expected that the use of Debye energy levels should increase the electronic partition function and its derivatives as compared with the corresponding results obtained by using energy levels from the Coulomb potential. The action of the Debye potential in fact is to decrease the energy of the levels as the Debye length decreases and to increase the Boltzmann factors as well as the number of levels included in the electronic partition function calculation, this last effect being predominant. The increase in the electronic partition function generates an increase of the atomic hydrogen molar fractions and, in turn, increases the importance of electronic excitation on the thermodynamic properties of the plasma. Figure 8.15 (left) shows the frozen specific heat of the mixture calculated with the two series of levels. The largest differences occur at $P = 100$ bar as a result of the combined effect of the specific heat of atomic hydrogen and of the molar fraction of the same species. Note that in any case the frozen specific heat calculated from

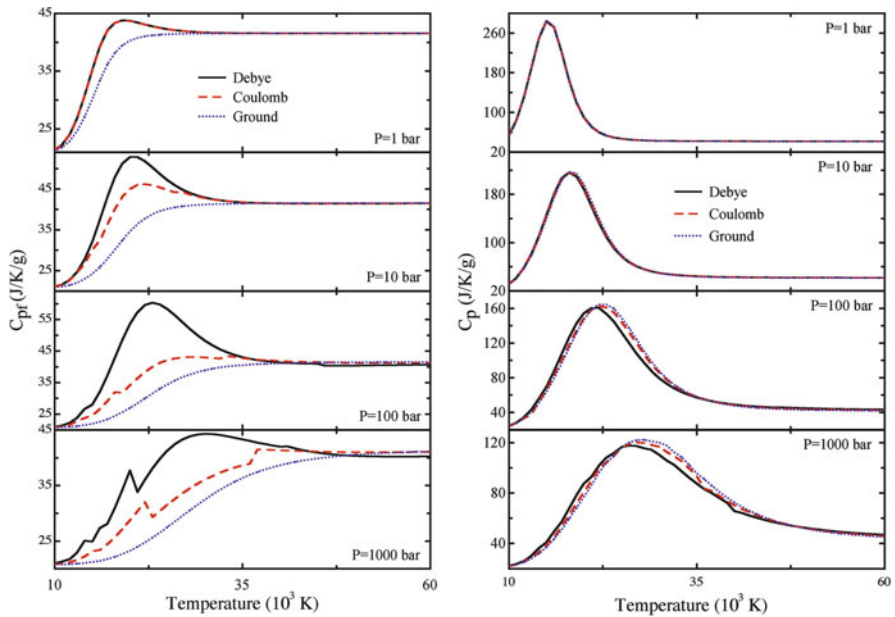


Fig. 8.15 Frozen (left) and total (right) specific heat of the (H, H^+, e^-) plasma calculated at different pressure using *Debye* and *Coulomb* levels, compared to *Ground* state approximation

the Debye energy levels overcomes the corresponding quantity calculated from Coulomb levels in all the considered temperature range. The maximum deviation can reach a value of 40%. On the other hand, an opposite trend is presented by the reactive contribution to the specific heat (see Fig. 8.15 (right)) so that the differences *Debye* and *Coulomb* levels are smoothed in the total specific heat (see (Capitelli et al. 2008)).

Chapter 9

Multi-Temperature Thermodynamics: A Multiplicity of Saha Equations

The multitemperature equilibrium model must be viewed in the framework of irreversible thermodynamics (Prigogine 1955)¹. It applies to systems which can be divided in subsystems with weak interaction between each other, but with a rapid internal relaxation. In this case, each subsystem reaches an internal equilibrium, while the overall system is outside equilibrium, relaxing very slowly. The theory was originally developed for systems whose volume was geometrically divided in different parts, with high ratio volumes/surfaces, limiting exchange of mass and energy through their interfaces.

This theory has been extended to gases and plasma considering as subsystems different degrees of freedom of the particles in the gas. This approach is commonly used to model nonequilibrium conditions in high enthalpy flowing plasma (Mostaghimi et al. 1987), encountered in shock wave formation or in nozzle expansion. In this chapter, we will derive a series of Saha equations for multitemperature plasmas obtained by using different thermodynamic potentials and different constraints (Giordano and Capitelli 1995, 2002). The results for an hydrogen plasma are discussed, focusing on the relevant differences coming from the selection of the particular method.

9.1 General Considerations

The equilibrium conditions of a one temperature chemical system can be obtained either by minimizing chemical potentials

$$(dG)_{P,T} = \sum_s \mu_s dn_s = 0 \quad (9.1)$$

¹The theory of irreversible thermodynamics is valid only for weak deviations from the equilibrium. In case of large deviations, the theory fails and a kinetic approach is necessary.

or by maximizing the entropy

$$(dS)_{V,U} = \frac{1}{T} \sum_s \mu_s dn_s = 0, \quad (9.2)$$

which are equivalent for the one temperature case (Capitelli and Giordano 2002; Capitelli et al. 2005b; Giordano 1998).

Let us assign a different temperature (T_s^d) to each degree of freedom d of each species s . This approach can be applied to degrees of freedom that are independent from each other. In particular, the separation of translational and internal degrees of freedom is exact. However, this method is often applied to molecules considering separable also rotation, vibration, and electronic excitation. In this case, we will consider the following temperatures for the s -th species

T^{tr}	translational temperature
T^{rot}	rotational temperature
T^{vib}	vibrational temperature
T^{el}	electronic excitation temperature
T^c	temperature linked to chemical processes

where for atoms only T^{tr} , T^{el} , and T^c can be considered and for electrons only the translational temperature is used, that for simplicity we will call T_e . For polyatomic molecules, we should distinguish also the different vibrational modes and rotational axes.

Under the hypothesis of separability of the different degrees of freedom, the partition function will be considered, neglecting nonlinear coupling, as the product of the contribution of the different degrees of freedom (see (4.6), (5.1)) each with its own temperature. In the general case of a diatomic molecule, the partition function is given by

$$\mathcal{Q}_s = \mathcal{Q}_s^{\text{tr}}(T_s^{\text{tr}}) \mathcal{Q}_s^{\text{rot}}(T_s^{\text{rot}}) \mathcal{Q}_s^{\text{vib}}(T_s^{\text{vib}}) \mathcal{Q}_s^{\text{el}}(T_s^{\text{el}}) \exp\left(-\frac{\varepsilon_s^f}{kT^c}\right), \quad (9.3)$$

where we are including the contribution of formation energy and where the temperature T^c should depend on the reaction more than on the species². Moreover, the nuclear partition functions are not considered in (9.3) for the reason discussed in Sect. 4.1.1.

Now, the calculation of the thermodynamic properties from the partition functions using the statistical thermodynamic theory (see Chap. 3) is not straightforward, and some assumptions are needed. Considering the general theory of irreversible thermodynamics, each degree of freedom must be considered independent; therefore, the formulae of statistical thermodynamics can be applied separately to each

²Considering a different T^c for different species in the same reaction will lead to a physical inconsistency, because the equation can depend on the reference of the energy.

partition function. The total properties can be calculated using the sum rule and in particular we have for the chemical potential

$$\mu_s = \mu_s^{\text{tr}}(T_s^{\text{tr}}) + \mu_s^{\text{rot}}(T_s^{\text{rot}}) + \mu_s^{\text{vib}}(T_s^{\text{vib}}) + \mu_s^{\text{el}}(T_s^{\text{el}}) + \varepsilon_s^f, \quad (9.4)$$

where (see (3.40))

$$\mu_s^d(T_s^d) = -k T_s^d \ln Q_s^d(T_s^d) \quad (9.5)$$

for each degree of freedom d . The translational contribution is rewritten as

$$\mu_s^{\text{tr}}(T_s^{\text{tr}}) = -k T_s^{\text{tr}} \ln \left[\frac{Q_s^{\text{tr}}(T_s^{\text{tr}})}{\mathcal{N}_s} \right] = -k T_s^{\text{tr}} \ln \mathcal{F}_s + k T_s^{\text{tr}} \ln P_s, \quad (9.6)$$

where, to simplify the notation, we define the function \mathcal{F}_s as

$$\mathcal{F}_s = \left(\frac{m_s k T_s^{\text{tr}}}{2\pi\hbar^2} \right)^{\frac{3}{2}} k T_s^{\text{tr}} = Q_s^{\text{tr}}(T_s^{\text{tr}}) P_s. \quad (9.7)$$

Similarly, the entropy is given by

$$S_s = S_s^{\text{tr}}(T_s^{\text{tr}}) + S_s^{\text{rot}}(T_s^{\text{rot}}) + S_s^{\text{vib}}(T_s^{\text{vib}}) + S_s^{\text{el}}(T_s^{\text{el}}), \quad (9.8)$$

where (see (3.39) when substituting (3.26), (9.5))

$$S_s^d(T_s^d) = \mathcal{N}_s k \left[-\frac{\mu_s^d(T_s^d)}{k T_s^d} + \frac{U_s^d(T_s^d)}{\mathcal{N}_s k T_s^d} \right] = \frac{H_s^d - G_s^d}{T_s^d} \quad (9.9)$$

for all the internal degrees of freedom while for the translation we have

$$S_s^{\text{tr}}(T_s^{\text{tr}}) = \mathcal{N}_s k \left[-\frac{\mu_s^{\text{tr}}(T_s^{\text{tr}})}{k T_s^{\text{tr}}} + 1 + \frac{U_s^{\text{tr}}(T_s^{\text{tr}})}{\mathcal{N}_s k T_s^{\text{tr}}} \right] = \frac{H_s^{\text{tr}} - G_s^{\text{tr}}}{T_s^{\text{tr}}}. \quad (9.10)$$

The equilibrium condition derived from the entropy maximization (see (9.2)) contains the derivative of the entropy of each degree of freedom of any species with respect to the number of particles, that, in all the cases is given by

$$\left(\frac{\partial S_s^d(T_s^d)}{\partial \mathcal{N}_s} \right)_{U_s^d, V} = -\frac{\mu_s^d}{T_s^d}. \quad (9.11)$$

Usually all the heavy species have the same translational temperature, namely T_h , while the electron temperature T_e is higher³. The internal temperatures are linked

³The condition $T_e > T_h$ is valid in discharge condition, where the applied electric field warms up directly the electrons, which transfer their energy to the gas through Joule effect.

with T_e or T_h depending on which excitation mechanism is dominant. In general, we should consider all the internal temperatures as independent quantities. Therefore, we define the nonequilibrium coefficient θ for the electron as

$$\theta_e = \frac{T_e}{T_h}. \quad (9.12)$$

Extending this definition to the internal degrees of freedom, we can define

$$\theta_s^d = \frac{T_s^d}{T_h}. \quad (9.13)$$

Let us consider a general reaction

$$\sum_{s \neq e} v_s X_s + v_e e = 0 \quad (9.14)$$

and where the contribution of free electrons is separated from those of heavy particles, where the stoichiometric coefficients v_s are positive for the product and negative for the reactants. In the following, we will obtain the multitemperature equilibrium equations resulting from the minimization of G and from the maximization of S .

9.1.1 Minimization of Gibbs Free Energy

In the multitemperature case, the minimization of Gibbs free energy (9.1) results in the following condition

$$\begin{aligned} \sum_{s \neq e} v_s & \left[k T_h (\ln P_s - \ln \mathcal{F}_s) + \varepsilon_s^f + \sum_d k T_s^d \ln \mathcal{Q}_s^d \right] + \\ & + v_e k T_e (\ln P_e - \ln \mathcal{F}_e) = 0, \end{aligned} \quad (9.15)$$

Dividing the equation by $k T_h$ and separating the pressure terms from the others, we obtain

$$\begin{aligned} \sum_{s \neq e} v_s \ln P_s + v_e \theta_e \ln P_e \\ = \sum_{s \neq e} \left(v_s \ln \mathcal{F}_s - v_s \frac{\varepsilon_s^f}{k T_h} + \sum_d v_s \theta_s^d \ln \mathcal{Q}_s^d \right) + v_e \theta_e \ln \mathcal{F}_e, \end{aligned} \quad (9.16)$$

which can be written as

$$P_e^{v_e \theta_e} \prod_{s \neq e} P_s^{v_s} = \mathcal{F}_e^{v_e \theta_e} \prod_{s \neq e} \left[\mathcal{F}_s \prod_d (\mathcal{Q}_s^d)^{\theta_s^d} \right]^{v_s} \exp \left(-\frac{\Delta \varepsilon^f}{k T_h} \right), \quad (9.17)$$

where

$$\Delta \varepsilon^f = \sum_s v_s \varepsilon_s^f \quad (9.18)$$

is the reaction energy.

This equation differs from the one-temperature equilibrium by the presence of the exponents θ applied to P_e and to electronic and internal partition functions. Moreover, it must be noted that the internal partition functions are calculated each with its own temperature.

9.1.2 Maximization of Entropy

The maximization of entropy (9.2) is based on (9.11) and gives the following relation

$$\sum_{s \neq e} v_s \left[(\ln P_s - \ln \mathcal{F}_s) + \frac{\varepsilon_s^f}{k T^c} + \sum_d \ln \mathcal{Q}_s^d \right] + v_e (\ln P_e - \ln \mathcal{F}_e) = 0. \quad (9.19)$$

Separating the pressure terms from the others, we have

$$\begin{aligned} & \sum_{s \neq e} v_s \ln P_s + v_e \ln P_e \\ &= \sum_{s \neq e} \left(v_s \ln \mathcal{F}_s - v_s \frac{\varepsilon_s^f}{k T^c} + \sum_d v_s \ln \mathcal{Q}_s^d \right) + v_e \ln \mathcal{F}_e \end{aligned} \quad (9.20)$$

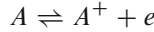
and calculating the exponential we have the equilibrium equation

$$P_e^{v_e} \prod_{s \neq e} P_s^{v_s} = \mathcal{F}_e^{v_e} \prod_{s \neq e} \left(\mathcal{F}_s \prod_d \mathcal{Q}_s^d \right)^{v_s} \exp \left(-\frac{\Delta \varepsilon^f}{k T^c} \right). \quad (9.21)$$

This equation is formally equal to the one-temperature equilibrium (the exponents θ are disappeared), being the internal partition functions calculated at the relevant temperature. Moreover, the exponential term depends on the temperature T^c related to the chemical process.

9.2 Free Energy Minimization for Atomic Ionization

In this section, we will show the different equations arising from minimizing the Gibbs potential (9.1). For the sake of simplicity, we will consider the ionization reaction in (1.49)⁴,



considering only three temperatures:

T_h the translational temperature for all heavy particles ($T_h = T_A^{\text{tr}} = T_{A^+}^{\text{tr}}$).

T_{int} the electronic excitation one for all heavy particles ($T_{\text{int}} = T_A^{\text{el}} = T_{A^+}^{\text{el}}$).

T_e the translational temperature of free electrons.

As in the one-temperature case, the minimization of the Gibbs potential leads to the equality of the chemical potentials of the left and right-hand side species in the reaction (see (1.50)).

To remember that we have many temperatures we write explicitly the equilibrium condition

$$\mu_{A^+}^{\text{tr}}(T_h) + \mu_{A^+}^{\text{el}}(T_{\text{int}}) + \mu_e(T_e) = \mu_A^{\text{tr}}(T_h) + \mu_A^{\text{el}}(T_{\text{int}}). \quad (9.22)$$

The application of (9.22), however, yields different equations depending on the hypotheses made on the thermal baths which govern the different degrees of freedom. This explains the different equations that are encountered in the literature (Giordano and Capitelli 2002) for multitemperature equilibrium calculations. In the following, we will discuss some of these cases to show the differences between the various assumptions.

9.2.1 Case a: $T_h = T_{\text{int}} \neq T_e$

Let us start with one of the most popular cases (Potapov 1966), considering one temperature for the translational and internal degrees of atoms and ions and one for the electrons.

With this premise, considering the explicit expression of the translational (4.29) and internal (4.38) chemical potential, being I the ionization potential⁵ and $Q_e^{\text{int}} = 2$ the contribution of electron spin degeneracy to the partition function, (9.22) becomes

⁴Compare with Sect. 1.3 for the one-temperature case.

⁵The ionization potential can include also its lowering (see Sect. 6.2.7) obtained in the framework of Debye–Hückel theory.

$$\begin{aligned}
& -kT_h \ln \left[\left(\frac{m_{A^+} k T_h}{2\pi \hbar^2} \right)^{\frac{3}{2}} \frac{k T_h}{P_{A^+}} \right] - kT_h \ln Q_{A^+}^{\text{int}}(T_h) + I + \\
& -kT_e \ln \left[\left(\frac{m_e k T_e}{2\pi \hbar^2} \right)^{\frac{3}{2}} \frac{k T_e}{P_e} \right] - kT_e \ln Q_e^{\text{int}} = \\
& = -kT_h \ln \left[\left(\frac{m_A k T_h}{2\pi \hbar^2} \right)^{\frac{3}{2}} \frac{k T_h}{P_A} \right] - kT_h \ln Q_A^{\text{int}}(T_h)
\end{aligned} \tag{9.23}$$

and, dividing by kT_e and bringing all the terms on one side, we have

$$\begin{aligned}
& -\frac{1}{\theta_e} \ln \left[\left(\frac{m_{A^+} k T_h}{2\pi \hbar^2} \right)^{\frac{3}{2}} k T_h \right] + \frac{\ln P_{A^+}}{\theta_e} - \frac{\ln Q_{A^+}^{\text{int}}(T_h)}{\theta_e} + \frac{I}{kT_e} + \\
& -\ln \left[\left(\frac{m_e k T_e}{2\pi \hbar^2} \right)^{\frac{3}{2}} k T_e \right] + \ln P_e - \ln Q_e^{\text{int}} + \\
& + \frac{1}{\theta_e} \ln \left[\left(\frac{m_A k T_h}{2\pi \hbar^2} \right)^{\frac{3}{2}} k T_h \right] - \frac{\ln P_A}{\theta_e} + \frac{\ln Q_A^{\text{int}}(T_h)}{\theta_e} = 0.
\end{aligned} \tag{9.24}$$

Considering that the atomic and ionic masses are almost equal we have that

$$\left[\left(\frac{m_{A^+} k T_h}{2\pi \hbar^2} \right)^{\frac{3}{2}} k T_h \right] \approx \left[\left(\frac{m_A k T_h}{2\pi \hbar^2} \right)^{\frac{3}{2}} k T_h \right]$$

and then these terms can be eliminated from (9.24). Calculating the exponential, we have the Saha equation

$$\left(\frac{P_{A^+}}{P_A} \right)^{\frac{1}{\theta_e}} P_e = \left(\frac{m_e k T_e}{2\pi \hbar^2} \right)^{\frac{3}{2}} k T_e \left[\frac{Q_{A^+}^{\text{int}}(T_h)}{Q_A^{\text{int}}(T_h)} \right]^{\frac{1}{\theta_e}} Q_e^{\text{int}} e^{-\frac{I}{kT_e}} \tag{9.25}$$

The exponent $\frac{1}{\theta_e}$ appears in the pressure and partition function ratios of heavy particle contribution. The internal partition function is calculated at the gas temperature.

9.2.2 Case b: $T_h \neq T_{\text{int}} = T_e$

A different Saha equation is obtained if the electronic excitation is governed by the electron temperature. In this case, (9.22) becomes

$$\begin{aligned} -kT_h \ln \left[\left(\frac{m_{A^+} + kT_h}{2\pi\hbar^2} \right)^{\frac{3}{2}} \frac{kT_h}{P_{A^+}} \right] - kT_e \ln Q_{A^+}^{\text{int}}(T_e) + I + \\ -kT_e \ln \left[\left(\frac{m_e kT_e}{2\pi\hbar^2} \right)^{\frac{3}{2}} \frac{kT_e}{P_e} \right] - kT_e \ln Q_e^{\text{int}} = \\ = -kT_h \ln \left[\left(\frac{m_A kT_h}{2\pi\hbar^2} \right)^{\frac{3}{2}} \frac{kT_h}{P_A} \right] - kT_e \ln Q_A^{\text{int}}(T_e). \end{aligned} \quad (9.26)$$

Proceeding in the same way as in case a, we obtain a different Saha equation

$$\left(\frac{P_{A^+}}{P_A} \right)^{\frac{1}{\theta_e}} P_e = \left(\frac{m_e kT_e}{2\pi\hbar^2} \right)^{\frac{3}{2}} kT_e \frac{Q_{A^+}^{\text{int}}(T_e)}{Q_A^{\text{int}}(T_e)} Q_e^{\text{int}} e^{-\frac{I}{kT_e}} \quad (9.27)$$

The exponent $\frac{1}{\theta_e}$ appears only in the pressure ratios of heavy particles, while the internal partition function is calculated at the electron temperature.

9.2.3 Case c: $T_h \neq T_{\text{int}} \neq T_e$

In the more general case of three independent temperatures, (9.22) becomes

$$\begin{aligned} -kT_h \ln \left[\left(\frac{m_{A^+} + kT_h}{2\pi\hbar^2} \right)^{\frac{3}{2}} \frac{kT_h}{P_{A^+}} \right] - kT_{\text{int}} \ln Q_{A^+}^{\text{int}}(T_{\text{int}}) + I + \\ -kT_e \ln \left[\left(\frac{m_e kT_e}{2\pi\hbar^2} \right)^{\frac{3}{2}} \frac{kT_e}{P_e} \right] - kT_e \ln Q_e^{\text{int}} = \\ = -kT_h \ln \left[\left(\frac{m_A kT_h}{2\pi\hbar^2} \right)^{\frac{3}{2}} \frac{kT_h}{P_A} \right] - kT_{\text{int}} \ln Q_A^{\text{int}}(T_{\text{int}}). \end{aligned} \quad (9.28)$$

Let us define another nonequilibrium coefficient δ given by

$$T_{\text{int}} = \delta T_e \quad (9.29)$$

and following the previous procedure we have

$$\left(\frac{P_{A+}}{P_A} \right)^{\frac{1}{\theta_e}} P_e = \left(\frac{m_e k T_e}{2\pi \hbar^2} \right)^{\frac{3}{2}} k T_e \left[\frac{\mathcal{Q}_{A+}^{\text{int}}(T_{\text{int}})}{\mathcal{Q}_A^{\text{int}}(T_{\text{int}})} \right]^\delta \mathcal{Q}_e^{\text{int}} e^{-\frac{I}{k T_e}}. \quad (9.30)$$

9.3 Entropy Maximization for Atomic Ionization

When the multitemperature equilibrium composition is calculated maximizing the entropy (9.2), it is not possible to equate the chemical potentials, but, considering (9.9), we obtain that the equilibrium condition will relate μ_s^d / T_s^d . In this section, we will analyze the same cases as in the previous section, using the same symbols. It should be noted that in the general equation reported in (9.8), we have introduced the temperature related to the chemical processes. For homogeneity with the previous section, we will consider $T_s^c = T_{\text{int}}$.

Under these assumptions, the equilibrium condition for the ionization process is given by

$$\frac{\mu_{A+}^{\text{tr}}(T_h)}{T_h} + \frac{\mu_{A+}^{\text{el}}(T_{\text{int}})}{T_{\text{int}}} + \frac{\mu_e(T_e)}{T_e} + \frac{I}{k T^c} = \frac{\mu_A^{\text{tr}}(T_h)}{T_h} + \frac{\mu_A^{\text{el}}(T_{\text{int}})}{T_{\text{int}}}. \quad (9.31)$$

From (3.40), we have that $\mu \propto T \ln \mathcal{Q}$, consequently we can deduce that the nonequilibrium coefficient θ_e will disappear from the equations. Also, in this case we have three different expressions for the cases considered above given by

case a $T_h = T_{\text{int}} \neq T_e$

$$\frac{P_{A+}}{P_A} P_e = \left(\frac{m_e k T_e}{2\pi \hbar^2} \right)^{\frac{3}{2}} k T_e \frac{\mathcal{Q}_{A+}^{\text{int}}(T_h)}{\mathcal{Q}_A^{\text{int}}(T_h)} \mathcal{Q}_e^{\text{int}} e^{-\frac{I}{k T_h}} \quad (9.32)$$

case b $T_h \neq T_{\text{int}} = T_e$

$$\frac{P_{A+}}{P_A} P_e = \left(\frac{m_e k T_e}{2\pi \hbar^2} \right)^{\frac{3}{2}} k T_e \frac{\mathcal{Q}_{A+}^{\text{int}}(T_e)}{\mathcal{Q}_A^{\text{int}}(T_e)} \mathcal{Q}_e^{\text{int}} e^{-\frac{I}{k T_e}} \quad (9.33)$$

case c $T_h \neq T_{\text{int}} \neq T_e$

$$\frac{P_{A+}}{P_A} P_e = \left(\frac{m_e k T_e}{2\pi \hbar^2} \right)^{\frac{3}{2}} k T_e \frac{\mathcal{Q}_{A+}^{\text{int}}(T_{\text{int}})}{\mathcal{Q}_A^{\text{int}}(T_{\text{int}})} \mathcal{Q}_e^{\text{int}} e^{-\frac{I}{k T_{\text{int}}}}. \quad (9.34)$$

These equations differ from corresponding cases in the previous section by the disappearance of θ_e and δ coefficients in the relevant equation.

9.4 Multitemperature Dissociation

In this section, we will consider the multitemperature equilibrium for the dissociation reaction in (1.36) for a homonuclear diatomic molecule⁶. Also in this case, a multiplicity of equations arise from the definition of different temperatures as can be appreciated by the following examples. In this case, we should consider the general description given in Sect. 9.1, considering the same translational temperature T_h for all the species, while a different temperature is assigned to each internal degree of freedom as described in Sect. 9.1: extending (9.12), we define a nonequilibrium coefficients for each internal degree as

$$\theta_s^d = \frac{T_s^d}{T_h}. \quad (9.35)$$

Let us now apply to dissociation the same approaches described in the previous sections for atomic ionization.

Model a – Minimization of Gibbs free energy

Minimizing the Gibbs free energy results in equating the chemical potentials (1.37) which in the multitemperature case is

$$\begin{aligned} -k T_h \ln \mathcal{F}_{A_2} - k T_{A_2}^{\text{rot}} \ln \mathcal{Q}_{A_2}^{\text{rot}} - k T_{A_2}^{\text{vib}} \ln \mathcal{Q}_{A_2}^{\text{vib}} - k T_{A_2}^{\text{el}} \ln \mathcal{Q}_{A_2}^{\text{el}} + k T_h \ln P_{A_2} = \\ = -2k T_h \ln \mathcal{F}_A - 2k T_A^{\text{el}} \ln \mathcal{Q}_A^{\text{el}} + D + 2k T_h \ln P_A. \end{aligned} \quad (9.36)$$

Dividing both terms by T_h , separating the partition functions from the pressures and calculating the exponential we get

$$\frac{P_A^2}{P_{A_2}} = \frac{\mathcal{F}_A^2}{\mathcal{F}_{A_2}} \frac{(\mathcal{Q}_A^{\text{el}})^{2\theta_A^{\text{el}}}}{(\mathcal{Q}_{A_2}^{\text{rot}})^{\theta_{A_2}^{\text{rot}}} (\mathcal{Q}_{A_2}^{\text{vib}})^{\theta_{A_2}^{\text{vib}}} (\mathcal{Q}_{A_2}^{\text{el}})^{\theta_{A_2}^{\text{el}}}} e^{-\frac{D}{kT_h}} \quad (9.37)$$

Model b – Maximization of entropy

Maximizing the entropy results in the equation

$$\frac{\mu_{A_2}^{\text{tr}}}{T_h} + \frac{\mu_{A_2}^{\text{rot}}}{T_{A_2}^{\text{rot}}} + \frac{\mu_{A_2}^{\text{vib}}}{T_{A_2}^{\text{vib}}} + \frac{\mu_{A_2}^{\text{el}}}{T_{A_2}^{\text{el}}} = \frac{\mu_A^{\text{tr}}}{T_h} + \frac{\mu_A^{\text{el}}}{T_A^{\text{el}}} + \frac{D}{kT^c} \quad (9.38)$$

⁶Compare with Sects. 1.2 for the one-temperature case.

and writing all the terms explicitly it becomes

$$\begin{aligned} \ln \mathcal{F}_{A_2} - \ln \mathcal{Q}_{A_2}^{\text{rot}} - \ln \mathcal{Q}_{A_2}^{\text{vib}} - \ln \mathcal{Q}_{A_2}^{\text{el}} + \ln P_{A_2} = \\ = -2 \ln \mathcal{F}_A - 2 \ln \mathcal{Q}_A^{\text{el}} + \frac{D}{kT_A^c} + 2 \ln P_A, \end{aligned} \quad (9.39)$$

and after simple algebra, we get

$$\frac{P_A^2}{P_{A_2}} = \frac{\mathcal{F}_A^2}{\mathcal{F}_{A_2}} \frac{(\mathcal{Q}_A^{\text{el}})^2}{\mathcal{Q}_{A_2}^{\text{rot}} \mathcal{Q}_{A_2}^{\text{vib}} \mathcal{Q}_{A_2}^{\text{el}}} e^{-\frac{D}{kT^c}}, \quad (9.40)$$

where the partition function of the rotational, vibrational, and electronic degrees of freedom are calculated at their own temperature (T^{rot} , T^{vib} , T^{el}).

We can put in evidence the differences between (9.37), (9.40). In **model a**, the internal partition functions are elevated to the power of the relevant nonequilibrium coefficient θ and the exponential depend on the translational temperature. The equilibrium equation obtained in **model b** does not contain the θ exponents, as in one-temperature case, and the exponential depends on the temperature T^c governing the chemical process.

9.5 Diatom Two-Temperature Ionization

We consider the process



We again obtain different two temperature Saha equations depending on the constraints used in the determination of equilibrium conditions as well as on the constraints on internal degrees of freedom.

Model a – **Minimization of Gibbs free energy**

$$P_e^{\theta_e} \frac{P_{A_2^+}}{P_{A_2}} = \mathcal{F}_e^{\theta_e} \frac{(\mathcal{Q}_{A_2^+}^{\text{rot}})^{\theta_{A_2^+}^{\text{rot}}} (\mathcal{Q}_{A_2^+}^{\text{vib}})^{\theta_{A_2^+}^{\text{vib}}} (\mathcal{Q}_{A_2^+}^{\text{el}})^{\theta_{A_2^+}^{\text{el}}}}{(\mathcal{Q}_{A_2}^{\text{rot}})^{\theta_{A_2}^{\text{rot}}} (\mathcal{Q}_{A_2}^{\text{vib}})^{\theta_{A_2}^{\text{vib}}} (\mathcal{Q}_{A_2}^{\text{el}})^{\theta_{A_2}^{\text{el}}}} \exp\left(-\frac{I_{A_2}}{kT_h}\right) \quad (9.42)$$

Case 1 $T_h = T_{A_2}^{\text{rot}} = T_{A_2^+}^{\text{rot}} = T_{A_2}^{\text{vib}} = T_{A_2^+}^{\text{vib}} = T_{A_2}^{\text{el}} = T_{A_2^+}^{\text{el}} \neq T_e$

$$P_e^{\theta_e} \frac{P_{A_2^+}}{P_{A_2}} = \mathcal{F}_e^{\theta_e} \frac{\mathcal{Q}_{A_2^+}^{\text{rot}} \mathcal{Q}_{A_2^+}^{\text{vib}} \mathcal{Q}_{A_2^+}^{\text{el}}}{\mathcal{Q}_{A_2}^{\text{rot}} \mathcal{Q}_{A_2}^{\text{vib}} \mathcal{Q}_{A_2}^{\text{el}}} \exp\left(-\frac{I_{A_2}}{kT_h}\right) \quad (9.43)$$

Case 2 $T_h = T_{A_2}^{\text{rot}} = T_{A_2^+}^{\text{rot}} = T_{A_2}^{\text{vib}} = T_{A_2^+}^{\text{vib}} \neq T_{A_2}^{\text{el}} = T_{A_2^+}^{\text{el}} = T_e$

$$P_e^{\theta_e} \frac{P_{A_2^+}}{P_{A_2}} = \mathcal{F}_e^{\theta_e} \frac{\mathcal{Q}_{A_2^+}^{\text{rot}} \mathcal{Q}_{A_2^+}^{\text{vib}} (\mathcal{Q}_{A_2^+}^{\text{el}})^{\theta_e}}{\mathcal{Q}_{A_2}^{\text{rot}} \mathcal{Q}_{A_2}^{\text{vib}} (\mathcal{Q}_{A_2}^{\text{el}})^{\theta_e}} \exp\left(-\frac{I_{A_2}}{kT_h}\right) \quad (9.44)$$

Case 3 $T_h = T_{A_2}^{\text{rot}} = T_{A_2^+}^{\text{rot}} \neq T_{A_2}^{\text{vib}} = T_{A_2^+}^{\text{vib}} \neq T_{A_2}^{\text{el}} = T_{A_2^+}^{\text{el}} = T_e$.

Considering $\gamma_v = \frac{T_{A_2}^{\text{vib}}}{T_h} = \frac{T_{A_2^+}^{\text{vib}}}{T_h}$

$$P_e^{\theta_e} \frac{P_{A_2^+}}{P_{A_2}} = \mathcal{F}_e^{\theta_e} \frac{\mathcal{Q}_{A_2^+}^{\text{rot}} (\mathcal{Q}_{A_2^+}^{\text{vib}})^{\gamma_v} (\mathcal{Q}_{A_2^+}^{\text{el}})^{\theta_e}}{\mathcal{Q}_{A_2}^{\text{rot}} (\mathcal{Q}_{A_2}^{\text{vib}})^{\gamma_v} (\mathcal{Q}_{A_2}^{\text{el}})^{\theta_e}} \exp\left(-\frac{I_{A_2}}{kT_h}\right). \quad (9.45)$$

Following (Andre et al. 1996, 1997, 2004; Aubreton et al. 1998) $\gamma_v = \sqrt{\theta_e}$

$$P_e^{\theta_e} \frac{P_{A_2^+}}{P_{A_2}} = \mathcal{F}_e^{\theta_e} \frac{\mathcal{Q}_{A_2^+}^{\text{rot}} (\mathcal{Q}_{A_2^+}^{\text{vib}})^{\sqrt{\theta_e}} (\mathcal{Q}_{A_2^+}^{\text{el}})^{\theta_e}}{\mathcal{Q}_{A_2}^{\text{rot}} (\mathcal{Q}_{A_2}^{\text{vib}})^{\sqrt{\theta_e}} (\mathcal{Q}_{A_2}^{\text{el}})^{\theta_e}} \exp\left(-\frac{I_{A_2}}{kT_h}\right) \quad (9.46)$$

Model b – **Maximization of entropy**

$$P_e \frac{P_{A_2^+}}{P_{A_2}} = \mathcal{F}_e \frac{\mathcal{Q}_{A_2^+}^{\text{rot}} \mathcal{Q}_{A_2^+}^{\text{vib}} \mathcal{Q}_{A_2^+}^{\text{el}}}{\mathcal{Q}_{A_2}^{\text{rot}} \mathcal{Q}_{A_2}^{\text{vib}} \mathcal{Q}_{A_2}^{\text{el}}} \exp\left(-\frac{I_{A_2}}{kT_c}\right) \quad (9.47)$$

Case 1 $T_h = T_{A_2}^{\text{rot}} = T_{A_2^+}^{\text{rot}} = T_{A_2}^{\text{vib}} = T_{A_2^+}^{\text{vib}} = T_{A_2}^{\text{el}} = T_{A_2^+}^{\text{el}} \neq T_e = T^c$

$$P_e \frac{P_{A_2^+}}{P_{A_2}} = \mathcal{F}_e(T_e) \frac{\mathcal{Q}_{A_2^+}^{\text{rot}}(T_h) \mathcal{Q}_{A_2^+}^{\text{vib}}(T_h) \mathcal{Q}_{A_2^+}^{\text{el}}(T_h)}{\mathcal{Q}_{A_2}^{\text{rot}}(T_h) \mathcal{Q}_{A_2}^{\text{vib}}(T_h) \mathcal{Q}_{A_2}^{\text{el}}(T_h)} \exp\left(-\frac{I_{A_2}}{kT_e}\right) \quad (9.48)$$

Case 2 $T_h = T_{A_2}^{\text{rot}} = T_{A_2^+}^{\text{rot}} = T_{A_2}^{\text{vib}} = T_{A_2^+}^{\text{vib}} \neq T_{A_2}^{\text{el}} = T_{A_2^+}^{\text{el}} = T_e = T^c$

$$P_e \frac{P_{A_2^+}}{P_{A_2}} = \mathcal{F}_e(T_e) \frac{\mathcal{Q}_{A_2^+}^{\text{rot}}(T_h) \mathcal{Q}_{A_2^+}^{\text{vib}}(T_h) \mathcal{Q}_{A_2^+}^{\text{el}}(T_e)}{\mathcal{Q}_{A_2}^{\text{rot}}(T_h) \mathcal{Q}_{A_2}^{\text{vib}}(T_h) \mathcal{Q}_{A_2}^{\text{el}}(T_e)} \exp\left(-\frac{I_{A_2}}{kT_e}\right) \quad (9.49)$$

Case 3 $T_h = T_{A_2}^{\text{rot}} = T_{A_2^+}^{\text{rot}} \neq T_{A_2}^{\text{vib}} = T_{A_2^+}^{\text{vib}} \neq T_{A_2}^{\text{el}} = T_{A_2^+}^{\text{el}} = T_e = T^c$.

Considering $\gamma_v = \frac{T_{A_2}^{\text{vib}}}{T_h} = \frac{T_{A_2^+}^{\text{vib}}}{T_h}$

$$P_e \frac{P_{A_2^+}}{P_{A_2}} = \mathcal{F}_e(T_e) \frac{\mathcal{Q}_{A_2^+}^{\text{rot}}(T_h) \mathcal{Q}_{A_2^+}^{\text{vib}}(T_v) \mathcal{Q}_{A_2^+}^{\text{el}}(T_e)}{\mathcal{Q}_{A_2}^{\text{rot}}(T_h) \mathcal{Q}_{A_2}^{\text{vib}}(T_v) \mathcal{Q}_{A_2}^{\text{el}}(T_e)} \exp\left(-\frac{I_{A_2}}{kT_e}\right). \quad (9.50)$$

9.6 Two-Temperature Hydrogen Plasma

Practically all the equations above reported have been used, by many authors (Andre et al. 1997, 2004; Aubreton et al. 1998; Boulos et al. 1994; Capitelli et al. 2001, 2002; Chen and Eddy 1998; Chen and Han 1999; Cliteur et al. 1999; Ghorui et al. 2008; Girard et al. 1999; Gleizes et al. 1999; Koalaga 2002; Koalaga and Zougmore 2002; Miller and Martinez Sanchez 1996; Rat et al. 2008; Tanaka et al. 1997; Van De Sanden et al. 1989), for numerous applications. We focus our attention on the thermodynamic properties of the hydrogen plasmas (Capitelli et al. 2001, 2002), calculated by using the different equations discussed above.

To simplify the problem, we consider only four components (H_2 , H , H^+ , and electrons e) linked by appropriate Saha equations, coupled with electroneutrality and mass conservation equations. The internal partition function of molecular hydrogen (vibrational and rotational) is calculated at T_h by summing over all of the rotational states up to the dissociation limit for each vibrational level of the ground electronic state; this procedure is repeated up to the dissociation limit for all of the 14 vibrational levels sustained by the ground state potential curve. No electronically excited states have been considered in this calculation of H_2 partition function (see Chap. 5). The partition function of atomic hydrogen is calculated at T_e by considering levels up to $n_{\max}=12$. This last assumption is roughly valid for atmospheric plasmas, when using Debye–Hückel cutoff criterion.

The multitemperature equilibrium composition is obtained by solving the system of the following equations

$$\begin{aligned} K_d(T_h, T_e) &= \frac{P_H^2}{P_{H_2}} \\ K_i(T_h, T_e) &= \left(\frac{P_{H^+}}{P_H} \right)^z P_e \\ P &= P_{H_2} + P_H + P_{H^+} + P_e = \left(\frac{\mathcal{N}_{H_2}}{V} + \frac{\mathcal{N}_H}{V} + \frac{\mathcal{N}_{H^+}}{V} \right) kT_h + \frac{\mathcal{N}_e}{V} kT_e \\ \frac{P_{H^+}}{kT_h} &= \frac{P_e}{kT_e} \Leftrightarrow \mathcal{N}_{H^+} = \mathcal{N}_e, \end{aligned} \quad (9.51)$$

where $z = 1/\theta_e$ in case of minimization of the Gibbs free energy and $z = 1$ for entropy maximization. Once the composition has been determined, one can calculate the mixture thermodynamic properties by taking into account the different temperatures acting in the system. As an example, the total enthalpy can be written as

$$\begin{aligned} H &= \frac{5}{2} kT_h(\mathcal{N}_{H_2} + \mathcal{N}_H + \mathcal{N}_{H^+}) + \frac{5}{2} kT_e\mathcal{N}_e \\ &\quad + \mathcal{N}_{H_2}\varepsilon_{H_2}^{\text{int}}(T_h) + \mathcal{N}_H\varepsilon_H^{\text{int}}(T_H^{\text{int}}) + \mathcal{N}_H D + \mathcal{N}_{H^+}(D + I), \end{aligned} \quad (9.52)$$

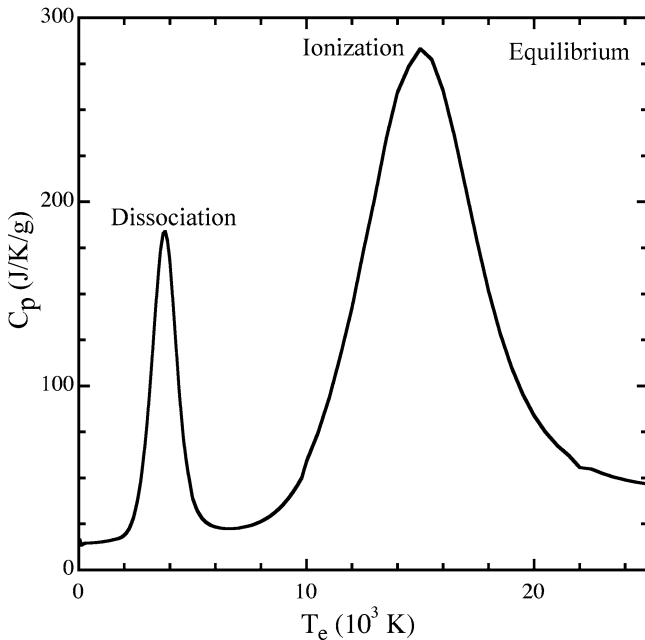


Fig. 9.1 Constant pressure specific heat for equilibrium conditions ($P = 1$ bar) as a function of the temperature

where \mathcal{N}_s is the number of particles of the s -th species and $\varepsilon_H^{\text{int}}$ is its internal energy per particle, each one depending on the relative temperature. Note that in the results we are discussing, the ro-vibrational partition function of H_2 is calculated at T_h .

The specific heat is not univocally defined: in this case, we can have

$$c_p^e = \left(\frac{\partial h}{\partial T_e} \right)_{T_h} \quad (9.53)$$

$$c_p^h = \left(\frac{\partial h}{\partial T_h} \right)_{T_e} \quad (9.54)$$

calculated as the derivative of the enthalpy per unit mass h with respect to the relevant temperature.

To better understand the multitemperature results, we recall the behaviors of the molar fractions (Figs. 1.5, 1.6) and the total specific heat (Fig. 9.1) of the equilibrium hydrogen plasma at $P = 1$ bar. Inspection of the figures shows the separation of the dissociation and ionization reactions in the examined temperature range. In particular, we note that the dissociation regime occurs in the temperature range 2,000–8,000 K with a strong peak in the specific heat at about $T = 4,000$ K, while the ionization regime is located in the temperature range 8,000–20,000 K with a peak at about $T = 15,000$ K (see Fig. 9.1).

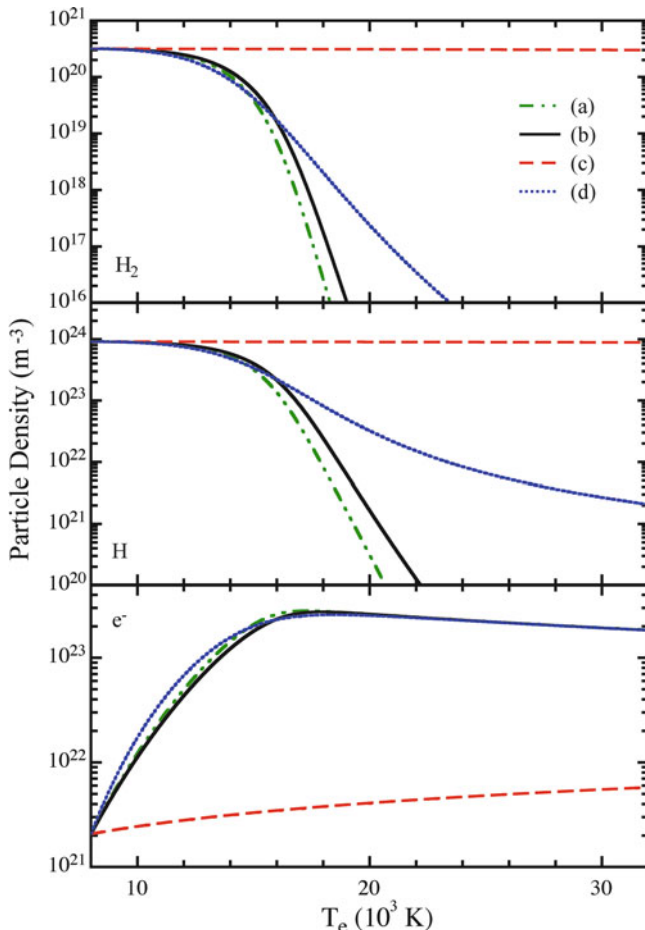


Fig. 9.2 Equilibrium composition as a function of the electron temperature for $T_h = 8,000$ K, calculated according to the different assumptions listed in Table 9.1

Table 9.1 Calculation conditions for the multitemperature hydrogen plasma

Case	K_{eq} calculation	Temperatures	Equation
(a)	minimization of Gibbs free energy	$T_{int} = T_h$	(9.25)
(b)	minimization of Gibbs free energy	$T_{int} = T_e$	(9.27)
(c)	maximization of entropy	$T_{int} = T_h$	(9.32)
(d)	maximization of entropy	$T_{int} = T_e$	(9.33)

Multitemperature results as a function of T_e for $T_h = 8,000$ K (ionization regime) and as a function of T_h for $T_e = 10,000$ K (dissociation regime) have been calculated under the conditions reported in Table 9.1.

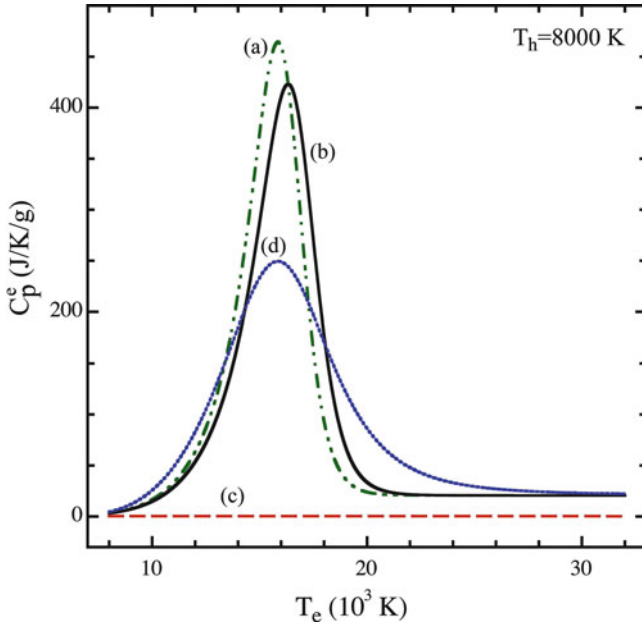


Fig. 9.3 Constant pressure specific heat c_p^e as a function of the electron temperature for $T_h = 8,000$ K, calculated according to the different assumptions listed in Table 9.1

In particular, Fig. 9.2 reports the number densities of the four components ($\mathcal{N}_e/V = \mathcal{N}_{H+}/V$) versus T_e at $T_h = 8,000$ K compared in the four cases. In the reported ionization regime, the dissociation of H_2 is practically complete and the H concentration starts decreasing from $T_e > 12,000$ K. This explains the exponential increase of \mathcal{N}_e according to (9.25), (9.27), (9.33) and the plateau of \mathcal{N}_e when use is made of (9.32) due to appearance of T_h in the corresponding exponential factor. It should be also noted that (9.25), (9.27), (9.33) produce small differences in \mathcal{N}_e , these differences however are exalted in the total specific heat of our plasma as reported in Fig. 9.3. In this figure, we can appreciate that the use of (9.32) does not produce any maximum in the total specific heat which remains very small.

In the dissociation regime, the use of (9.25), (9.27) and (9.32), (9.33) does not alter the concentration of molecular and atomic hydrogen having strong effects on the electron density. These points can be appreciated by looking at Fig. 9.4 where the number density of the different species are reported as a function of T_h for $T_e = 10,000$ K. Note, however, that in this regime the electron density is always a minority species due to the selected electron temperature. The total specific heat (see Fig. 9.5) in the dissociation regime is practically not affected by the selection of Saha equations for the ionization reaction, the only exception being represented

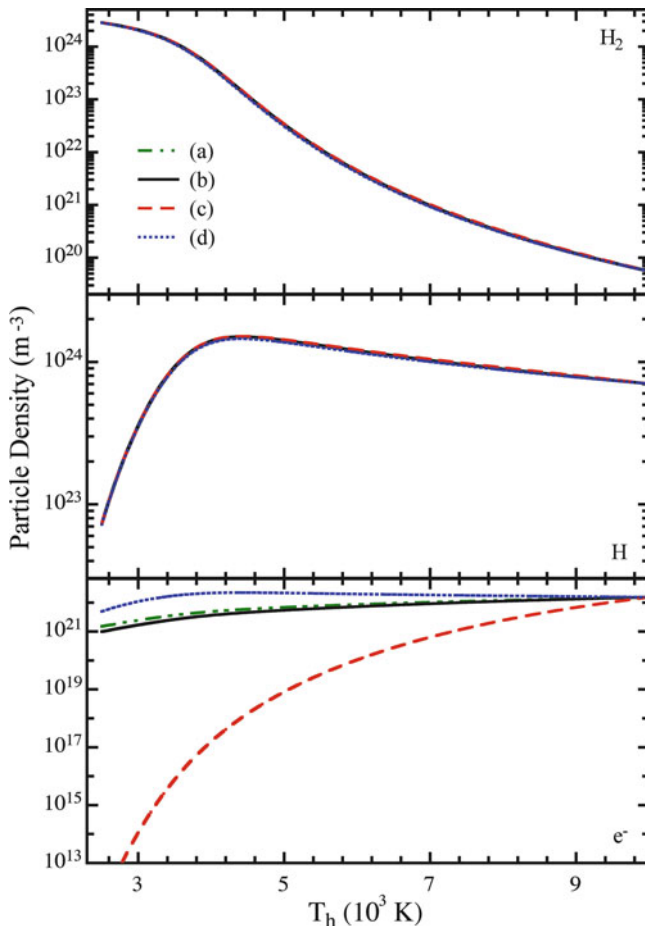


Fig. 9.4 Equilibrium composition as a function of the translational temperature for $T_e = 10,000$ K, calculated according to the different assumptions listed in Table 9.1

by the use of (9.32). The ionization equation in this case exponentially increases as a function of T_h preparing the onset of the second peak in the total specific heat for $T_h > 8,000$ K.

As a final remark, we can say that (9.33) is nowadays preferred to the other equations even though many authors tend to define a $T_{\text{int}} \neq T_e$ on the basis of kinetic considerations, mixing concepts of thermodynamics and kinetics. Our point of view is indeed more neutral, i.e., each equation has its thermodynamic explanation without a priori preference thus implying that further work is to be expected to completely clarify this intricate problem.

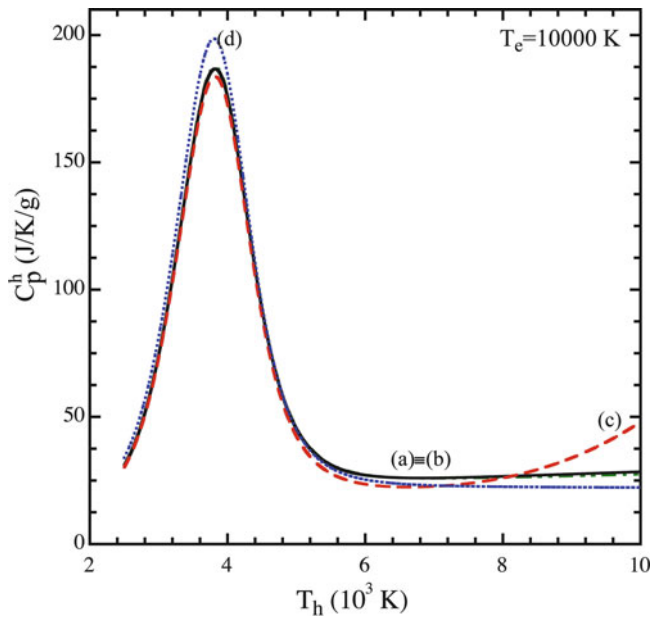


Fig. 9.5 Constant pressure specific heat as a function of the translational temperature for $T_e = 10,000$ K, calculated according to the different assumptions listed in Table 9.1

Chapter 10

Thermodynamics of Planetary Plasmas

In this chapter, we report, in graphical and tabular form, the thermodynamic properties of high temperature planetary atmospheres (Earth, Mars, Jupiter).

All the concepts (cutoff criteria and level completion for atomic species, state-to-state calculations of molecular partition function, nonideal Debye-Hückel effects) described in detail in the previous chapters have been implemented in an equilibrium computer program to produce the results here presented.

The relevant data can be used, with a fair amount of confidence, in fluid dynamic equilibrium plasma codes. For air plasma, we report also a comparison with existing data.

10.1 Basic Equations

Thermodynamic properties of high temperature equilibrium plasmas have been calculated in a wide pressure (0.01÷100 bar) and temperature range (100÷50,000 K). The thermodynamic properties have been obtained by using a self-consistent approach including Debye–Hückel corrections. The partition functions of the species are expressed as the product of the translational and internal contributions

$$\mathcal{Q}_s = \mathcal{Q}_s^{\text{tr}} \mathcal{Q}_s^{\text{int}}. \quad (10.1)$$

As a consequence, the mean energy is given by the sum of the two contributions

$$\bar{U}_s = \bar{U}_s^{\text{tr}} + \bar{U}_s^{\text{int}}. \quad (10.2)$$

The translational partition function and the associated energy are given by Sect. 4.1

$$\mathcal{Q}_s^{\text{tr}} = \frac{\mathcal{N}kT}{P} \left(\frac{m_s k T}{2\pi\hbar^2} \right)^{\frac{3}{2}} \quad (10.3)$$

$$\bar{U}_s^{\text{tr}} = \frac{3}{2} RT \quad (10.4)$$

while the internal partition function and the internal energy are calculated as the sum over atomic or molecular levels

$$Q_s^{\text{int}} = \sum_{i=1}^{n_{\text{max},s}} g_{si} \exp\left(-\frac{\varepsilon_{si}}{kT}\right) \quad (10.5)$$

$$\bar{U}_s^{\text{int}} = \frac{N_a}{Q_s^{\text{int}}} \sum_{i=1}^{n_{\text{max},s}} g_{si} \varepsilon_{si} \exp\left(-\frac{\varepsilon_{si}}{kT}\right). \quad (10.6)$$

For all molecules but H_2 , $n_{\text{max},s}$ has been restricted to the bound electronic states originating by the spin and angular momentum coupling of valence electrons. Each bound state supports a finite number of ro-vibrational levels as described in Chap. 5. The internal partition function is calculated as in (5.35)

$$Q_s^{\text{int}} = \frac{1}{\sigma} \sum_{n=1}^{n_s^m} \sum_{v=0}^{v_s^m(n)} \sum_{J=0}^{J_s^m(nv)} g_{s,nvJ} \exp\left(-\frac{\varepsilon_{s,nvJ}}{kT}\right), \quad (10.7)$$

where n runs over n_s^m the electronic states and v and J are, respectively, the vibrational and rotational quantum numbers. The statistical weight of a (nvJ) state depends only on the electronic and rotational contribution

$$g_{s,nvJ} = g_{s,n}^{\text{el}} (2J + 1). \quad (10.8)$$

The electronic energies as well as the spectroscopic data of the most important diatomic molecules for the planetary atmospheres can be found on reports published by European Space Agency (Capitelli et al. 1994, 2005a; Giordano et al. 1994; Pagano et al. 2009). For atomic species, the cutoff selected, in the compilation of the present tables, is the largest between the Fermi and Griem values (D'Angola et al. 2008). It must be pointed out that the Griem cutoff depends on the plasma composition making necessary a self-consistent solution of the problem. The formation of the plasma potential induces in the system real gas properties. The corrections to the perfect gas behavior have been determined in the framework of the Debye–Hückel theory (see Chap. 6):

$$\Delta_{\text{DH}} = \frac{kT}{24\pi\lambda_D^3} \quad (10.9)$$

$$P_{\text{DH}} = -\Delta_{\text{DH}} \quad (10.10)$$

$$F_{\text{DH}} = -2V\Delta_{\text{DH}} \quad (10.11)$$

$$G_{\text{DH}} = U_{\text{DH}} = \frac{3}{2} F_{\text{DH}} \quad (10.12)$$

$$H_{\text{DH}} = 2F_{\text{DH}} \quad (10.13)$$

$$S_{\text{DH}} = \frac{1}{2}F_{\text{DH}}. \quad (10.14)$$

It must be noted that there is also a correction to the pressure leading to the result

$$P = \sum_s P_s + P_{\text{DH}}, \quad (10.15)$$

where P_s follows the perfect gas role

$$P_s = \mathcal{N}_s kT. \quad (10.16)$$

The partial pressures are calculated solving the equilibrium equation system. Given a reaction

$$\sum_s v_{rs} X_s = 0 \quad (10.17)$$

the sum running over all the species, where the reactants have negative coefficients, the products have positive coefficients and species not involved in the reaction have null coefficients, its equilibrium equation can be written as

$$K_p^r = \prod_s P_s^{v_{rs}}. \quad (10.18)$$

In a mixture, there are many of such reactions and the equilibrium compositions are obtained solving the system of nonlinear coupled equilibrium equations and the conservation of mass and charge.

The determination of equilibrium composition is a complex problem and many algorithms have been developed (Smith and Missen 1982; Capitelli et al. 1968; Bottin et al. 1999; Meintjes and Morgan 1985; Reynolds 1986.; Gordon and McBride 1994; Mioshi and do Lago 1996; Bishnuy et al. 1997; McDonald and Floudas 1997; Phoenix and Heidemann 1998; Sofyan et al. 2003). We have applied a new approach (Colonna and D'Angola 2004; Colonna 2007), which consists in solving one equilibrium equation at a time. The method is based on the idea in (Villars 1960, 1959) soon abandoned because the method was not easily automatized. The reaction ordering is chosen determining, at each step, which reaction is farther from equilibrium, defining a reaction distance. The algorithm (details can be found in (Colonna and D'Angola 2004; Colonna 2007)) is very fast and stable, finding in very few steps the concentration of principal species and refining the solution of minority species in a second stage. A crucial aspect is the automatic determination of a *shortcut reaction* that produces in a single step the same advancement resulting from hundreds of thousand steps with the original reaction set. Once the reaction farther from equilibrium is solved, calculating the new composition, Debye length and cutoffs are updated. It should be noted that the Debye length and cutoffs converge faster than the mixture composition, being related to the concentration of the majority species. In hierarchical methods, the

concept of accuracy differs completely respect to global minimization approaches, where the tolerance is the maximum percentage error for each concentration. In fact, the concentration precision is given by the machine error for all the species except for those with molar fraction below a given tolerance which are affected by large errors. Details about error analysis are reported in (Colonna 2007).

The thermodynamic properties of the mixture are calculated using the traditional transformation equation from energy or partition function

$$F = -kT \sum_s N_s \ln Q_f + F_{\text{DH}} \quad (10.19)$$

$$U = - \sum_s N_s \bar{U}_s + U_{\text{DH}} \quad (10.20)$$

$$H = U + PV \quad (10.21)$$

$$G = F + PV \quad (10.22)$$

$$S = \frac{U - F}{T} \quad (10.23)$$

$$c_p = \left(\frac{\partial h}{\partial T} \right)_P . \quad (10.24)$$

It should be noted that virial corrections have been neglected in these calculations, being their effects appreciable at high pressures (>20 bar) and low temperature ($<1,500$ K) as discussed in Sect. 1.10 and in Chap. 7.

In the next sections, thermodynamic properties of planetary plasma have been reported in a wide pressure ($0.01 \div 100$ bar) and temperature range ($100 \div 50,000$ K). In particular, species considered, equilibrium compositions and thermodynamic properties of air, Mars and Jupiter atmosphere have been reported in different tables. Figures 10.1–10.4 show, respectively, density, enthalpy, entropy and specific heat of air, Mars and Jupiter atmospheres at $P = 1$ bar. Note that air and Mars atmosphere behave similarly, presenting large differences with the corresponding thermodynamic properties of Jupiter atmosphere.

10.2 Air Plasmas

Thermodynamic properties of high temperature equilibrium air have been calculated in the pressure range ($0.01 \div 100$ bar) and in the temperature range ($100 \div 50,000$ K). In Table 10.1, species considered in the calculations, volume percentage compositions and enthalpies of formation have been reported while temperature dependence of molar fractions of air species at atmospheric pressure has been represented in Figs. 10.5, 10.6, where, respectively, species with molar fractions $\chi_i \geq 0.1$ and $10^{-8} \leq \chi_i \leq 0.1$ are shown.

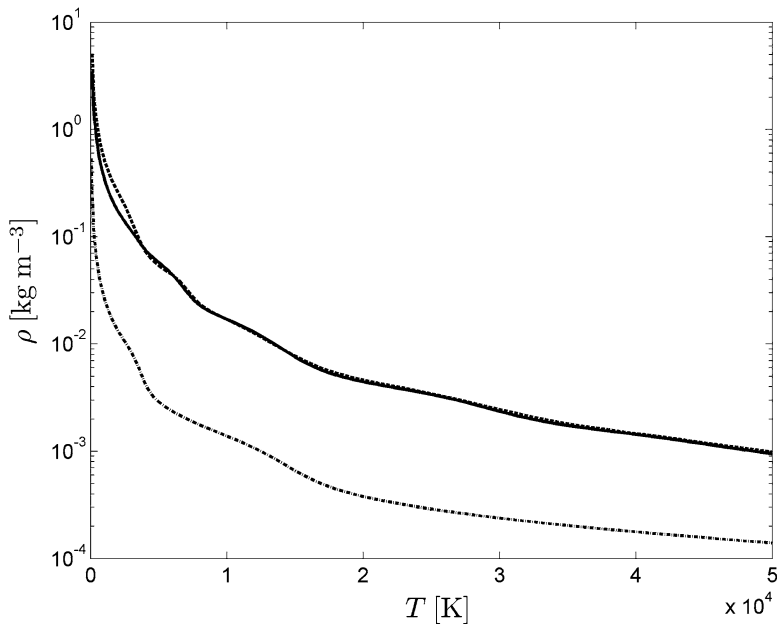


Fig. 10.1 Comparison of density of air (full line), Mars (dashed line), and Jupiter (dash-dotted line) atmospheres at $P = 1$ bar

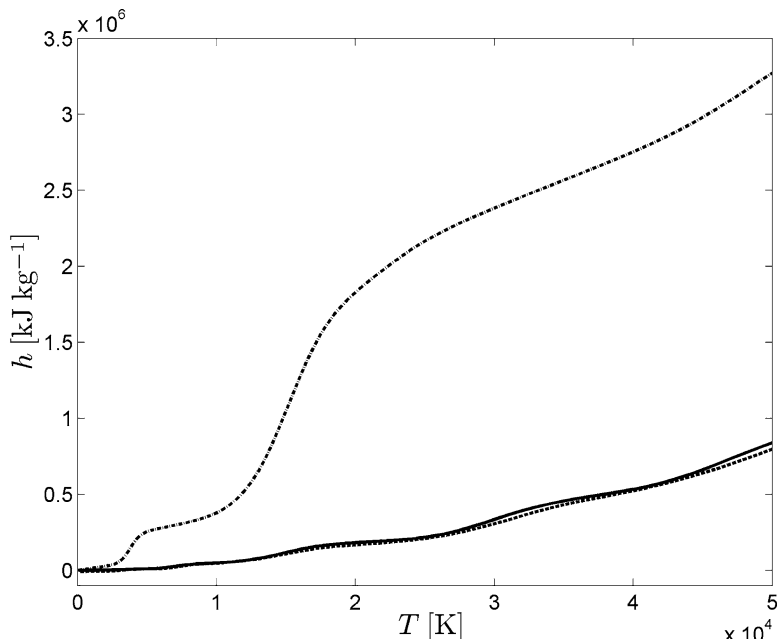


Fig. 10.2 Comparison of specific enthalpy of air (full line), Mars (dashed line) and Jupiter (dash-dotted line) atmospheres at $P = 1$ bar

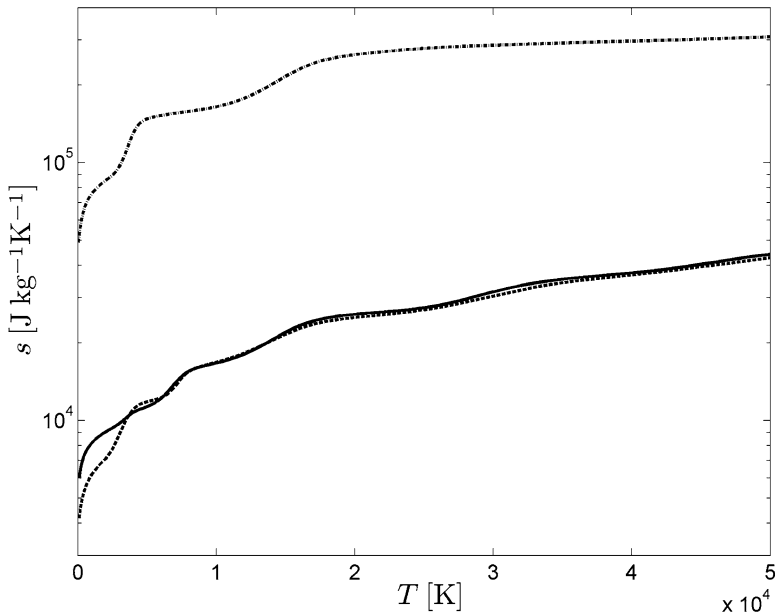


Fig. 10.3 Comparison of specific entropy of air (full line), Mars (dashed line), and Jupiter (dash-dotted line) atmospheres at $P = 1$ bar

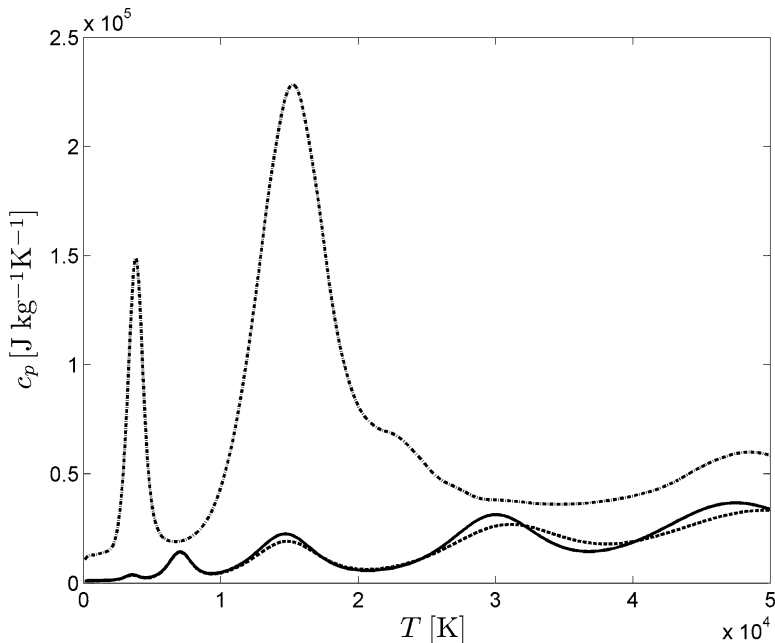


Fig. 10.4 Comparison of specific heat of air (full line), Mars (dashed line) and Jupiter (dash-dotted line) atmospheres at $P = 1$ bar

Table 10.1 Air species, volume compositions, and enthalpies of formation

Species	Volume (%)	h_f (eV)
N_2	80	0.0
N_2^+	0.0	15.5808
N	0.0	4.8795
N^+	0.0	19.4285
N^{+2}	0.0	49.0425
N^{+3}	0.0	96.4825
N^{+4}	0.0	173.9555
O_2	20	0.0
O_2^+	0.0	12.071
O_2^-	0.0	-0.44
O	0.0	2.5575
O^-	0.0	0.95
O^+	0.0	16.1755
O^{+2}	0.0	51.3315
O^{+3}	0.0	106.2805
O^{+4}	0.0	183.6965
NO	0.0	0.941
NO^+	0.0	10.20536
e	0.0	0.0

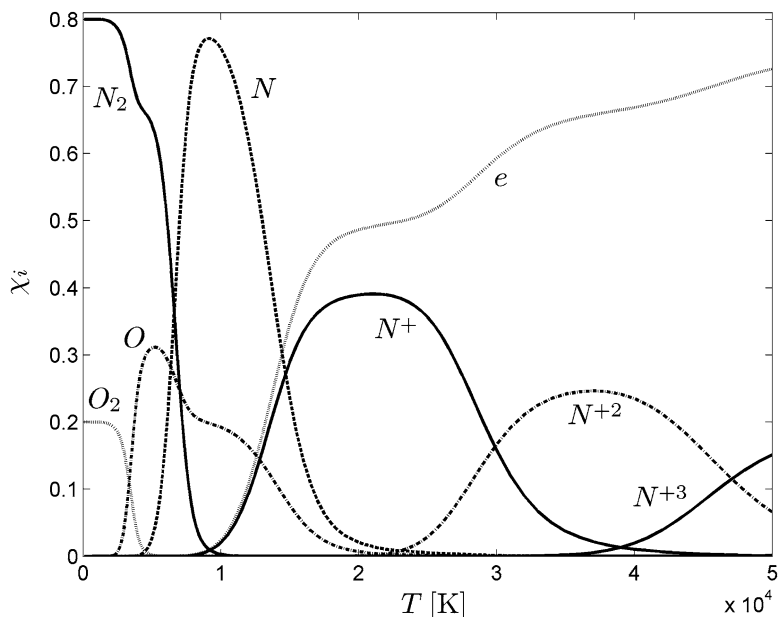


Fig. 10.5 Molar fractions of air species at atmospheric pressure. Species with $\chi_i > 10^{-1}$ have been considered

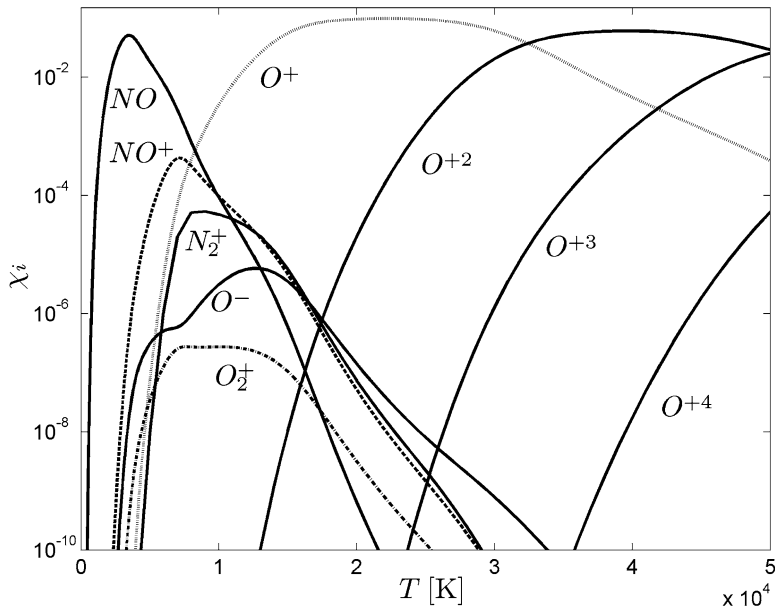


Fig. 10.6 Molar fractions of air species at atmospheric pressure. Species with $10^{-8} \leq \chi_i \leq 0.1$ have been considered

Specific enthalpy, specific entropy, density, specific heat, equilibrium, frozen and total isentropic coefficients have been reported in Tables 10.2–10.8 and shown in Figs. 10.7–10.17 in the pressure range (0.01–100 bar) and in the temperature range (100–50,000 K). Isentropic exponent has been compared with data reported in (Henderson and Menart 2008) in Fig. 10.18. In this case, we report γ_f , γ_{eq} and γ . The data reported in the different figures can be used with fair amount of confidence for different applications. It is interesting to compare the relevant data with the corresponding values reported in the literature. We refer, in particular, to the atmospheric tables of Boulos et al. (1994) and to the pioneeristic tables of Yos (1967). The relevant differences for density, enthalpy and the specific heat are reported in Figs. 10.11–10.13. In general, the agreement is satisfactory up to $T = 15,000$ K, the differences becoming important for higher temperatures especially with Yos results. A similar trend is observed comparing our results with those in (Lisal et al. 2002) at $P = 10$ bar (see Fig. 10.14 for enthalpy and specific heat) by using REMC method Sect. 7.4. The agreement is rather satisfactory, even though many compensation effects are such to hide the strong differences either in the method or in the input data.

Table 10.2 Specific enthalpy h [kJ kg⁻¹] of air as a function of temperature for different pressures

T (K)	P (bar)				
	10^{-2}	10^{-1}	1	10	10^2
100	100.958	100.958	100.958	100.958	100.958
200	201.916	201.916	201.916	201.916	201.916
300	303.240	303.240	303.240	303.240	303.240
400	404.808	404.808	404.808	404.808	404.808
500	508.248	508.248	508.248	508.248	508.248
600	612.579	612.579	612.579	612.579	612.579
700	720.163	720.163	720.163	720.163	720.163
800	829.321	829.321	829.321	829.321	829.321
900	941.415	941.415	941.415	941.415	941.415
1,000	1,055.425	1,055.425	1,055.425	1,055.425	1,055.425
1,500	1,654.368	1,654.259	1,654.221	1,654.213	1,654.209
2,000	2,323.130	2,305.327	2,299.679	2,297.896	2,297.331
2,500	3,498.021	3,152.698	3,036.460	2,998.996	2,987.081
3,000	6,070.441	4,804.604	4,094.762	3,829.926	3,742.003
3,500	7,660.881	7,023.943	5,789.172	4,945.197	4,608.160
4,000	8,698.956	8,340.692	7,620.688	6,422.216	5,646.193
4,500	10,577.950	9,510.274	8,929.649	7,983.307	6,863.672
5,000	15,049.494	11,475.684	10,175.724	9,328.274	8,174.183
6,000	33,236.326	22,160.691	14,960.316	12,156.206	10,731.689
7,000	40,446.037	36,908.484	26,338.112	17,495.214	13,731.197
8,000	44,739.726	42,579.756	38,411.294	27,273.108	18,496.571
9,000	53,430.686	47,098.151	44,274.573	38,054.914	25,983.993
10,000	72,082.461	54,698.867	48,741.888	44,957.858	35,217.812
11,000	103,389.677	68,354.953	54,759.995	49,658.797	43,303.235
12,000	135,571.933	90,261.128	64,040.455	54,531.395	49,186.526
13,000	154,883.548	117,569.949	77,801.211	60,800.710	53,985.855
14,000	164,365.813	142,041.377	96,334.081	69,155.888	58,847.149
15,000	169,871.874	158,386.225	117,805.248	80,237.510	64,370.794
16,000	174,122.732	168,220.181	138,488.040	93,874.755	71,103.168
17,000	178,361.867	174,593.747	155,176.206	109,816.833	79,256.961
18,000	183,959.618	179,537.520	167,288.618	126,631.859	88,659.677
19,000	193,464.910	184,168.540	175,923.474	142,712.940	99,586.806
20,000	210,984.575	189,574.536	182,447.346	156,853.857	111,679.541
22,000	279,812.636	209,290.177	193,424.717	178,182.253	137,192.225
24,000	362,905.544	254,714.026	207,299.354	192,937.792	161,050.705
26,000	419,073.559	324,232.491	232,796.547	205,756.099	181,025.090
28,000	449,704.188	390,543.029	276,868.060	221,105.745	197,503.079
30,000	473,912.266	436,641.372	334,847.704	243,944.321	212,326.863
35,000	628,974.590	509,759.647	456,654.276	345,876.572	257,609.617
40,000	849,979.015	666,287.352	533,201.540	456,846.869	335,320.393
45,000	975,976.574	863,540.060	662,213.596	537,790.273	431,910.288
50,000	1,200,753.306	994,645.516	840,160.969	634,877.978	518,237.917

Table 10.3 Specific entropy s [$\text{J kg}^{-1} \text{ K}^{-1}$] of air as a function of temperature for different pressures

T (K)	P (bar)				
	10^{-2}	10^{-1}	1	10	10^2
100	7319.489	6654.542	5989.594	5324.647	4659.699
200	7819.896	7154.948	6490.001	5825.053	5160.105
300	8230.788	7565.841	6900.893	6235.946	5570.998
400	8522.692	7857.744	7192.797	6527.849	5862.902
500	8753.887	8088.939	7423.992	6759.044	6094.097
600	8943.382	8278.434	7613.486	6948.539	6283.591
700	9109.891	8444.943	7779.995	7115.048	6450.100
800	9254.838	8589.890	7924.943	7259.995	6595.047
900	9387.601	8722.654	8057.706	7392.758	6727.811
1000	9506.925	8841.977	8177.030	7512.082	6847.135
1500	9991.966	9326.934	8661.945	7996.997	7332.050
2000	10374.514	9700.062	9032.100	8366.231	7700.949
2500	10890.202	10075.241	9359.926	8678.776	8008.679
3000	11823.314	10670.855	9742.725	8980.393	8283.207
3500	12319.994	11357.156	10262.768	9322.957	8549.864
4000	12596.448	11710.856	10753.000	9716.390	8826.319
4500	13035.602	11985.636	11062.363	10084.536	9112.905
5000	13970.891	12397.366	11324.373	10368.275	9388.899
6000	17279.175	14313.497	12183.588	10880.865	9855.392
7000	18411.453	16602.881	13923.622	11696.161	10315.689
8000	18981.905	17367.726	15545.002	12995.618	10948.398
9000	19997.245	17897.942	16240.095	14268.489	11827.040
10000	21949.676	18693.978	16709.937	14999.085	12799.466
11000	24924.062	19988.411	17280.850	15447.199	13571.512
12000	27728.255	21886.790	18084.003	15869.437	14083.893
13000	29280.176	24066.857	19178.810	16367.960	14466.776
14000	29985.485	25880.286	20543.958	16981.410	14824.119
15000	30366.400	27009.256	22017.125	17738.425	15199.842
16000	30640.886	27644.687	23346.350	18607.395	15627.022
17000	30897.830	28032.175	24354.951	19562.656	16111.393
18000	31217.116	28314.784	25045.605	20512.724	16634.408
19000	31729.496	28565.615	25512.308	21372.442	17209.590
20000	32625.472	28842.949	25847.377	22090.143	17813.327
22000	35888.245	29775.056	26369.722	23099.790	18995.512
24000	39505.807	31739.000	26971.198	23738.277	20006.749
26000	41761.739	34514.011	27984.194	24248.271	20788.006
28000	42900.465	36971.663	29607.500	24813.824	21386.844
30000	43734.894	38564.824	31599.371	25594.955	21889.511
35000	48435.833	40818.914	35371.510	28690.005	23256.962
40000	54368.947	44955.346	37411.486	31642.243	25282.578
45000	57340.319	49613.580	40423.931	33539.827	27513.263
50000	62046.283	52378.961	44166.135	35565.736	29303.288

Table 10.4 Density ρ [kg m^{-3}] of air as a function of temperature for different pressures

T (K)	P (bar)				
	10^{-2}	10^{-1}	1	10	10^2
100	0.03465120	0.34651200	3.46512000	34.6512000	346.512000
200	0.01732560	0.17325600	1.73256000	17.3256000	173.256000
300	0.01155040	0.11550400	1.15504000	11.5504000	115.504000
400	0.00866281	0.08662810	0.86628100	8.66281000	86.6281000
500	0.00693025	0.06930250	0.69302500	6.93025000	69.3025000
600	0.00577521	0.05775200	0.57752000	5.77520000	57.7520000
700	0.00495018	0.04950180	0.49501800	4.95018000	49.5018000
800	0.00433140	0.04331400	0.43314000	4.33140000	43.3140000
900	0.00385014	0.03850140	0.38501400	3.85014000	38.5014000
1,000	0.00346512	0.03465120	0.34651200	3.46512000	34.6512000
1,500	0.00231006	0.02310080	0.23100800	2.31008000	23.1008000
2,000	0.00173001	0.01731750	0.17323100	1.73248000	17.3254000
2,500	0.00134653	0.01372700	0.13817400	1.38468000	13.8562000
3,000	0.00101631	0.01086230	0.11295300	1.14655000	11.5231000
3,500	0.00083214	0.00859941	0.09180140	0.96185800	9.80484000
4,000	0.00071898	0.00729257	0.07569730	0.80757500	8.43599000
4,500	0.00062014	0.00637863	0.06527960	0.68592900	7.29747000
5,000	0.00051192	0.00555825	0.05761850	0.59777100	6.35892000
6,000	0.00031352	0.00380173	0.04419050	0.47461300	5.01336000
7,000	0.00024800	0.00260883	0.03105880	0.37068700	4.08181000
8,000	0.00021184	0.00216573	0.02295250	0.27559000	3.29544000
9,000	0.00017757	0.00187718	0.01933550	0.21114100	2.59484000
10,000	0.00014036	0.00160975	0.01696560	0.17719800	2.04911000
11,000	0.00010536	0.00133530	0.01489580	0.15616600	1.69664000
12,000	0.00008212	0.00106728	0.01288570	0.13942700	1.47733000
13,000	0.00007001	0.00084792	0.01091190	0.12427700	1.32233000
14,000	0.00006312	0.00070257	0.00908662	0.10986700	1.19611000
15,000	0.00005830	0.00061502	0.00757016	0.09613230	1.08400000
16,000	0.00005440	0.00055905	0.00644765	0.08339210	0.98021800
17,000	0.00005104	0.00051886	0.00567209	0.07220580	0.88296600
18,000	0.00004792	0.00048632	0.00513651	0.06293000	0.79208000
19,000	0.00004477	0.00045856	0.00474947	0.05560990	0.70894000
20,000	0.00004127	0.00043317	0.00444922	0.04999950	0.63478700
22,000	0.00003329	0.00038244	0.00397611	0.04238760	0.51540300
24,000	0.00002692	0.00032463	0.00358058	0.03750020	0.43155300
26,000	0.00002318	0.00026839	0.00317687	0.03387140	0.37389700
28,000	0.00002093	0.00022758	0.00274892	0.03078790	0.33286300
30,000	0.00001922	0.00020155	0.00235249	0.02779030	0.30155000
35,000	0.00001478	0.00016333	0.00173932	0.02052750	0.24163100
40,000	0.00001131	0.00012852	0.00143504	0.01575240	0.18981200
45,000	0.00000954	0.00010172	0.00117183	0.01306980	0.15005200
50,000	0.00000792	0.00008657	0.00094912	0.01103000	0.12422300

Table 10.5 Specific heat c_p [J kg⁻¹ K⁻¹] of air as a function of temperature for different pressures

T (K)	P (bar)				
	10^{-2}	10^{-1}	1	10	10^2
100	1014.520	1007.379	999.692	991.135	980.921
200	1024.986	1019.193	1012.905	1005.712	996.771
300	1035.496	1031.067	1026.177	1020.358	1012.707
400	1046.007	1042.975	1039.520	1035.057	1028.671
500	1056.632	1055.002	1052.987	1049.905	1044.764
600	1067.303	1067.108	1066.540	1064.828	1060.917
700	1078.075	1079.354	1080.253	1079.881	1077.178
800	1089.129	1091.868	1094.242	1095.180	1093.577
900	1100.460	1104.679	1108.478	1110.624	1110.069
1000	1112.283	1117.918	1123.082	1126.371	1126.802
1500	1197.811	1201.673	1207.825	1212.330	1214.302
2000	1576.336	1414.532	1353.060	1326.512	1314.418
2500	3852.955	2310.936	1732.113	1523.123	1443.388
3000	4780.056	4396.216	2736.026	1926.976	1633.423
3500	2224.724	3534.237	3782.774	2627.059	1925.484
4000	2521.479	2304.186	3108.601	3128.177	2293.618
4500	5381.352	2819.383	2493.950	2877.939	2541.829
5000	13324.183	5163.011	2899.424	2605.873	2543.750
6000	14199.251	16723.042	7450.140	3634.367	2651.560
7000	3986.872	9129.795	14323.441	7355.384	3674.722
8000	5566.082	4161.324	8416.463	11594.896	5921.948
9000	12436.343	5550.852	4507.565	9193.429	8779.046
10000	25858.943	9990.580	4871.495	5453.854	9341.867
11000	35022.360	17849.586	7112.580	4465.663	7153.383
12000	25917.821	26178.366	11059.886	5095.517	5214.909
13000	12890.191	27101.316	16452.059	6677.107	4555.560
14000	6447.673	19688.604	21274.323	9130.361	4774.278
15000	4484.200	11760.530	22257.378	12337.200	5541.464
16000	4539.567	7201.355	18702.803	15649.028	6758.608
17000	5836.254	5381.051	13514.762	17795.560	8396.067
18000	8580.667	5132.901	9384.078	17691.110	10338.294
19000	13520.980	5895.724	6976.605	15504.099	12268.423
20000	21472.278	7616.617	5932.350	12482.605	13669.132
22000	41635.856	15119.992	6368.178	7927.448	13373.046
24000	38583.471	28861.573	9512.442	6462.797	10341.591
26000	19648.378	37528.527	16242.392	7012.757	7963.109
28000	11861.544	28695.069	25924.269	9149.809	7124.192
30000	14464.231	17113.209	31322.438	13188.905	7395.310
35000	49705.790	18594.428	16157.240	25600.297	11542.517
40000	29666.227	42697.574	18627.342	17641.543	19040.416
45000	30732.499	31126.417	33526.227	16552.424	18912.212
50000	55626.641	26315.412	33745.157	24246.007	15715.859

Table 10.6 Equilibrium isentropic coefficient γ_{eq} of air as a function of temperature for different pressures

T (K)	P (bar)				
	10^{-2}	10^{-1}	1	10	10^2
100	1.40073	1.40073	1.40073	1.40073	1.40073
200	1.40098	1.40098	1.40098	1.40098	1.40098
300	1.39740	1.39740	1.39742	1.39742	1.39742
400	1.39155	1.39155	1.39154	1.39154	1.39155
500	1.38275	1.38274	1.38268	1.38266	1.38267
600	1.37219	1.37219	1.37209	1.37220	1.37208
700	1.36137	1.36140	1.36132	1.36135	1.36135
800	1.35126	1.35144	1.35125	1.35086	1.35120
900	1.34330	1.34264	1.34245	1.34203	1.34234
1,000	1.33383	1.33477	1.33476	1.33398	1.33463
1,500	1.30367	1.30325	1.30284	1.30396	1.30344
2,000	1.24559	1.26628	1.27400	1.27701	1.27759
2,500	1.16097	1.19366	1.22840	1.24696	1.25427
3,000	1.18204	1.17805	1.18942	1.21490	1.23331
3,500	1.26262	1.21437	1.20206	1.20397	1.21936
4,000	1.21162	1.25609	1.23544	1.22233	1.22046
4,500	1.15710	1.20498	1.25251	1.24862	1.23668
5,000	1.18074	1.17045	1.21607	1.25857	1.25744
6,000	1.20001	1.22581	1.19698	1.21481	1.26261
7,000	1.25416	1.21551	1.25006	1.22565	1.23511
8,000	1.19854	1.24953	1.23604	1.27051	1.24718
9,000	1.18964	1.21041	1.25185	1.26396	1.28540
10,000	1.24408	1.20251	1.23013	1.26180	1.29917
11,000	1.27509	1.23834	1.21747	1.25555	1.28957
12,000	1.25587	1.28289	1.23326	1.24001	1.28065
13,000	1.26381	1.29509	1.26803	1.23822	1.26989
14,000	1.34550	1.28188	1.30300	1.25132	1.25971
15,000	1.43566	1.29159	1.31924	1.27685	1.25297
16,000	1.46077	1.34207	1.31827	1.30453	1.25440
17,000	1.39019	1.40511	1.31972	1.32883	1.26803
18,000	1.28075	1.43262	1.33758	1.34540	1.28640
19,000	1.21647	1.39566	1.37205	1.35210	1.30640
20,000	1.20809	1.31841	1.40361	1.35865	1.32759
22,000	1.23741	1.22895	1.37495	1.38533	1.36675
24,000	1.23133	1.24564	1.27975	1.40487	1.39602
26,000	1.23565	1.26042	1.25198	1.36358	1.41848
28,000	1.26725	1.25583	1.27075	1.30398	1.42120
30,000	1.23898	1.26336	1.28467	1.28132	1.39747
35,000	1.21766	1.23682	1.29011	1.31139	1.31423
40,000	1.22304	1.23992	1.26196	1.32144	1.32654
45,000	1.20879	1.24190	1.26214	1.30438	1.35301
50,000	1.20421	1.23192	1.26853	1.28797	1.35465

Table 10.7 Frozen isentropic coefficient γ_f of air as a function of temperature for different pressures

T (K)	P (bar)				
	10^{-2}	10^{-1}	1	10	10^2
100	1.39993	1.39993	1.39993	1.39993	1.39993
200	1.39980	1.39980	1.39980	1.39980	1.39980
300	1.39852	1.39852	1.39852	1.39852	1.39852
400	1.39393	1.39393	1.39393	1.39393	1.39393
500	1.38549	1.38549	1.38549	1.38549	1.38549
600	1.37466	1.37466	1.37466	1.37466	1.37466
700	1.36329	1.36329	1.36329	1.36329	1.36329
800	1.35261	1.35261	1.35261	1.35261	1.35260
900	1.34314	1.34314	1.34314	1.34314	1.34314
1000	1.33500	1.33500	1.33500	1.33500	1.33500
1500	1.30938	1.30938	1.30938	1.30938	1.30937
2000	1.29724	1.29689	1.29678	1.29674	1.29671
2500	1.29933	1.29251	1.29022	1.28948	1.28922
3000	1.33264	1.30629	1.29194	1.28666	1.28488
3500	1.34856	1.33447	1.30813	1.29076	1.28393
4000	1.35044	1.34462	1.32897	1.30334	1.28729
4500	1.35840	1.34785	1.33866	1.31860	1.29497
5000	1.38558	1.35588	1.34309	1.32882	1.30486
6000	1.47236	1.40747	1.36114	1.33943	1.32031
7000	1.45599	1.44289	1.39815	1.35399	1.32831
8000	1.43048	1.42646	1.41412	1.37458	1.33497
9000	1.41644	1.41111	1.40738	1.38901	1.34436
10000	1.40056	1.39878	1.39910	1.39311	1.35807
11000	1.39914	1.38004	1.38829	1.39187	1.37201
12000	1.41739	1.38249	1.37686	1.38457	1.38056
13000	1.45180	1.39838	1.37341	1.37925	1.38226
14000	1.48074	1.42046	1.37878	1.37126	1.38629
15000	1.50764	1.44605	1.38898	1.37916	1.38240
16000	1.52711	1.47033	1.40631	1.37558	1.38228
17000	1.53938	1.49112	1.43065	1.37736	1.38961
18000	1.53961	1.51346	1.45650	1.39684	1.39682
19000	1.52499	1.52478	1.47689	1.41189	1.40022
20000	1.49545	1.52850	1.48886	1.42390	1.40638
22000	1.44035	1.50208	1.51248	1.46444	1.42935
24000	1.42721	1.45341	1.50072	1.49253	1.45707
26000	1.44384	1.42374	1.46797	1.49672	1.48140
28000	1.46293	1.42543	1.43230	1.48242	1.49367
30000	1.47819	1.43651	1.41391	1.45782	1.49477
35000	1.43304	1.47113	1.43761	1.41780	1.44485
40000	1.43538	1.45900	1.46521	1.43346	1.41969
45000	1.47289	1.46757	1.46771	1.45447	1.43052
50000	1.49658	1.48721	1.47373	1.47102	1.45438

Table 10.8 Isentropic coefficient γ of air as a function of temperature for different pressures

T (K)	P (bar)				
	10^{-2}	10^{-1}	1	10	10^2
100	1.40064	1.40064	1.40064	1.40064	1.40064
200	1.39977	1.39977	1.39977	1.39977	1.39977
300	1.39744	1.39744	1.39744	1.39744	1.39744
400	1.39173	1.39173	1.39173	1.39173	1.39173
500	1.38279	1.38279	1.38279	1.38278	1.38277
600	1.37216	1.37216	1.37216	1.37216	1.37215
700	1.36136	1.36136	1.36136	1.36133	1.36129
800	1.35131	1.35127	1.35130	1.35127	1.35043
900	1.34242	1.34241	1.34229	1.34221	1.34218
1,000	1.33464	1.33471	1.33440	1.33428	1.33406
1,500	1.30283	1.30323	1.30335	1.30335	1.30325
2,000	1.24469	1.26607	1.27400	1.27661	1.27732
2,500	1.14557	1.18808	1.22641	1.24650	1.25411
3,000	1.14930	1.14978	1.17699	1.21058	1.23197
3,500	1.25430	1.18600	1.16985	1.18822	1.21357
4,000	1.20513	1.24508	1.20511	1.19121	1.20565
4,500	1.13644	1.19447	1.23536	1.21402	1.21011
5,000	1.11762	1.14597	1.20115	1.23190	1.22279
6,000	1.12856	1.12820	1.14627	1.18693	1.22909
7,000	1.24391	1.16181	1.14411	1.16018	1.19547
8,000	1.18333	1.23578	1.17645	1.16137	1.17777
9,000	1.14317	1.19234	1.23105	1.18107	1.17793
10,000	1.13537	1.15973	1.21203	1.22248	1.18783
11,000	1.13541	1.14980	1.18285	1.23193	1.21004
12,000	1.15263	1.15018	1.16923	1.21176	1.23304
13,000	1.21444	1.15631	1.16578	1.19564	1.23571
14,000	1.32092	1.17918	1.16836	1.18393	1.22553
15,000	1.42232	1.22984	1.17535	1.18285	1.20999
16,000	1.45144	1.30555	1.19212	1.18363	1.19831
17,000	1.38149	1.38138	1.22318	1.18872	1.19433
18,000	1.26799	1.41522	1.26897	1.20115	1.19273
19,000	1.19129	1.38069	1.32222	1.21651	1.19385
20,000	1.15815	1.30197	1.36590	1.23957	1.19978
22,000	1.14102	1.18974	1.34917	1.30279	1.22320
24,000	1.15197	1.16107	1.24751	1.34776	1.25933
26,000	1.18763	1.15920	1.19345	1.31971	1.30037
28,000	1.24058	1.17556	1.17773	1.25673	1.32417
30,000	1.21914	1.20769	1.17808	1.21567	1.31752
35,000	1.14052	1.20051	1.22420	1.19840	1.23596
40,000	1.18115	1.15721	1.21333	1.22884	1.21309
45,000	1.18029	1.18831	1.17766	1.23592	1.23070
50,000	1.14522	1.19894	1.19075	1.20481	1.24883

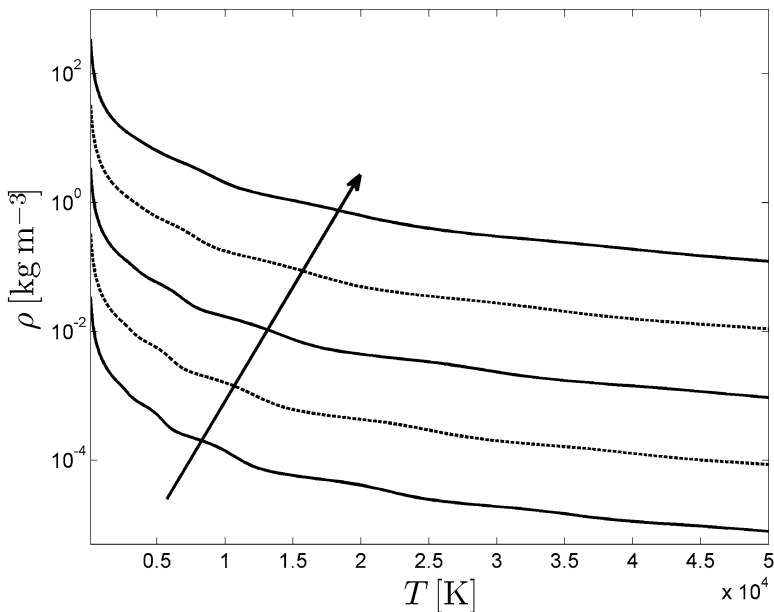


Fig. 10.7 Density of air at $P = 10^{-2}, 10^{-1}, 1, 10, 100$ bar

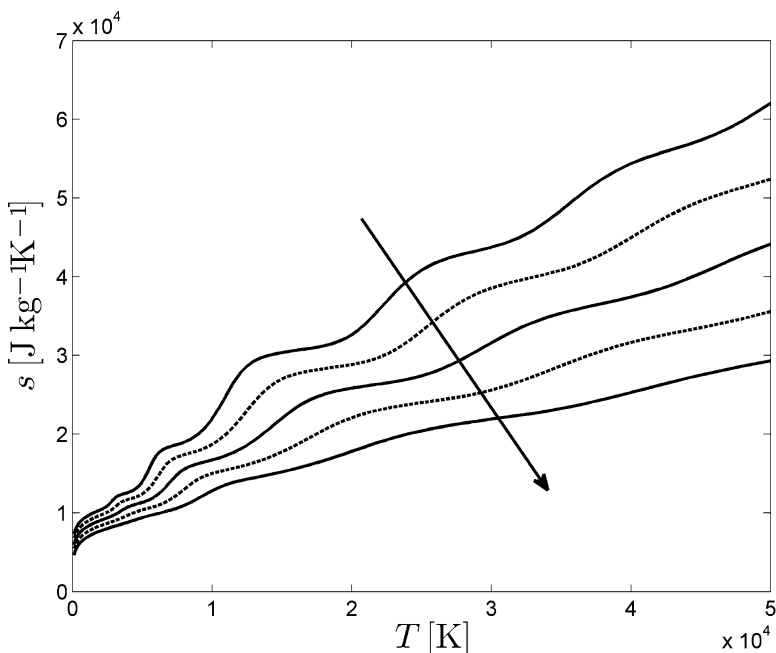


Fig. 10.8 Specific entropy of air at $P = 10^{-2}, 10^{-1}, 1, 10, 100$ bar

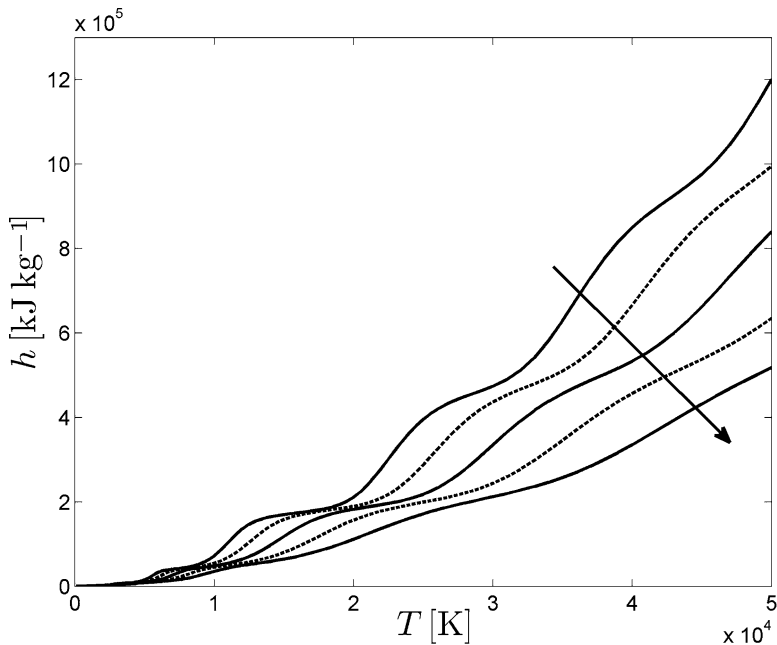


Fig. 10.9 Specific enthalpy of air at $P = 10^{-2}, 10^{-1}, 1, 10, 100$ bar

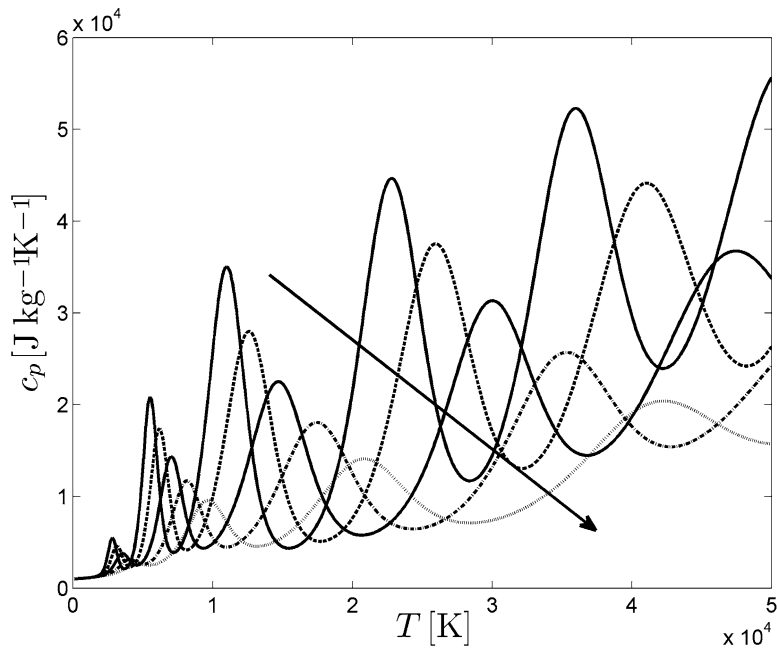


Fig. 10.10 Specific heat of air at $P = 10^{-2}, 10^{-1}, 1, 10, 100$ bar

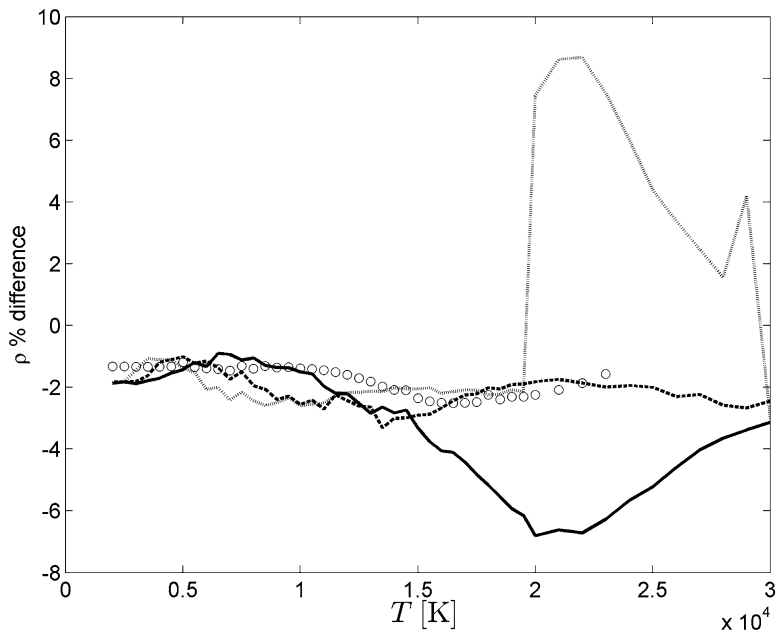


Fig. 10.11 Percentage differences of density of air with data obtained by Yos at $P = 10^{-2}$ (dotted line), 1 (dashed line), 100 (full line) bar and by Boulos et al. (o) at $P = 1$ bar

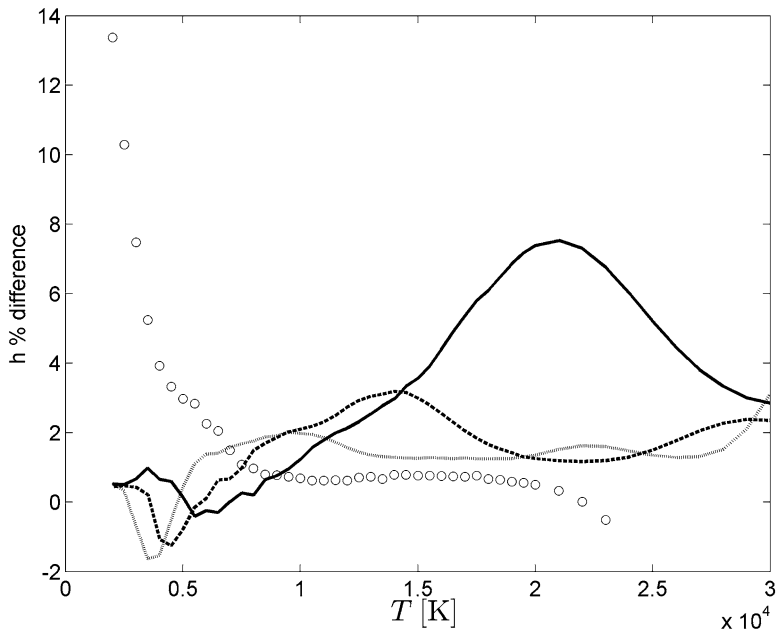


Fig. 10.12 Percentage differences of enthalpy of air with data obtained by Yos at $P = 10^{-2}$ (dotted line), 1 (dashed line), 100 (full line) bar and by Boulos et al. (o) at $P = 1$ bar

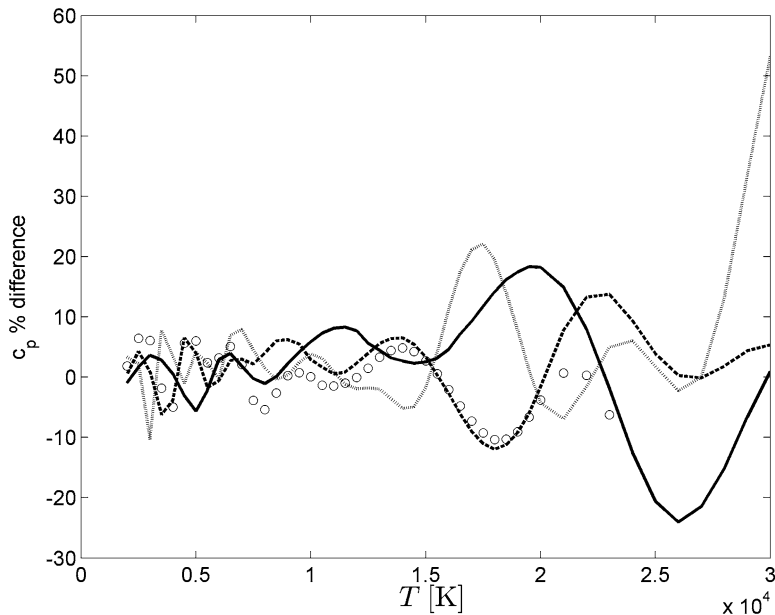


Fig. 10.13 Percentage differences of specific heat of air with data obtained by Yos at $P = 10^{-2}$ (dotted line), 1 (dashed line), 100 (full line) bar and by Boulos et al. (o) at $P = 1$ bar

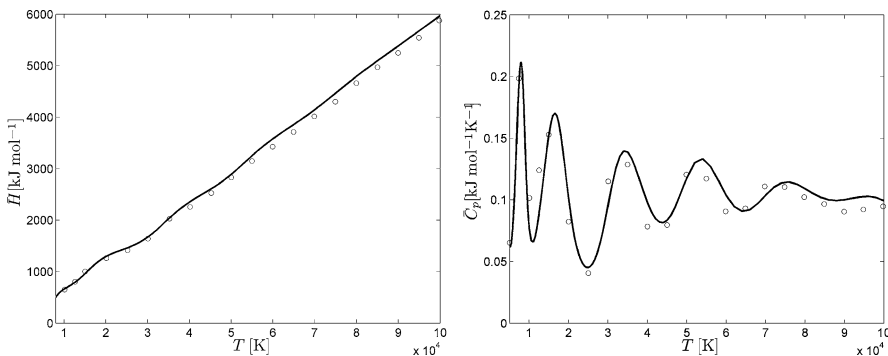


Fig. 10.14 Comparison of molar enthalpy (left) and specific heat (right) of air with data obtained by Lisal (o) at $P = 10$ bar. Solid curves correspond to the results obtained by using the Debye–Hückel approximation

Thermodynamic properties of high temperature air plasmas including enthalpy, entropy, density, specific heat, and isentropic (frozen, equilibrium, and total) coefficients have been reported in Figs. 10.7–10.17 as a function of temperature for different pressures (see also Tables 10.2–10.8). Figure 10.18 reports the present

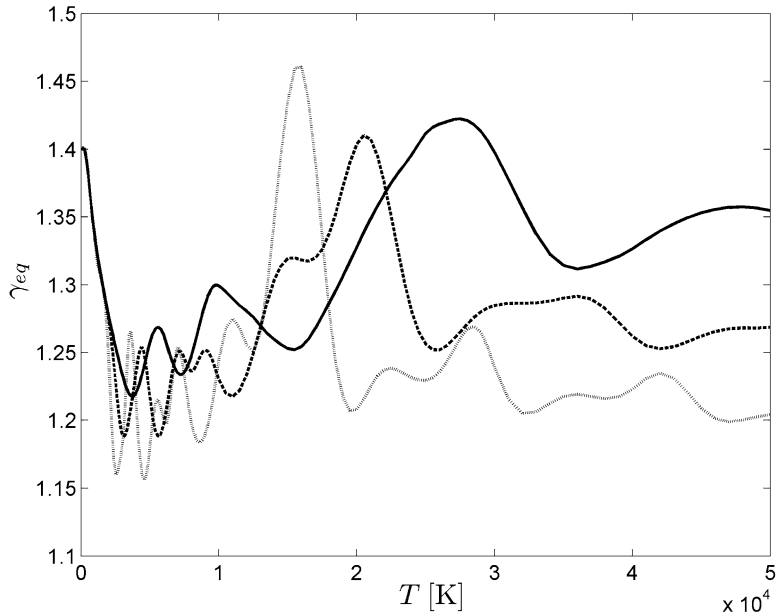


Fig. 10.15 Equilibrium isentropic coefficient of air atmosphere at $P = 10^{-2}$ (dotted line), 1 (dashed line), 100 (full line) bar

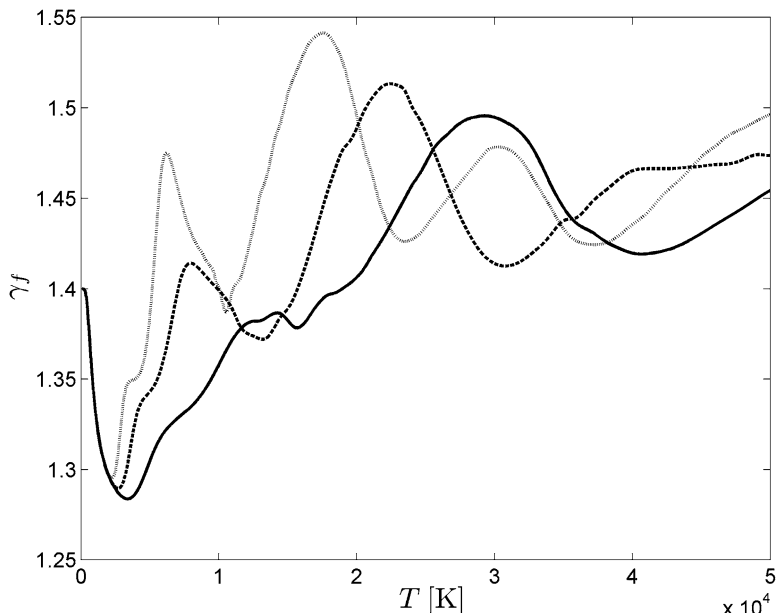


Fig. 10.16 Frozen isentropic coefficient of air atmosphere at $P = 10^{-2}$ (dotted line), 1 (dashed line), 100 (full line) bar

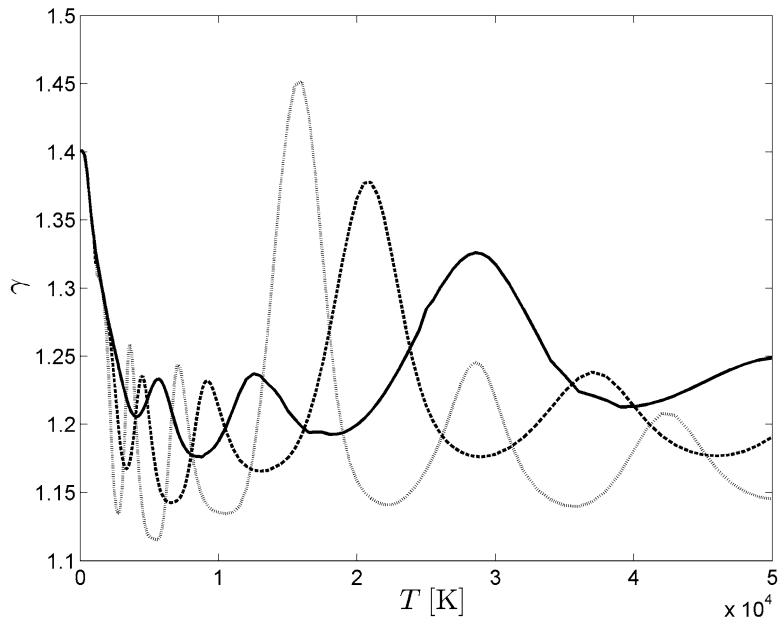


Fig. 10.17 Isentropic coefficient of air atmosphere at $P = 10^{-2}$ (dotted line), 1 (dashed line), 100 (full line) bar

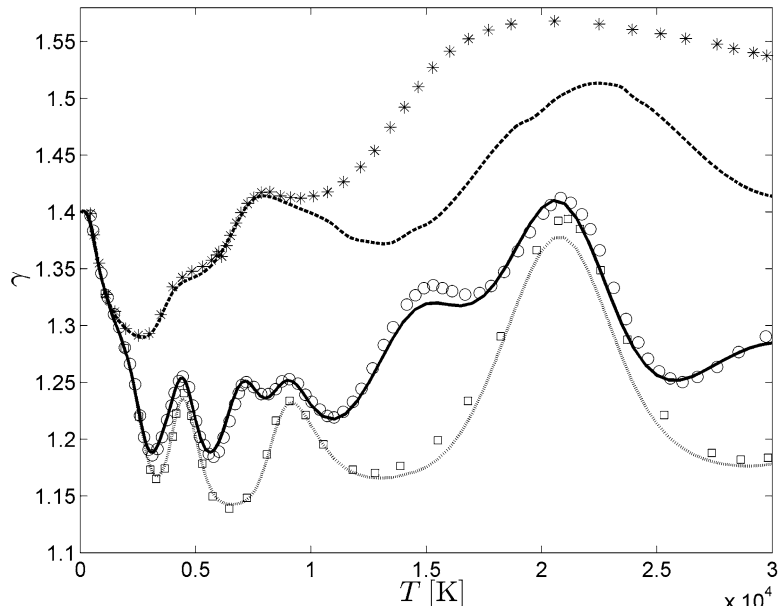


Fig. 10.18 Comparison of frozen (dashed line), equilibrium (full line), and isentropic (dotted line) coefficients of air with data obtained by Henderson (Henderson and Menart 2008) at $P = 1$ bar (*, o, □)

isentropic coefficients with the corresponding ones in (Henderson and Menart 2008). Large differences are observed in the frozen isentropic coefficient while a satisfactory agreement holds for the other two coefficients.

10.3 Thermodynamic Properties of High-Temperature Mars-Atmosphere Species

Thermodynamic properties of high temperature equilibrium Mars-atmosphere have been calculated in the pressure range (0.01÷100 bar) and in the temperature range (100 ÷ 50,000 K). In Table 10.9, species considered in the calculations, volume percentage compositions, and enthalpies of formation have been reported while temperature dependence of molar fractions of Mars-atmosphere species at $P = 1$ bar has been represented in Figs. 10.19–10.24.

Table 10.9 Mars species, volume compositions, and enthalpies of formation

Species	Volume (%)	h_f (eV)	Species	Volume (%)	h_f (eV)
C_2	0.0	8.54273074	C_2N	0.0	5.7674
C_2^+	0.	19.94273074	CNO	0.0	1.3163
C_2^-	0.	5.26973074	C^-	0.0	6.182
CN	0.0	4.69264775	C	0.0	7.35351324
CN^+	0.0	18.29064775	C^+	0.0	18.619034
CN^-	0.0	0.83064775	C^{+2}	0.0	43.00231
CO	0.0	-1.17950394	C^{+3}	0.0	90.890014
CO^+	0.0	12.83449606	C^{+4}	0.0	155.38376
CO_2	95.3	-4.07475247	N	0.0	4.87933027
CO_2^+	0.0	9.70224753	N^+	0.0	19.428233
CO_2^-	0.0	-3.475	N^{+2}	0.0	49.043795
C_2O	0.0	2.9704	N^{+3}	0.0	96.492844
N_2	2.7	0.0	N^{+4}	0.0	173.96623
N_2^+	0.0	15.581	N^-	0.0	4.9497068
N_2^-	0.0	0.352	O	0.0	2.55800581
N_2O	0.0	0.885928879	O^-	0.0	0.95
N_2O^+	0.0	13.77492888	O^+	0.0	16.1755
NO_2	0.0	0.372497752	O^{+2}	0.0	51.3315
NO	0.0	0.930593918	O^{+3}	0.0	106.2805
NO^+	0.0	10.194793918	O^{+4}	0.0	183.6965
N_3	0.0	4.2931	Ar	1.6	0.0
C_3	0.0	8.15696357	Ar^+	0.0	15.7596
O_2	0.4	0.0	Ar^{+2}	0.0	43.3893
O_2^+	0.0	12.0697	Ar^{+3}	0.0	84.1243
O_2^-	0.0	-0.4510	Ar^{+4}	0.0	143.8103
O_3	0.0	1.50907122	e	0.0	0.0
O_3^-	0.0	-0.594			

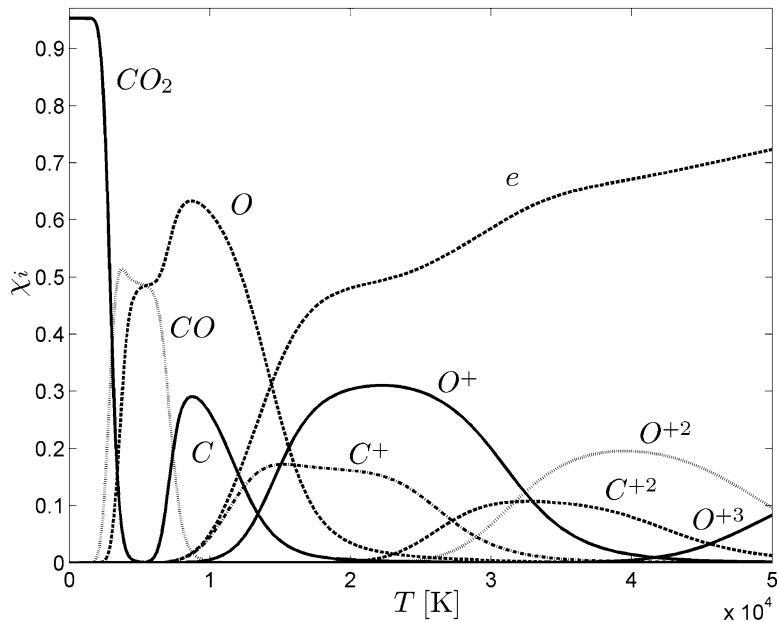


Fig. 10.19 Molar fractions of Mars species (with $\chi_i > 10^{-1}$) as a function of the temperature at $P = 1$ bar

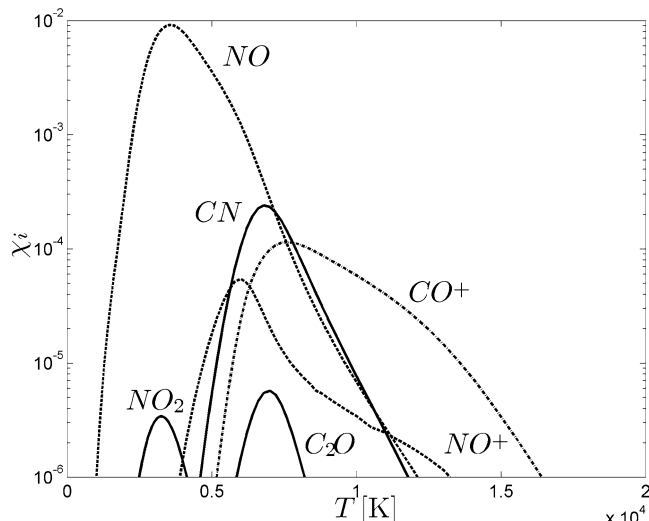


Fig. 10.20 Molar fractions of Mars species ($10^{-6} < \chi_i < 10^{-1}$) as a function of the temperature at $P = 1$ bar

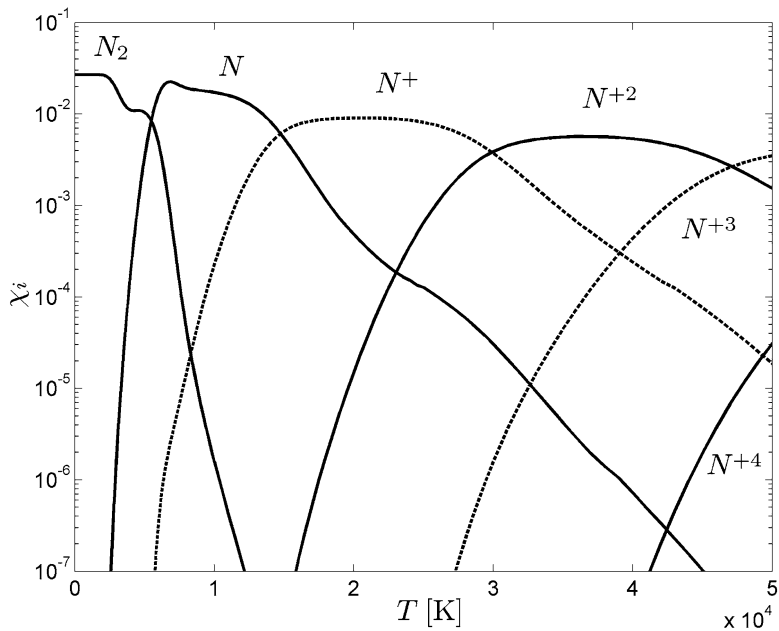


Fig. 10.21 Molar fractions of Mars species (nitrogen compounds) as a function of the temperature at $P = 1$ bar

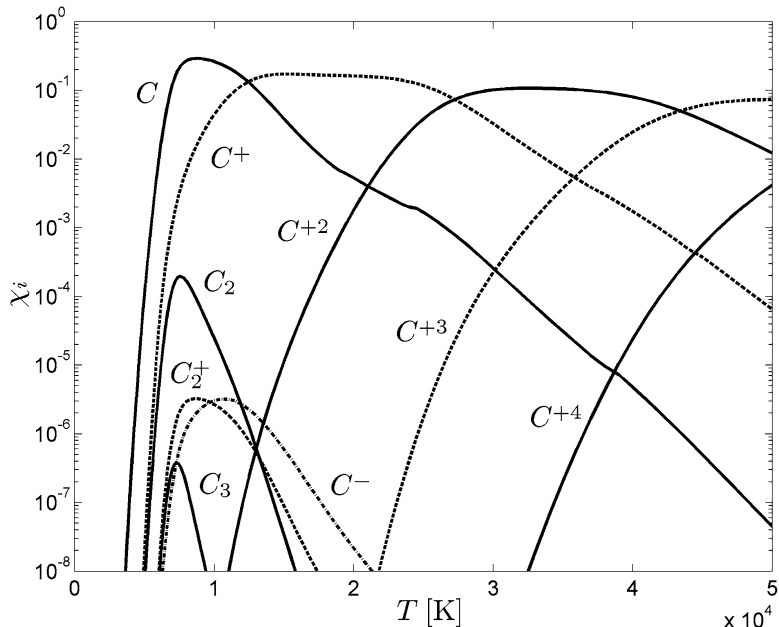


Fig. 10.22 Molar fractions of Mars species (carbon compounds) as a function of the temperature at $P = 1$ bar

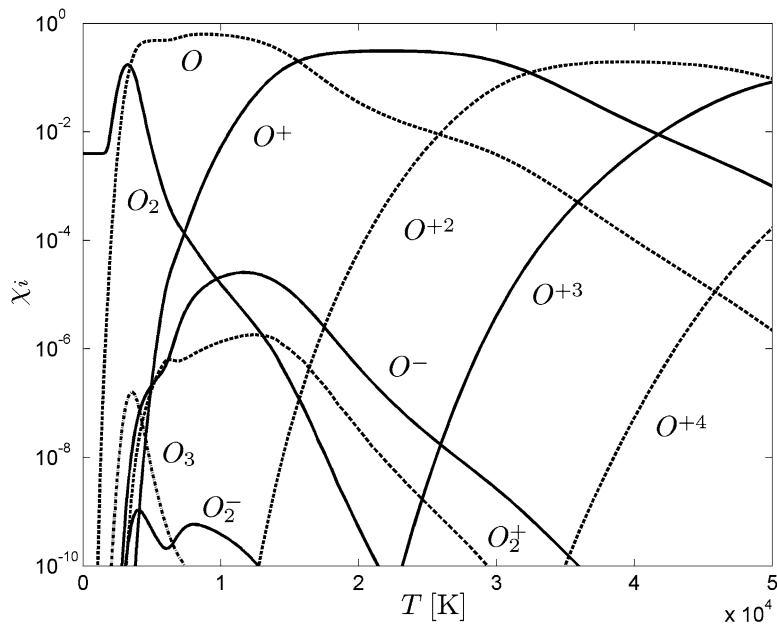


Fig. 10.23 Molar fractions of Mars species (oxygen compounds) as a function of the temperature at $P = 1$ bar

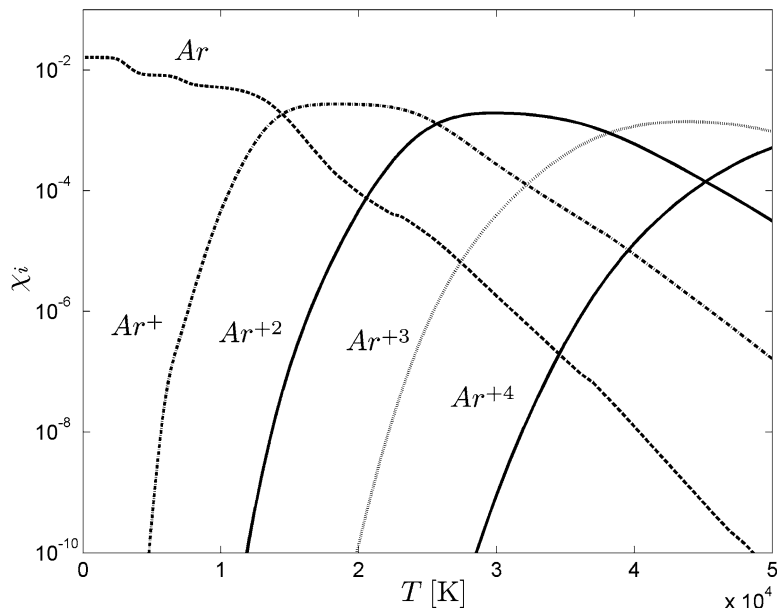


Fig. 10.24 Molar fractions of Mars species (argon compounds) as a function of the temperature at $P = 1$ bar

Specific enthalpy, specific entropy, density, specific heat, frozen, equilibrium, and isentropic coefficients have been reported in Tables 10.10–10.16 and shown in Figs. 10.25–10.31 in the pressure range (0.01 ÷ 100 bar) and in the temperature range (100 ÷ 50000 K).

Table 10.10 Specific enthalpy h [kJ kg⁻¹] of Mars as a function of temperature for different pressures

T (K)	P (bar)				
	10^{-2}	10^{-1}	1	10	10^2
100	-8559.452	-8559.452	-8559.452	-8559.452	-8559.452
200	-8489.826	-8489.826	-8489.826	-8489.826	-8489.826
300	-8410.695	-8410.695	-8410.695	-8410.695	-8410.695
400	-8321.767	-8321.767	-8321.767	-8321.767	-8321.767
500	-8224.885	-8224.885	-8224.885	-8224.885	-8224.885
600	-8121.471	-8121.471	-8121.471	-8121.471	-8121.471
700	-8012.614	-8012.614	-8012.614	-8012.614	-8012.614
800	-7899.277	-7899.277	-7899.277	-7899.277	-7899.277
900	-7782.173	-7782.173	-7782.173	-7782.173	-7782.173
1000	-7661.928	-7661.928	-7661.928	-7661.928	-7661.928
1500	-7024.278	-7027.460	-7028.507	-7028.842	-7028.925
2000	-5940.483	-6174.609	-6283.759	-6333.079	-6353.971
2500	-2277.334	-3948.609	-4847.854	-5296.344	-5511.504
3000	3949.492	645.877	-1841.664	-3377.722	-4213.093
3500	7055.595	5484.289	2288.693	-440.640	-2244.422
4000	8014.959	7697.222	6058.844	2901.511	241.053
4500	8887.195	8676.850	8151.700	6003.453	2875.352
5000	10319.080	9595.936	9263.462	8231.542	5416.044
6000	26413.140	15008.254	11512.988	10696.688	9407.740
7000	38337.313	32531.310	19984.141	13555.267	11955.700
8000	45074.670	40360.961	34626.218	22008.500	14982.548
9000	56489.562	46314.800	41528.744	34347.293	21519.650
10000	73383.300	55364.150	46614.156	41696.467	31533.847
11000	97031.183	68428.641	53282.473	46425.750	39923.608
12000	122483.997	86055.906	62592.660	51354.870	45447.714
13000	139751.616	107508.650	74996.055	57538.355	49854.321
14000	149091.111	128108.962	90574.719	65376.045	54396.999
15000	154903.645	143280.670	108318.796	75172.738	59635.523
16000	159871.702	153127.605	125830.087	86983.282	65734.016
17000	165784.301	159901.847	140712.905	100486.968	72971.737
18000	174749.077	165497.086	152160.872	114963.666	81439.122
19000	188766.902	171283.663	160800.753	129334.439	91032.336
20000	207898.066	178638.196	167690.551	142559.703	101597.726
22000	259342.115	202619.349	180273.141	163712.672	124418.298
24000	330004.413	240008.729	196841.565	179281.707	146928.628
26000	391994.174	290404.822	222612.575	193250.128	166810.067
28000	429050.704	352954.776	258841.374	209856.651	183822.710

(continued)

Table 10.10 (continued)

T (K)	P (bar)				
	10^{-2}	10^{-1}	1	10	10^2
30000	461125.778	408874.514	305247.865	232693.552	199332.292
35000	591674.389	503487.821	431420.432	322273.068	244597.880
40000	800658.511	635644.163	523144.847	431458.114	315035.766
45000	983667.726	822182.850	639353.668	521143.556	406374.576
50000	1148455.987	987239.066	797510.038	617142.694	495859.471

Table 10.11 Specific entropy s [J kg⁻¹ K⁻¹] of Mars as a function of temperature for different pressures

T (K)	P (bar)				
	10^{-2}	10^{-1}	1	10	10^2
100	5,014.154	4,573.409	4,132.631	3,691.862	3,251.088
200	5,493.835	5,053.049	4,612.304	4,171.518	3,730.749
300	5,813.246	5,372.460	4,931.715	4,490.929	4,050.168
400	6,068.432	5,627.687	5,186.901	4,746.156	4,305.370
500	6,284.387	5,843.642	5,402.856	4,962.070	4,521.325
600	6,472.793	6,032.048	5,591.262	5,150.476	4,709.731
700	6,640.474	6,199.688	5,758.943	5,318.157	4,877.371
800	6,791.743	6,350.999	5,910.212	5,469.426	5,028.682
900	6,929.656	6,488.870	6,048.126	5,607.339	5,166.553
1,000	7,056.307	6,615.521	6,174.776	5,733.990	5,293.204
1,500	7,571.660	7,128.697	6,687.199	6,246.203	5,805.333
2,000	8,179.835	7,611.895	7,112.117	6,644.828	6,192.863
2,500	9,782.626	8,586.499	7,743.110	7,102.571	6,566.410
3,000	12,052.206	10,251.589	8,829.794	7,796.031	7,036.504
3,500	13,027.396	11,749.752	10,101.409	8,698.412	7,640.784
4,000	13,285.093	12,347.962	11,112.060	9,590.786	8,303.597
4,500	13,490.121	12,579.576	11,608.782	10,322.848	8,924.122
5,000	13,789.686	12,772.922	11,843.871	10,794.240	9,459.865
6,000	16,658.524	13,731.825	12,250.284	11,247.461	10,192.806
7,000	18,531.865	16,431.892	13,532.073	11,683.517	10,586.952
8,000	19,426.752	17,488.975	15,494.844	12,799.927	10,988.424
9,000	20,763.723	18,187.041	16,313.531	14,255.803	11,752.683
10,000	22,536.498	19,134.890	16,847.223	15,033.710	12,806.333
11,000	24,783.051	20,373.555	17,477.964	15,482.912	13,607.226
12,000	26,998.496	21,900.481	18,281.453	15,907.328	14,086.489
13,000	28,385.122	23,612.003	19,266.230	16,395.509	14,434.830
14,000	29,079.922	25,137.212	20,412.367	16,966.840	14,764.666
15,000	29,482.064	26,184.917	21,629.009	17,631.661	15,116.567
16,000	29,802.898	26,821.394	22,753.667	18,381.643	15,496.980
17,000	30,161.037	27,232.831	23,652.866	19,187.183	15,920.265
18,000	30,672.287	27,552.996	24,305.839	20,002.228	16,387.135
19,000	31,428.675	27,866.336	24,772.584	20,769.040	16,887.165
20,000	32,408.846	28,242.897	25,126.494	21,439.724	17,409.719
22,000	34,855.277	29,379.445	25,725.458	22,442.504	18,459.852

(continued)

Table 10.11 (continued)

T (K)	P (bar)				
	10^{-2}	10^{-1}	1	10	10^2
24,000	37,924.034	31,000.114	26,442.698	23,118.002	19,410.675
26,000	40,411.580	33,010.238	27,468.046	23,677.275	20,188.540
28,000	41,788.283	35,324.073	28,803.467	24,290.809	20,808.522
30,000	42,893.347	37,254.439	30,396.629	25,071.145	21,336.310
35,000	46,889.229	40,176.240	34,285.370	27,791.727	22,703.300
40,000	52,449.718	43,685.490	36,732.764	30,688.825	24,538.751
45,000	56,772.171	48,070.326	39,453.975	32,793.404	26,643.790
50,000	60,240.516	51,552.906	42,773.186	34,800.472	28,498.920

Table 10.12 Density ρ [kg m⁻³] of Mars as a function of temperature for different pressures

T (K)	P (bar)				
	10^{-2}	10^{-1}	1	10	10^2
100	0.05227500	0.52274999	5.22749988	52.27499877	522.74998767
200	0.02613750	0.26137499	2.61374994	26.13749938	261.37499384
300	0.01742500	0.17425000	1.74249996	17.42499959	174.24999589
400	0.01306875	0.13068750	1.30687497	13.06874969	130.68749692
500	0.01045500	0.10455000	1.04549998	10.45499975	104.54999753
600	0.00871250	0.08712500	0.87124998	8.71249979	87.12499795
700	0.00746786	0.07467857	0.74678570	7.46785697	74.67856967
800	0.00653437	0.06534375	0.65343748	6.53437485	65.34374846
900	0.00580833	0.05808333	0.58083332	5.80833320	58.08333196
1,000	0.00522750	0.05227500	0.52274999	5.22749988	52.27499877
1,500	0.00348374	0.03484591	0.34848716	3.48495983	34.84991900
2,000	0.00252985	0.02575389	0.25971404	2.60708087	26.11308423
2,500	0.00164631	0.01839228	0.19617560	2.02882912	20.62558106
3,000	0.00100946	0.01199546	0.13930426	1.54454482	16.40802244
3,500	0.00077335	0.00830311	0.09746954	1.14106887	12.83422423
4,000	0.00066844	0.00677529	0.07298476	0.85585320	9.98621687
4,500	0.00059103	0.00594701	0.06081871	0.67185358	7.91106952
5,000	0.00052354	0.00531714	0.05374773	0.56235665	6.44297740
6,000	0.00033876	0.00409619	0.04381878	0.44772332	4.73068567
7,000	0.00025131	0.00271510	0.03297746	0.37117899	3.86922552
8,000	0.00020738	0.00218794	0.02358167	0.28603459	3.25826477
9,000	0.00016723	0.00185315	0.01956045	0.21521145	2.63650200
10,000	0.00013272	0.00155015	0.01694195	0.17935874	2.06917786
11,000	0.00010427	0.00127805	0.01465477	0.15729020	1.70774837
12,000	0.00008387	0.00104518	0.01255987	0.13943796	1.48948445
13,000	0.00007199	0.00085628	0.01067883	0.12345517	1.33273962
14,000	0.00006492	0.00072112	0.00904941	0.10879002	1.20285415
15,000	0.00005990	0.00063356	0.00770505	0.09544519	1.08756058
16,000	0.00005580	0.00057556	0.00666694	0.08351665	0.98225121
17,000	0.00005212	0.00053322	0.00590765	0.07311315	0.88559568
18,000	0.00004850	0.00049898	0.00535795	0.06435142	0.79736776

(continued)

Table 10.12 (continued)

T (K)	P (bar)				
	10^{-2}	10^{-1}	1	10	10^2
19,000	0.00004477	0.00046907	0.00494650	0.05724153	0.71761674
20,000	0.00004106	0.00044064	0.00462208	0.05161573	0.64650232
22,000	0.00003461	0.00038415	0.00410363	0.04376385	0.53016955
24,000	0.00002922	0.00032998	0.00365797	0.03859954	0.44553487
26,000	0.00002525	0.00028197	0.00322937	0.03477183	0.38565435
28,000	0.00002259	0.00024061	0.00282525	0.03147991	0.34239283
30,000	0.00002046	0.00021025	0.00246055	0.02833135	0.30924773
35,000	0.00001570	0.00016606	0.00180610	0.02133358	0.24635212
40,000	0.00001189	0.00013263	0.00146195	0.01641877	0.19539125
45,000	0.00000962	0.00010563	0.00120116	0.01346741	0.15543242
50,000	0.00000814	0.00008790	0.00098518	0.01132572	0.12804555

Table 10.13 Specific heat c_p [J kg⁻¹ K⁻¹] of Mars as a function of temperature for different pressures

T (K)	P (bar)				
	10^{-2}	10^{-1}	1	10	10^2
100	695.447	695.447	695.447	695.447	695.447
200	790.822	790.822	790.822	790.822	790.822
300	888.635	888.635	888.635	888.635	888.635
400	968.418	968.418	968.418	968.418	968.418
500	1033.570	1033.570	1033.570	1033.570	1033.570
600	1087.600	1087.600	1087.600	1087.600	1087.600
700	1132.660	1132.660	1132.660	1132.660	1132.660
800	1170.250	1170.250	1170.250	1170.250	1170.250
900	1201.560	1201.560	1201.560	1201.560	1201.560
1000	1227.720	1227.710	1227.710	1227.710	1227.710
1500	1433.480	1352.330	1322.630	1312.670	1309.450
2000	4331.680	2766.200	2006.900	1642.740	1469.360
2500	11748.100	7517.010	4604.380	2963.460	2128.870
3000	10090.300	10627.000	7792.040	5183.530	3383.950
3500	2426.320	6591.600	8397.130	6584.290	4672.590
4000	1626.350	2318.620	5562.480	6609.900	5249.010
4500	2089.180	1730.670	2630.040	5281.890	5215.400
5000	6084.740	2294.140	1878.310	3145.610	4713.830
6000	20304.900	15021.400	4041.150	2126.030	2900.680
7000	5817.690	11783.800	15688.200	5194.300	2423.820
8000	9188.220	5293.440	9467.910	12779.000	4623.600
9000	14621.600	7562.800	4903.010	9480.600	9325.380
10000	21909.400	11962.500	6063.830	4884.790	9219.270
11000	26484.000	16364.500	8523.330	4682.520	5975.110
12000	19748.200	20816.900	11526.900	5745.620	4452.860
13000	10699.600	21503.900	14722.000	7271.990	4306.630
14000	6269.210	16679.000	17312.500	9184.180	4875.020
15000	4949.050	10887.100	17786.400	11111.700	5657.120

(continued)

Table 10.13 (continued)

T (K)	P (bar)				
	10^{-2}	10^{-1}	1	10	10^2
16000	5437.740	7275.940	15630.500	12904.100	6588.000
17000	7901.020	5699.100	12215.300	14097.700	7763.830
18000	12590.600	5537.990	9184.640	14296.600	8850.010
19000	17975.600	6796.050	7171.340	13407.800	9848.690
20000	22139.900	9332.420	6265.730	11787.500	10472.100
22000	32065.900	16428.600	7024.650	8501.260	11055.600
24000	35877.200	22345.200	10838.400	6749.020	10190.200
26000	22043.700	29900.600	16112.800	7552.820	8789.740
28000	15200.800	30798.800	21209.000	10019.700	7784.410
30000	19995.600	21607.500	26212.100	14095.000	7732.910
35000	35048.100	21691.400	19744.900	21972.500	11523.300
40000	41652.000	34048.000	19785.600	19260.500	16874.400
45000	32204.000	36349.700	28617.200	17390.200	18188.900
50000	40401.600	29857.900	33050.500	22956.500	16513.500

Table 10.14 Equilibrium isentropic coefficient γ_{eq} of Mars as a function of temperature for different pressures

T (K)	P (bar)				
	10^{-2}	10^{-1}	1	10	10^2
100	1.39064	1.39064	1.39064	1.39064	1.39064
200	1.33973	1.33973	1.33973	1.33973	1.33973
300	1.29229	1.29229	1.29229	1.29229	1.29229
400	1.25860	1.25860	1.25860	1.25860	1.25860
500	1.23726	1.23726	1.23726	1.23726	1.23726
600	1.22201	1.22201	1.22201	1.22201	1.22201
700	1.20968	1.20968	1.20968	1.20968	1.20968
800	1.20013	1.20013	1.20014	1.20014	1.20014
900	1.19338	1.19337	1.19332	1.19332	1.19332
1,000	1.18809	1.18813	1.18811	1.18810	1.18810
1,500	1.17066	1.17078	1.17274	1.17331	1.17325
2,000	1.10952	1.12129	1.13742	1.15079	1.15968
2,500	1.15935	1.13809	1.12749	1.12970	1.13879
3,000	1.19222	1.19504	1.17333	1.15345	1.14347
3,500	1.24929	1.20836	1.21793	1.19751	1.17510
4,000	1.32978	1.26878	1.23215	1.23586	1.21310
4,500	1.26933	1.31754	1.26870	1.25692	1.24770
5,000	1.16624	1.26641	1.30840	1.27371	1.27577
6,000	1.20170	1.19283	1.20731	1.29400	1.30323
7,000	1.21687	1.20557	1.23070	1.20947	1.29064
8,000	1.21382	1.24045	1.22753	1.25296	1.23223
9,000	1.22825	1.23400	1.26010	1.25704	1.26474
10,000	1.24631	1.24225	1.25588	1.27399	1.29005
11,000	1.26367	1.25922	1.25259	1.28232	1.29220
12,000	1.25689	1.27820	1.26108	1.27305	1.30258
13,000	1.26256	1.28810	1.27413	1.27463	1.30331

(continued)

Table 10.14 (continued)

T (K)	P (bar)				
	10^{-2}	10^{-1}	1	10	10^2
14,000	1.31844	1.28318	1.28793	1.28351	1.29450
15,000	1.37265	1.28721	1.29814	1.29620	1.28489
16,000	1.35030	1.31871	1.30331	1.31317	1.29124
17,000	1.27821	1.35549	1.31033	1.32783	1.30229
18,000	1.22961	1.35426	1.32740	1.34052	1.31402
19,000	1.21351	1.31324	1.35180	1.34845	1.32919
20,000	1.20246	1.26849	1.36933	1.35304	1.34351
22,000	1.16541	1.23919	1.33260	1.36793	1.37244
24,000	1.16491	1.23636	1.27807	1.37437	1.39271
26,000	1.19550	1.23971	1.26450	1.34041	1.40436
28,000	1.24638	1.24469	1.26555	1.30204	1.40392
30,000	1.23609	1.24638	1.27231	1.28522	1.38456
35,000	1.23186	1.23752	1.27764	1.29268	1.32293
40,000	1.23286	1.23149	1.26476	1.30689	1.32580
45,000	1.22130	1.23659	1.25670	1.30379	1.34415
50,000	1.20787	1.23989	1.26220	1.28973	1.34863

Table 10.15 Frozen isentropic coefficient γ_f of Mars as a function of temperature for different pressures

T (K)	P (bar)				
	10^{-2}	10^{-1}	1	10	10^2
100	1.40066	1.40066	1.40066	1.40066	1.40066
200	1.35016	1.35016	1.35016	1.35016	1.35016
300	1.29366	1.29366	1.29366	1.29366	1.29366
400	1.25849	1.25849	1.25849	1.25849	1.25849
500	1.23565	1.23565	1.23565	1.23565	1.23565
600	1.21965	1.21965	1.21965	1.21965	1.21965
700	1.20789	1.20789	1.20789	1.20789	1.20789
800	1.19900	1.19900	1.19900	1.19900	1.19900
900	1.19215	1.19215	1.19215	1.19215	1.19215
1000	1.18680	1.18680	1.18680	1.18680	1.18680
1500	1.17228	1.17222	1.17220	1.17219	1.17219
2000	1.17381	1.16966	1.16774	1.16687	1.16650
2500	1.22619	1.19433	1.17803	1.17014	1.16642
3000	1.33833	1.26804	1.21859	1.19000	1.17519
3500	1.38930	1.35367	1.28489	1.23012	1.19637
4000	1.39172	1.38473	1.34789	1.28070	1.22803
4500	1.39010	1.38727	1.37587	1.32859	1.26383
5000	1.39260	1.38620	1.38124	1.35884	1.29881
6000	1.50252	1.41049	1.38225	1.37326	1.34710
7000	1.56316	1.52549	1.42749	1.37681	1.35961
8000	1.54931	1.54992	1.51641	1.41751	1.36125
9000	1.51185	1.52577	1.53110	1.48710	1.38192
10000	1.46494	1.48156	1.50117	1.51009	1.43081
11000	1.43847	1.45467	1.45341	1.48949	1.47116

(continued)

Table 10.15 (continued)

T (K)	P (bar)				
	10 ⁻²	10 ⁻¹	1	10	10 ²
12000	1.42674	1.41943	1.39722	1.46683	1.48082
13000	1.43745	1.40252	1.34170	1.43956	1.48107
14000	1.45062	1.40067	1.29755	1.42744	1.46694
15000	1.46410	1.41248	1.27549	1.41110	1.44675
16000	1.47360	1.43241	1.27652	1.39414	1.45126
17000	1.47466	1.45001	1.29697	1.38350	1.44882
18000	1.45660	1.46351	1.32902	1.38631	1.44046
19000	1.40321	1.46867	1.36523	1.39102	1.43538
20000	1.31172	1.47018	1.39895	1.40021	1.43439
22000	1.14243	1.45541	1.44498	1.42702	1.44245
24000	1.09840	1.44211	1.45841	1.44155	1.45738
26000	1.13030	1.43741	1.44990	1.45094	1.47237
28000	1.23178	1.43521	1.44331	1.44059	1.48227
30000	1.36291	1.44951	1.44129	1.42049	1.48488
35000	1.50663	1.47691	1.46161	1.36206	1.45979
40000	1.53229	1.50038	1.48015	1.36484	1.43957
45000	1.53381	1.51834	1.48658	1.40431	1.44216
50000	1.53909	1.52202	1.48951	1.42432	1.45659

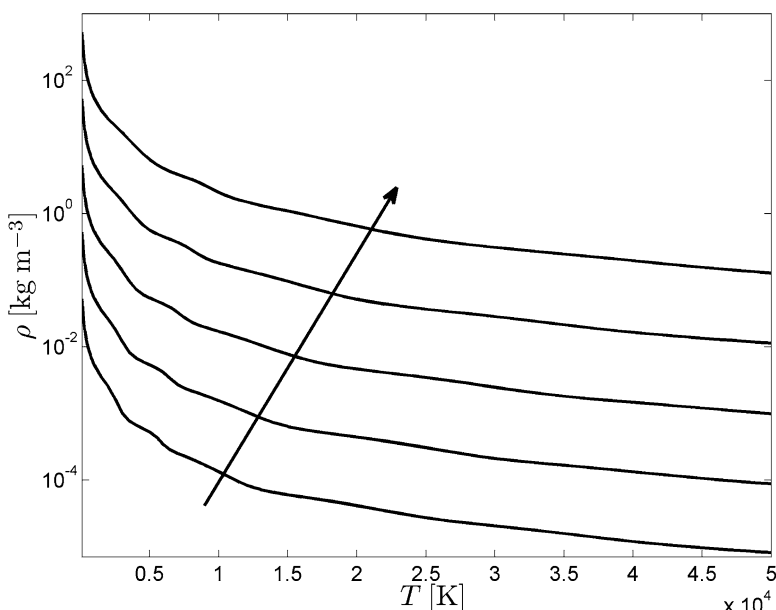
Table 10.16 Isentropic coefficient γ of Mars as a function of temperature for different pressures

T (K)	P (bar)				
	10 ⁻²	10 ⁻¹	1	10	10 ²
100	1.39061	1.39061	1.39061	1.39061	1.39061
200	1.33941	1.33941	1.33941	1.33941	1.33941
300	1.29168	1.29168	1.29168	1.29168	1.29168
400	1.25950	1.25950	1.25950	1.25950	1.25950
500	1.23746	1.23746	1.23746	1.23746	1.23746
600	1.22163	1.22163	1.22163	1.22163	1.22163
700	1.20987	1.20987	1.20987	1.20987	1.20987
800	1.20091	1.20091	1.20091	1.20091	1.20091
900	1.19397	1.19397	1.19397	1.19397	1.19397
1,000	1.18851	1.18851	1.18851	1.18851	1.18851
1,500	1.16577	1.17068	1.17246	1.17305	1.17324
2,000	1.09749	1.11562	1.13450	1.14956	1.15915
2,500	1.09367	1.09692	1.10506	1.11819	1.13324
3,000	1.11609	1.11269	1.11147	1.11444	1.12211
3,500	1.23478	1.14523	1.13299	1.12865	1.12827
4,000	1.32684	1.25258	1.16674	1.15139	1.14442
4,500	1.26574	1.31264	1.24288	1.17984	1.16590
5,000	1.15561	1.26069	1.29848	1.22642	1.19023
6,000	1.10624	1.12698	1.19295	1.28008	1.24887
7,000	1.19547	1.13548	1.13548	1.18040	1.26472
8,000	1.17572	1.21702	1.16015	1.15220	1.19501

(continued)

Table 10.16 (continued)

T (K)	P (bar)				
	10 ⁻²	10 ⁻¹	1	10	10 ²
9,000	1.15950	1.19698	1.23263	1.17256	1.17177
10,000	1.15178	1.17822	1.22425	1.23405	1.18198
11,000	1.14932	1.16960	1.20134	1.25226	1.21920
12,000	1.16119	1.16491	1.18605	1.23550	1.25829
13,000	1.20887	1.16719	1.17561	1.21843	1.26748
14,000	1.29161	1.18263	1.16989	1.20690	1.25488
15,000	1.35679	1.22010	1.17121	1.20218	1.24156
16,000	1.33799	1.27706	1.18294	1.19905	1.23099
17,000	1.26224	1.32782	1.20800	1.19910	1.22464
18,000	1.20266	1.33419	1.24551	1.20592	1.22027
19,000	1.17173	1.29266	1.28722	1.21660	1.21945
20,000	1.15179	1.24247	1.31647	1.23295	1.22143
22,000	1.10958	1.18951	1.29114	1.27880	1.23913
24,000	1.09341	1.17141	1.22886	1.30928	1.25683
26,000	1.12526	1.16036	1.19738	1.28683	1.28414
28,000	1.18177	1.16143	1.18345	1.24357	1.30280
30,000	1.17011	1.18388	1.17762	1.21414	1.29874
35,000	1.15092	1.19570	1.20611	1.18942	1.23933
40,000	1.15502	1.17066	1.21318	1.21094	1.21618
45,000	1.17773	1.17100	1.19008	1.22874	1.22478
50,000	1.16812	1.19198	1.18570	1.21080	1.24306

**Fig. 10.25** Mass density of Mars atmosphere at $P = 10^{-2}, 10^{-1}, 1, 10, 100$ bar

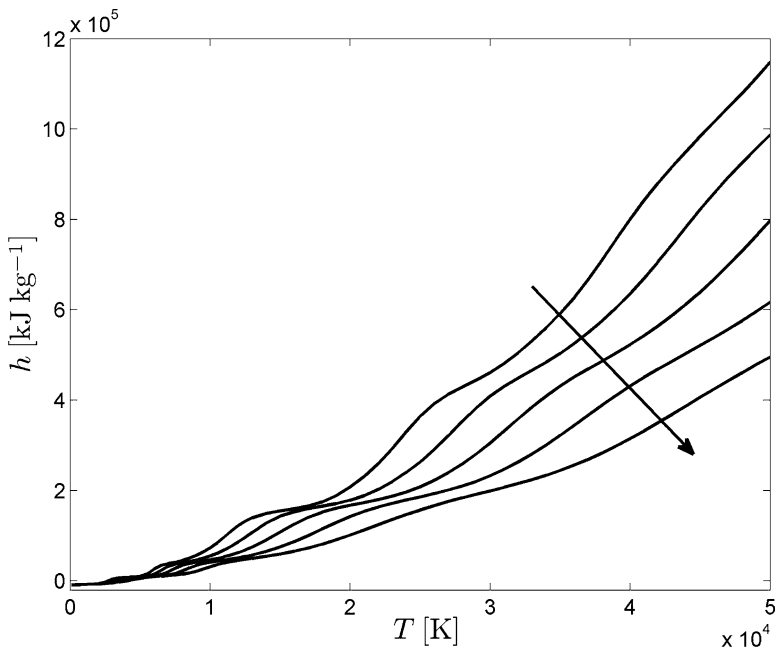


Fig. 10.26 Specific enthalpy of Mars atmosphere at $P = 10^{-2}, 10^{-1}, 1, 10, 100$ bar

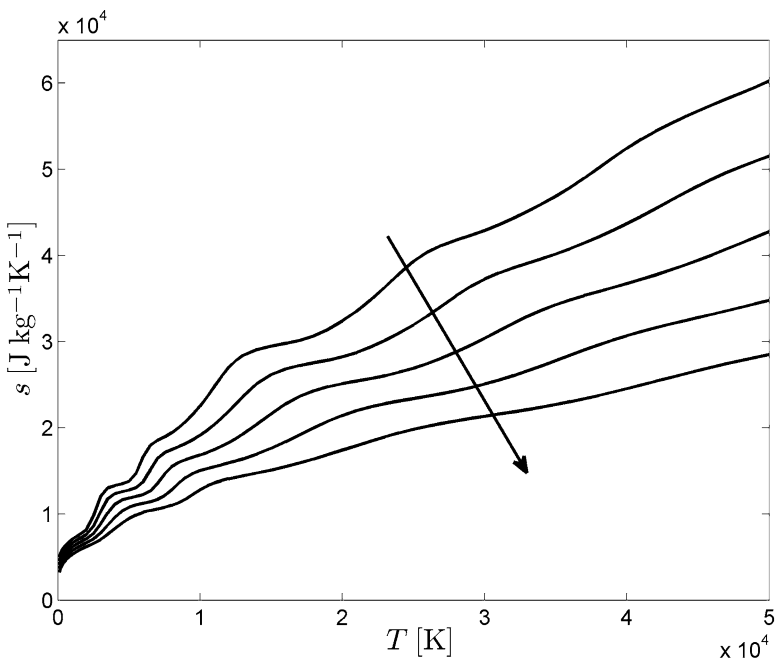


Fig. 10.27 Specific entropy of Mars atmosphere at $P = 10^{-2}, 10^{-1}, 1, 10, 100$ bar

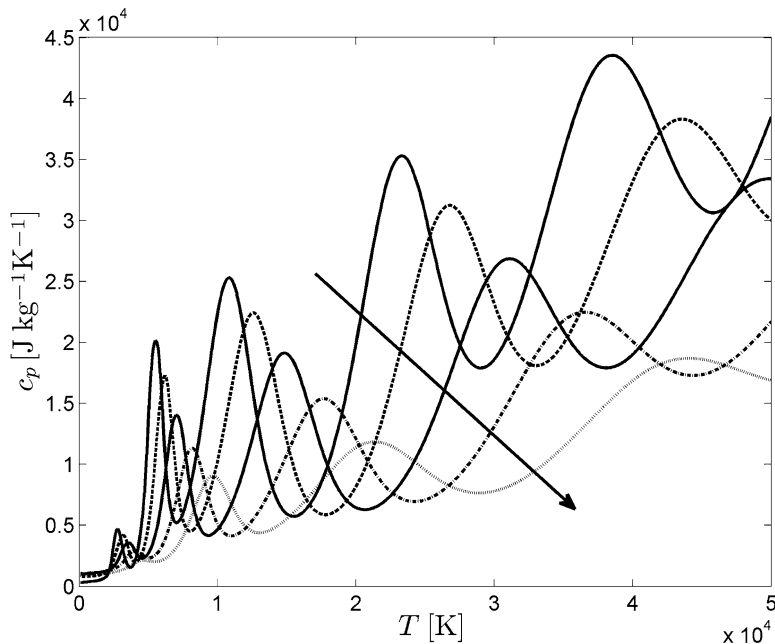


Fig. 10.28 Specific heat of Mars atmosphere at $P = 10^{-2}, 10^{-1}, 1, 10, 100$ bar

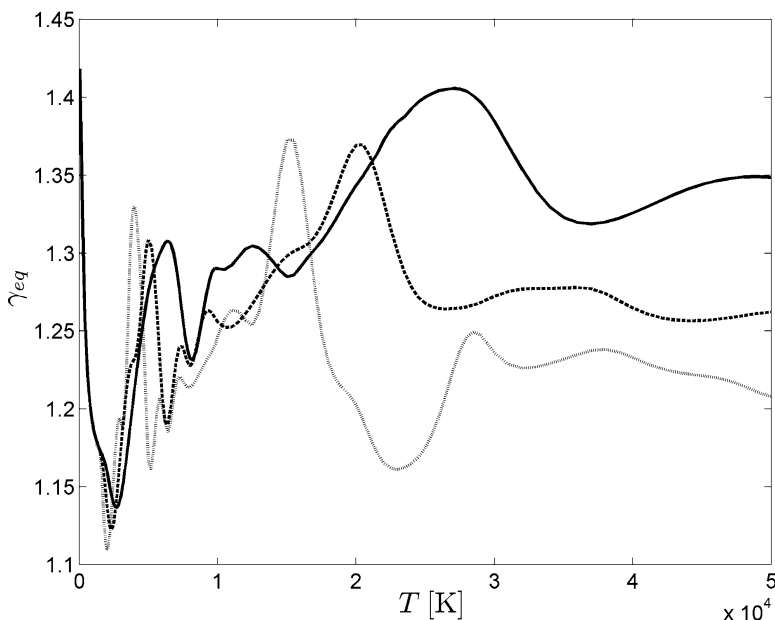


Fig. 10.29 Equilibrium isentropic coefficient of Mars atmosphere at $P = 10^{-2}$ (dotted line), 1 (dashed line), 100 (full line) bar

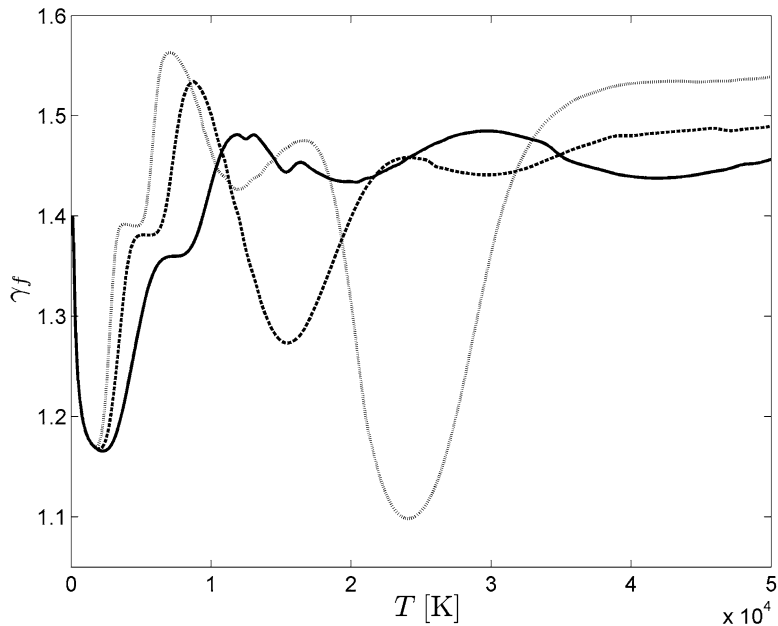


Fig. 10.30 Frozen isentropic coefficient of Jupiter atmosphere at $P = 10^{-2}$ (dotted line), 1 (dashed line), 100 (full line) bar

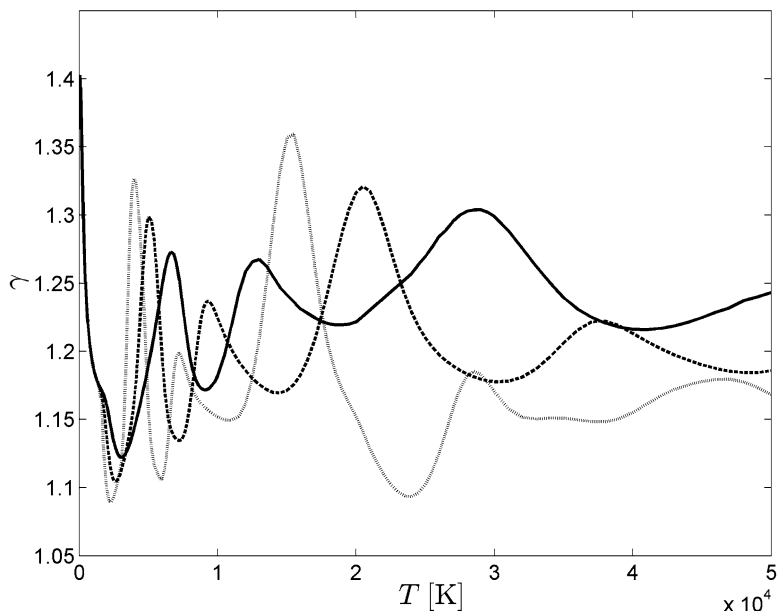


Fig. 10.31 Isentropic coefficient of Mars at $P = 10^{-2}$ (dotted line), 1 (dashed line), 100 (full line) bar

10.4 Thermodynamic Properties of High-Temperature Jupiter-Atmosphere Species

Thermodynamic properties of high-temperature equilibrium Jupiter atmosphere have been calculated in the pressure range (0.01÷100 bar) and in the temperature range (100÷50,000 K). In Table 10.17, species considered in the calculations, volume percentage compositions, and enthalpies of formation have been reported while temperature dependence of molar fractions of Jupiter-atmosphere species at $P=1$ bar pressure has been represented in Figs. 10.32, 10.33, where, respectively, species with molar fractions $\chi_i \geq 0.1$ and $10^{-15} \leq \chi_i \leq 0.1$ are shown.

Table 10.17 Jupiter species, volume compositions, and enthalpies of formation of Jupiter

Species	Volume (%)	h_f (eV)
H_2	89	0.0
H_2^+	0.0	15.4258
H	0.	2.2391
H^+	0.0	15.8191
H^-	0.0	1.4848893
H_3^+	0.0	11.334
He	11	0.0
He^+	0.	24.5873876
He^{+2}	0.	79.0047712
e	0.0	0.0

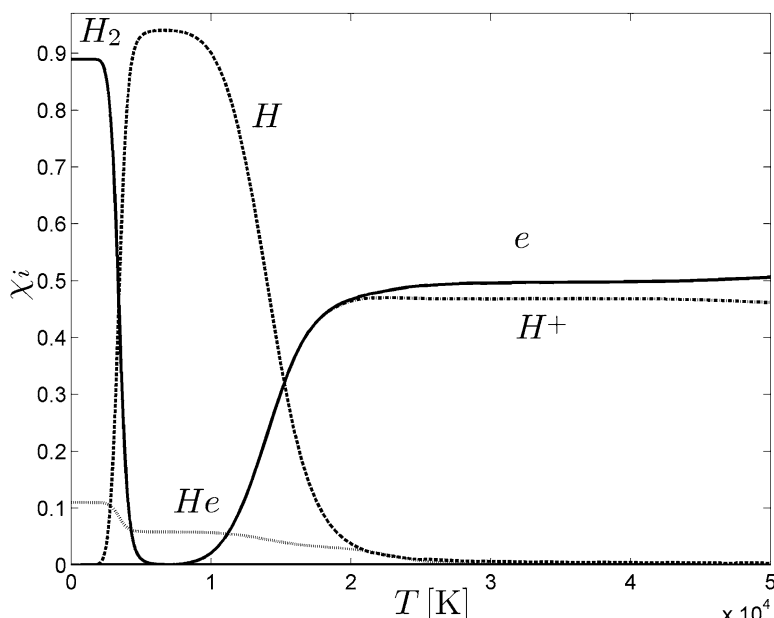


Fig. 10.32 Molar fractions of Jupiter species (with $\chi_i > 10^{-1}$) as a function of the temperature at $P = 1$ bar

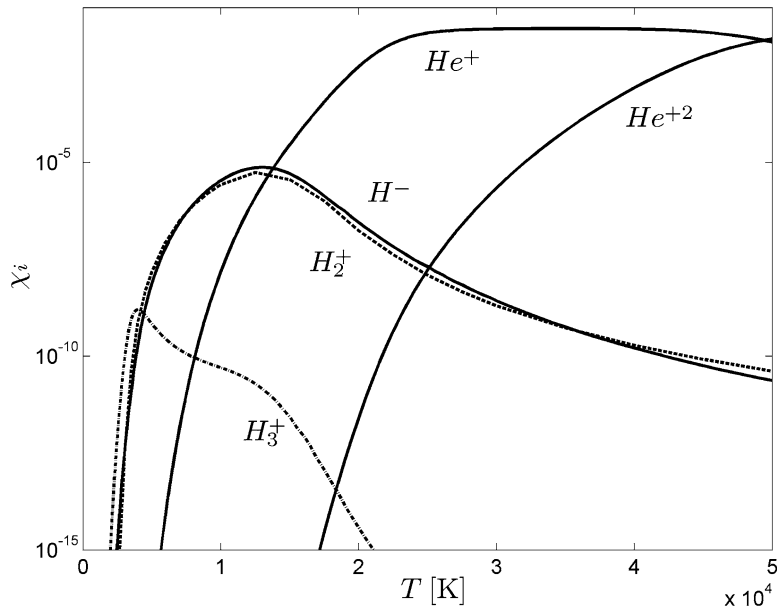


Fig. 10.33 Molar fractions of Jupiter species (with $10^{-15} < \chi_i < 10^{-1}$) as a function of the temperature at $P = 1$ bar

Table 10.18 Specific enthalpy h [kJ kg^{-1}] of Jupiter as a function of temperature for different pressures

T (K)	P (bar)				
	10^{-2}	10^{-1}	1	10	10^2
100	1376.0	1376.0	1376.0	1376.0	1376.0
200	2489.7	2489.7	2489.7	2489.7	2489.7
300	3724.5	3724.5	3724.5	3724.5	3724.5
400	4992.3	4992.3	4992.3	4992.3	4992.3
500	6266.8	6266.8	6266.8	6266.8	6266.8
600	7544.0	7544.0	7544.0	7544.0	7544.0
700	8824.6	8824.6	8824.6	8824.6	8824.6
800	10111.2	10111.2	10111.2	10111.2	10111.2
900	11406.7	11406.7	11406.7	11406.7	11406.7
1000	12713.9	12713.9	12713.9	12713.9	12713.9
1500	19503.6	19492.6	19489.2	19488.1	19487.7

(continued)

Density, specific enthalpy, specific entropy and specific heat have been reported in Tables 10.18–10.21 and shown in Figs. 10.34–10.37 in the pressure range (0.01÷100 bar) and in the temperature range (100÷50,000 K). The quantities γ_f (frozen), γ_{eq} (equilibrium) and γ isentropic coefficients for the same conditions have been reported in Figs. 10.38–10.40 and in Tables 10.22–10.24.

Table 10.18 (continued)

T (K)	P (bar)				
	10^{-2}	10^{-1}	1	10	10^2
2000	28195.8	27163.2	26836.5	26733.1	26700.5
2500	57584.4	41710.8	36611.3	34994.0	34482.1
3000	156940.1	87590.3	56999.4	46839.2	43601.2
3500	225474.2	177162.6	103624.8	67908.1	55848.7
4000	242554.6	231098.2	175096.6	104916.1	73746.2
4500	252523.9	249842.3	228270.7	157422.8	99597.5
5000	261622.1	260805.2	253430.0	209175.2	133895.8
6000	280066.3	279453.6	278080.1	267050.8	212072.3
7000	302810.0	298844.9	297275.1	293724.9	269014.8
8000	342950.3	323685.6	317461.6	314338.7	302994.1
9000	431224.9	363945.6	342425.3	335051.3	327637.6
10000	618318.2	437700.9	378169.2	358846.9	349889.3
11000	936215.4	570745.8	433803.5	389061.7	372944.2
12000	1288917.0	784259.0	520980.5	429906.7	399078.6
13000	1524399.0	1065132.0	651569.5	486052.9	430265.7
14000	1645908.0	1341466.0	829268.9	562383.7	468571.5
15000	1717538.0	1544530.0	1046882.0	664274.9	516931.7
16000	1778309.0	1673072.0	1271410.0	790919.8	575009.9
17000	1846551.0	1758698.0	1470318.0	943539.4	646764.0
18000	1919145.0	1827588.0	1625186.0	1112517.0	732469.1
19000	1982015.0	1895537.0	1740160.0	1285079.0	826511.5
20000	2032297.0	1964554.0	1829591.0	1447952.0	936687.3
22000	2113763.0	2084769.0	1976916.0	1715375.0	1181957.0
24000	2187094.0	2174746.0	2108903.0	1910753.0	1434957.0
26000	2258712.0	2251781.0	2216014.0	2065123.0	1668072.0
28000	2330262.0	2324828.0	2304628.0	2199165.0	1873730.0
30000	2402984.0	2397077.0	2382652.0	2312619.0	2012467.0
35000	2632138.0	2580959.0	2566947.0	2533433.0	2381774.0
40000	2979635.0	2821414.0	2754230.0	2726036.0	2635900.0
45000	3225603.0	3142575.0	2981737.0	2913461.0	2848279.0
50000	3418256.0	3394043.0	3272324.0	3123026.0	3039291.0

Table 10.19 Specific entropy s [$\text{J kg}^{-1} \text{ K}^{-1}$] of Jupiter as a function of temperature for different pressures

T (K)	P (bar)				
	10^{-2}	10^{-1}	1	10	10^2
100	68836.35	60213.64	51590.94	42968.24	34345.54
200	74347.90	65725.19	57102.49	48479.79	39857.09
300	78635.57	70012.87	61390.16	52767.46	44144.76
400	81926.81	73304.11	64681.41	56058.71	47436.01

(continued)

Table 10.19 (continued)

<i>T</i> (K)	<i>P</i> (bar)				
	10^{-2}	10^{-1}	1	10	10^2
500	84,557.66	75,934.96	67,312.25	58,689.55	50,066.85
600	86,744.03	78,121.33	69,498.63	60,875.93	52,253.22
700	88,616.63	79,993.92	71,371.22	62,748.52	54,125.82
800	90,258.42	81,635.72	73,013.02	64,390.31	55,767.61
900	91,724.94	83,102.24	74,479.54	65,856.84	57,234.13
1,000	93,054.73	84,432.03	75,809.32	67,186.62	58,563.92
1,500	98,405.32	89,774.91	81,149.77	72,526.30	63,903.35
2,000	103,269.40	94,092.53	85,294.51	76,616.36	67,976.13
2,500	115,979.50	100,423.00	89,574.57	80,246.03	71,399.97
3,000	151,810.60	116,852.00	96,884.23	84,504.98	74,685.60
3,500	173,307.20	144,402.40	111,109.70	90,930.72	78,424.54
4,000	177,917.50	158,975.30	130,167.90	100,747.30	83,169.20
4,500	180,270.30	163,426.10	142,771.50	113,085.10	89,228.38
5,000	182,188.00	165,741.50	148,106.70	124,007.70	96,434.35
6,000	185,547.10	169,144.60	152,638.90	134,711.60	110,690.40
7,000	189,036.50	172,128.80	155,599.30	138,848.10	119,524.70
8,000	194,353.90	175,432.30	158,290.90	141,603.20	124,083.70
9,000	204,669.90	180,148.00	161,222.80	144,040.80	126,991.50
10,000	224,266.00	187,877.10	164,975.20	146,543.70	129,336.30
11,000	254,478.90	200,503.70	170,258.50	149,417.50	131,532.30
12,000	285,204.30	219,025.60	177,820.80	152,963.80	133,803.70
13,000	304,134.80	241,484.80	188,244.50	157,447.40	136,299.00
14,000	313,180.20	261,989.70	201,387.90	163,091.70	139,134.50
15,000	318,136.50	276,035.30	216,397.90	170,115.40	142,472.10
16,000	322,061.90	284,363.20	230,881.80	178,272.60	146,212.10
17,000	326,199.40	289,562.80	242,957.80	187,528.40	150,566.20
18,000	330,353.00	293,512.20	251,848.70	197,195.40	155,473.00
19,000	333,758.70	297,185.40	258,074.20	206,537.20	160,533.70
20,000	336,343.10	300,734.60	262,666.00	214,904.00	166,199.60
22,000	340,231.20	306,485.10	269,718.90	227,690.50	177,913.90
24,000	343,424.60	310,413.60	275,467.20	236,211.70	188,954.80
26,000	346,292.80	313,505.00	279,780.40	242,453.90	198,313.80
28,000	348,943.90	316,218.10	283,067.10	247,425.70	205,946.80
30,000	351,453.40	318,710.50	285,776.00	251,343.30	210,756.90
35,000	358,471.90	324,386.50	291,474.90	258,217.40	222,406.60
40,000	367,752.50	330,780.20	296,483.00	263,364.70	229,212.70
45,000	373,571.90	338,346.30	301,835.90	267,806.10	234,221.30
50,000	377,635.30	343,663.30	307,961.20	272,216.30	238,321.80

Table 10.20 Density ρ [kg m^{-3}] of Jupiter as a function of temperature for different pressures

T (K)	P (bar)				
	10^{-2}	10^{-1}	1	10	10^2
100	0.00267038	0.02670375	0.26703750	2.67037500	26.70375000
200	0.00133519	0.01335188	0.13351880	1.33518800	13.35188000
300	0.00089013	0.00890125	0.08901251	0.89012510	8.90125100
400	0.00066759	0.00667594	0.06675938	0.66759380	6.67593800
500	0.00053408	0.00534075	0.05340751	0.53407510	5.34075100
600	0.00044506	0.00445063	0.04450626	0.44506260	4.45062600
700	0.00038148	0.00381482	0.03814822	0.38148220	3.81482200
800	0.00033380	0.00333797	0.03337969	0.33379690	3.33796900
900	0.00029671	0.00296708	0.02967084	0.29670840	2.96708400
1000	0.00026704	0.00267038	0.02670375	0.26703750	2.67037500
1500	0.00017801	0.00178021	0.01780236	0.17802460	1.78024900
2000	0.00013254	0.00133207	0.01334201	0.13348760	1.33508900
2500	0.00009594	0.00103076	0.01056011	0.10642790	1.06692300
3000	0.00005725	0.00072972	0.00830347	0.08702008	0.88371870
3500	0.00004139	0.00047359	0.00606935	0.07030801	0.74281000
4000	0.00003545	0.00036517	0.00428109	0.05460651	0.62220590
4500	0.00003142	0.00031637	0.00334818	0.04141411	0.51341970
5000	0.00002826	0.00028321	0.00288605	0.03259165	0.41780050
6000	0.00002354	0.00023552	0.00236280	0.02430693	0.28384190
7000	0.00002009	0.00020157	0.00201933	0.02036235	0.21727500
8000	0.00001727	0.00017538	0.00176276	0.01770753	0.18210150
9000	0.00001458	0.00015323	0.00155800	0.01568410	0.15919630
10000	0.00001172	0.00013242	0.00138351	0.01404516	0.14211470
11000	0.00000899	0.00011148	0.00122437	0.01265238	0.12841490
12000	0.00000703	0.00009094	0.00107159	0.01141586	0.11691030
13000	0.00000595	0.00007329	0.00092249	0.01027463	0.10699320
14000	0.00000534	0.00006068	0.00078282	0.00919611	0.09803056
15000	0.00000491	0.00005269	0.00066112	0.00817265	0.08982313
16000	0.00000457	0.00004758	0.00056440	0.00721216	0.08219873
17000	0.00000426	0.00004391	0.00049386	0.00634134	0.07512572
18000	0.00000399	0.00004100	0.00044432	0.00558281	0.06848987
19000	0.00000376	0.00003846	0.00040768	0.00494979	0.06229172
20000	0.00000356	0.00003623	0.00037933	0.00443953	0.05661300
22000	0.00000322	0.00003254	0.00033639	0.00371597	0.04692373
24000	0.00000295	0.00002968	0.00030293	0.00324537	0.03946328
26000	0.00000272	0.00002734	0.00027704	0.00291689	0.03394311
28000	0.00000253	0.00002536	0.00025579	0.00265327	0.02984037
30000	0.00000236	0.00002365	0.00023822	0.00244289	0.02713648
35000	0.00000201	0.00002025	0.00020349	0.00206458	0.02180179
40000	0.00000173	0.00001760	0.00017761	0.00179317	0.01853651
45000	0.00000153	0.00001542	0.00015699	0.00158926	0.01623744
50000	0.00000137	0.00001379	0.00013975	0.00142254	0.01455033

Table 10.21 Specific heat c_p [J kg⁻¹ K⁻¹] of Jupiter as a function of temperature for different pressures

T (K)	P (bar)				
	10^{-2}	10^{-1}	1	10	10^2
100	10,211.849	10,211.849	10,211.849	10,211.849	10,211.849
200	11,907.825	11,907.825	11,907.825	11,907.825	11,907.825
300	12,611.177	12,611.177	12,611.177	12,611.177	12,611.177
400	12,724.869	12,724.869	12,724.869	12,724.869	12,724.869
500	12,759.968	12,759.968	12,759.968	12,759.968	12,759.968
600	12,785.599	12,785.599	12,785.598	12,785.598	12,785.598
700	12,831.698	12,831.697	12,831.699	12,831.698	12,831.698
800	12,905.290	12,905.293	12,905.288	12,905.289	12,905.289
900	13,008.731	13,008.722	13,008.741	13,008.735	13,008.736
1,000	13,138.985	13,139.019	13,138.948	13,138.972	13,138.967
1,500	14,173.992	14,042.200	14,000.425	13,987.240	13,982.999
2,000	25,130.434	18,058.249	15,819.725	15,111.618	14,887.750
2,500	116,379.067	48,306.267	25,881.216	18,741.034	16,479.515
3,000	231,187.503	146,757.777	61,488.488	30,571.792	20,604.387
3,500	58,023.954	168,531.473	126,948.849	56,202.036	29,257.776
4,000	22,586.727	57,876.068	139,248.345	92,199.496	43,152.688
4,500	18,557.604	25,720.120	72,333.177	111,678.317	60,490.528
5,000	18,029.482	19,686.849	34,914.399	89,484.230	75,661.555
6,000	19,442.848	18,453.558	19,949.100	35,014.862	71,906.903
7,000	28,069.546	21,023.012	19,148.006	21,922.451	42,634.524
8,000	57,222.667	30,271.068	21,812.226	20,114.449	27,608.167
9,000	128,214.337	53,275.128	29,103.847	21,772.700	22,739.095
10,000	253,892.718	98,668.808	43,920.042	26,354.840	22,259.228
11,000	365,601.424	171,423.614	69,747.500	34,895.528	24,289.109
12,000	308,146.786	255,036.727	105,779.132	47,994.140	28,773.689
13,000	167,083.441	293,431.856	153,941.869	66,405.620	34,561.938
14,000	87,783.256	245,549.048	202,350.204	87,189.746	42,651.642
15,000	61,700.036	161,498.941	228,448.856	116,085.152	51,320.218
16,000	63,031.144	101,568.042	215,744.563	138,711.832	65,758.549
17,000	72,781.939	74,037.568	177,943.085	162,450.623	79,374.902
18,000	69,476.080	66,685.827	132,426.680	173,102.523	94,125.302
19,000	55,995.228	69,309.975	99,770.399	169,694.342	98,436.480
20,000	45,481.089	67,817.856	81,260.827	154,524.346	114,768.720
22,000	37,606.629	50,928.801	68,976.942	113,177.327	127,013.369
24,000	36,098.737	40,277.177	60,425.519	85,494.986	27,871.321
26,000	35,602.397	36,858.824	48,589.630	69,509.535	55,111.952
28,000	35,914.187	35,818.259	41,177.918	61,844.596	72,310.198
30,000	37,065.760	35,883.009	38,801.902	52,122.307	41,974.077
35,000	61,472.775	39,183.437	36,769.908	40,664.731	58,199.809
40,000	62,214.193	59,841.547	39,778.027	38,156.053	45,322.209
45,000	40,995.483	59,869.904	53,118.375	39,132.636	41,854.437
50,000	37,178.300	43,090.901	59,124.990	45,071.512	39,718.505

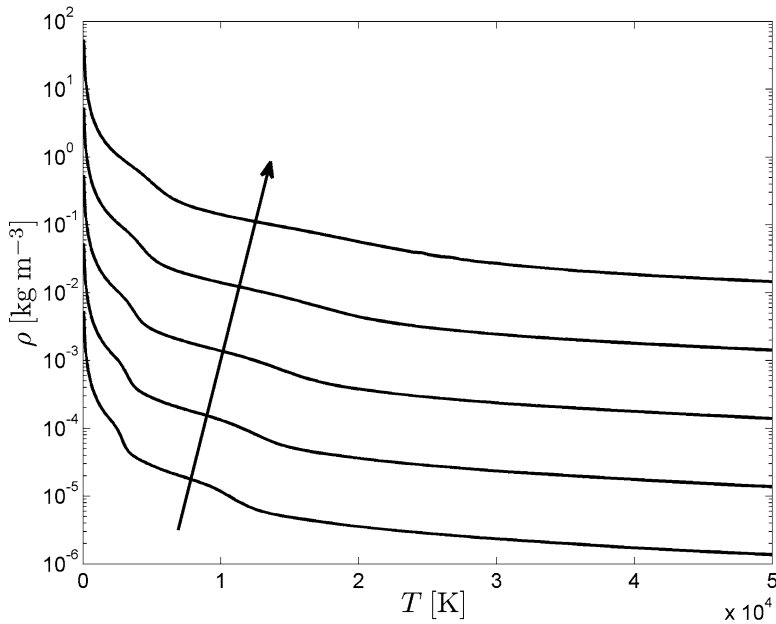


Fig. 10.34 Mass density of Jupiter atmosphere at $P = 10^{-2}, 10^{-1}, 1, 10, 100$ bar

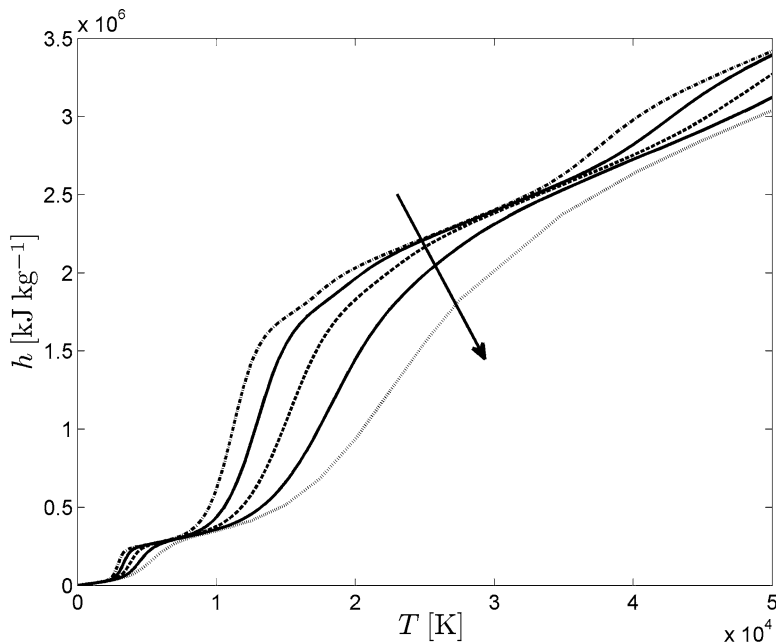


Fig. 10.35 Specific enthalpy of Jupiter atmosphere at $P = 10^{-2}, 10^{-1}, 1, 10, 100$ bar

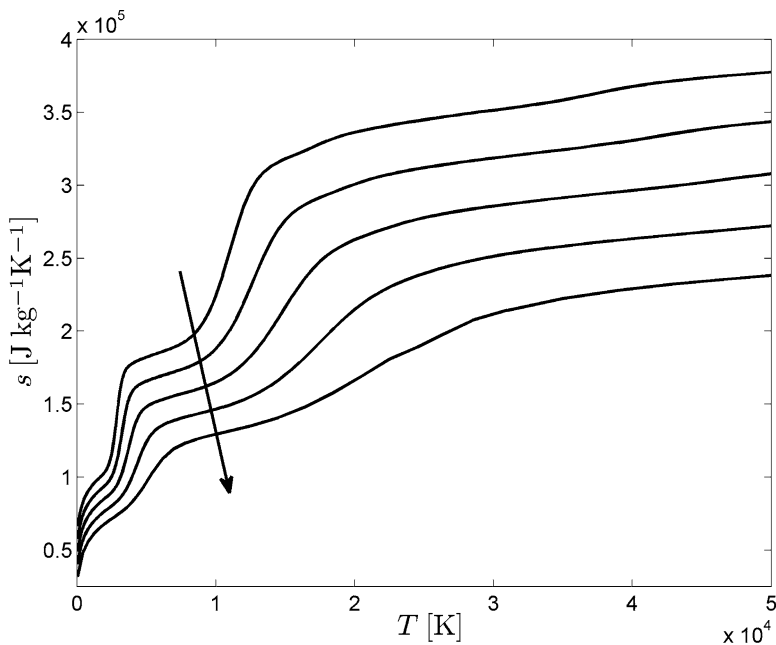


Fig. 10.36 Specific entropy of Jupiter atmosphere at $P = 10^{-2}, 10^{-1}, 1, 10, 100$ bar

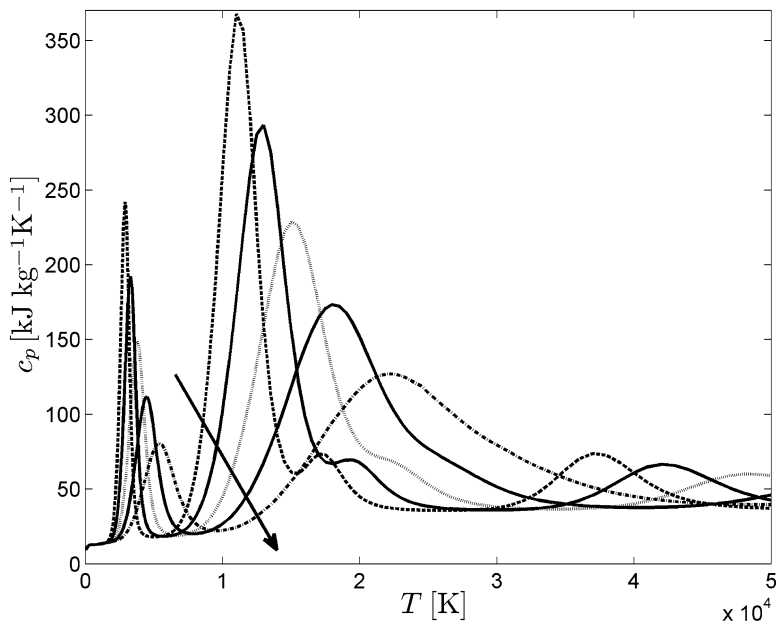


Fig. 10.37 Specific heat of Jupiter atmosphere at $P = 10^{-2}, 10^{-1}, 1, 10, 100$ bar

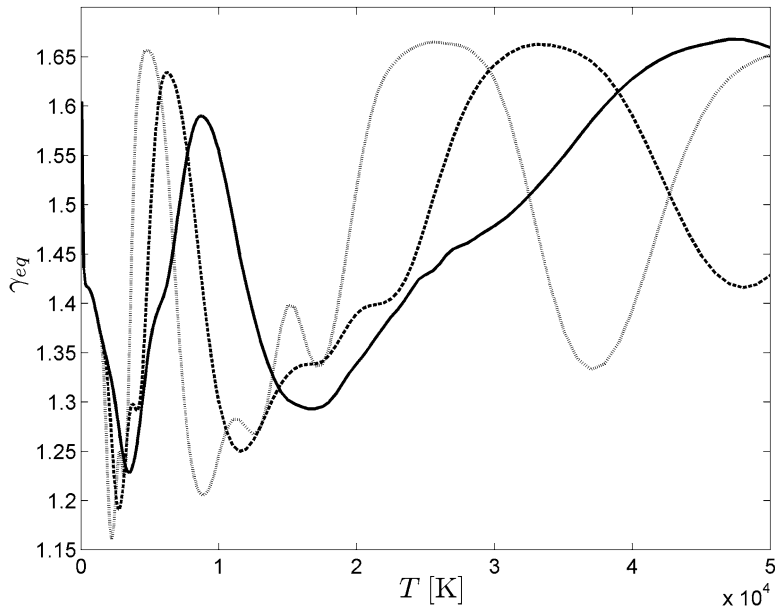


Fig. 10.38 Equilibrium isentropic coefficient of Jupiter atmosphere at $P = 10^{-2}$ (dotted line), 1 (dashed line), 100 (full line) bar

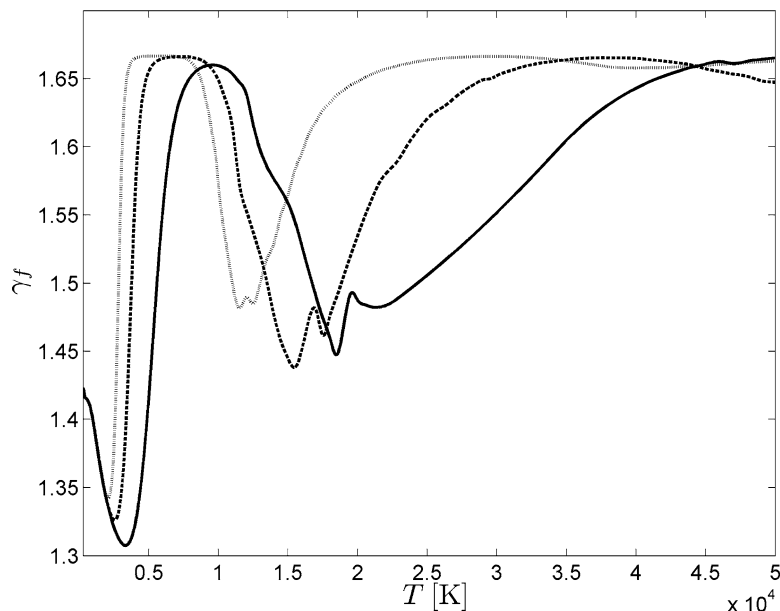


Fig. 10.39 Frozen isentropic coefficient of Jupiter atmosphere at $P = 10^{-2}$ (dotted line), 1 (dashed line), 100 (full line) bar

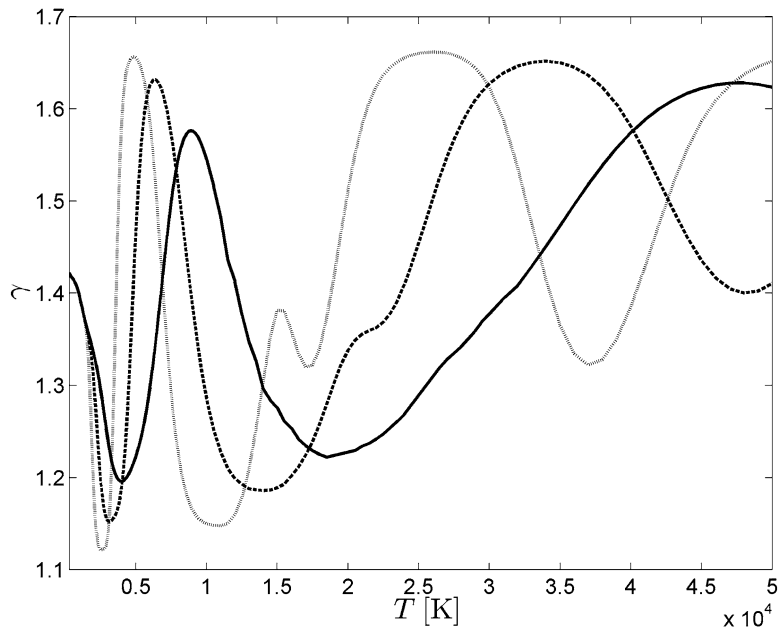


Fig. 10.40 Isentropic coefficient of Jupiter at $P = 10^{-2}$ (dotted line), 1 (dashed line), 100 (full line) bar

Table 10.22 Frozen isentropic coefficient γ_f of Jupiter as a function of temperature for different pressures

T (K)	P (bar)				
	10^{-2}	10^{-1}	1	10	10^2
100	1.59169	1.59169	1.59169	1.59169	1.59169
200	1.45582	1.45582	1.45582	1.45582	1.45582
300	1.42322	1.42322	1.42322	1.42322	1.42322
400	1.41690	1.41690	1.41690	1.41690	1.41690
500	1.41544	1.41544	1.41544	1.41544	1.41544
600	1.41420	1.41420	1.41420	1.41420	1.41420
700	1.41211	1.41211	1.41211	1.41211	1.41211
800	1.40880	1.40880	1.40880	1.40880	1.40880
900	1.40423	1.40423	1.40423	1.40423	1.40423
1000	1.39863	1.39863	1.39863	1.39863	1.39863
1500	1.36586	1.36584	1.36583	1.36583	1.36583
2000	1.34184	1.34005	1.33948	1.33930	1.33925
2500	1.36093	1.33325	1.32445	1.32167	1.32079
3000	1.51876	1.38605	1.33175	1.31424	1.30871
3500	1.64365	1.53516	1.38885	1.32482	1.30412
4000	1.66305	1.63441	1.50550	1.36609	1.31077
4500	1.66586	1.65877	1.60360	1.44381	1.33336
5000	1.66642	1.66426	1.64434	1.53369	1.37507
6000	1.66662	1.66628	1.66289	1.63290	1.49756
7000	1.66633	1.66644	1.66564	1.65723	1.59417

(continued)

Table 10.22 (continued)

T (K)	P (bar)				
	10^{-2}	10^{-1}	1	10	10^2
8000	1.66242	1.66512	1.66575	1.66308	1.63711
9000	1.63883	1.65568	1.66228	1.66348	1.65279
10000	1.57118	1.62324	1.64891	1.65873	1.65654
11000	1.50004	1.54469	1.61436	1.63934	1.65205
12000	1.48951	1.49790	1.55343	1.60255	1.63815
13000	1.49966	1.47275	1.50448	1.56727	1.59705
14000	1.52940	1.46719	1.47599	1.53796	1.57563
15000	1.56424	1.48829	1.44464	1.48755	1.53059
16000	1.59576	1.50572	1.46914	1.48703	1.52638
17000	1.61835	1.54253	1.48055	1.46198	1.49052
18000	1.63230	1.56662	1.47531	1.45015	1.45992
19000	1.64135	1.59382	1.50522	1.45085	1.49854
20000	1.64777	1.60962	1.53485	1.46165	1.48735
22000	1.65717	1.63358	1.57129	1.50067	1.48347
24000	1.66207	1.64756	1.60762	1.54406	1.49953
26000	1.66480	1.65601	1.62692	1.55766	1.52655
28000	1.66603	1.66127	1.64351	1.59131	1.55762
30000	1.66632	1.66436	1.65223	1.61613	1.56640
35000	1.66298	1.66540	1.66389	1.64757	1.60482
40000	1.65790	1.65836	1.66496	1.66248	1.64308
45000	1.65980	1.65090	1.65727	1.66523	1.66075
50000	1.66290	1.65366	1.64749	1.66088	1.66524

Table 10.23 Equilibrium isentropic coefficient γ_{eq} of Jupiter as a function of temperature for different pressures

T (K)	P (bar)				
	10^{-2}	10^{-1}	1	10	10^2
100	1.59060	1.59060	1.59060	1.59060	1.59060
200	1.45519	1.45519	1.45519	1.45519	1.45519
300	1.42303	1.42303	1.42303	1.42303	1.42303
400	1.41685	1.41685	1.41685	1.41685	1.41685
500	1.41541	1.41541	1.41541	1.41541	1.41541
600	1.41415	1.41415	1.41415	1.41415	1.41415
700	1.41202	1.41202	1.41202	1.41202	1.41202
800	1.40864	1.40864	1.40864	1.40864	1.40864
900	1.40400	1.40400	1.40400	1.40400	1.40400
1,000	1.39832	1.39833	1.39833	1.39833	1.39833
1,500	1.35964	1.36353	1.36479	1.36518	1.36531
2,000	1.21915	1.28179	1.31738	1.33159	1.33646
2,500	1.18346	1.18037	1.22526	1.27525	1.30331
3,000	1.25353	1.23692	1.20104	1.22079	1.26135
3,500	1.27949	1.27287	1.26926	1.22614	1.23544
4,000	1.52776	1.30211	1.30829	1.28418	1.24470

(continued)

Table 10.23 (continued)

T (K)	P (bar)				
	10^{-2}	10^{-1}	1	10	10^2
4,500	1.63595	1.48304	1.31520	1.33960	1.28572
5,000	1.65216	1.60492	1.41254	1.35471	1.34112
6,000	1.58488	1.63239	1.60315	1.44437	1.41410
7,000	1.38873	1.53369	1.60804	1.57390	1.46186
8,000	1.23879	1.37103	1.51731	1.59037	1.53560
9,000	1.20649	1.26025	1.39276	1.52874	1.57207
10,000	1.24327	1.22715	1.29973	1.43753	1.54841
11,000	1.28397	1.24466	1.25657	1.35499	1.48986
12,000	1.27310	1.28468	1.25214	1.30094	1.42331
13,000	1.27157	1.30789	1.27401	1.27727	1.36156
14,000	1.33530	1.30186	1.30533	1.27618	1.32468
15,000	1.40042	1.30316	1.32803	1.28762	1.29930
16,000	1.37443	1.33749	1.33774	1.31178	1.29411
17,000	1.33594	1.38061	1.33859	1.33466	1.29340
18,000	1.35515	1.38671	1.34736	1.35414	1.30050
19,000	1.42854	1.37030	1.36918	1.36785	1.32181
20,000	1.51988	1.37600	1.39010	1.37741	1.33893
22,000	1.62951	1.47768	1.40081	1.39779	1.37722
24,000	1.65930	1.59240	1.43937	1.42069	1.41165
26,000	1.66488	1.64508	1.52633	1.43997	1.43911
28,000	1.65818	1.66212	1.60091	1.47416	1.46261
30,000	1.62567	1.66373	1.64269	1.52876	1.48036
35,000	1.37246	1.58835	1.66106	1.64072	1.54949
40,000	1.39361	1.39366	1.59098	1.66098	1.62782
45,000	1.58936	1.41491	1.44815	1.62298	1.66119
50,000	1.65294	1.56521	1.42629	1.52769	1.65936

Table 10.24 Isentropic coefficient γ of Jupiter as a function of temperature for different pressures

T (K)	P (bar)				
	10^{-2}	10^{-1}	1	10	10^2
100	1.59060	1.59060	1.59060	1.59060	1.59060
200	1.45519	1.45519	1.45519	1.45519	1.45519
300	1.42303	1.42303	1.42303	1.42303	1.42303
400	1.41685	1.41685	1.41685	1.41685	1.41685
500	1.41541	1.41541	1.41541	1.41541	1.41541
600	1.41415	1.41415	1.41415	1.41415	1.41415
700	1.41202	1.41202	1.41202	1.41202	1.41202
800	1.40864	1.40864	1.40864	1.40864	1.40864
900	1.40400	1.40400	1.40400	1.40400	1.40400
1000	1.39832	1.39833	1.39833	1.39833	1.39833
1500	1.35959	1.36351	1.36478	1.36518	1.36531
2000	1.21469	1.28029	1.31689	1.33143	1.33641

(continued)

Table 10.24 (continued)

T (K)	P (bar)				
	10^{-2}	10^{-1}	1	10	10^2
2500	1.12713	1.16009	1.21833	1.27294	1.30256
3000	1.13046	1.14084	1.16230	1.20727	1.25682
3500	1.25017	1.15692	1.16098	1.18031	1.21933
4000	1.52225	1.26346	1.18043	1.18364	1.20408
4500	1.63467	1.47199	1.24774	1.20161	1.20712
5000	1.65176	1.60133	1.38471	1.23767	1.22173
6000	1.58436	1.63167	1.59761	1.40322	1.27719
7000	1.38551	1.53242	1.60619	1.56005	1.37866
8000	1.22537	1.36617	1.51510	1.58452	1.49278
9000	1.16507	1.24533	1.38719	1.52452	1.54930
10000	1.14998	1.19003	1.28623	1.43155	1.53465
11000	1.14777	1.16963	1.22794	1.34402	1.47916
12000	1.15949	1.16557	1.19903	1.28098	1.41191
13000	1.20861	1.16865	1.18808	1.24331	1.34650
14000	1.30289	1.18416	1.18601	1.22276	1.30302
15000	1.38122	1.22357	1.18890	1.21041	1.26813
16000	1.35910	1.28658	1.20176	1.20903	1.25033
17000	1.31995	1.34666	1.22419	1.20958	1.23462
18000	1.33999	1.36026	1.25834	1.21535	1.22494
19000	1.41665	1.34698	1.30184	1.22655	1.22803
20000	1.51102	1.35392	1.33806	1.24381	1.22865
22000	1.62427	1.46172	1.36260	1.29394	1.24182
24000	1.65536	1.58121	1.40973	1.34400	1.26896
26000	1.66159	1.63627	1.50282	1.37730	1.30463
28000	1.65543	1.65455	1.58324	1.42354	1.34353
30000	1.62298	1.65747	1.62726	1.48802	1.37764
35000	1.36518	1.58219	1.64988	1.61261	1.47308
40000	1.38497	1.38312	1.58114	1.64176	1.57404
45000	1.58641	1.40368	1.43530	1.60577	1.62234
50000	1.65160	1.55932	1.41071	1.51173	1.62349

Appendix A

Spectral Terms for Atoms and Molecules

In previous chapters, the calculation of the electronic partition function of atomic hydrogen has been carried out by using the analytical formulation of the energy levels and of the corresponding statistical weights. The situation is deeply different when dealing with the multielectron atoms. In principle, one can write the Schrödinger equation for the system and solve it through numerical methods. This approach is in general followed for the ground state and for the so-called *low-lying* excited states, i.e., for electronic states arising from the rearrangement of valence electrons. On the other hand, the solution of the Schrödinger equation for *high-lying* excited states (i.e., states characterized by values of principal quantum number different from that of the ground state) is still a prohibitive task despite the enormous progress of quantum chemistry calculations. In this case, semiempirical methods, based on known electronic levels, can be used to get a complete set of energy levels, ready for the cutoff criterion. In doing so, we must be aware of the enormous number of energy levels arising from the coupling of the angular and spin momenta in the multielectron systems. This kind of problems will be analyzed in the first part of this appendix that will give us the recipes to get complete sets of energy levels for multielectron atoms.

In the second part, we will consider similar problems for diatomic molecules.

A.1 Atomic Electronic Terms

The electrons in multielectron atoms can be identified through four quantum numbers (principal, angular, magnetic, and spin) in the order

$$(n_1, l_1, m_1, s_1)$$

$$(n_2, l_2, m_2, s_2)$$

$$(n_3, l_3, m_3, s_3)$$

...

In the frame of the *vector model* for angular momentum, let us define the following total quantities:

- L Quantum number for the *orbital* angular momentum, associated to the squared modulus of the vector \mathbf{L} , i.e. $|\mathbf{L}|^2 = L(L+1)$, with $(2L+1)$ values of the projection on the quantization axis (the z -axis) $M_L = -L, -L+1, \dots, 0, \dots, L-1, L$.
- S Quantum number associated to the *spin* angular momentum, corresponding to a vector \mathbf{S} with modulus $|\mathbf{S}|^2 = S(S+1)$, with $(2S+1)$ values of the projection on the quantization axis $M_S = -S, -S+1, \dots, 0, \dots, S-1, S$.
- J Total angular momentum for $\mathbf{J} = \mathbf{L} + \mathbf{S}$ with $|\mathbf{J}|^2 = J(J+1)$.

The sum rules are those of vector addition, considering their possible relative orientation. In the following, we will present the practical rules for obtaining L , S and J ¹.

A.1.1 Calculation of L

One-electron atoms $L_1 = \ell_1$.

Two-electron atoms L_2 assumes all the integer values in the interval $\ell_1 + \ell_2, \ell_1 + \ell_2 - 1 \dots |\ell_1 - \ell_2|$

Three-electron atoms L_3 assumes, for each possible value of L_2 , all the values in the interval $L_2 + \ell_3, L_2 + \ell_3 - 1 \dots |L_2 - \ell_3|$.

The procedure is extended adding one electron at a time.

A.1.2 Calculation of S

One-electron atoms $S_1 = s_1$

Two-electron atoms S_2 assumes all the integer values in the interval $s_1 + s_2, s_1 + s_2 - 1 \dots |s_1 - s_2|$

Three-electron atoms S_3 assumes, for each possible value of S_2 , all the values in the interval $S_2 + s_3, S_2 + s_3 - 1 \dots |S_2 - s_3|$.

The procedure is extended adding one electron at a time.

¹It should be noted that the scheme presented in this chapter is the so-called Russell–Saunders coupling scheme, widely used for the derivation of atomic term symbols of light atoms ($Z \lesssim 40$). Alternatively, the $j - j$ coupling scheme can be considered. Within this frame, the orbital and spin angular momenta of each electron are coupled ($j_i = \ell_i + s_i$) and then the coupling of one-electron total angular momenta ($j_1, j_2, j_3 \dots$) results in the total angular momentum of the atom J . This scheme is more appropriate for heavy atoms, when the spin-orbit coupling is the relevant interaction.

A.1.3 Calculation of J

J can assume, for each possible value of L and S , all the integer values in the range $L + S, L + S - 1 \dots |L - S|$.

Before passing to practical examples, we want to remind that each electronic term, corresponding to a given electronic configuration, is characterized by a term symbol written in the form $^{2S+1}L_J$. Capital letters in the series (S, P, D, F, G, \dots) correspond to different values of the orbital angular momentum L ($0, 1, 2, 3, 4, \dots$). On the left of the capital letter, the value of spin multiplicity $2S + 1$ is reported², while on the right the value of J is found. The total multiplicity of the state, i.e., the statistical weight is $2J + 1 = (2L + 1)(2S + 1)$. Therefore,

$^2S_{1/2}$ identifies a state with $L = 0$ (state S), total spin $S = \frac{1}{2}$, resulting in a doublet (multiplicity $2S + 1 = 2$) and with $J = \frac{1}{2}$ ($J = L + S = 0 + \frac{1}{2} = \frac{1}{2}$). The statistical weight of the state is $2J + 1 = 2$.

A.1.3.1 Hydrogen

For $n = 1$ (ground state,) we have $H(1s)$ which corresponds to

$$\begin{aligned} S &= s_1 = \frac{1}{2} \\ L &= \ell_1 = 0 \\ J &= \frac{1}{2}. \end{aligned}$$

The electronic term is written as $^2S_{1/2}$. The statistical weight is given by $g_1 = 2J + 1 = 2$ having energy $\varepsilon_1 = 0$.

For $n = 2$, we have $H(2s)$ and $H(2p)$ states. The angular momentum of $H(2s)$ is analogous to the $H(1s)$ and therefore the electronic term is $^2S_{1/2}$ and the statistical weight is $g_{2s} = 2$.

Let us now consider the excited state $H(2p)$

$$\begin{aligned} S &= s_1 = \frac{1}{2} \\ L &= \ell_1 = 1 \\ J &= \{\frac{3}{2}, \frac{1}{2}\}. \end{aligned}$$

Therefore, we have two terms $\{^2P_{3/2}, ^2P_{1/2}\}$ with statistical weights of 4 and 2, respectively. The energy of the state is given by

$$\varepsilon_2 = I_H \left(1 - \frac{1}{2^2} \right) = \frac{3}{4} I_H$$

independently of the angular momentum³. Therefore, summing the contribution of the three terms we have $g_{n=2} = 2 + 4 + 2 = 8$, in agreement with the general formula $g_n = 2n^2$.

²Depending on the spin multiplicity, electronic states of atoms are classified as doublets ($2S + 1 = 2$), triplets ($2S + 1 = 3$), quartets ($2S + 1 = 4$), ...

³If the spin-orbit coupling is neglected.

A.1.3.2 Helium

The ground state configuration is $He(1s^2)$. The two electrons are not independent because, due to the *Pauli exclusion principle*, their spins must be antiparallel. Therefore, we have:

$$L = 0 \text{ being } \ell_1 = \ell_2 = 0$$

$$S = 0 \text{ being } s_1 = s_2 = \frac{1}{2} \text{ with } m_{s_1} = -m_{s_2}$$

$$J = 0$$

giving a configuration 1S_0 , corresponding to a *closed shell atom*, characteristic of noble gas ground state, having degeneracy $g_1 = 1$.

Let us consider the $He(1s2s)$ excited configuration. The two electrons are now independent because they do not occupy the same orbital. Therefore, we have:

$$L = 0 \text{ being } \ell_1 = \ell_2 = 0$$

$$S = \{1, 0\} \text{ being } s_1 = s_2 = \frac{1}{2}$$

$$J = \{1, 0\}$$

giving the configurations 3S_1 and 1S_0 , corresponding to a triplet ($g = 3$) and a singlet ($g = 1$) states.

A.1.3.3 Two Not-Equivalent p Electrons (np, mp)

The two electrons are independent because are not in the same orbital. Therefore:

$$L = \{2, 1, 0\} \text{ being } \ell_1 = \ell_2 = 1$$

$$S = \{1, 0\} \text{ being } s_1 = s_2 = \frac{1}{2}.$$

To calculate J , we have to combine the different contributions giving the following terms

L	S	J	Terms
2	1	{3,2,1}	${}^3D_3, {}^3D_2, {}^3D_1$
2	0	2	1D_2
1	1	{2,1,0}	${}^3P_2, {}^3P_1, {}^3P_0$
1	0	1	1P_1
0	1	1	3S_1
0	0	0	1S_0

A.1.3.4 Two Equivalent p Electrons (np^2)

For two equivalent p electrons, characterized by the same principal and orbital quantum numbers (n, ℓ), not all the electronic terms derived in the previous example do exist. In this case in fact the *Pauli exclusion principle* restricts the number of allowed configurations. For the configuration np^2 , i.e. $(\ell_i = 1, s_i = \frac{1}{2})$, with

m												
1	↑↓				↑		↑		↑		↑	
0		↑↓		↑↓	↓	↑		↑	↑		↑	↓
-1			↑↓		↓		↓		↑		↑	↑
M_L	2	0	-2	1	-1	0	1	0	-1	1	0	-1
M_S	0	0	0	0	0	0	1	1	1	0	0	0
	1D_2			1S_0			$^3P_{2,1,0}$					

Fig. A.1 Arrangements of two electrons on three equivalent p orbitals

axial projections $m_{\ell_i} = \pm 1, 0, m_{s_i} = \pm \frac{1}{2}$, let us consider the possible values of the electrons angular momentum projections, algebraically summing in the resulting total angular and spin momentum projections, $M_L = m_{\ell_1} + m_{\ell_2}$ and $M_S = m_{s_1} + m_{s_2}$, as shown in Fig. A.1, where uparrows correspond to $m_s = \frac{1}{2}$ and downarrows to $-\frac{1}{2}$. The configurations originating negative total spin projection are implicitly included.

The maximum M_L value of 2, found in constructing the allowed configurations, with maximum $M_S = 0$, implies the existence of a term 1D , thus accounting for five configurations with ($M_L = \pm 2, \pm 1, 0$ and $M_S = 0$). Repeating the procedure on the remaining configurations, $(M_L)_{\text{max}} = 1$ and $(M_S)_{\text{max}} = 1$, one accounts for a 3P term with nine configurations arising from allowed values $M_L = \pm 1, 0$ and $M_S = \pm 1, 0$. Finally, the last arrangement ($M_L = 0$ and $S = 0$) leads to the 1S term. The group theory offers an elegant and compact derivation of allowed terms (Bishop 1993), though beyond the scope of this book. It can be demonstrated that the spatial wavefunction for D and S terms is even, while spin wavefunction is even for triplets and odd for singlets. It is straightforward that due to the antisymmetric nature of the total (spatial+spin) electronic wavefunction, only $^1S, ^1D$ and 3P terms could exist.

This is the case of ground and low-lying excited states of carbon atom.

Term	Energy (cm $^{-1}$)	g
3P_0	0	1
3P_1	16.40	3
3P_2	43.40	5
1D_2	10,192.63	5
1S_0	21,648.01	1

A.1.3.5 Three Not-Equivalent p Electrons ($n_1 p, n_2 p, n_3 p$)

The results of the two-electron case with configuration (L_2, S_2) must be combined with the third electron (l_3, s_3), i.e.,

L_2	ℓ_3	L	S_2	s_3	S
2	1	{3,2,1}	1	1/2	{3/2,1/2}
1	1	{2,1,0}	0	1/2	1/2
0	1	1			

Let us now compose L and S :

L	S	J	Terms	# of terms
3	3/2	{9/2,7/2,5/2,3/2}	$^4F_{9/2,7/2,5/2,3/2}$	1
2	3/2	{7/2,5/2,3/2,1/2}	$^4D_{7/2,5/2,3/2,1/2}$	2
1	3/2	{5/2,3/2,1/2}	$^4P_{5/2,3/2,1/2}$	3
0	3/2	3/2	$^4S_{3/2}$	1
3	1/2	{7/2,5/2}	$^2F_{7/2,5/2}$	2
2	1/2	{5/2,3/2}	$^2D_{5/2,3/2}$	4
1	1/2	{3/2,1/2}	$^2P_{3/2,1/2}$	6
0	1/2	1/2	$^2S_{1/2}$	2

A.1.3.6 Three Equivalent p Electrons (np^3)

It turns out (see Fig. A.2) that for np^3 electronic configuration only the terms 4S , 2D , 2P survive. This is the case of the nitrogen atoms in ground and low-lying states with three electrons having principal quantum number $n = 2$

Term	Energy (cm $^{-1}$)	g
$^4S_{3/2}$	0	4
$^2D_{5/2}$	19224.464	6
$^2D_{3/2}$	19233.177	4
$^2P_{1/2}$	28838.920	2
$^2P_{3/2}$	28839.306	4

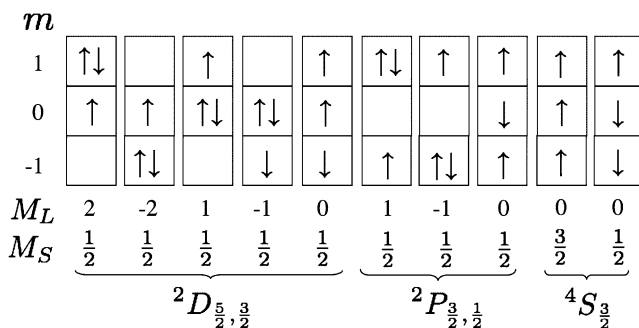


Fig. A.2 Arrangements of three electrons on three equivalent p orbitals

Table A.1 Electronic terms for atoms with equivalent-electron configurations

Configuration	Electronic terms	Atoms
$p\ p^5$	2P	B, F
$p^2\ p^4$	$^1S\ ^3P\ ^1D$	C, O, N ⁺
p^3	$^4S\ ^2P\ ^2D$	N, O ⁺
p^6	1S	Ne
$d\ d^9$	2D	Sc
$d^2\ d^8$	$^1S\ ^3P\ ^1D\ ^3F\ ^1G$	Ti, Ni
$d^3\ d^7$	$^2P\ ^4P\ ^2D\ ^2F\ ^4F\ ^2G\ ^2H$	V, Co
$d^4\ d^6$	$^2^1S\ ^2^3P\ ^2^1D\ ^3D\ ^5D\ ^1F$ $^2^3F\ ^2^1G\ ^3G\ ^3H\ ^1I$	Fe
d^5	$^2S\ ^6S\ ^2P\ ^4P\ ^3^2D\ ^4D\ ^2^2F$ $^4F\ ^2^2G\ ^4G\ ^2H\ ^2I$	Mn
d^{10}	1S	Zn

A.1.3.7 Four Equivalent p Electrons (np^4)

This situation gives the same terms as the two equivalent p electrons. This is the case of the oxygen atoms in ground and low-lying excited states, having four electrons with principal quantum number $n = 2$, reported below

Term	Energy (cm ⁻¹)	g
3P_2	0	5
3P_1	158.265	3
3P_0	226.977	1
1D_2	15867.862	5
1S_0	33792.583	1

In Table A.1, the electronic terms for equivalent-electron configurations are given. It should be noted that configurations having equal number of electrons or *electron-holes* have to be considered as equivalent, giving rise to the same electronic terms. Complete shell configurations, i.e. p^6 , always give the 1S term. We give here the definition of the parity of atomic terms $P = (-1)^{\sum_i \ell_i}$, being the exponent the algebraic sum of orbital angular momenta of electrons, in a given electronic configuration.

A.2 Complete Sets of Electronic Levels

The calculation of electronic partition function of atomic species needs of complete sets of energy levels and of corresponding statistical weights. Here, we want to present a very simple and rapid method based on the calculation of energy levels by an hydrogenic approximation and by calculating the statistical weight through the

L–S coupling. Some examples will explain the procedure which closely follows that one described in the previous pages. A better set of energy levels can be obtained by using semiempirical methods with the aid of existing tabulated energy levels ([Capitelli and Molinari 1970](#)) (see also Sect. A.3).

A.2.1 Helium

We want to calculate the complete set of levels with energies and statistical weights for the configurations derived from the interaction of the Helium core (2S) with the (*optical*) electron jumping on the excited levels.

Let us start with the interaction

$${}^2S + 2s$$

We note that the core configuration ($1s^1$) is characterized by quantum numbers $S_{\text{core}} = 1/2$ and $L_{\text{core}} = 0$, while the $2s$ excited electron has spin $1/2$ and $\ell = 0$. In the frame of L–S coupling scheme, the singlet 1S_0 ($g = 1$) and triplet 3S_1 ($g = 3$) states are obtained.

Consider now the interaction

$${}^2S + 2p$$

i.e., $(L_{\text{core}} = 0, S_{\text{core}} = 1/2) + (\ell = 1, s = 1/2)$. We obtain a triplet state ($L = 1$), which corresponds to 1P_1 ($g = 3$), ${}^3P_{2,1,0}$ ($g = 9$) and the total statistical weight is $g_{n=2} = 16$.

Let us now consider the interaction of the core with one electron in the $n = 3$ shell. The interactions with the $3s$ and $3p$ states follow directly from the cases above considered for the shell $n = 2$. Additionally, the interaction with the $3d$ electron must be considered

$${}^2S + 3d$$

originating, in the L–S coupling, 1D_2 ($g = 5$) and ${}^3D_{3,2,1}$ ($g = 15$), leading to the total statistical weight $g_{n=3} = g_{3s} + g_{3p} + g_{3d} = 36$.

The procedure can be continued to get all excited states coming from the interaction of the core electron with the optical electron. By comparing the total statistical weight coming from $n = 2$ and $n = 3$ we can deduce that the statistical weight of helium follows the relation

$$g = 4n^2$$

with respect to the principal quantum number.

Concerning the energy of levels, to a first approximation we can use an hydrogenic formula, inserting the helium ionization potential I_{He} in place of the corresponding one of the hydrogen atom

$$E_n = I_{\text{He}} - \frac{I_H}{n^2}$$

neglecting the splitting between singlet and triplet states due to spin–orbit coupling. Note also that the He ground state has a statistical weight $g = 1$.

A.2.2 Oxygen

We have already studied the spectroscopic terms coming from the different interactions occurring in the p^4 configuration. Now we want to study the interaction of the most stable atomic oxygen core (i.e., the ${}^4S_{3/2}$ state $L_{\text{core}} = 0, S_{\text{core}} = 3/2$) with the optical electron jumping on the excited states with $n \geq 3$. The stable core derives from the elimination of one electron from the p^4 to obtain the p^3 configuration.

Combining the core and an electron with $n = 4$, thus with $\ell = 0, \dots, n - 1 = 0, 1, 2, 3$, the following atomic terms can be derived

ℓ	s	L	S	J	Terms	g
0	1/2	0	{2,1}	{2,1}	${}^5S_2, {}^3S_1$	8
1	1/2	1	2	{3,2,1}	${}^5P_{3,2,1}$	15
1	1/2	1	1	{2,1,0}	${}^3P_{2,1,0}$	9
2	1/2	2	2	{4,3,2,1,0}	${}^5D_{4,3,2,1,0}$	25
2	1/2	2	1	{3,2,1}	${}^3D_{3,2,1}$	15
3	1/2	3	2	{5,4,3,2,1}	${}^5F_{5,4,3,2,1}$	35
3	1/2	3	1	{4,3,2}	${}^3F_{4,3,2}$	21

giving a total statistical weight $g = 128$. For $n = 3$, only the contribution of state with $\ell = 0 - 2$ must be considered, giving a total statistical weight $g = 72$.

We can deduce that the statistical weight for states obtained by the interaction of the 4S core with the optical electron with $n > 2$ is reproduced by the general formula

$$g_n = 8n^2.$$

Again, we can approximate the energy of the excited states through an hydrogenic form

$$E_n = I_O - \frac{I_H}{n^2}.$$

We must note that other sequences can arise forming electronically excited states of oxygen atoms from different core configurations. In fact, keeping in mind that low-lying excited states of oxygen are formed from different $L - S$ of the core electrons as 1S or 1D states. The new series are obtained repeating the previous procedure to each core configuration, obtaining plenty of the different levels. The corresponding energy can be calculated by the hydrogenic formula

$$E_n^* = I_O - \frac{I_H}{n^2} + E_{\text{core}},$$

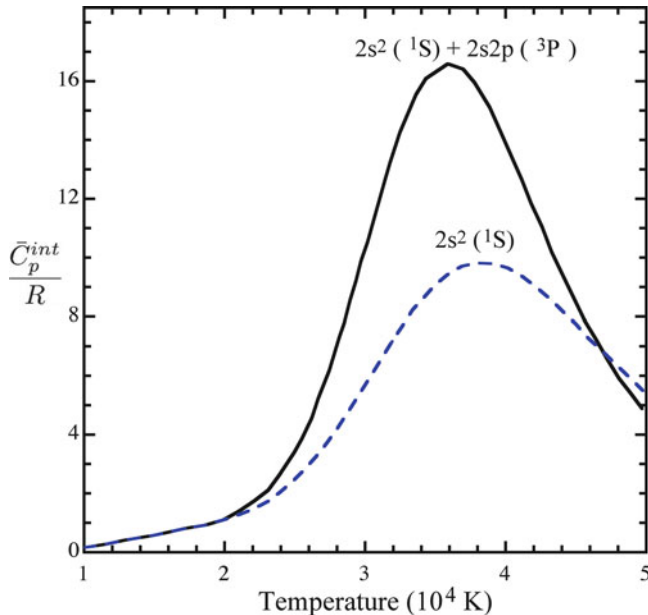


Fig. A.3 Reduced internal specific heat of C^+ as a function of temperature: comparison between calculations including levels having core $2s^2 ({}^1S)$ and $2s^2 ({}^1S) + 2s2p({}^3P)$

where E_{core} is the energy of the excited core configuration with respect to the ground state. The energy of the states of these series rapidly overcomes the ionization potential of the ground I_O forming the autoionizing states of the atom.

These states, while having energies above the ionization potential, are in same case considered, especially in the astrophysical literature. In this context, it is interesting to analyze their effects on the partition function and on thermodynamic properties. In Fig. A.3, we can see the effects on the internal specific heat of C^+ of the autoionizing states coming from $2s2p({}^3P)$ core.

As a general rule, we can calculate the statistical weight of excited states obtained from the interaction of a given core with the excited electron using the general formula

$$g_n = 2g_{\text{core}}n^2,$$

where g_{core} is the statistical weight of the relative core configuration. Keeping in mind that the electronic configuration of the helium core is a 2S state we have $g_{\text{core}} = 2$, while for 4S core of oxygen $g_{\text{core}} = 4$.

A.3 Beyond the Hydrogenoid Approximation

The available database for observed atomic electronic energy levels, as Moore (1949) and NIST tables (Chase Jr. 1998; NIST 2009), miss most of the predicted electronic levels, especially for higher quantum numbers.

In this section, we present an useful semi-empirical procedure which, applying a simplified formula to available, experimental or calculated, electronic levels, allows to complete, interpolating and/or extrapolating, the level series. We apply this method to estimate level energies of neutral carbon atom (see (Capitelli and Molinari 1970) for the nitrogen atom). The structure of the ground state is very complex, due to the presence of a few of low-lying states resulting from different L–S coupling:

Configuration	Terms
$2s^2 2p^2$	$^1S, ^3P, ^1D$
$2s^1 2p^3$	$^5S, ^3S, ^3P, ^1P, ^3D, ^1D$
$2p^4$	$^1S, ^3P, ^1D$

The first three states results from rearrangement of the spin of the p electrons, while the others are obtained from different rearrangements of the angular momenta.

The first step of the procedure is to determine the energy of the ground state configuration. If one of these terms has not been observed, it can be derived through extrapolation from energy levels of isoelectronic species. Practically, for carbon, the term $2p^4(^1S)$ is missing. We have to consider the energies of N^+ , O^{+2} and F^{+3} , corresponding to the same term, and, relating these energies to the atomic number Z , we extrapolate to obtain the corresponding value for $Z = 6$ (carbon).

The excited states come from the excitation of one electron toward higher values of the principal quantum numbers ($n > 2$) giving for carbon atoms

$$\begin{aligned} & 2s^2 2p(^2P)nl \\ & 2s2p^2(^4P)nl \\ & 2s2p^2(^2D)nl \\ & 2s2p^2(^2S)nl \\ & 2s2p^2(^2P)nl \\ & 2p^3(^4S)nl, \end{aligned}$$

where each series arises from the interaction of different atomic cores, $2s^2 2p(^2P)$, $2s2p^2(^4P)$, ..., with the excited electron, where $x = s, p, d, \dots$. It should be noted that in the previous section we have discussed only the excited states coming from the interaction of the more stable core, $2s^2 2p(^2P)$, with the excited electron. In this case, for $\ell = s$, there are two spectroscopic terms: 3P ($L = 1, S = 1$), and 1P ($L = 1, S = 0$). NIST's tables (NIST 2009) report observed levels up to

$n = 10$ for the former and $n = 14$ (missing values $n = 11, 12$) for the latter. To extrapolate to higher principal quantum numbers, the following Ritz–Rydberg series can be used:

$$E_n = I - \frac{I_H(z+1)^2}{(n + A + \frac{B}{n^2})^2}, \quad (\text{A.1})$$

where z is the charge of the species and A, B are adjustable parameters. The ionization energy I is related to the specific core configuration. It is calculated as the sum of the ionization energy from the ground state and the energy of the excited state of the successive ion in the corresponding electronic state. For example, if we consider C in the $2s2p^2(^4P)n\ell$ series, I is the sum of the ionization potential of C from the ground state (11.260 eV) and the energy of the C^+ in the excited state $2s2p^2(^4P)$ (5.336 eV).

The constants A and B can be determined when at least two observed levels are available. If we have only two levels, it is straightforward to calculate A and B by solving a system of two equations in two unknowns. If more than two levels are available, the two parameters are calculated by a *best fit* procedure. When only one observed energy level is known in a series, (A.1) cannot be used and the following formula with a single adjustable parameter should be applied:

$$E_n = I - \frac{I_H(z+1)^2}{(n + A)^2} \quad (\text{A.2})$$

obtained from (A.1) considering $B = 0$.

In some cases, as for $2s2p^2(^2P)n\ell$ for $n > 4$ and $\ell = g$, no level has been observed. As an example, to obtain the energy level of the terms corresponding to $5g$, we relate the energy levels ($5s, 5p, 5d, 5f$) as a function of the azimuthal quantum number $\ell (= 0 - 3)$, and extrapolate to $\ell = 4$ (see also (Capitelli and Molinari 1970)).

This method has been applied up to $n = 20$ and $\ell = 19$, with the exception of those series where no observed energies are present. For $n > 20$, we assume an hydrogen-like behavior and use the following formulas:

$$E_n = I - \frac{I_H(z+1)^2}{n^2}. \quad (\text{A.3})$$

At fixed n and for each series, the sum over the statistical weights of all the corresponding predicted spectroscopic terms for different ℓ is equal to

$$g_n = 2n^2 g_{\text{core}} \quad (\text{A.4})$$

and for $n > 20$ we apply this last equation to determine the total statistical weight. This method is more accurate than the hydrogenic approximation (see Sect. A.2) and has been extensively used in the calculation of thermodynamic properties of thermal plasmas.

A.4 Electronic Terms of Diatomic Molecules

Analogously to the case of atomic systems, also molecular electronic states are classified through the value of quantum numbers associated with total orbital and spin angular momenta and the information is condensed in the corresponding *molecular term symbol*.

In diatoms the electric field has an axial symmetry, with respect to the internuclear axis and therefore the Hamiltonian commutes with the operator corresponding to the axial projection of orbital angular momentum, corresponding to the quantum number Λ . Capital greek letters (Σ , Π , Δ , Φ , ...) are used for classification of molecular terms depending on the value assumed by Λ in the sequence (0, 1, 2, 3, ...). Moreover, each electronic term is characterized by the total spin S , with multiplicity $(2S + 1)$ originating *doublets* ($2S + 1 = 2$), *triplets* ($2S + 1 = 3$), *quartets* ($2S + 1 = 4$), ..., as seen for atoms. The general term symbol assumes the form: ${}^{(2S+1)}\Lambda$.

In the case of diatomic molecules, the term symbol also retains information about the parity of the electronic wavefunction with respect to some symmetry operations. More in detail, the reflection about a plane containing the internuclear axis returns a state with the same energy but with opposite sign of the projection of the orbital angular momentum, thus leading to the conclusion that all terms with $\Lambda \neq 0$ are doubly degenerate. However for Σ states ($\Lambda = 0$), which are nondegenerate, the parity is usually specified adding the sign plus or minus as superscript to the term symbol for even or odd states, i.e. ${}^{(2S+1)}\Sigma^{+/-}$.

Finally in the case of homonuclear diatomic molecules, a new symmetry arises due to the inversion center bisecting the internuclear axis. In this case, the subscripts g and u are used (${}^{(2S+1)}\Lambda_{g/u}$) for even (*gerade*) and odd (*ungerade*), respectively.

In the following, the *Wigner–Withmer rules* for the construction of molecular electronic terms for diatomic molecules arising from the interaction of atoms in given electronic states are illustrated.

The Λ value is determined as the modulus of the algebraic sum of axial projections of orbital angular momenta of atoms, i.e., $\Lambda = |M_{L_1} + M_{L_2}|$, assuming values in the series, $M_{L_1} = L_1, L_1 - 1, \dots, 0, \dots, -L_1$ and $L_2 = L_2, L_2 - 1, \dots, 0, \dots, -L_2$. If $L_1 \geq L_2$ it can be demonstrated that, accounting for double degeneracy of terms with $\Lambda \neq 0$, $(2L_2 + 1)(L_1 + 1)$ terms arise with Λ assuming values from 0 to $L_1 + L_2$. The number of molecular terms for each symmetry, given the orbital angular momenta of atoms, is given in Table A.2.

The atomic spin S_1 and S_2 vectorially sum in the total spin S , assuming values in the series $S_1 + S_2, S_1 + S_2 - 1, \dots, |S_1 - S_2|$.

Table A.2 Number of molecular terms per symmetry in diatomic molecules, for given orbital angular momenta of atoms

Number of terms	Λ
1	$L_1 + L_2$
2	$L_1 + L_2 - 1$
3	$L_1 + L_2 - 2$
...	...
$(2L_2+1)$	$L_1 - L_2$
$(2L_2+1)$	$L_1 - L_2 - 1$
...	...
$(2L_2+1)$	0

A.4.1 H_2 Molecule

(a) – Molecular states arising from two atoms in the ground state

The ground state of the hydrogen atom is a 2S state therefore $S = 1/2$ and $L = 0$. Using the combination rules, we have

$$\begin{aligned}\Lambda &= L_1 + L_2 = 0 & \Rightarrow \Sigma \\ S &= S_1 + S_2, |S_1 - S_2| = 1, 0 & \Rightarrow \text{triplet and singlet}\end{aligned}$$

Therefore, two molecular states arise: $^1\Sigma$ and $^3\Sigma$.

To characterize better the symmetry of the states, we must know the parity of the wave functions. For the hydrogen molecule, we can use either Heitler–London or molecular orbital (MO) wave functions. By using Heitler–London wave functions we must remind that the spatial part of these wave functions for the two states are written (neglecting the normalization factor) as

$$^1\Sigma \quad 1s_a(1)1s_b(2) + 1s_a(2)1s_b(1)$$

$$^3\Sigma \quad 1s_a(1)1s_b(2) - 1s_a(2)1s_b(1),$$

where $1s_a(1)$ represents an hydrogen wave function centered on the atom a describing electron 1. On the other hand, $1s_b(2)$ represents an hydrogen wave function centered on the atom b describing electron 2. The other terms mix the coordinates of the two electrons. By applying the symmetry operations generated by inversion through the molecule center and by reflection through a plane containing the internuclear axis to the first wave function one finds its invariants so that in the molecular state should appear the g and $+$ characters, i.e., the singlet state should be better written as $^1\Sigma_g^+$. The same operators applied to the triplet state should add the characters u and $+$ to the wavefunction, i.e., the triplet state should be written as $^3\Sigma_u^+$. To conclude we have written the first two molecular states of molecular hydrogen, the ground $X^1\Sigma_g^+$ and the first excited state $b^3\Sigma_u^+$. The triplet state is repulsive so that it does not enter in the electronic partition function. However, the repulsive state, which plays an important role on the transport properties and on the chemical kinetics of a plasma, should be taken into account also in thermodynamics

when considering real gas effects, i.e., the virial coefficients (see Chap. 7). The statistical weight of the Σ states is equal to the spin multiplicity, which is the number of total wave functions (space and spin) describing the state. According to the Pauli exclusion principle, the total wave function (space and spin) must be antisymmetric under the exchange of every couple of electrons (Capitelli et al. 2011b; Pauling and Wilson 1985). Keeping in mind the spin wave-functions α and β we can write the following (a part the normalization factor) wave functions for the two electron spin system

$$\sigma_{\text{singlet}} = \alpha(1)\beta(2) - \alpha(2)\beta(1)$$

$$\sigma_{\text{triplet}} = \begin{cases} \alpha(1)\alpha(2) \\ \beta(1)\beta(2) \\ \alpha(1)\beta(2) + \alpha(2)\beta(1). \end{cases}$$

To keep antisymmetric the total wavefunction we must couple symmetric space part with the antisymmetric spin part and vice versa. Therefore for the first two states of hydrogen molecule, we obtain

$$\begin{aligned} {}^1\Sigma_g^+ &\propto [1s_a(1)1s_b(2) + 1s_a(2)1s_b(1)][\alpha(1)\beta(2) - \alpha(2)\beta(1)] \\ {}^3\Sigma_u^+ &\propto [1s_a(1)1s_b(2) - 1s_a(2)1s_b(1)] \cdot \begin{cases} \alpha(1)\alpha(2) \\ \beta(1)\beta(2) \\ \alpha(1)\beta(2) + \alpha(2)\beta(1) \end{cases} \end{aligned}$$

To get the energies of the different states, we must apply the Hamiltonian operator of H_2 molecule to the relevant wave functions. These energies depend on the internuclear distance resulting in the potential energy curves. Nowadays, molecular states are obtained by quantum chemistry approaches, i.e., Hartree–Fock (HF), configuration interaction (CI) and high-level post-HF methods (see (Szabo and Ostlund 1996)).

(b) – Molecular states arising from excited atoms

Many other bound states can enter in the electronic partition function of molecular hydrogen. As an example from the interaction between $H(1s) + H(2s, 2p)$ atomic states, we can obtain the following 12 (bound and unbound) molecular states: ${}^{1,3}\Sigma_{g,u}^+$ (from $1s + 2s$) and ${}^{1,3}\Sigma_{g,u}^+, {}^{1,3}\Pi_{g,u}$ (from $1s + 2p$), while in the interaction between $H(1s) + H(3s, 3p, 3d)$ we obtain 24 molecular states (Capitelli et al. 1974) and so on. Most of these states have been inserted in the results of Fig. 5.4, which in particular includes a series of excited states with a total multiplicity of 129 and energy ranging from 91700 to 123488.0 cm⁻¹ (see (Pagano et al. 2008) for details). The potential curves of the most important electronic states of H_2 , H_2^+ and H_2^- are reported in Fig. A.4 adapted from (Sharp 1970).

Note also that other excited states can be constructed from the interaction between $H(2s)$ and $H(ns, np, \dots)$ with $n > 1$. These states are characterized by very large excitation energies and many terms are purely repulsive (Celiberto et al. 1998).

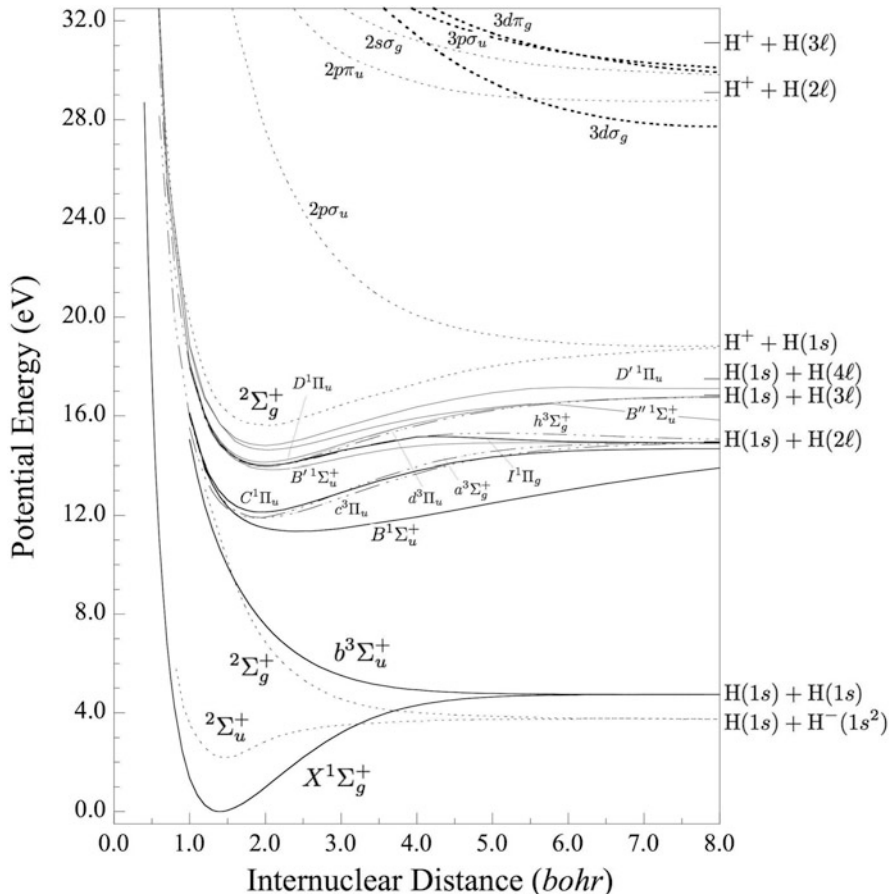


Fig. A.4 Energy diagram for H_2 molecule and its molecular ions

A.4.2 N_2 Molecule

(a) – Molecular states arising from two atoms in the ground state

The ground state of the nitrogen atom is 4S ; therefore, $S = 3/2$ and $L = 0$. Using the combination rules, we have

$$\begin{aligned} \Lambda &= L_1 + L_2 = 0 && \Rightarrow \Sigma \\ S &= S_1 + S_2, \dots |S_1 - S_2| = 3, 2, 1, 0 && \Rightarrow \text{septet, quintet,} \\ &&& \text{triplet and singlet (ground).} \end{aligned}$$

In the interaction, we form four Σ states (${}^1\Sigma$, ${}^3\Sigma$, ${}^5\Sigma$, ${}^7\Sigma$). Considering the interaction of two identical atoms the *gerade/ungerade* symmetry should be

taken into account and being the two atoms in identical quantum states there are restrictions on the number of terms, in particular if S is even $N_g^+ = N_u^- + 1 = L + 1$, while for S odd $N_u^+ = N_g^- + 1 = L + 1$. Therefore, the different molecular wave functions show the following symmetries: ${}^1\Sigma_g^+$, ${}^3\Sigma_u^+$, ${}^5\Sigma_g^+$, ${}^7\Sigma_u^+$. The increase of spin multiplicity gives more antibonding character to the potential curves. So the singlet state in which all the spins are paired is strongly bounded, while the septet state, in which all spins are unpaired, is the most repulsive state. It should be noted that the triplet state is bounded and represents a metastable state playing an important role in the kinetics of nitrogen plasmas ([Colonna and Capitelli 2001a](#)).

(b) – Molecular states arising from one atom in the ground state and one atom in the excited 2D state

The excited 2D state of the nitrogen atom is characterized by $L_1 = 2$ and $S_1 = 1/2$, and the interaction with the 4S ground state, $L_2 = 0$ and $S_2 = 3/2$, leads to

$$\begin{aligned} \Lambda &= L_1 + L_2, \dots, |L_1 - L_2| = 2, 1, 0 &\Rightarrow \Delta, \Pi \text{ and } \Sigma \\ S &= S_1 + S_2, \dots, |S_1 - S_2| = 2, 1 &\Rightarrow \text{quintet and triplet} \end{aligned}$$

Therefore, we obtain the following states: ${}^3\Sigma$, ${}^3\Pi$, ${}^3\Delta$, ${}^5\Sigma$, ${}^5\Pi$, ${}^5\Delta$. In this case considering an homonuclear diatomic system, i.e. identical atoms, states with *gerade/ungerade* parity arise and, being the atoms in different quantum states, all the states exist. Therefore in the interaction ${}^4S + {}^2D$ 12 states arise: ${}^3\Sigma_{g,u}$, ${}^3\Pi_{g,u}$, ${}^3\Delta_{g,u}$, ${}^5\Sigma_{g,u}$, ${}^5\Pi_{g,u}$, ${}^5\Delta_{g,u}$. It can be demonstrated ([Landau and Lifshitz 1981](#)) that, concerning the parity of Σ states, $(2L_2 + 1)\Sigma^+$ terms and $L_2\Sigma^-$ terms are found when the factor $(-1)^{L_1+L_2}P_1P_2 = 1$ and the opposite is true when the factor is equal to -1 , being P_i the parity of the state of i -th atom. In this case we have ${}^3\Sigma_{g,u}^+$, ${}^3\Pi_{g,u}$, ${}^3\Delta_{g,u}$, ${}^5\Sigma_{g,u}^+$, ${}^5\Pi_{g,u}$, ${}^5\Delta_{g,u}$. Some of them are repulsive and do not enter in the partition function.

(c) – Molecular states arising from one atoms in the ground state and one atom in the excited 2P state

The excited 2P state of the nitrogen atom is characterized by $L_1 = 1$ and $S_1 = 1/2$, and the interaction with the 4S ground state, $L_2 = 0$ and $S_2 = 3/2$, leads to

$$\begin{aligned} \Lambda &= L_1 + L_2, \dots, |L_1 - L_2| = 1, 0 &\Rightarrow \Pi \text{ and } \Sigma \\ S &= S_1 + S_2, \dots, |S_1 - S_2| = 2, 1 &\Rightarrow \text{quintet and triplet.} \end{aligned}$$

The following states arise: ${}^{3,5}\Sigma_{g,u}^-$, ${}^{3,5}\Pi_{g,u}$.

(d) – Molecular states arising from one atom in the 2D state and one atom in the excited 2P state

Let us consider the interaction between N(2D), with $L_1 = 2$ and $S_1 = 1/2$, and N(2P), with $L_2 = 1$ and $S_2 = 1/2$.

$$\begin{aligned} \Lambda &= L_1 + L_2, \dots, |L_1 - L_2| = 3, 2, 1, 0 & \Rightarrow \Phi, \Delta, \Pi \text{ and } \Sigma \\ S &= S_1 + S_2, \dots, |S_1 - S_2| = 1, 0 & \Rightarrow \text{triplet and singlet.} \end{aligned}$$

In this case, the number of terms for each symmetry is higher than 1, in fact following Table A.2 we have 3 states of symmetry ${}^1, {}^3\Sigma_{g,u}$, 3 states of symmetry ${}^1, {}^3\Pi_{g,u}$, 2 states of symmetry ${}^1, {}^3\Delta_{g,u}$ and 1 state of symmetry ${}^1, {}^3\Phi_{g,u}$. Moreover being $(-1)^{L_1+L_2} P_1 P_2 = -1$ two of the three Σ terms are odd (–) and only one is even (+). Therefore, the electronic terms are ${}^1, {}^3\Phi_{g,u}$, $(2){}^1, {}^3\Delta_{g,u}$, $(3){}^1, {}^3\Pi_{g,u}$, $(2){}^1, {}^3\Sigma_{g,u}^-$ and ${}^1, {}^3\Sigma_{g,u}^+$.

(e) – Molecular states arising from two atoms in the 2D state

The excited 2D state of the nitrogen atom, with $L = 2$ and $S = 1/2$,

$$\begin{aligned} \Lambda &= L_1 + L_2, \dots, |L_1 - L_2| = 4, 3, 2, 1, 0 & \Rightarrow \Gamma, \Phi, \Delta, \Pi \text{ and } \Sigma \\ S &= S_1 + S_2, \dots, |S_1 - S_2| = 1, 0 & \Rightarrow \text{triplet and singlet.} \end{aligned}$$

In the interaction, the number of states per symmetry is the following: five states ${}^1, {}^3\Sigma$, four states ${}^1, {}^3\Pi$, three states ${}^1, {}^3\Delta$, two states ${}^1, {}^3\Phi$, and one ${}^1, {}^3\Gamma$. Being the interaction of two identical atoms in the identical quantum state, restrictions occurs on the number of state of gerade/ungerade symmetry, in particular

Λ odd	S even or odd	$N_g = N_u$
Λ even	S even	$N_g = N_u + 1$
Λ even	S odd	$N_u = N_g + 1$
$\Lambda = 0$	S even	$N_g^+ = N_u^- + 1$
$\Lambda = 0$	S odd	$N_u^+ = N_g^- + 1$

i.e., ${}^1\Gamma_g$, ${}^3\Gamma_u$, ${}^1, {}^3\Phi_{g,u}$, $(2){}^1\Delta_g$, ${}^1\Delta_u$, $(2){}^3\Delta_u$, ${}^3\Delta_g$, $(2){}^1, {}^3\Pi_{g,u}$, $(3){}^1\Sigma_g^+$, $(2){}^1\Sigma_u^-$, $(3){}^3\Sigma_u^+$, $(2){}^3\Sigma_u^-$.

(f) – Molecular states arising from two atoms in the 2P state

The excited 2P state of the nitrogen atom, with $S = 1/2$ and $L = 1$,

$$\begin{aligned} \Lambda &= L_1 + L_2, \dots, |L_1 - L_2| = 2, 1, 0 & \Rightarrow \Delta, \Pi \text{ and } \Sigma \\ S &= S_1 + S_2, \dots, |S_1 - S_2| = 1, 0 & \Rightarrow \text{triplet and singlet.} \end{aligned}$$

The electronic terms are: ${}^1\Delta_g$, ${}^3\Delta_u$, ${}^1, {}^3\Pi_{g,u}$, $(2){}^1\Sigma_g^+$, ${}^1\Sigma_u^-$, $(2){}^3\Sigma_u^+$, ${}^3\Sigma_g^-$.

A.4.3 N_2^+ Molecule

(a) – Molecular states arising from $N(^4S)$ and $N^+(^3P)$

The nitrogen ion in the ground state (3P), $L_1 = 1$ and $S_1 = 1$, interacting with the nitrogen atom in the ground state (4S), $L_2 = 0$ and $S_2 = 3/2$, originates

$$\begin{aligned} \Lambda &= L_1 + L_2, \dots, |L_1 - L_2| = 1, 0 && \Rightarrow \Pi \text{ and } \Sigma \\ S &= S_1 + S_2, \dots, |S_1 - S_2| = 5/2, 3/2, 1/2 && \Rightarrow \text{sestet, quartet, and doublet} \end{aligned}$$

and considering the *gerade/ungerade* symmetry, being the atoms different, and the $+/-$ parity ($((-1)^{L_1+L_2} P_1 P_2 = 1)$ we have ${}^{2,4,6}\Sigma_{g,u}^+$, ${}^{2,4,6}\Pi_{g,u}$.

Appendix B

Tables of Partition Function of Atmospheric Species

In this appendix, we report tables of internal partition functions of species considered in the planetary atmospheres (Chap. 10).

For molecules, negative atomic ions and some positive atomic ions, as H^+ , He^{+2} and C^{+4} , internal partitions functions are independent of the pressure (see Tables B.1–B.7). For other species, self-consistent partition functions are reported with cutoff depending on the neutral or electron density as discussed in Chap. 8. For other species self-consistent partition functions in the relevant atmospheres are reported as a function of temperature for different pressures (see Tables B.8–B.39).

It should be noted that the atomic species reported in the *air* section are also present in the *Mars* section, because, due to the different composition of the two mixtures, the internal partition functions calculated using the self-consistent cutoff are slightly different.

B.1 Partition Functions Independent of the Pressure

Table B.1 Internal partition function as a function of temperature

T (K)	C_2	C_2^+	C_2^-	CN	CN^+
100	19.4	84.2	40.3	74.2	269.9
200	41.8	167.8	80.3	147.8	537.9
300	78.5	251.9	120.4	221.4	806.7
400	134.7	337.9	160.7	295.2	1,079.4
500	209.2	427.9	201.8	369.7	1,361.8
600	299.8	523.5	244.3	445.7	1,659.7
700	405.2	625.9	288.7	524.1	1,977.3
800	524.4	735.7	335.3	605.5	2,317.7
900	657.0	853.4	384.6	690.4	2,682.9

(continued)

Table B.1 (continued)

T (K)	C_2	C_2^+	C_2^-	CN	CN^+
1,000	802.8	979.1	436.6	779.3	3,074.4
1,500	1,730.0	1,734.2	742.5	1,292.6	5,455.3
2,000	3,005.5	2,704.2	1,129.2	1,935.4	8,602.9
2,500	4,667.8	3,891.4	1,600.3	2,730.1	12,600.4
3,000	6,763.0	5,297.1	2,158.8	3,707.1	17,538.1
3,500	9,339.3	6,922.1	2,810.0	4,901.5	23,507.7
4,000	12,444.9	8,767.3	3,562.1	6,349.6	30,599.4
4,500	16,128.1	10,833.4	4,427.6	8,086.6	38,900.9
5,000	20,437.5	13,121.2	5,421.9	10,145.4	48,496.2
6,000	31,133.9	18,363.4	7,867.5	15,351.4	71,881.8
7,000	44,939.3	24,491.1	11,037.4	22,199.3	101,310.0
8,000	62,262.3	31,486.8	15,046.9	30,909.5	137,169.0
9,000	83,490.3	39,313.9	19,975.3	41,704.8	179,640.0
10,000	108,959.0	47,916.3	25,865.6	54,818.1	228,677.0
11,000	138,926.0	57,221.7	32,729.4	70,493.5	284,036.0
12,000	173,560.0	67,147.4	40,553.3	88,980.2	345,316.0
13,000	212,931.0	77,605.5	49,303.7	110,522.0	412,003.0
14,000	257,023.0	88,507.5	58,932.7	135,347.0	483,518.0
15,000	305,741.0	99,768.3	69,381.9	163,654.0	559,257.0
16,000	358,924.0	111,308.0	80,586.2	195,606.0	638,612.0
17,000	416,363.0	123,053.0	92,476.5	231,323.0	720,998.0
18,000	477,812.0	134,937.0	104,983.0	270,881.0	805,864.0
19,000	542,999.0	146,904.0	118,035.0	314,312.0	892,701.0
20,000	611,639.0	158,901.0	131,564.0	361,606.0	981,045.0
22,000	758,109.0	182,821.0	159,801.0	467,549.0	1,160,630.0
24,000	914,914.0	206,418.0	189,215.0	587,944.0	1,341,830.0
26,000	1,079,880.0	229,499.0	219,398.0	721,641.0	1,522,480.0
28,000	1,251,030.0	251,931.0	250,006.0	867,258.0	1,700,990.0
30,000	1,426,640.0	273,631.0	280,759.0	1,023,300.0	1,876,200.0
35,000	1,875,870.0	324,428.0	356,908.0	1,449,250.0	2,294,990.0
40,000	2,326,520.0	370,250.0	430,302.0	1,909,420.0	2,681,970.0
45,000	2,767,530.0	411,383.0	499,756.0	2,386,370.0	3,035,950.0
50,000	3,192,450.0	448,284.0	564,792.0	2,867,250.0	3,358,320.0

Table B.2 Internal partition function as a function of temperature

<i>T</i> (K)	<i>CN</i> ⁻	<i>CO</i>	<i>CO</i> ⁺	<i>CO</i> ₂	<i>CO</i> ₂ ⁺
100	36.5	36.5	71.3	88.9	403.6
200	72.7	72.7	142.0	180.7	1,022.0
300	108.9	108.9	212.8	290.0	1,966.0
400	145.1	145.1	283.6	432.7	3,374.5
500	181.7	181.7	355.0	621.9	5,423.3
600	218.8	218.8	427.4	870.8	8,331.7
700	257.0	257.0	501.7	1,194.3	12,366.4
800	296.4	296.4	578.4	1,609.3	17,844.9
900	337.5	337.5	658.1	2,135.3	25,139.7
1,000	380.3	380.3	741.1	2,794.3	34,683.4
1,500	625.6	625.6	1,215.8	9,057.6	136,041.0
2,000	928.3	928.3	1,800.2	23,748.9	400,984.0
2,500	1,291.7	1,291.7	2,501.0	53,594.1	978,579.0
3,000	1,717.3	1,717.3	3,322.2	108,246.0	2,089,820.0
3,500	2,206.4	2,206.4	4,267.7	200,822.0	4,041,990.0
4,000	2,760.2	2,760.2	5,343.7	348,462.0	7,242,990.0
4,500	3,379.8	3,379.8	6,559.0	572,935.0	12,215,900.0
5,000	4,066.2	4,066.2	7,925.9	901,355.0	19,613,200.0
6,000	5,644.2	5,644.7	11,180.2	2,010,980.0	45,025,600.0
7,000	7,503.8	7,508.3	15,266.1	4,042,960.0	91,818,700.0
8,000	9,655.5	9,677.9	20,378.5	7,538,410.0	171,203,000.0
9,000	12,110.6	12,192.9	26,732.5	13,289,000.0	297,463,000.0
10,000	14,881.4	15,122.0	34,548.8	22,428,500.0	487,950,000.0
11,000	17,980.5	18,573.5	44,037.7	36,529,500.0	762,868,000.0
12,000	21,420.7	22,700.7	55,386.3	57,695,300.0	1,144,870,000.0
13,000	25,213.7	27,701.0	68,747.5	88,632,800.0	1,658,500,000.0
14,000	29,370.0	33,810.0	84,233.8	132,700,000.0	2,329,600,000.0
15,000	33,897.5	41,291.0	101,915.0	193,921,000.0	3,184,620,000.0
16,000	38,801.5	50,422.5	121,821.0	276,974,000.0	4,249,980,000.0
17,000	44,084.1	61,486.4	143,941.0	387,151,000.0	5,551,490,000.0
18,000	49,744.1	74,756.7	168,233.0	530,289,000.0	7,113,780,000.0
19,000	55,777.4	90,490.2	194,628.0	712,691,000.0	8,959,920,000.0
20,000	62,176.7	108,920.0	223,033.0	941,037,000.0	11,111,000,000.0
22,000	76,031.0	154,658.0	285,432.0	1,563,550,000.0	16,401,400,000.0
24,000	91,202.0	213,232.0	354,450.0	2,455,030,000.0	23,107,400,000.0
26,000	107,559.0	285,412.0	429,037.0	3,672,620,000.0	31,312,000,000.0
28,000	124,959.0	371,519.0	508,158.0	5,270,860,000.0	41,060,200,000.0
30,000	143,253.0	471,506.0	590,843.0	7,299,850,000.0	52,363,000,000.0
35,000	191,954.0	779,484.0	807,644.0	14,530,900,000.0	87,241,400,000.0
40,000	243,299.0	1,161,730.0	1,030,590.0	25,217,400,000.0	130,814,000,000.0
45,000	295,677.0	1,605,250.0	1,252,370.0	39,601,000,000.0	181,761,000,000.0
50,000	347,918.0	2,096,840.0	1,468,410.0	57,697,300,000.0	238,617,000,000.0

Table B.3 Internal partition function as a function of temperature

<i>T</i> (K)	<i>CO</i> ₂ ⁻	<i>C</i> ₂ <i>O</i>	<i>N</i> ₂	<i>N</i> ₂ ⁺	<i>N</i> ₂ ⁻
100	506.7	515.7	17.6	36.5	83.2
200	1,436.5	1,168.2	35.1	72.7	,165.7
300	2,691.8	2,188.9	52.6	108.9	,248.3
400	4,328.1	3,752.3	70.1	145.1	,331.2
500	6,452.3	6,052.5	87.7	181.7	,415.1
600	9,197.3	9,325.7	105.5	218.8	,501.0
700	12,714.7	13,858.6	123.6	256.8	,589.9
800	17,173.6	19,994.0	142.3	296.1	,682.6
900	22,760.6	28,137.4	161.6	337.0	,779.6
1000	29,681.6	38,764.4	181.6	379.5	,881.5
1500	92,946.6	151,657.0	294.9	623.3	1,472.3
2000	232,951.0	452,222.0	433.1	926.5	2,209.4
2500	502,149.0	1,129,800.0	597.9	1,300.5	3,099.4
3000	971,748.0	2,489,200.0	790.0	1,760.2	4,145.6
3500	1,735,150.0	4,990,270.0	1,010.1	2,322.6	5,350.9
4000	2,911,330.0	9,290,960.0	1,258.6	3,005.2	6,717.8
4500	4,647,740.0	16,289,300.0	1,535.9	3,825.1	8,248.9
5000	7,122,000.0	27,158,900.0	1,842.5	4,798.9	9,946.8
6000	15,147,200.0	66,716,300.0	2,545.6	7,271.3	13,853.4
7000	28,996,500.0	143,419,000.0	3,372.4	10,547.6	18,459.9
8000	51,058,600.0	277,136,000.0	4,330.3	14,753.8	23,789.1
9000	83,959,900.0	490,902,000.0	5,432.2	20,018.5	29,863.5
10000	130,402,000.0	809,212,000.0	6,700.6	26,471.2	36,702.2
11000	193,006,000.0	1,256,250,000.0	8,170.8	34,236.0	44,318.8
12000	274,190,000.0	1,854,330,000.0	9,893.0	43,425.2	52,718.8
13000	376,077,000.0	2,622,810,000.0	11,932.4	54,132.2	61,898.5
14000	500,439,000.0	3,577,330,000.0	14,368.2	66,426.9	71,844.8
15000	648,679,000.0	4,729,550,000.0	17,290.2	80,353.2	82,535.6
16000	821,828,000.0	6,087,160,000.0	20,795.2	95,928.7	93,941.1
17000	1,020,570,000.0	7,654,090,000.0	24,983.0	113,146.0	106,025.0
18000	1,245,250,000.0	9,430,900,000.0	29,952.5	131,976.0	118,748.0
19000	1,495,960,000.0	11,415,200,000.0	35,798.2	152,370.0	132,065.0
20000	1,772,520,000.0	13,602,300,000.0	42,607.4	174,265.0	145,931.0
22000	2,401,460,000.0	18,556,000,000.0	59,417.9	222,241.0	175,130.0
24000	3,127,150,000.0	24,221,600,000.0	80,876.4	275,211.0	205,992.0
26000	3,942,870,000.0	30,515,500,000.0	107,290.0	332,421.0	238,187.0
28000	4,840,950,000.0	37,349,100,000.0	138,790.0	393,117.0	271,427.0
30000	5,813,280,000.0	44,635,100,000.0	175,354.0	456,588.0	305,458.0
35000	8,516,540,000.0	64,303,800,000.0	287,738.0	623,307.0	392,681.0
40000	11,517,600,000.0	85,209,100,000.0	426,328.0	795,278.0	481,109.0
45000	14,719,600,000.0	106,552,000,000.0	585,469.0	966,882.0	569,161.0
50000	18,046,800,000.0	127,785,000,000.0	759,530.0	1,134,550.0	655,843.0

Table B.4 Internal partition function as a function of temperature

<i>T</i> (K)	<i>N₂O</i>	<i>N₂O⁺</i>	<i>NO₂</i>	<i>NO</i>	<i>NO⁺</i>
100	166.3	389.8	861.9	168.5	35.3
200	341.9	1009.1	2446.7	335.6	70.3
300	563.9	1965.4	4609.0	502.9	105.3
400	866.5	3408.2	7469.7	670.8	140.3
500	1279.2	5518.6	11236.0	841.0	175.5
600	1833.7	8519.4	16161.2	1015.8	211.1
700	2566.9	12680.8	22533.7	1197.1	247.4
800	3521.4	18324.3	30676.2	1386.8	284.7
900	4746.1	25827.5	40946.7	1586.0	323.3
1000	6297.2	35628.0	53741.2	1795.6	363.3
1500	21450.5	139193.0	172308.0	3016.3	589.5
2000	57938.4	408191.0	438169.0	4546.1	865.1
2500	132975.0	989336.0	953588.0	6398.4	1193.9
3000	269926.0	2087540.0	1858040.0	8580.8	1577.3
3500	497077.0	3956690.0	3336340.0	11099.8	2016.6
4000	845383.0	6879780.0	5628370.0	13961.8	2512.7
4500	1345940.0	11144400.0	9039470.0	17173.4	3066.7
5000	2027870.0	17019800.0	13950700.0	20742.1	3679.5
6000	4036200.0	34488300.0	30232100.0	28988.3	5085.7
7000	7040820.0	60562400.0	59362700.0	38800.9	6741.1
8000	11186600.0	95725500.0	107886000.0	50330.7	8660.9
9000	16629800.0	139802000.0	184018000.0	63781.4	10871.9
10000	23561200.0	192163000.0	297492000.0	79395.7	13420.2
11000	32206900.0	251921000.0	459265000.0	97432.6	16378.0
12000	42814300.0	318074000.0	681110000.0	118143.0	19846.7
13000	55630600.0	389604000.0	975169000.0	141748.0	23955.6
14000	70883200.0	465541000.0	1353510000.0	168428.0	28857.4
15000	88765300.0	544992000.0	1827750000.0	198307.0	34720.3
16000	109427000.0	627158000.0	2408710000.0	231460.0	41719.2
17000	132970000.0	711337000.0	3106170000.0	267905.0	50027.6
18000	159453000.0	796919000.0	3928740000.0	307614.0	59809.7
19000	188888000.0	883384000.0	4883710000.0	350518.0	71214.7
20000	221254000.0	970288000.0	5977070000.0	396510.0	84372.4
22000	294528000.0	1143980000.0	8596430000.0	497205.0	116355.0
24000	378550000.0	1315680000.0	11809600000.0	608415.0	156345.0
26000	472339000.0	1483820000.0	15622300000.0	728686.0	204579.0
28000	574789000.0	1647380000.0	20025900000.0	856525.0	260988.0
30000	684761000.0	1805690000.0	25001400000.0	990496.0	325270.0
35000	985446000.0	2176650000.0	39754100000.0	1343790.0	517034.0
40000	1310990000.0	2511750000.0	57378000000.0	1710180.0	745158.0
45000	1649450000.0	2813070000.0	77304000000.0	2077580.0	999324.0
50000	1992130000.0	3083860000.0	99000100000.0	2438070.0	1270330.0

Table B.5 Internal partition function as a function of temperature

T (K)	N_3	C_3	O_2	O_2^+	O_2^-	O_3
100	219.0	180.2	73.4	83.4	121.5	649.8
200	520.3	798.6	146.4	166.1	242.6	1,849.7
300	878.2	2,035.8	219.6	248.9	365.8	3,536.3
400	1,332.7	4,037.9	293.7	332.1	495.4	5,900.8
500	1,925.8	6,972.8	369.9	416.5	635.5	9,217.9
600	2,700.6	11,044.5	449.8	503.2	788.6	13,806.1
700	3,704.8	16,493.6	534.2	593.3	956.0	20,028.8
800	4,992.8	23,594.9	623.9	687.5	1,138.6	28,300.3
900	6,626.0	32,656.5	719.4	786.5	1,337.0	39,090.5
1,000	8,674.0	44,017.7	820.9	890.8	1,551.4	52,929.1
1,500	28,221.0	149,384.0	1,426.6	1,499.2	2,872.2	190,983.0
2,000	74,308.0	381,187.0	2,207.2	2,264.1	4,622.2	526,364.0
2,500	168,295.0	818,489.0	3,179.2	3,193.0	6,819.4	1,238,070.0
3,000	340,902.0	1,566,530.0	4,362.5	4,291.2	9,482.5	2,675,800.0
3,500	633,930.0	2,768,050.0	5,779.1	5,563.0	12,633.0	5,506,510.0
4,000	1,101,980.0	4,621,180.0	7,452.3	7,013.3	16,295.7	10,836,500.0
4,500	1,814,090.0	7,402,970.0	9,405.7	8,647.5	20,499.8	20,243,300.0
5,000	2,855,290.0	11,497,700.0	11,663.6	10,472.4	25,277.0	35,707,800.0
6,000	6,351,960.0	25,892,500.0	17,194.2	14,732.6	36,674.1	93,931,100.0
7,000	12,628,900.0	54,286,400.0	24,249.0	19,901.3	50,681.7	204,051,000.0
8,000	23,012,100.0	107,075,000.0	33,019.3	26,139.0	67,365.5	382,505,000.0
9,000	39,087,700.0	199,666,000.0	43,654.5	33,648.5	86,643.2	641,412,000.0

10,000	62,645,100.0	353,459,000.0	56,242.5	42,650.8	108,310.0	988,037,000.0
11,000	95,603,500.0	596,628,000.0	70,804.9	53,358.5	132,080.0	1,425,220,000.0
12,000	139,932,000.0	964,670,000.0	87,303.6	65,954.3	157,630.0	1,952,240,000.0
13,000	197,572,000.0	1,500,680,000.0	105,653.0	80,578.1	184,630.0	2,565,730,000.0
14,000	270,372,000.0	2,255,340,000.0	125,733.0	97,320.8	212,761.0	3,260,510,000.0
15,000	360,034,000.0	3,286,590,000.0	147,403.0	116,225.0	241,734.0	4,030,260,000.0
16,000	468,072,000.0	4,659,120,000.0	170,511.0	137,291.0	271,289.0	4,868,080,000.0
17,000	595,788,000.0	6,443,490,000.0	194,902.0	160,478.0	301,203.0	5,766,840,000.0
18,000	744,257,000.0	8,715,230,000.0	220,422.0	185,717.0	331,282.0	6,719,450,000.0
19,000	914,323,000.0	11,553,700,000.0	246,924.0	212,914.0	361,365.0	7,719,080,000.0
20,000	1,106,610,000.0	15,040,800,000.0	274,269.0	241,957.0	391,319.0	8,759,260,000.0
22,000	1,559,250,000.0	24,295,000,000.0	330,983.0	305,081.0	450,420.0	10,937,500,000.0
24,000	2,103,130,000.0	37,141,500,000.0	389,654.0	374,034.0	507,938.0	13,211,400,000.0
26,000	2,736,580,000.0	54,214,700,000.0	449,531.0	447,748.0	563,471.0	15,545,600,000.0
28,000	3,455,920,000.0	76,091,400,000.0	510,008.0	525,213.0	616,795.0	17,911,400,000.0
30,000	4,256,040,000.0	103,272,000,000.0	570,600.0	605,510.0	667,801.0	20,286,200,000.0
35,000	6,568,700,000.0	196,892,000,000.0	720,293.0	813,593.0	785,151.0	26,154,800,000.0
40,000	9,243,160,000.0	329,859,000,000.0	864,612.0	1,024,820.0	888,765.0	31,796,600,000.0
45,000	12,177,400,000.0	502,778,000,000.0	1,001,620.0	1,232,930.0	980,153.0	37,125,100,000.0
50,000	15,282,600,000.0	713,774,000,000.0	1,130,530.0	1,434,160.0	1,060,940.0	42,108,400,000.0

Table B.6 Internal partition function as a function of temperature

T (K)	O_3^-	C_2N	CNO	H_2	H_2^+	H_3^+
100	650.0	263.8	449.0	2.3	5.1	0.6
200	1876.9	691.4	1123.2	2.5	7.0	1.5
300	3720.6	1411.2	2062.6	3.0	9.3	2.7
400	6483.7	2559.7	3396.9	3.5	11.7	4.0
500	10555.4	4308.1	5267.5	4.0	14.1	5.5
600	16392.6	6874.9	7840.0	4.6	16.7	7.1
700	24526.4	10529.7	11311.4	5.2	19.3	8.8
800	35569.9	15597.9	15912.9	5.8	22.0	10.7
900	50224.0	22465.0	21913.0	6.4	24.8	12.8
1000	69282.4	31581.9	29620.4	7.0	27.9	14.9
1500	265417.0	131936.0	107743.0	10.2	45.6	28.1
2000	750528.0	402924.0	302976.0	13.9	68.5	45.8
2500	1746700.0	1005810.0	716363.0	18.1	97.7	69.4
3000	3546140.0	2181850.0	1495660.0	22.9	134.3	100.9
3500	6503050.0	4268600.0	2844340.0	28.5	178.9	142.4
4000	11024400.0	7716250.0	5030530.0	34.9	231.8	197.0
4500	17565500.0	13104000.0	8395630.0	42.0	292.6	268.6
5000	26630000.0	21157000.0	13362200.0	50.2	360.7	362.1
6000	54598400.0	48987800.0	30230900.0	69.3	514.2	639.9
7000	99933900.0	100564000.0	60823500.0	92.7	684.0	1097.2
8000	168161000.0	188625000.0	11175000.0	120.3	862.4	1829.0
9000	264840000.0	329722000.0	191076000.0	151.9	1043.7	2961.7

10000	395048000.0	544469000.0	307699000.0	187.2	1223.7	4649.2
11000	562980000.0	857597000.0	471354000.0	225.7	1400.0	7063.5
12000	771731000.0	1297760000.0	692060000.0	267.0	1571.1	10381.5
13000	1023250000.0	1897150000.0	979789000.0	310.5	1736.6	14772.3
14000	1318400000.0	2690910000.0	1344130000.0	356.1	1896.9	20386.0
15000	1657090000.0	3716430000.0	1794030000.0	403.6	2053.1	27346.8
16000	2038460000.0	5012570000.0	2337530000.0	453.2	2206.9	35748.5
17000	2461030000.0	6618890000.0	2981700000.0	505.3	2360.3	45654.0
18000	2922860000.0	8574810000.0	3732460000.0	560.5	2515.6	57096.3
19000	3421680000.0	10918900000.0	4594590000.0	619.7	2675.5	70081.6
20000	3955020000.0	13688200000.0	5571690000.0	684.0	2842.6	84592.6
22000	5114870000.0	20640200000.0	7879780000.0	833.2	3208.5	118028.0
24000	6381510000.0	29678400000.0	10664500000.0	1019.9	3632.9	156940.0
26000	7734860000.0	41001300000.0	13919500000.0	1257.3	4131.7	200718.0
28000	9156490000.0	54753500000.0	17627200000.0	1558.0	4717.2	248690.0
30000	10630000000.0	71026700000.0	21762000000.0	1933.8	5397.4	300177.0
35000	14452100000.0	122907000000.0	33755100000.0	3262.1	7532.0	440139.0
40000	18343800000.0	190266000000.0	47668900000.0	5213.6	10265.3	589554.0
45000	22195100000.0	271594000000.0	62960700000.0	7808.0	13517.2	742174.0
50000	25939200000.0	364836000000.0	79155100000.0	11008.1	17181.2	893800.0

Table B.7 Internal partition function as a function of temperature

T (K)	N^-	O^-	C^-	H^-	H^+	He^{+2}	C^{+4}
100	6.5	4.2	4.000	1	1	1	1
200	7.4	4.6	4.000	1	1	1	1
300	7.9	4.9	4.000	1	1	1	1
400	8.1	5.1	4.000	1	1	1	1
500	8.3	5.2	4.000	1	1	1	1
600	8.4	5.3	4.000	1	1	1	1
700	8.5	5.4	4.000	1	1	1	1
800	8.5	5.5	4.000	1	1	1	1
900	8.6	5.5	4.000	1	1	1	1
1,000	8.6	5.6	4.000	1	1	1	1
1,500	8.7	5.7	4.001	1	1	1	1
2,000	8.8	5.8	4.008	1	1	1	1
2,500	8.9	5.8	4.033	1	1	1	1
3,000	8.9	5.8	4.086	1	1	1	1
3,500	8.9	5.9	4.169	1	1	1	1
4,000	9.0	5.9	4.282	1	1	1	1
4,500	9.1	5.9	4.419	1	1	1	1
5,000	9.1	6.0	4.576	1	1	1	1
6,000	9.3	6.0	4.927	1	1	1	1
7,000	9.5	6.1	5.302	1	1	1	1
8,000	9.7	6.3	5.680	1	1	1	1
9,000	9.9	6.4	6.048	1	1	1	1
10,000	10.1	6.5	6.400	1	1	1	1
11,000	10.2	6.7	6.732	1	1	1	1
12,000	10.4	6.8	7.044	1	1	1	1
13,000	10.6	7.0	7.336	1	1	1	1
14,000	10.7	7.1	7.608	1	1	1	1
15,000	10.9	7.2	7.862	1	1	1	1
16,000	11.0	7.4	8.098	1	1	1	1
17,000	11.1	7.5	8.319	1	1	1	1
18,000	11.3	7.6	8.525	1	1	1	1
19,000	11.4	7.7	8.718	1	1	1	1
20,000	11.5	7.9	8.899	1	1	1	1
22,000	11.7	8.1	9.227	1	1	1	1
24,000	11.9	8.3	9.517	1	1	1	1
26,000	12.0	8.4	9.776	1	1	1	1
28,000	12.2	8.6	10.007	1	1	1	1
30,000	12.3	8.8	10.214	1	1	1	1
35,000	12.6	9.1	10.651	1	1	1	1
40,000	12.8	9.3	10.999	1	1	1	1
45,000	13.0	9.6	11.282	1	1	1	1
50,000	13.2	9.8	11.517	1	1	1	1

B.2 Selfconsistent Partition Functions of Atomic Species in Air Atmosphere

Table B.8 Internal partition function of N as a function of pressure and temperature

T (K)	P (bar)				
	10^{-2}	10^{-1}	1	10^1	10^2
100	4.000	4.000	4.000	4.000	4.000
200	4.000	4.000	4.000	4.000	4.000
300	4.000	4.000	4.000	4.000	4.000
400	4.000	4.000	4.000	4.000	4.000
500	4.000	4.000	4.000	4.000	4.000
600	4.000	4.000	4.000	4.000	4.000
700	4.000	4.000	4.000	4.000	4.000
800	4.000	4.000	4.000	4.000	4.000
900	4.000	4.000	4.000	4.000	4.000
1000	4.000	4.000	4.000	4.000	4.000
1500	4.000	4.000	4.000	4.000	4.000
2000	4.000	4.000	4.000	4.000	4.000
2500	4.000	4.000	4.000	4.000	4.000
3000	4.001	4.001	4.001	4.001	4.001
3500	4.004	4.004	4.004	4.004	4.004
4000	4.010	4.010	4.010	4.010	4.010
4500	4.022	4.022	4.022	4.022	4.022
5000	4.041	4.041	4.041	4.041	4.041
6000	4.105	4.105	4.105	4.105	4.105
7000	4.208	4.208	4.208	4.208	4.208
8000	4.349	4.348	4.348	4.348	4.348
9000	4.524	4.523	4.522	4.522	4.522
10000	4.734	4.727	4.725	4.724	4.724
11000	4.990	4.961	4.952	4.949	4.948
12000	5.339	5.226	5.202	5.194	5.190
13000	5.886	5.538	5.474	5.454	5.448
14000	6.933	5.945	5.770	5.734	5.715
15000	8.969	6.531	6.117	6.022	5.996
16000	13.421	7.496	6.535	6.342	6.292
17000	20.994	9.189	7.055	6.698	6.583
18000	31.899	11.416	7.720	7.075	6.892
19000	51.586	15.737	8.649	7.522	7.224
20000	76.701	20.827	10.243	8.098	7.579
22000	157.071	40.912	14.091	9.476	8.366
24000	290.849	70.806	22.766	11.361	9.290
26000	533.113	115.802	33.449	14.015	10.400
28000	908.347	178.946	48.161	18.253	11.690
30000	1456.560	262.752	67.473	25.647	13.217
35000	3482.800	734.684	138.765	45.545	20.230
40000	6818.060	1330.920	295.223	73.924	30.919
45000	12485.900	2382.080	464.643	111.993	42.185
50000	19402.700	3873.690	693.668	157.473	56.773

Table B.9 Internal partition function of N^+ as a function of pressure and temperature

T (K)	P (bar)				
	10^{-2}	10^{-1}	1	10^1	10^2
100	3.250	3.250	3.250	3.250	3.250
200	5.065	5.065	5.065	5.065	5.065
300	6.045	6.045	6.045	6.045	6.045
400	6.641	6.641	6.641	6.641	6.641
500	7.039	7.039	7.039	7.039	7.039
600	7.323	7.323	7.323	7.323	7.323
700	7.536	7.536	7.536	7.536	7.536
800	7.700	7.700	7.700	7.700	7.700
900	7.832	7.832	7.832	7.832	7.832
1,000	7.939	7.939	7.939	7.939	7.939
1,500	8.274	8.274	8.274	8.274	8.274
2,000	8.448	8.448	8.448	8.448	8.448
2,500	8.555	8.555	8.555	8.555	8.555
3,000	8.630	8.630	8.630	8.630	8.630
3,500	8.688	8.688	8.688	8.688	8.688
4,000	8.738	8.738	8.738	8.738	8.738
4,500	8.786	8.786	8.786	8.786	8.786
5,000	8.835	8.835	8.835	8.835	8.835
6,000	8.938	8.938	8.938	8.938	8.938
7,000	9.054	9.054	9.054	9.054	9.054
8,000	9.180	9.180	9.180	9.180	9.180
9,000	9.314	9.314	9.314	9.314	9.314
10,000	9.453	9.453	9.453	9.453	9.453
11,000	9.596	9.596	9.596	9.596	9.596
12,000	9.740	9.740	9.740	9.740	9.740
13,000	9.886	9.886	9.886	9.886	9.886
14,000	10.031	10.031	10.031	10.031	10.031
15,000	10.177	10.177	10.177	10.177	10.177
16,000	10.322	10.321	10.321	10.321	10.321
17,000	10.467	10.466	10.466	10.466	10.466
18,000	10.613	10.610	10.610	10.610	10.610
19,000	10.763	10.755	10.753	10.753	10.753
20,000	10.923	10.901	10.897	10.896	10.896
22,000	11.304	11.207	11.187	11.183	11.182
24,000	11.917	11.559	11.492	11.475	11.472
26,000	13.176	12.029	11.826	11.778	11.766
28,000	16.075	12.742	12.222	12.102	12.071
30,000	22.390	14.048	12.731	12.459	12.391
35,000	69.675	23.333	15.019	13.638	13.342
40,000	225.137	51.463	21.169	15.674	14.601
45,000	640.863	111.804	35.915	19.772	16.371
50,000	1,478.330	258.378	60.511	26.071	18.844

Table B.10 Internal partition function of N^{+2} as a function of pressure and temperature

T (K)	<i>P</i> (bar)				
	10^{-2}	10^{-1}	1	10^1	10^2
100	2.325	2.325	2.325	2.325	2.325
200	3.141	3.141	3.141	3.141	3.141
300	3.733	3.733	3.733	3.733	3.733
400	4.136	4.136	4.136	4.136	4.136
500	4.422	4.422	4.422	4.422	4.422
600	4.633	4.633	4.633	4.633	4.633
700	4.795	4.795	4.795	4.795	4.795
800	4.923	4.923	4.923	4.923	4.923
900	5.027	5.027	5.027	5.027	5.027
1000	5.112	5.112	5.112	5.112	5.112
1500	5.384	5.384	5.384	5.384	5.384
2000	5.528	5.528	5.528	5.528	5.528
2500	5.618	5.618	5.618	5.618	5.618
3000	5.679	5.679	5.679	5.679	5.679
3500	5.723	5.723	5.723	5.723	5.723
4000	5.757	5.757	5.757	5.757	5.757
4500	5.783	5.783	5.783	5.783	5.783
5000	5.804	5.804	5.804	5.804	5.804
6000	5.836	5.836	5.836	5.836	5.836
7000	5.859	5.859	5.859	5.859	5.859
8000	5.877	5.877	5.877	5.877	5.877
9000	5.891	5.891	5.891	5.891	5.891
10000	5.904	5.904	5.904	5.904	5.904
11000	5.917	5.917	5.917	5.917	5.917
12000	5.930	5.930	5.930	5.930	5.930
13000	5.945	5.945	5.945	5.945	5.945
14000	5.963	5.963	5.963	5.963	5.963
15000	5.984	5.984	5.984	5.984	5.984
16000	6.008	6.008	6.008	6.008	6.008
17000	6.038	6.038	6.038	6.038	6.038
18000	6.071	6.071	6.071	6.071	6.071
19000	6.109	6.109	6.109	6.109	6.109
20000	6.152	6.152	6.152	6.152	6.152
22000	6.252	6.252	6.252	6.252	6.252
24000	6.371	6.371	6.371	6.371	6.371
26000	6.507	6.507	6.507	6.507	6.507
28000	6.660	6.659	6.659	6.659	6.659
30000	6.830	6.826	6.826	6.825	6.825
35000	7.379	7.308	7.299	7.298	7.298
40000	8.474	7.909	7.849	7.838	7.836
45000	12.158	8.787	8.494	8.442	8.429
50000	23.634	10.443	9.315	9.115	9.076

Table B.11 Internal partition function of N^{+3} as a function of pressure and temperature

T (K)	P (bar)				
	10^{-2}	10^{-1}	1	10^1	10^2
100	1.000	1.000	1.000	1.000	1.000
200	1.000	1.000	1.000	1.000	1.000
300	1.000	1.000	1.000	1.000	1.000
400	1.000	1.000	1.000	1.000	1.000
500	1.000	1.000	1.000	1.000	1.000
600	1.000	1.000	1.000	1.000	1.000
700	1.000	1.000	1.000	1.000	1.000
800	1.000	1.000	1.000	1.000	1.000
900	1.000	1.000	1.000	1.000	1.000
1,000	1.000	1.000	1.000	1.000	1.000
1,500	1.000	1.000	1.000	1.000	1.000
2,000	1.000	1.000	1.000	1.000	1.000
2,500	1.000	1.000	1.000	1.000	1.000
3,000	1.000	1.000	1.000	1.000	1.000
3,500	1.000	1.000	1.000	1.000	1.000
4,000	1.000	1.000	1.000	1.000	1.000
4,500	1.000	1.000	1.000	1.000	1.000
5,000	1.000	1.000	1.000	1.000	1.000
6,000	1.000	1.000	1.000	1.000	1.000
7,000	1.000	1.000	1.000	1.000	1.000
8,000	1.000	1.000	1.000	1.000	1.000
9,000	1.000	1.000	1.000	1.000	1.000
10,000	1.001	1.001	1.001	1.001	1.001
11,000	1.001	1.001	1.001	1.001	1.001
12,000	1.003	1.003	1.003	1.003	1.003
13,000	1.005	1.005	1.005	1.005	1.005
14,000	1.009	1.009	1.009	1.009	1.009
15,000	1.014	1.014	1.014	1.014	1.014
16,000	1.021	1.021	1.021	1.021	1.021
17,000	1.030	1.030	1.030	1.030	1.030
18,000	1.041	1.041	1.041	1.041	1.041
19,000	1.055	1.055	1.055	1.055	1.055
20,000	1.071	1.071	1.071	1.071	1.071
22,000	1.111	1.111	1.111	1.111	1.111
24,000	1.160	1.160	1.160	1.160	1.160
26,000	1.219	1.219	1.219	1.219	1.219
28,000	1.287	1.287	1.287	1.287	1.287
30,000	1.364	1.364	1.364	1.364	1.364
35,000	1.585	1.585	1.585	1.585	1.585
40,000	1.842	1.842	1.842	1.842	1.842
45,000	2.127	2.126	2.125	2.125	2.125
50,000	2.443	2.431	2.428	2.428	2.428

Table B.12 Internal partition function of N^{+4} as a function of pressure and temperature

T (K)	P (bar)				
	10^{-2}	10^{-1}	1	10^1	10^2
100	2.000	2.000	2.000	2.000	2.000
200	2.000	2.000	2.000	2.000	2.000
300	2.000	2.000	2.000	2.000	2.000
400	2.000	2.000	2.000	2.000	2.000
500	2.000	2.000	2.000	2.000	2.000
600	2.000	2.000	2.000	2.000	2.000
700	2.000	2.000	2.000	2.000	2.000
800	2.000	2.000	2.000	2.000	2.000
900	2.000	2.000	2.000	2.000	2.000
1000	2.000	2.000	2.000	2.000	2.000
1500	2.000	2.000	2.000	2.000	2.000
2000	2.000	2.000	2.000	2.000	2.000
2500	2.000	2.000	2.000	2.000	2.000
3000	2.000	2.000	2.000	2.000	2.000
3500	2.000	2.000	2.000	2.000	2.000
4000	2.000	2.000	2.000	2.000	2.000
4500	2.000	2.000	2.000	2.000	2.000
5000	2.000	2.000	2.000	2.000	2.000
6000	2.000	2.000	2.000	2.000	2.000
7000	2.000	2.000	2.000	2.000	2.000
8000	2.000	2.000	2.000	2.000	2.000
9000	2.000	2.000	2.000	2.000	2.000
10000	2.000	2.000	2.000	2.000	2.000
11000	2.000	2.000	2.000	2.000	2.000
12000	2.000	2.000	2.000	2.000	2.000
13000	2.001	2.001	2.001	2.001	2.001
14000	2.002	2.002	2.002	2.002	2.002
15000	2.003	2.003	2.003	2.003	2.003
16000	2.004	2.004	2.004	2.004	2.004
17000	2.007	2.007	2.007	2.007	2.007
18000	2.010	2.010	2.010	2.010	2.010
19000	2.013	2.013	2.013	2.013	2.013
20000	2.018	2.018	2.018	2.018	2.018
22000	2.031	2.031	2.031	2.031	2.031
24000	2.048	2.048	2.048	2.048	2.048
26000	2.069	2.069	2.069	2.069	2.069
28000	2.095	2.095	2.095	2.095	2.095
30000	2.126	2.126	2.126	2.126	2.126
35000	2.218	2.218	2.218	2.218	2.218
40000	2.330	2.330	2.330	2.330	2.330
45000	2.456	2.456	2.456	2.456	2.456
50000	2.590	2.589	2.589	2.589	2.589

Table B.13 Internal partition function of O as a function of pressure and temperature

T (K)	P (bar)				
	10^{-2}	10^{-1}	1	10^1	10^2
100	5.346	5.346	5.346	5.346	5.346
200	6.156	6.156	6.156	6.156	6.156
300	6.741	6.741	6.741	6.741	6.741
400	7.140	7.140	7.140	7.140	7.140
500	7.423	7.423	7.423	7.423	7.423
600	7.633	7.633	7.633	7.633	7.633
700	7.794	7.794	7.794	7.794	7.794
800	7.922	7.922	7.922	7.922	7.922
900	8.025	8.025	8.025	8.025	8.025
1,000	8.110	8.110	8.110	8.110	8.110
1,500	8.382	8.382	8.382	8.382	8.382
2,000	8.527	8.527	8.527	8.527	8.527
2,500	8.617	8.617	8.617	8.617	8.617
3,000	8.680	8.680	8.680	8.680	8.680
3,500	8.729	8.729	8.729	8.729	8.729
4,000	8.772	8.772	8.772	8.772	8.772
4,500	8.813	8.813	8.813	8.813	8.813
5,000	8.855	8.855	8.855	8.855	8.855
6,000	8.947	8.947	8.947	8.947	8.947
7,000	9.051	9.051	9.051	9.051	9.051
8,000	9.166	9.166	9.166	9.166	9.166
9,000	9.292	9.290	9.290	9.290	9.290
10,000	9.431	9.422	9.420	9.419	9.418
11,000	9.600	9.566	9.555	9.552	9.550
12,000	9.847	9.723	9.697	9.689	9.685
13,000	10.268	9.913	9.848	9.828	9.821
14,000	11.127	10.179	10.011	9.975	9.957
15,000	12.813	10.643	10.207	10.121	10.097
16,000	16.469	11.295	10.456	10.289	10.244
17,000	22.474	12.571	10.776	10.479	10.380
18,000	30.786	14.197	11.197	10.678	10.530
19,000	45.510	17.378	11.839	10.926	10.693
20,000	63.599	20.980	12.903	11.263	10.870
22,000	119.269	34.913	15.408	12.084	11.272
24,000	208.037	54.645	21.150	13.208	11.755
26,000	364.340	83.334	27.833	14.731	12.332
28,000	599.187	122.388	36.825	17.664	13.016
30,000	933.420	172.861	48.349	21.854	13.845
35,000	2,113.170	450.162	89.066	33.184	18.615
40,000	3,975.420	780.587	177.202	48.770	23.441
45,000	7,060.660	1,351.720	267.024	68.198	29.256
50,000	10,708.900	2,142.700	393.197	92.912	36.572

Table B.14 Internal partition function of O^+ as a function of pressure and temperature

T (K)	P (bar)				
	10^{-2}	10^{-1}	1	10^1	10^2
100	7.000	7.000	7.000	7.000	7.000
200	7.000	7.000	7.000	7.000	7.000
300	7.000	7.000	7.000	7.000	7.000
400	7.000	7.000	7.000	7.000	7.000
500	7.000	7.000	7.000	7.000	7.000
600	7.000	7.000	7.000	7.000	7.000
700	7.000	7.000	7.000	7.000	7.000
800	7.000	7.000	7.000	7.000	7.000
900	7.000	7.000	7.000	7.000	7.000
1000	7.000	7.000	7.000	7.000	7.000
1500	7.000	7.000	7.000	7.000	7.000
2000	7.000	7.000	7.000	7.000	7.000
2500	7.000	7.000	7.000	7.000	7.000
3000	7.000	7.000	7.000	7.000	7.000
3500	7.000	7.000	7.000	7.000	7.000
4000	7.001	7.001	7.001	7.001	7.001
4500	7.003	7.003	7.003	7.003	7.003
5000	7.008	7.008	7.008	7.008	7.008
6000	7.030	7.030	7.030	7.030	7.030
7000	7.075	7.075	7.075	7.075	7.075
8000	7.152	7.152	7.152	7.152	7.152
9000	7.263	7.263	7.263	7.263	7.263
10000	7.409	7.409	7.409	7.409	7.409
11000	7.590	7.590	7.590	7.590	7.590
12000	7.801	7.801	7.801	7.801	7.801
13000	8.039	8.039	8.039	8.039	8.039
14000	8.300	8.300	8.300	8.300	8.300
15000	8.581	8.581	8.581	8.581	8.581
16000	8.877	8.877	8.877	8.877	8.877
17000	9.186	9.186	9.186	9.186	9.186
18000	9.505	9.505	9.505	9.505	9.505
19000	9.832	9.831	9.831	9.831	9.831
20000	10.164	10.163	10.163	10.163	10.163
22000	10.842	10.835	10.834	10.834	10.834
24000	11.545	11.516	11.509	11.508	11.508
26000	12.322	12.208	12.185	12.180	12.178
28000	13.334	12.934	12.864	12.846	12.841
30000	14.867	13.763	13.556	13.508	13.496
35000	25.683	17.316	15.519	15.188	15.116
40000	66.816	27.004	18.760	17.081	16.777
45000	189.602	50.258	25.666	19.850	18.613
50000	485.379	112.798	38.146	23.834	20.813

Table B.15 Internal partition function of O^{+2} as a function of pressure and temperature

T (K)	P (bar)				
	10^{-2}	10^{-1}	1	10^1	10^2
100	1.650	1.650	1.650	1.650	1.650
200	2.882	2.882	2.882	2.882	2.882
300	3.895	3.895	3.895	3.895	3.895
400	4.659	4.659	4.659	4.659	4.659
500	5.238	5.238	5.238	5.238	5.238
600	5.686	5.686	5.686	5.686	5.686
700	6.042	6.042	6.042	6.042	6.042
800	6.330	6.330	6.330	6.330	6.330
900	6.568	6.568	6.568	6.568	6.568
1,000	6.768	6.768	6.768	6.768	6.768
1,500	7.419	7.419	7.419	7.419	7.419
2,000	7.777	7.777	7.777	7.777	7.777
2,500	8.003	8.003	8.003	8.003	8.003
3,000	8.159	8.159	8.159	8.159	8.159
3,500	8.274	8.274	8.274	8.274	8.274
4,000	8.362	8.362	8.362	8.362	8.362
4,500	8.435	8.435	8.435	8.435	8.435
5,000	8.497	8.497	8.497	8.497	8.497
6,000	8.604	8.604	8.604	8.604	8.604
7,000	8.704	8.704	8.704	8.704	8.704
8,000	8.803	8.803	8.803	8.803	8.803
9,000	8.904	8.904	8.904	8.904	8.904
10,000	9.009	9.009	9.009	9.009	9.009
11,000	9.118	9.118	9.118	9.118	9.118
12,000	9.228	9.228	9.228	9.228	9.228
13,000	9.341	9.341	9.341	9.341	9.341
14,000	9.455	9.455	9.455	9.455	9.455
15,000	9.570	9.570	9.570	9.570	9.570
16,000	9.684	9.684	9.684	9.684	9.684
17,000	9.799	9.799	9.799	9.799	9.799
18,000	9.914	9.914	9.914	9.914	9.914
19,000	10.029	10.029	10.029	10.029	10.029
20,000	10.143	10.143	10.143	10.143	10.143
22,000	10.369	10.369	10.369	10.369	10.369
24,000	10.594	10.594	10.594	10.594	10.594
26,000	10.818	10.818	10.818	10.818	10.818
28,000	11.041	11.041	11.041	11.041	11.041
30,000	11.264	11.263	11.263	11.263	11.263
35,000	11.841	11.827	11.824	11.823	11.823
40,000	12.586	12.435	12.403	12.396	12.394
45,000	14.254	13.225	13.036	12.998	12.987
50,000	19.250	14.728	13.838	13.655	13.616

Table B.16 Internal partition function of O^{+3} as a function of pressure and temperature

T (K)	P (bar)				
	10^{-2}	10^{-1}	1	10^1	10^2
100	3.027	3.027	3.027	3.027	3.027
200	3.436	3.436	3.436	3.436	3.436
300	4.100	4.100	4.100	4.100	4.100
400	4.747	4.747	4.747	4.747	4.747
500	5.306	5.306	5.306	5.306	5.306
600	5.775	5.775	5.775	5.775	5.775
700	6.167	6.167	6.167	6.167	6.167
800	6.497	6.497	6.497	6.497	6.497
900	6.777	6.777	6.777	6.777	6.777
1000	7.018	7.018	7.018	7.018	7.018
1500	7.834	7.834	7.834	7.834	7.834
2000	8.303	8.303	8.303	8.303	8.303
2500	8.606	8.606	8.606	8.606	8.606
3000	8.817	8.817	8.817	8.817	8.817
3500	8.973	8.973	8.973	8.973	8.973
4000	9.093	9.093	9.093	9.093	9.093
4500	9.187	9.187	9.187	9.187	9.187
5000	9.264	9.264	9.264	9.264	9.264
6000	9.381	9.381	9.381	9.381	9.381
7000	9.466	9.466	9.466	9.466	9.466
8000	9.531	9.531	9.531	9.531	9.531
9000	9.581	9.581	9.581	9.581	9.581
10000	9.623	9.623	9.623	9.623	9.623
11000	9.657	9.657	9.657	9.657	9.657
12000	9.687	9.687	9.687	9.687	9.687
13000	9.715	9.715	9.715	9.715	9.715
14000	9.741	9.741	9.741	9.741	9.741
15000	9.767	9.767	9.767	9.767	9.767
16000	9.795	9.795	9.795	9.795	9.795
17000	9.824	9.824	9.824	9.824	9.824
18000	9.856	9.856	9.856	9.856	9.856
19000	9.892	9.892	9.892	9.892	9.892
20000	9.932	9.932	9.932	9.932	9.932
22000	10.024	10.024	10.024	10.024	10.024
24000	10.136	10.136	10.136	10.136	10.136
26000	10.267	10.267	10.267	10.267	10.267
28000	10.419	10.419	10.419	10.419	10.419
30000	10.592	10.592	10.592	10.592	10.592
35000	11.102	11.102	11.102	11.102	11.102
40000	11.714	11.714	11.714	11.714	11.714
45000	12.408	12.407	12.407	12.407	12.407
50000	13.174	13.168	13.167	13.166	13.166

Table B.17 Internal partition function of O^{+4} as a function of pressure and temperature

T (K)	P (bar)				
	10^{-2}	10^{-1}	1	10^1	10^2
100	1.000	1.000	1.000	1.000	1.000
200	1.000	1.000	1.000	1.000	1.000
300	1.000	1.000	1.000	1.000	1.000
400	1.000	1.000	1.000	1.000	1.000
500	1.000	1.000	1.000	1.000	1.000
600	1.000	1.000	1.000	1.000	1.000
700	1.000	1.000	1.000	1.000	1.000
800	1.000	1.000	1.000	1.000	1.000
900	1.000	1.000	1.000	1.000	1.000
1,000	1.000	1.000	1.000	1.000	1.000
1,500	1.000	1.000	1.000	1.000	1.000
2,000	1.000	1.000	1.000	1.000	1.000
2,500	1.000	1.000	1.000	1.000	1.000
3,000	1.000	1.000	1.000	1.000	1.000
3,500	1.000	1.000	1.000	1.000	1.000
4,000	1.000	1.000	1.000	1.000	1.000
4,500	1.000	1.000	1.000	1.000	1.000
5,000	1.000	1.000	1.000	1.000	1.000
6,000	1.000	1.000	1.000	1.000	1.000
7,000	1.000	1.000	1.000	1.000	1.000
8,000	1.000	1.000	1.000	1.000	1.000
9,000	1.000	1.000	1.000	1.000	1.000
10,000	1.000	1.000	1.000	1.000	1.000
11,000	1.000	1.000	1.000	1.000	1.000
12,000	1.000	1.000	1.000	1.000	1.000
13,000	1.001	1.001	1.001	1.001	1.001
14,000	1.002	1.002	1.002	1.002	1.002
15,000	1.003	1.003	1.003	1.003	1.003
16,000	1.006	1.006	1.006	1.006	1.006
17,000	1.009	1.009	1.009	1.009	1.009
18,000	1.013	1.013	1.013	1.013	1.013
19,000	1.018	1.018	1.018	1.018	1.018
20,000	1.024	1.024	1.024	1.024	1.024
22,000	1.042	1.042	1.042	1.042	1.042
24,000	1.065	1.065	1.065	1.065	1.065
26,000	1.096	1.096	1.096	1.096	1.096
28,000	1.133	1.133	1.133	1.133	1.133
30,000	1.176	1.176	1.176	1.176	1.176
35,000	1.312	1.312	1.312	1.312	1.312
40,000	1.483	1.483	1.483	1.483	1.483
45,000	1.681	1.681	1.681	1.681	1.681
50,000	1.901	1.901	1.901	1.901	1.901

B.3 Selfconsistent Partition Functions of Atomic Species in Mars Atmosphere

Table B.18 Internal partition function of C as a function of pressure and temperature

T (K)	P (bar)				
	10^{-2}	10^{-1}	1	10^1	10^2
100	6.047	6.047	6.047	6.047	6.047
200	7.325	7.325	7.325	7.325	7.325
300	7.834	7.834	7.834	7.834	7.834
400	8.105	8.105	8.105	8.105	8.105
500	8.275	8.275	8.275	8.275	8.275
600	8.390	8.390	8.390	8.390	8.390
700	8.474	8.474	8.474	8.474	8.474
800	8.537	8.537	8.537	8.537	8.537
900	8.587	8.587	8.587	8.587	8.587
1000	8.627	8.627	8.627	8.627	8.627
1500	8.750	8.750	8.750	8.750	8.750
2000	8.814	8.814	8.814	8.814	8.814
2500	8.863	8.863	8.863	8.863	8.863
3000	8.911	8.911	8.911	8.911	8.911
3500	8.967	8.967	8.967	8.967	8.967
4000	9.033	9.033	9.033	9.033	9.033
4500	9.109	9.109	9.109	9.109	9.109
5000	9.192	9.192	9.192	9.192	9.192
6000	9.378	9.378	9.378	9.378	9.378
7000	9.578	9.578	9.578	9.578	9.578
8000	9.794	9.787	9.785	9.785	9.785
9000	10.059	10.015	10.001	9.996	9.995
10000	10.506	10.296	10.235	10.215	10.209
11000	11.314	10.645	10.499	10.450	10.429
12000	13.039	11.233	10.808	10.699	10.664
13000	16.402	12.046	11.188	10.994	10.903
14000	23.527	13.513	11.726	11.291	11.170
15000	36.631	16.531	12.505	11.693	11.473
16000	59.096	20.524	13.591	12.197	11.751
17000	95.356	28.253	15.071	12.820	12.066
18000	150.983	37.545	17.064	13.361	12.462
19000	215.735	55.117	19.811	14.209	12.907
20000	323.235	72.823	25.318	15.448	13.411
22000	575.124	137.332	36.182	18.752	14.584
24000	934.721	216.856	59.810	22.829	16.026
26000	1527.220	322.346	84.249	28.147	17.778
28000	2351.650	455.038	114.686	35.746	19.775
30000	3450.040	697.270	151.049	45.106	22.015
35000	6892.110	1449.310	267.842	82.834	30.906
40000	11781.900	2297.410	504.874	122.770	43.203
45000	19413.000	3703.310	717.414	168.181	54.469
50000	27720.300	5535.600	986.138	222.399	75.323

Table B.19 Internal partition function of C^+ as a function of pressure and temperature

T (K)	P (bar)				
	10^{-2}	10^{-1}	1	10^1	10^2
100	3.606	3.606	3.606	3.606	3.606
200	4.535	4.535	4.535	4.535	4.535
300	4.951	4.951	4.951	4.951	4.951
400	5.184	5.184	5.184	5.184	5.184
500	5.333	5.333	5.333	5.333	5.333
600	5.436	5.436	5.436	5.436	5.436
700	5.511	5.511	5.511	5.511	5.511
800	5.569	5.569	5.569	5.569	5.569
900	5.614	5.614	5.614	5.614	5.614
1,000	5.651	5.651	5.651	5.651	5.651
1,500	5.764	5.764	5.764	5.764	5.764
2,000	5.822	5.822	5.822	5.822	5.822
2,500	5.857	5.857	5.857	5.857	5.857
3,000	5.880	5.880	5.880	5.880	5.880
3,500	5.897	5.897	5.897	5.897	5.897
4,000	5.910	5.910	5.910	5.910	5.910
4,500	5.920	5.920	5.920	5.920	5.920
5,000	5.928	5.928	5.928	5.928	5.928
6,000	5.940	5.940	5.940	5.940	5.940
7,000	5.950	5.950	5.950	5.950	5.950
8,000	5.960	5.960	5.960	5.960	5.960
9,000	5.972	5.972	5.972	5.972	5.972
10,000	5.988	5.988	5.988	5.988	5.988
11,000	6.011	6.011	6.011	6.011	6.011
12,000	6.040	6.040	6.040	6.040	6.040
13,000	6.077	6.077	6.077	6.077	6.077
14,000	6.123	6.123	6.123	6.123	6.123
15,000	6.178	6.177	6.177	6.177	6.177
16,000	6.242	6.241	6.240	6.240	6.240
17,000	6.317	6.313	6.312	6.312	6.312
18,000	6.406	6.395	6.393	6.392	6.392
19,000	6.514	6.487	6.482	6.481	6.480
20,000	6.648	6.591	6.579	6.577	6.576
22,000	7.063	6.849	6.803	6.793	6.791
24,000	7.826	7.201	7.070	7.040	7.033
26,000	9.372	7.715	7.405	7.324	7.302
28,000	12.341	8.578	7.819	7.643	7.598
30,000	18.241	9.835	8.350	8.008	7.921
35,000	52.700	17.567	10.477	9.174	8.891
40,000	136.351	35.910	15.086	10.864	10.084
45,000	316.524	72.906	24.128	13.760	11.554
50,000	641.095	137.719	36.760	17.431	13.382

Table B.20 Internal partition function of C^{+2} as a function of pressure and temperature

T (K)	P (bar)				
	10^{-2}	10^{-1}	1	10^1	10^2
100	1.000	1.000	1.000	1.000	1.000
200	1.000	1.000	1.000	1.000	1.000
300	1.000	1.000	1.000	1.000	1.000
400	1.000	1.000	1.000	1.000	1.000
500	1.000	1.000	1.000	1.000	1.000
600	1.000	1.000	1.000	1.000	1.000
700	1.000	1.000	1.000	1.000	1.000
800	1.000	1.000	1.000	1.000	1.000
900	1.000	1.000	1.000	1.000	1.000
1000	1.000	1.000	1.000	1.000	1.000
1500	1.000	1.000	1.000	1.000	1.000
2000	1.000	1.000	1.000	1.000	1.000
2500	1.000	1.000	1.000	1.000	1.000
3000	1.000	1.000	1.000	1.000	1.000
3500	1.000	1.000	1.000	1.000	1.000
4000	1.000	1.000	1.000	1.000	1.000
4500	1.000	1.000	1.000	1.000	1.000
5000	1.000	1.000	1.000	1.000	1.000
6000	1.000	1.000	1.000	1.000	1.000
7000	1.000	1.000	1.000	1.000	1.000
8000	1.001	1.001	1.001	1.001	1.001
9000	1.002	1.002	1.002	1.002	1.002
10000	1.005	1.005	1.005	1.005	1.005
11000	1.009	1.009	1.009	1.009	1.009
12000	1.017	1.017	1.017	1.017	1.017
13000	1.027	1.027	1.027	1.027	1.027
14000	1.041	1.041	1.041	1.041	1.041
15000	1.059	1.059	1.059	1.059	1.059
16000	1.081	1.081	1.081	1.081	1.081
17000	1.107	1.107	1.107	1.107	1.107
18000	1.137	1.137	1.137	1.137	1.137
19000	1.172	1.172	1.172	1.172	1.172
20000	1.210	1.210	1.210	1.210	1.210
22000	1.297	1.297	1.297	1.297	1.297
24000	1.398	1.398	1.398	1.398	1.398
26000	1.512	1.511	1.511	1.511	1.511
28000	1.636	1.635	1.635	1.635	1.635
30000	1.772	1.769	1.768	1.768	1.768
35000	2.200	2.147	2.137	2.134	2.134
40000	3.037	2.645	2.561	2.543	2.539
45000	5.601	3.505	3.081	3.001	2.979
50000	13.175	5.381	3.847	3.532	3.463

Table B.21 Internal partition function of C^{+3} as a function of pressure and temperature

T (K)	P (bar)				
	10^{-2}	10^{-1}	1	10^1	10^2
100	2.000	2.000	2.000	2.000	2.000
200	2.000	2.000	2.000	2.000	2.000
300	2.000	2.000	2.000	2.000	2.000
400	2.000	2.000	2.000	2.000	2.000
500	2.000	2.000	2.000	2.000	2.000
600	2.000	2.000	2.000	2.000	2.000
700	2.000	2.000	2.000	2.000	2.000
800	2.000	2.000	2.000	2.000	2.000
900	2.000	2.000	2.000	2.000	2.000
1,000	2.000	2.000	2.000	2.000	2.000
1,500	2.000	2.000	2.000	2.000	2.000
2,000	2.000	2.000	2.000	2.000	2.000
2,500	2.000	2.000	2.000	2.000	2.000
3,000	2.000	2.000	2.000	2.000	2.000
3,500	2.000	2.000	2.000	2.000	2.000
4,000	2.000	2.000	2.000	2.000	2.000
4,500	2.000	2.000	2.000	2.000	2.000
5,000	2.000	2.000	2.000	2.000	2.000
6,000	2.000	2.000	2.000	2.000	2.000
7,000	2.000	2.000	2.000	2.000	2.000
8,000	2.000	2.000	2.000	2.000	2.000
9,000	2.000	2.000	2.000	2.000	2.000
10,000	2.001	2.001	2.001	2.001	2.001
11,000	2.001	2.001	2.001	2.001	2.001
12,000	2.003	2.003	2.003	2.003	2.003
13,000	2.005	2.005	2.005	2.005	2.005
14,000	2.008	2.008	2.008	2.008	2.008
15,000	2.012	2.012	2.012	2.012	2.012
16,000	2.018	2.018	2.018	2.018	2.018
17,000	2.025	2.025	2.025	2.025	2.025
18,000	2.034	2.034	2.034	2.034	2.034
19,000	2.045	2.045	2.045	2.045	2.045
20,000	2.058	2.058	2.058	2.058	2.058
22,000	2.088	2.088	2.088	2.088	2.088
24,000	2.125	2.125	2.125	2.125	2.125
26,000	2.169	2.169	2.169	2.169	2.169
28,000	2.218	2.218	2.218	2.218	2.218
30,000	2.271	2.271	2.271	2.271	2.271
35,000	2.423	2.422	2.422	2.422	2.422
40,000	2.592	2.589	2.589	2.589	2.589
45,000	2.791	2.768	2.764	2.763	2.763
50,000	3.097	2.971	2.945	2.940	2.939

Table B.22 Internal partition function of N as a function of pressure and temperature

T (K)	P (bar)				
	10^{-2}	10^{-1}	1	10^1	10^2
100	4.000	4.000	4.000	4.000	4.000
200	4.000	4.000	4.000	4.000	4.000
300	4.000	4.000	4.000	4.000	4.000
400	4.000	4.000	4.000	4.000	4.000
500	4.000	4.000	4.000	4.000	4.000
600	4.000	4.000	4.000	4.000	4.000
700	4.000	4.000	4.000	4.000	4.000
800	4.000	4.000	4.000	4.000	4.000
900	4.000	4.000	4.000	4.000	4.000
1000	4.000	4.000	4.000	4.000	4.000
1500	4.000	4.000	4.000	4.000	4.000
2000	4.000	4.000	4.000	4.000	4.000
2500	4.000	4.000	4.000	4.000	4.000
3000	4.001	4.001	4.001	4.001	4.001
3500	4.004	4.004	4.004	4.004	4.004
4000	4.010	4.010	4.010	4.010	4.010
4500	4.022	4.022	4.022	4.022	4.022
5000	4.041	4.041	4.041	4.041	4.041
6000	4.105	4.105	4.105	4.105	4.105
7000	4.208	4.208	4.208	4.208	4.208
8000	4.349	4.348	4.348	4.348	4.348
9000	4.524	4.523	4.522	4.522	4.522
10000	4.734	4.727	4.725	4.724	4.724
11000	4.990	4.958	4.951	4.949	4.948
12000	5.339	5.226	5.199	5.192	5.190
13000	5.886	5.538	5.470	5.453	5.446
14000	6.933	5.946	5.770	5.726	5.715
15000	8.969	6.593	6.117	6.021	5.996
16000	13.421	7.496	6.535	6.342	6.279
17000	19.851	9.189	7.055	6.697	6.576
18000	31.899	11.416	7.720	7.075	6.891
19000	48.156	15.737	8.684	7.522	7.224
20000	76.701	20.827	10.246	8.098	7.579
22000	157.071	40.912	14.091	9.476	8.366
24000	290.849	70.806	21.609	11.361	9.290
26000	533.113	115.802	33.418	13.991	10.400
28000	908.347	178.946	48.161	17.828	11.690
30000	1456.560	262.752	67.473	23.687	13.217
35000	3482.800	734.684	138.765	45.545	18.921
40000	6818.060	1330.920	295.223	73.924	28.148
45000	12485.900	2382.080	464.643	111.993	42.185
50000	19402.700	3873.690	713.616	157.473	56.313

Table B.23 Internal partition function of N^+ as a function of pressure and temperature

T (K)	P (bar)				
	10^{-2}	10^{-1}	1	10^1	10^2
100	3.250	3.250	3.250	3.250	3.250
200	5.065	5.065	5.065	5.065	5.065
300	6.045	6.045	6.045	6.045	6.045
400	6.641	6.641	6.641	6.641	6.641
500	7.039	7.039	7.039	7.039	7.039
600	7.323	7.323	7.323	7.323	7.323
700	7.536	7.536	7.536	7.536	7.536
800	7.700	7.700	7.700	7.700	7.700
900	7.832	7.832	7.832	7.832	7.832
1,000	7.939	7.939	7.939	7.939	7.939
1,500	8.274	8.274	8.274	8.274	8.274
2,000	8.448	8.448	8.448	8.448	8.448
2,500	8.555	8.555	8.555	8.555	8.555
3,000	8.630	8.630	8.630	8.630	8.630
3,500	8.688	8.688	8.688	8.688	8.688
4,000	8.738	8.738	8.738	8.738	8.738
4,500	8.786	8.786	8.786	8.786	8.786
5,000	8.835	8.835	8.835	8.835	8.835
6,000	8.938	8.938	8.938	8.938	8.938
7,000	9.054	9.054	9.054	9.054	9.054
8,000	9.180	9.180	9.180	9.180	9.180
9,000	9.314	9.314	9.314	9.314	9.314
10,000	9.453	9.453	9.453	9.453	9.453
11,000	9.596	9.596	9.596	9.596	9.596
12,000	9.740	9.740	9.740	9.740	9.740
13,000	9.886	9.886	9.886	9.886	9.886
14,000	10.031	10.031	10.031	10.031	10.031
15,000	10.177	10.177	10.177	10.177	10.177
16,000	10.322	10.321	10.321	10.321	10.321
17,000	10.467	10.466	10.466	10.466	10.466
18,000	10.613	10.610	10.610	10.610	10.610
19,000	10.763	10.755	10.753	10.753	10.753
20,000	10.920	10.901	10.897	10.896	10.896
22,000	11.304	11.207	11.187	11.183	11.182
24,000	11.941	11.559	11.489	11.475	11.472
26,000	13.249	12.029	11.826	11.778	11.766
28,000	16.278	12.742	12.222	12.102	12.071
30,000	22.390	14.048	12.731	12.459	12.391
35,000	72.363	23.333	15.019	13.638	13.342
40,000	225.137	51.463	21.169	15.734	14.601
45,000	640.863	119.811	35.915	19.772	16.369
50,000	1,478.330	258.378	60.511	26.071	18.844

Table B.24 Internal partition function of N^{+2} as a function of pressure and temperature

T (K)	P (bar)				
	10^{-2}	10^{-1}	1	10^1	10^2
100	2.325	2.325	2.325	2.325	2.325
200	3.141	3.141	3.141	3.141	3.141
300	3.733	3.733	3.733	3.733	3.733
400	4.136	4.136	4.136	4.136	4.136
500	4.422	4.422	4.422	4.422	4.422
600	4.633	4.633	4.633	4.633	4.633
700	4.795	4.795	4.795	4.795	4.795
800	4.923	4.923	4.923	4.923	4.923
900	5.027	5.027	5.027	5.027	5.027
1000	5.112	5.112	5.112	5.112	5.112
1500	5.384	5.384	5.384	5.384	5.384
2000	5.528	5.528	5.528	5.528	5.528
2500	5.618	5.618	5.618	5.618	5.618
3000	5.679	5.679	5.679	5.679	5.679
3500	5.723	5.723	5.723	5.723	5.723
4000	5.757	5.757	5.757	5.757	5.757
4500	5.783	5.783	5.783	5.783	5.783
5000	5.804	5.804	5.804	5.804	5.804
6000	5.836	5.836	5.836	5.836	5.836
7000	5.859	5.859	5.859	5.859	5.859
8000	5.877	5.877	5.877	5.877	5.877
9000	5.891	5.891	5.891	5.891	5.891
10000	5.904	5.904	5.904	5.904	5.904
11000	5.917	5.917	5.917	5.917	5.917
12000	5.930	5.930	5.930	5.930	5.930
13000	5.945	5.945	5.945	5.945	5.945
14000	5.963	5.963	5.963	5.963	5.963
15000	5.984	5.984	5.984	5.984	5.984
16000	6.008	6.008	6.008	6.008	6.008
17000	6.038	6.038	6.038	6.038	6.038
18000	6.071	6.071	6.071	6.071	6.071
19000	6.109	6.109	6.109	6.109	6.109
20000	6.152	6.152	6.152	6.152	6.152
22000	6.252	6.252	6.252	6.252	6.252
24000	6.371	6.371	6.371	6.371	6.371
26000	6.507	6.507	6.507	6.507	6.507
28000	6.660	6.659	6.659	6.659	6.659
30000	6.831	6.826	6.826	6.825	6.825
35000	7.382	7.308	7.299	7.298	7.298
40000	8.494	7.909	7.849	7.838	7.836
45000	12.053	8.787	8.494	8.442	8.429
50000	23.634	10.443	9.315	9.115	9.076

Table B.25 Internal partition function of N^{+3} as a function of pressure and temperature

T (K)	P (bar)				
	10^{-2}	10^{-1}	1	10^1	10^2
100	1.000	1.000	1.000	1.000	1.000
200	1.000	1.000	1.000	1.000	1.000
300	1.000	1.000	1.000	1.000	1.000
400	1.000	1.000	1.000	1.000	1.000
500	1.000	1.000	1.000	1.000	1.000
600	1.000	1.000	1.000	1.000	1.000
700	1.000	1.000	1.000	1.000	1.000
800	1.000	1.000	1.000	1.000	1.000
900	1.000	1.000	1.000	1.000	1.000
1,000	1.000	1.000	1.000	1.000	1.000
1,500	1.000	1.000	1.000	1.000	1.000
2,000	1.000	1.000	1.000	1.000	1.000
2,500	1.000	1.000	1.000	1.000	1.000
3,000	1.000	1.000	1.000	1.000	1.000
3,500	1.000	1.000	1.000	1.000	1.000
4,000	1.000	1.000	1.000	1.000	1.000
4,500	1.000	1.000	1.000	1.000	1.000
5,000	1.000	1.000	1.000	1.000	1.000
6,000	1.000	1.000	1.000	1.000	1.000
7,000	1.000	1.000	1.000	1.000	1.000
8,000	1.000	1.000	1.000	1.000	1.000
9,000	1.000	1.000	1.000	1.000	1.000
10,000	1.001	1.001	1.001	1.001	1.001
11,000	1.001	1.001	1.001	1.001	1.001
12,000	1.003	1.003	1.003	1.003	1.003
13,000	1.005	1.005	1.005	1.005	1.005
14,000	1.009	1.009	1.009	1.009	1.009
15,000	1.014	1.014	1.014	1.014	1.014
16,000	1.021	1.021	1.021	1.021	1.021
17,000	1.030	1.030	1.030	1.030	1.030
18,000	1.041	1.041	1.041	1.041	1.041
19,000	1.055	1.055	1.055	1.055	1.055
20,000	1.071	1.071	1.071	1.071	1.071
22,000	1.111	1.111	1.111	1.111	1.111
24,000	1.160	1.160	1.160	1.160	1.160
26,000	1.219	1.219	1.219	1.219	1.219
28,000	1.287	1.287	1.287	1.287	1.287
30,000	1.364	1.364	1.364	1.364	1.364
35,000	1.585	1.585	1.585	1.585	1.585
40,000	1.842	1.842	1.842	1.842	1.842
45,000	2.127	2.126	2.125	2.125	2.125
50,000	2.443	2.431	2.428	2.428	2.428

Table B.26 Internal partition function of N^{+4} as a function of pressure and temperature

T (K)	P (bar)				
	10^{-2}	10^{-1}	1	10^1	10^2
100	2.000	2.000	2.000	2.000	2.000
200	2.000	2.000	2.000	2.000	2.000
300	2.000	2.000	2.000	2.000	2.000
400	2.000	2.000	2.000	2.000	2.000
500	2.000	2.000	2.000	2.000	2.000
600	2.000	2.000	2.000	2.000	2.000
700	2.000	2.000	2.000	2.000	2.000
800	2.000	2.000	2.000	2.000	2.000
900	2.000	2.000	2.000	2.000	2.000
1000	2.000	2.000	2.000	2.000	2.000
1500	2.000	2.000	2.000	2.000	2.000
2000	2.000	2.000	2.000	2.000	2.000
2500	2.000	2.000	2.000	2.000	2.000
3000	2.000	2.000	2.000	2.000	2.000
3500	2.000	2.000	2.000	2.000	2.000
4000	2.000	2.000	2.000	2.000	2.000
4500	2.000	2.000	2.000	2.000	2.000
5000	2.000	2.000	2.000	2.000	2.000
6000	2.000	2.000	2.000	2.000	2.000
7000	2.000	2.000	2.000	2.000	2.000
8000	2.000	2.000	2.000	2.000	2.000
9000	2.000	2.000	2.000	2.000	2.000
10000	2.000	2.000	2.000	2.000	2.000
11000	2.000	2.000	2.000	2.000	2.000
12000	2.000	2.000	2.000	2.000	2.000
13000	2.001	2.001	2.001	2.001	2.001
14000	2.002	2.002	2.002	2.002	2.002
15000	2.003	2.003	2.003	2.003	2.003
16000	2.004	2.004	2.004	2.004	2.004
17000	2.007	2.007	2.007	2.007	2.007
18000	2.010	2.010	2.010	2.010	2.010
19000	2.013	2.013	2.013	2.013	2.013
20000	2.018	2.018	2.018	2.018	2.018
22000	2.031	2.031	2.031	2.031	2.031
24000	2.048	2.048	2.048	2.048	2.048
26000	2.069	2.069	2.069	2.069	2.069
28000	2.095	2.095	2.095	2.095	2.095
30000	2.126	2.126	2.126	2.126	2.126
35000	2.218	2.218	2.218	2.218	2.218
40000	2.330	2.330	2.330	2.330	2.330
45000	2.456	2.456	2.456	2.456	2.456
50000	2.590	2.589	2.589	2.589	2.589

Table B.27 Internal partition function of O as a function of pressure and temperature

T (K)	P (bar)				
	10^{-2}	10^{-1}	1	10^1	10^2
100	5.346	5.346	5.346	5.346	5.346
200	6.156	6.156	6.156	6.156	6.156
300	6.741	6.741	6.741	6.741	6.741
400	7.140	7.140	7.140	7.140	7.140
500	7.423	7.423	7.423	7.423	7.423
600	7.633	7.633	7.633	7.633	7.633
700	7.794	7.794	7.794	7.794	7.794
800	7.922	7.922	7.922	7.922	7.922
900	8.025	8.025	8.025	8.025	8.025
1,000	8.110	8.110	8.110	8.110	8.110
1,500	8.382	8.382	8.382	8.382	8.382
2,000	8.527	8.527	8.527	8.527	8.527
2,500	8.617	8.617	8.617	8.617	8.617
3,000	8.680	8.680	8.680	8.680	8.680
3,500	8.729	8.729	8.729	8.729	8.729
4,000	8.772	8.772	8.772	8.772	8.772
4,500	8.813	8.813	8.813	8.813	8.813
5,000	8.855	8.855	8.855	8.855	8.855
6,000	8.947	8.947	8.947	8.947	8.947
7,000	9.051	9.051	9.051	9.051	9.051
8,000	9.166	9.166	9.166	9.166	9.166
9,000	9.292	9.290	9.290	9.290	9.290
10,000	9.432	9.422	9.422	9.420	9.418
11,000	9.601	9.565	9.565	9.555	9.550
12,000	9.850	9.733	9.732	9.694	9.685
13,000	10.275	9.952	9.950	9.837	9.819
14,000	11.144	10.271	10.266	9.985	9.956
15,000	12.845	10.761	10.750	10.141	10.098
16,000	16.020	11.518	11.497	10.323	10.233
17,000	21.614	12.669	12.628	10.539	10.375
18,000	30.941	14.352	14.285	10.800	10.528
19,000	43.050	17.610	16.637	11.118	10.692
20,000	63.931	21.312	19.839	11.508	10.868
22,000	119.886	35.529	29.536	12.578	11.268
24,000	209.062	55.669	44.835	14.986	11.748
26,000	365.905	84.897	66.939	17.715	12.323
28,000	601.422	124.622	96.927	24.212	13.003
30,000	936.450	175.889	135.577	30.131	13.795
35,000	2,118.650	455.643	272.798	50.405	16.906
40,000	3,983.830	788.986	468.622	97.460	23.395
45,000	6,609.160	1,363.260	716.958	169.424	29.194
50,000	10,723.700	2,157.420	1,011.150	239.463	38.069

Table B.28 Internal partition function of O^+ as a function of pressure and temperature

T (K)	P (bar)				
	10^{-2}	10^{-1}	1	10^1	10^2
100	4.000	4.000	4.000	4.000	4.000
200	4.000	4.000	4.000	4.000	4.000
300	4.000	4.000	4.000	4.000	4.000
400	4.000	4.000	4.000	4.000	4.000
500	4.000	4.000	4.000	4.000	4.000
600	4.000	4.000	4.000	4.000	4.000
700	4.000	4.000	4.000	4.000	4.000
800	4.000	4.000	4.000	4.000	4.000
900	4.000	4.000	4.000	4.000	4.000
1000	4.000	4.000	4.000	4.000	4.000
1500	4.000	4.000	4.000	4.000	4.000
2000	4.000	4.000	4.000	4.000	4.000
2500	4.000	4.000	4.000	4.000	4.000
3000	4.000	4.000	4.000	4.000	4.000
3500	4.000	4.000	4.000	4.000	4.000
4000	4.001	4.001	4.001	4.001	4.001
4500	4.002	4.002	4.002	4.002	4.002
5000	4.005	4.005	4.005	4.005	4.005
6000	4.016	4.016	4.016	4.016	4.016
7000	4.042	4.042	4.042	4.042	4.042
8000	4.085	4.085	4.085	4.085	4.085
9000	4.147	4.147	4.147	4.147	4.147
10000	4.229	4.229	4.229	4.229	4.229
11000	4.330	4.330	4.330	4.330	4.330
12000	4.448	4.448	4.448	4.448	4.448
13000	4.582	4.582	4.582	4.582	4.582
14000	4.729	4.729	4.729	4.729	4.729
15000	4.887	4.887	4.887	4.887	4.887
16000	5.055	5.055	5.055	5.055	5.055
17000	5.230	5.229	5.229	5.229	5.229
18000	5.412	5.409	5.409	5.409	5.409
19000	5.607	5.594	5.594	5.594	5.594
20000	5.833	5.781	5.781	5.781	5.781
22000	6.594	6.163	6.162	6.162	6.162
24000	8.569	6.552	6.546	6.546	6.544
26000	14.406	6.953	6.931	6.931	6.926
28000	30.234	7.395	7.321	7.320	7.304
30000	68.213	7.920	7.723	7.721	7.680
35000	430.487	10.831	8.913	8.899	8.627
40000	1819.130	20.863	10.842	10.794	9.648
45000	5626.660	48.597	14.500	14.407	10.868
50000	13908.700	130.543	21.288	21.099	12.468

Table B.29 Internal partition function of O^{+2} as a function of pressure and temperature

T (K)	<i>P</i> (bar)				
	10^{-2}	10^{-1}	1	10^1	10^2
100	1.650	1.650	1.650	1.650	1.650
200	2.882	2.882	2.882	2.882	2.882
300	3.895	3.895	3.895	3.895	3.895
400	4.659	4.659	4.659	4.659	4.659
500	5.238	5.238	5.238	5.238	5.238
600	5.686	5.686	5.686	5.686	5.686
700	6.042	6.042	6.042	6.042	6.042
800	6.330	6.330	6.330	6.330	6.330
900	6.568	6.568	6.568	6.568	6.568
1,000	6.768	6.768	6.768	6.768	6.768
1,500	7.419	7.419	7.419	7.419	7.419
2,000	7.777	7.777	7.777	7.777	7.777
2,500	8.003	8.003	8.003	8.003	8.003
3,000	8.159	8.159	8.159	8.159	8.159
3,500	8.274	8.274	8.274	8.274	8.274
4,000	8.362	8.362	8.362	8.362	8.362
4,500	8.435	8.435	8.435	8.435	8.435
5,000	8.497	8.497	8.497	8.497	8.497
6,000	8.604	8.604	8.604	8.604	8.604
7,000	8.704	8.704	8.704	8.704	8.704
8,000	8.803	8.803	8.803	8.803	8.803
9,000	8.904	8.904	8.904	8.904	8.904
10,000	9.009	9.009	9.009	9.009	9.009
11,000	9.118	9.118	9.118	9.118	9.118
12,000	9.228	9.228	9.228	9.228	9.228
13,000	9.341	9.341	9.341	9.341	9.341
14,000	9.455	9.455	9.455	9.455	9.455
15,000	9.570	9.570	9.570	9.570	9.570
16,000	9.684	9.684	9.684	9.684	9.684
17,000	9.799	9.799	9.799	9.799	9.799
18,000	9.914	9.914	9.914	9.914	9.914
19,000	10.029	10.029	10.029	10.029	10.029
20,000	10.143	10.143	10.143	10.143	10.143
22,000	10.369	10.369	10.369	10.369	10.369
24,000	10.594	10.594	10.594	10.594	10.594
26,000	10.818	10.818	10.818	10.818	10.818
28,000	11.041	11.041	11.041	11.041	11.041
30,000	11.263	11.263	11.263	11.263	11.263
35,000	11.824	11.823	11.823	11.823	11.822
40,000	12.410	12.401	12.399	12.398	12.393
45,000	13.078	13.026	13.014	13.013	12.984
50,000	13.988	13.795	13.724	13.720	13.602

Table B.30 Internal partition function of O^{+3} as a function of pressure and temperature

T (K)	P (bar)				
	10^{-2}	10^{-1}	1	10^1	10^2
100	2.016	2.016	2.016	2.016	2.016
200	2.249	2.249	2.249	2.249	2.249
300	2.628	2.628	2.628	2.628	2.628
400	2.998	2.998	2.998	2.998	2.998
500	3.318	3.318	3.318	3.318	3.318
600	3.586	3.586	3.586	3.586	3.586
700	3.810	3.810	3.810	3.810	3.810
800	3.998	3.998	3.998	3.998	3.998
900	4.158	4.158	4.158	4.158	4.158
1000	4.296	4.296	4.296	4.296	4.296
1500	4.763	4.763	4.763	4.763	4.763
2000	5.030	5.030	5.030	5.030	5.030
2500	5.203	5.203	5.203	5.203	5.203
3000	5.324	5.324	5.324	5.324	5.324
3500	5.413	5.413	5.413	5.413	5.413
4000	5.482	5.482	5.482	5.482	5.482
4500	5.536	5.536	5.536	5.536	5.536
5000	5.580	5.580	5.580	5.580	5.580
6000	5.646	5.646	5.646	5.646	5.646
7000	5.695	5.695	5.695	5.695	5.695
8000	5.732	5.732	5.732	5.732	5.732
9000	5.761	5.761	5.761	5.761	5.761
10000	5.784	5.784	5.784	5.784	5.784
11000	5.804	5.804	5.804	5.804	5.804
12000	5.821	5.821	5.821	5.821	5.821
13000	5.837	5.837	5.837	5.837	5.837
14000	5.852	5.852	5.852	5.852	5.852
15000	5.867	5.867	5.867	5.867	5.867
16000	5.883	5.883	5.883	5.883	5.883
17000	5.900	5.900	5.900	5.900	5.900
18000	5.918	5.918	5.918	5.918	5.918
19000	5.938	5.938	5.938	5.938	5.938
20000	5.961	5.961	5.961	5.961	5.961
22000	6.014	6.014	6.014	6.014	6.014
24000	6.077	6.077	6.077	6.077	6.077
26000	6.153	6.153	6.153	6.153	6.153
28000	6.239	6.239	6.239	6.239	6.239
30000	6.338	6.338	6.338	6.338	6.338
35000	6.629	6.629	6.629	6.629	6.629
40000	6.978	6.978	6.978	6.978	6.978
45000	7.373	7.373	7.373	7.373	7.373
50000	7.808	7.807	7.807	7.807	7.806

Table B.31 Internal partition function of O^{+4} as a function of pressure and temperature

T (K)	P (bar)				
	10^{-2}	10^{-1}	1	10^1	10^2
100	1.000	1.000	1.000	1.000	1.000
200	1.000	1.000	1.000	1.000	1.000
300	1.000	1.000	1.000	1.000	1.000
400	1.000	1.000	1.000	1.000	1.000
500	1.000	1.000	1.000	1.000	1.000
600	1.000	1.000	1.000	1.000	1.000
700	1.000	1.000	1.000	1.000	1.000
800	1.000	1.000	1.000	1.000	1.000
900	1.000	1.000	1.000	1.000	1.000
1000	1.000	1.000	1.000	1.000	1.000
1,500	1.000	1.000	1.000	1.000	1.000
2,000	1.000	1.000	1.000	1.000	1.000
2,500	1.000	1.000	1.000	1.000	1.000
3,000	1.000	1.000	1.000	1.000	1.000
3,500	1.000	1.000	1.000	1.000	1.000
4,000	1.000	1.000	1.000	1.000	1.000
4,500	1.000	1.000	1.000	1.000	1.000
5,000	1.000	1.000	1.000	1.000	1.000
6,000	1.000	1.000	1.000	1.000	1.000
7,000	1.000	1.000	1.000	1.000	1.000
8,000	1.000	1.000	1.000	1.000	1.000
9,000	1.000	1.000	1.000	1.000	1.000
10,000	1.000	1.000	1.000	1.000	1.000
11,000	1.000	1.000	1.000	1.000	1.000
12,000	1.000	1.000	1.000	1.000	1.000
13,000	1.001	1.001	1.001	1.001	1.001
14,000	1.002	1.002	1.002	1.002	1.002
15,000	1.003	1.003	1.003	1.003	1.003
16,000	1.006	1.006	1.006	1.006	1.006
17,000	1.009	1.009	1.009	1.009	1.009
18,000	1.013	1.013	1.013	1.013	1.013
19,000	1.018	1.018	1.018	1.018	1.018
20,000	1.024	1.024	1.024	1.024	1.024
22,000	1.042	1.042	1.042	1.042	1.042
24,000	1.065	1.065	1.065	1.065	1.065
26,000	1.096	1.096	1.096	1.096	1.096
28,000	1.133	1.133	1.133	1.133	1.133
30,000	1.176	1.176	1.176	1.176	1.176
35,000	1.312	1.312	1.312	1.312	1.312
40,000	1.483	1.483	1.483	1.483	1.483
45,000	1.681	1.681	1.681	1.681	1.681
50,000	1.901	1.901	1.901	1.901	1.901

Table B.32 Internal partition function of *Ar* as a function of pressure and temperature

T (K)	P (bar)				
	10 ⁻²	10 ⁻¹	1	10 ¹	10 ²
100	1.000	1.000	1.000	1.000	1.000
200	1.000	1.000	1.000	1.000	1.000
300	1.000	1.000	1.000	1.000	1.000
400	1.000	1.000	1.000	1.000	1.000
500	1.000	1.000	1.000	1.000	1.000
600	1.000	1.000	1.000	1.000	1.000
700	1.000	1.000	1.000	1.000	1.000
800	1.000	1.000	1.000	1.000	1.000
900	1.000	1.000	1.000	1.000	1.000
1000	1.000	1.000	1.000	1.000	1.000
1500	1.000	1.000	1.000	1.000	1.000
2000	1.000	1.000	1.000	1.000	1.000
2500	1.000	1.000	1.000	1.000	1.000
3000	1.000	1.000	1.000	1.000	1.000
3500	1.000	1.000	1.000	1.000	1.000
4000	1.000	1.000	1.000	1.000	1.000
4500	1.000	1.000	1.000	1.000	1.000
5000	1.000	1.000	1.000	1.000	1.000
6000	1.000	1.000	1.000	1.000	1.000
7000	1.000	1.000	1.000	1.000	1.000
8000	1.000	1.000	1.000	1.000	1.000
9000	1.000	1.000	1.000	1.000	1.000
10000	1.000	1.000	1.000	1.000	1.000
11000	1.002	1.002	1.001	1.000	1.000
12000	1.007	1.006	1.002	1.001	1.001
13000	1.021	1.016	1.006	1.003	1.002
14000	1.056	1.043	1.014	1.006	1.004
15000	1.133	1.115	1.031	1.013	1.008
16000	1.284	1.245	1.065	1.027	1.013
17000	1.551	1.545	1.126	1.049	1.023
18000	1.997	1.987	1.225	1.085	1.038
19000	2.694	2.681	1.456	1.140	1.059
20000	3.728	3.708	1.732	1.220	1.090
22000	7.220	7.175	2.659	1.488	1.178
24000	13.363	13.274	4.916	1.949	1.329
26000	23.119	22.952	7.988	2.685	1.586
28000	37.426	37.144	12.448	4.226	1.940
30000	57.132	56.697	18.590	6.182	2.437
35000	134.284	133.268	42.582	13.574	4.334
40000	256.011	254.101	96.117	24.788	8.588
45000	423.601	420.154	158.724	40.332	13.110
50000	633.946	628.876	281.687	59.970	18.614

Table B.33 Internal partition function of Ar^+ as a function of pressure and temperature

T (K)	P (bar)				
	10^{-2}	10^{-1}	1	10^1	10^2
100	4.000	4.000	4.000	4.000	4.000
200	4.000	4.000	4.000	4.000	4.000
300	4.002	4.002	4.002	4.002	4.002
400	4.012	4.012	4.012	4.012	4.012
500	4.033	4.033	4.033	4.033	4.033
600	4.065	4.065	4.065	4.065	4.065
700	4.105	4.105	4.105	4.105	4.105
800	4.152	4.152	4.152	4.152	4.152
900	4.203	4.203	4.203	4.203	4.203
1,000	4.255	4.255	4.255	4.255	4.255
1,500	4.507	4.507	4.507	4.507	4.507
2,000	4.714	4.714	4.714	4.714	4.714
2,500	4.877	4.877	4.877	4.877	4.877
3,000	5.007	5.007	5.007	5.007	5.007
3,500	5.110	5.110	5.110	5.110	5.110
4,000	5.195	5.195	5.195	5.195	5.195
4,500	5.265	5.265	5.265	5.265	5.265
5,000	5.325	5.325	5.325	5.325	5.325
6,000	5.419	5.419	5.419	5.419	5.419
7,000	5.490	5.490	5.490	5.490	5.490
8,000	5.546	5.546	5.546	5.546	5.546
9,000	5.591	5.591	5.591	5.591	5.591
10,000	5.628	5.628	5.628	5.628	5.628
11,000	5.658	5.658	5.658	5.658	5.658
12,000	5.685	5.685	5.685	5.685	5.685
13,000	5.707	5.707	5.707	5.707	5.707
14,000	5.726	5.726	5.726	5.726	5.726
15,000	5.744	5.744	5.744	5.744	5.744
16,000	5.759	5.759	5.759	5.759	5.759
17,000	5.773	5.773	5.773	5.773	5.773
18,000	5.787	5.787	5.787	5.786	5.786
19,000	5.801	5.801	5.800	5.799	5.799
20,000	5.817	5.817	5.815	5.812	5.812
22,000	5.864	5.862	5.856	5.844	5.841
24,000	5.957	5.950	5.930	5.891	5.880
26,000	6.150	6.132	6.092	5.975	5.939
28,000	6.540	6.491	6.395	6.115	6.030
30,000	7.252	7.148	6.941	6.351	6.167
35,000	11.742	11.489	10.365	7.689	6.891
40,000	23.458	22.662	20.771	10.847	8.382
45,000	47.438	45.501	41.158	18.050	10.995
50,000	88.945	84.930	76.092	29.737	15.160

Table B.34 Internal partition function of Ar^{+2} as a function of pressure and temperature

T (K)	P (bar)				
	10^{-2}	10^{-1}	1	10^1	10^2
100	5.597	5.597	5.597	5.597	5.597
200	6.339	6.339	6.339	6.339	6.339
300	6.752	6.752	6.752	6.752	6.752
400	7.007	7.007	7.007	7.007	7.007
500	7.183	7.183	7.183	7.183	7.183
600	7.316	7.316	7.316	7.316	7.316
700	7.422	7.422	7.422	7.422	7.422
800	7.511	7.511	7.511	7.511	7.511
900	7.589	7.589	7.589	7.589	7.589
1000	7.657	7.657	7.657	7.657	7.657
1500	7.916	7.916	7.916	7.916	7.916
2000	8.091	8.091	8.091	8.091	8.091
2500	8.219	8.219	8.219	8.219	8.219
3000	8.320	8.320	8.320	8.320	8.320
3500	8.405	8.405	8.405	8.405	8.405
4000	8.482	8.482	8.482	8.482	8.482
4500	8.556	8.556	8.556	8.556	8.556
5000	8.630	8.630	8.630	8.630	8.630
6000	8.781	8.781	8.781	8.781	8.781
7000	8.938	8.938	8.938	8.938	8.938
8000	9.099	9.099	9.099	9.099	9.099
9000	9.262	9.262	9.262	9.262	9.262
10000	9.424	9.424	9.424	9.424	9.424
11000	9.584	9.584	9.584	9.584	9.584
12000	9.739	9.739	9.739	9.739	9.739
13000	9.889	9.889	9.889	9.889	9.889
14000	10.034	10.034	10.034	10.034	10.034
15000	10.174	10.174	10.174	10.174	10.174
16000	10.307	10.307	10.307	10.307	10.307
17000	10.435	10.435	10.435	10.435	10.435
18000	10.558	10.558	10.558	10.558	10.558
19000	10.676	10.676	10.676	10.676	10.676
20000	10.789	10.789	10.789	10.789	10.789
22000	11.004	11.004	11.004	11.004	11.004
24000	11.205	11.205	11.205	11.205	11.205
26000	11.398	11.398	11.398	11.397	11.397
28000	11.588	11.588	11.588	11.587	11.586
30000	11.781	11.781	11.781	11.779	11.777
35000	12.341	12.341	12.341	12.316	12.304
40000	13.181	13.181	13.181	13.058	12.988
45000	14.657	14.656	14.656	14.211	13.953
50000	17.318	17.317	17.317	16.198	15.341

Table B.35 Internal partition function of Ar^{+3} as a function of pressure and temperature

T (K)	P (bar)				
	10^{-2}	10^{-1}	1	10^1	10^2
100	4.000	4.000	4.000	4.000	4.000
200	4.000	4.000	4.000	4.000	4.000
300	4.000	4.000	4.000	4.000	4.000
400	4.000	4.000	4.000	4.000	4.000
500	4.000	4.000	4.000	4.000	4.000
600	4.000	4.000	4.000	4.000	4.000
700	4.000	4.000	4.000	4.000	4.000
800	4.000	4.000	4.000	4.000	4.000
900	4.000	4.000	4.000	4.000	4.000
1,000	4.000	4.000	4.000	4.000	4.000
1,500	4.000	4.000	4.000	4.000	4.000
2,000	4.000	4.000	4.000	4.000	4.000
2,500	4.000	4.000	4.000	4.000	4.000
3,000	4.000	4.000	4.000	4.000	4.000
3,500	4.002	4.002	4.002	4.002	4.002
4,000	4.005	4.005	4.005	4.005	4.005
4,500	4.012	4.012	4.012	4.012	4.012
5,000	4.023	4.023	4.023	4.023	4.023
6,000	4.064	4.064	4.064	4.064	4.064
7,000	4.134	4.134	4.134	4.134	4.134
8,000	4.233	4.233	4.233	4.233	4.233
9,000	4.362	4.362	4.362	4.362	4.362
10,000	4.515	4.515	4.515	4.515	4.515
11,000	4.689	4.689	4.689	4.689	4.689
12,000	4.881	4.881	4.881	4.881	4.881
13,000	5.086	5.086	5.086	5.086	5.086
14,000	5.301	5.301	5.301	5.301	5.301
15,000	5.523	5.523	5.523	5.523	5.523
16,000	5.749	5.749	5.749	5.749	5.749
17,000	5.979	5.979	5.979	5.979	5.979
18,000	6.209	6.209	6.209	6.209	6.209
19,000	6.440	6.440	6.440	6.440	6.440
20,000	6.669	6.669	6.669	6.669	6.669
22,000	7.121	7.121	7.121	7.121	7.121
24,000	7.561	7.561	7.561	7.561	7.561
26,000	7.989	7.989	7.989	7.989	7.989
28,000	8.404	8.404	8.404	8.404	8.404
30,000	8.807	8.807	8.807	8.807	8.807
35,000	9.776	9.776	9.776	9.776	9.776
40,000	10.720	10.720	10.720	10.719	10.719
45,000	11.691	11.691	11.690	11.685	11.678
50,000	12.756	12.756	12.755	12.734	12.701

Table B.36 Internal partition function of Ar^{+4} as a function of pressure and temperature

T (K)	P (bar)				
	10^{-2}	10^{-1}	1	10^1	10^2
100	1.000	1.000	1.000	1.000	1.000
200	1.012	1.012	1.012	1.012	1.012
300	1.077	1.077	1.077	1.077	1.077
400	1.195	1.195	1.195	1.195	1.195
500	1.346	1.346	1.346	1.346	1.346
600	1.517	1.517	1.517	1.517	1.517
700	1.700	1.700	1.700	1.700	1.700
800	1.888	1.888	1.888	1.888	1.888
900	2.078	2.078	2.078	2.078	2.078
1000	2.268	2.268	2.268	2.268	2.268
1500	3.154	3.154	3.154	3.154	3.154
2000	3.892	3.892	3.892	3.892	3.892
2500	4.487	4.487	4.487	4.487	4.487
3000	4.970	4.970	4.970	4.970	4.970
3500	5.368	5.368	5.368	5.368	5.368
4000	5.703	5.703	5.703	5.703	5.703
4500	5.990	5.990	5.990	5.990	5.990
5000	6.242	6.242	6.242	6.242	6.242
6000	6.671	6.671	6.671	6.671	6.671
7000	7.034	7.034	7.034	7.034	7.034
8000	7.353	7.353	7.353	7.353	7.353
9000	7.641	7.641	7.641	7.641	7.641
10000	7.905	7.905	7.905	7.905	7.905
11000	8.149	8.149	8.149	8.149	8.149
12000	8.377	8.377	8.377	8.377	8.377
13000	8.590	8.590	8.590	8.590	8.590
14000	8.790	8.790	8.790	8.790	8.790
15000	8.979	8.979	8.979	8.979	8.979
16000	9.157	9.157	9.157	9.157	9.157
17000	9.327	9.327	9.327	9.327	9.327
18000	9.488	9.488	9.488	9.488	9.488
19000	9.641	9.641	9.641	9.641	9.641
20000	9.788	9.788	9.788	9.788	9.788
22000	10.065	10.065	10.065	10.065	10.065
24000	10.323	10.323	10.323	10.323	10.323
26000	10.567	10.567	10.567	10.567	10.567
28000	10.800	10.800	10.800	10.800	10.800
30000	11.026	11.026	11.026	11.026	11.026
35000	11.579	11.579	11.579	11.579	11.579
40000	12.139	12.139	12.139	12.139	12.139
45000	12.729	12.729	12.729	12.729	12.729
50000	13.366	13.366	13.366	13.366	13.365

B.4 Selfconsistent Partition Functions of Atomic Species in Jupiter Atmosphere

Table B.37 Internal partition function of H as a function of pressure and temperature

T (K)	P (bar)				
	10^{-2}	10^{-1}	1	10^1	10^2
100	2.000	2.000	2.000	2.000	2.000
200	2.000	2.000	2.000	2.000	2.000
300	2.000	2.000	2.000	2.000	2.000
400	2.000	2.000	2.000	2.000	2.000
500	2.000	2.000	2.000	2.000	2.000
600	2.000	2.000	2.000	2.000	2.000
700	2.000	2.000	2.000	2.000	2.000
800	2.000	2.000	2.000	2.000	2.000
900	2.000	2.000	2.000	2.000	2.000
1,000	2.000	2.000	2.000	2.000	2.000
1,500	2.000	2.000	2.000	2.000	2.000
2,000	2.000	2.000	2.000	2.000	2.000
2,500	2.000	2.000	2.000	2.000	2.000
3,000	2.000	2.000	2.000	2.000	2.000
3,500	2.000	2.000	2.000	2.000	2.000
4,000	2.000	2.000	2.000	2.000	2.000
4,500	2.000	2.000	2.000	2.000	2.000
5,000	2.000	2.000	2.000	2.000	2.000
6,000	2.000	2.000	2.000	2.000	2.000
7,000	2.000	2.000	2.000	2.000	2.000
8,000	2.000	2.000	2.000	2.000	2.000
9,000	2.001	2.000	2.000	2.000	2.000
10,000	2.003	2.001	2.000	2.000	2.000
11,000	2.014	2.005	2.002	2.001	2.000
12,000	2.042	2.013	2.005	2.002	2.001
13,000	2.127	2.030	2.011	2.005	2.003
14,000	2.328	2.070	2.022	2.009	2.006
15,000	2.757	2.146	2.044	2.018	2.011
16,000	3.585	2.322	2.068	2.026	2.015
17,000	5.069	2.572	2.119	2.044	2.024
18,000	7.562	3.093	2.243	2.071	2.038
19,000	11.529	3.728	2.381	2.108	2.040
20,000	17.562	4.975	2.570	2.159	2.057
22,000	33.846	8.884	3.416	2.310	2.106
24,000	64.303	16.090	4.544	2.543	2.177
26,000	113.016	28.212	7.108	3.197	2.273
28,000	173.160	47.204	9.825	3.809	2.398
30,000	269.420	67.715	15.712	4.589	2.552
35,000	609.149	192.913	36.505	9.190	3.722
40,000	1,142.980	371.747	73.552	14.390	4.875
45,000	1,891.330	574.449	132.056	27.130	6.287
50,000	2,864.220	896.095	217.103	37.351	11.248

Table B.38 Internal partition function of He as a function of pressure and temperature

T (K)	P (bar)				
	10^{-2}	10^{-1}	1	10^1	10^2
100	1.000	1.000	1.000	1.000	1.000
200	1.000	1.000	1.000	1.000	1.000
300	1.000	1.000	1.000	1.000	1.000
400	1.000	1.000	1.000	1.000	1.000
500	1.000	1.000	1.000	1.000	1.000
600	1.000	1.000	1.000	1.000	1.000
700	1.000	1.000	1.000	1.000	1.000
800	1.000	1.000	1.000	1.000	1.000
900	1.000	1.000	1.000	1.000	1.000
1000	1.000	1.000	1.000	1.000	1.000
1500	1.000	1.000	1.000	1.000	1.000
2000	1.000	1.000	1.000	1.000	1.000
2500	1.000	1.000	1.000	1.000	1.000
3000	1.000	1.000	1.000	1.000	1.000
3500	1.000	1.000	1.000	1.000	1.000
4000	1.000	1.000	1.000	1.000	1.000
4500	1.000	1.000	1.000	1.000	1.000
5000	1.000	1.000	1.000	1.000	1.000
6000	1.000	1.000	1.000	1.000	1.000
7000	1.000	1.000	1.000	1.000	1.000
8000	1.000	1.000	1.000	1.000	1.000
9000	1.000	1.000	1.000	1.000	1.000
10000	1.000	1.000	1.000	1.000	1.000
11000	1.000	1.000	1.000	1.000	1.000
12000	1.000	1.000	1.000	1.000	1.000
13000	1.000	1.000	1.000	1.000	1.000
14000	1.000	1.000	1.000	1.000	1.000
15000	1.000	1.000	1.000	1.000	1.000
16000	1.001	1.000	1.000	1.000	1.000
17000	1.003	1.001	1.000	1.000	1.000
18000	1.009	1.002	1.000	1.000	1.000
19000	1.023	1.004	1.001	1.000	1.000
20000	1.053	1.010	1.002	1.001	1.000
22000	1.194	1.041	1.009	1.002	1.001
24000	1.614	1.137	1.025	1.006	1.002
26000	2.646	1.384	1.076	1.018	1.004
28000	4.601	1.942	1.165	1.039	1.009
30000	8.621	2.855	1.389	1.075	1.017
35000	32.750	10.919	2.793	1.379	1.093
40000	95.074	31.308	6.851	2.030	1.243
45000	222.978	67.850	16.128	3.961	1.523
50000	447.439	139.700	34.252	6.721	2.462

Table B.39 Internal partition function of He^+ as a function of pressure and temperature

T (K)	P (bar)				
	10^{-2}	10^{-1}	1	10^1	10^2
100	2.000	2.000	2.000	2.000	2.000
200	2.000	2.000	2.000	2.000	2.000
300	2.000	2.000	2.000	2.000	2.000
400	2.000	2.000	2.000	2.000	2.000
500	2.000	2.000	2.000	2.000	2.000
600	2.000	2.000	2.000	2.000	2.000
700	2.000	2.000	2.000	2.000	2.000
800	2.000	2.000	2.000	2.000	2.000
900	2.000	2.000	2.000	2.000	2.000
1,000	2.000	2.000	2.000	2.000	2.000
1,500	2.000	2.000	2.000	2.000	2.000
2,000	2.000	2.000	2.000	2.000	2.000
2,500	2.000	2.000	2.000	2.000	2.000
3,000	2.000	2.000	2.000	2.000	2.000
3,500	2.000	2.000	2.000	2.000	2.000
4,000	2.000	2.000	2.000	2.000	2.000
4,500	2.000	2.000	2.000	2.000	2.000
5,000	2.000	2.000	2.000	2.000	2.000
6,000	2.000	2.000	2.000	2.000	2.000
7,000	2.000	2.000	2.000	2.000	2.000
8,000	2.000	2.000	2.000	2.000	2.000
9,000	2.000	2.000	2.000	2.000	2.000
10,000	2.000	2.000	2.000	2.000	2.000
11,000	2.000	2.000	2.000	2.000	2.000
12,000	2.000	2.000	2.000	2.000	2.000
13,000	2.000	2.000	2.000	2.000	2.000
14,000	2.000	2.000	2.000	2.000	2.000
15,000	2.000	2.000	2.000	2.000	2.000
16,000	2.000	2.000	2.000	2.000	2.000
17,000	2.000	2.000	2.000	2.000	2.000
18,000	2.000	2.000	2.000	2.000	2.000
19,000	2.000	2.000	2.000	2.000	2.000
20,000	2.000	2.000	2.000	2.000	2.000
22,000	2.000	2.000	2.000	2.000	2.000
24,000	2.000	2.000	2.000	2.000	2.000
26,000	2.000	2.000	2.000	2.000	2.000
28,000	2.000	2.000	2.000	2.000	2.000
30,000	2.000	2.000	2.000	2.000	2.000
35,000	2.002	2.001	2.000	2.000	2.000
40,000	2.023	2.007	2.002	2.000	2.000
45,000	2.146	2.045	2.011	2.002	2.001
50,000	2.619	2.197	2.049	2.010	2.003

Appendix C

Constants

a_0	$0.529177249 \times 10^{-10}$	(m)	Bohr radius
c	299792458	(ms $^{-1}$)	Speed of light
e	2.718281828		Neper number
ϵ_0	8.85415×10^{-12}	(C 2 m $^{-1}$ J $^{-1}$)	Vacuum dielectric constant
m_e	$9.1093897 \times 10^{-31}$	(kg)	Electron mass
m_p	$1.67262158 \times 10^{-27}$	(kg)	Proton mass
AMU	$1.66053886 \times 10^{-27}$	(kg)	Atomic Mass Unit
N_a	6.0221367×10^{23}	(mol $^{-1}$)	Avogadro number
h	$6.6260755 \times 10^{-34}$	(Js)	Plank Constant
$\hbar = \frac{h}{2\pi}$	$1.05457266 \times 10^{-34}$	(Js)	Reduced Plank Constant
k	1.380658×10^{-23}	(JK $^{-1}$)	Boltzmann Constant
	8.617386×10^{-5}	(eVK $^{-1}$)	
	6.950388×10^{-1}	(cm $^{-1}$ K $^{-1}$)	
I_H	13.6	(eV)	Atomic hydrogen ionization potential
q_e	$1.6021773 \times 10^{-19}$	(C)	Electron charge
R	8.314510	(JK $^{-1}$ mol $^{-1}$)	Ideal gas constant

C.1 Conversion Factors

$$\text{cm}^{-1} = 1.239842447 \times 10^{-4} \text{ eV}$$

$$\text{J} = q_e \text{ eV}$$

$$R = N_a k$$

References

- Allen MP, Tildesley DJ (1989) Computer Simulation of Liquids. 2nd ed. Oxford University Press, USA
- Anderson JD (2000) Hypersonic and High Temperatur Gas Dynamics. American Institute of Aeronautics and Astronautics
- Andre P, Abbaoui M, Lefort A, Parizet M (1996) Numerical method and composition in multi-temperature plasmas: Application to an Ar-H₂ mixture. *Plasma Chemistry and Plasma Processing* 16(3):379–398
- Andre P, Abbaoui M, Bessege R, Lefort A (1997) Comparison between Gibbs free energy minimization and mass action law for a multitemperature plasma with application to nitrogen. *Plasma Chemistry and Plasma Processing* 17(2):207–217
- Andre P, Aubreton J, Elchinger M, Rat V, Fauchais P, Lefort A, Murphy A (2004) A statistical mechanical view of the determination of the composition of multi-temperature Plasmas. *Plasma Chemistry and Plasma Processing* 24(3):435–446
- Atkins PW (1986) Physical Chemistry. Oxford University Press
- Aubreton J, Elchinger M, Fauchais P (1998) New method to calculate thermodynamic and transport properties of a multi-temperature plasma: Application to N₂ plasma. *Plasma Chemistry and Plasma Processing* 18(1):1–27
- Babou Y, Rivier P, Perrin MY, Souflani A (2007) High temperature nonequilibrium partition function and thermodynamic data of diatomic molecules. *International Journal of Thermophysics* 30(2):416–438
- Biolsi L, Holland PM (1996) Thermodynamic properties of oxygen molecules at high temperatures. *International Journal of Thermophysics* 17(1):191–200
- Biolsi L, Holland PM (2010) The transport properties of sodium atoms and the heat capacity of sodium dimers at high temperatures. *International Journal of Thermophysics* 17:831–843
- Bishnuy PS, Hamirouney D, Metghalchiy M, Keckz JC (1997) Constrained-equilibrium calculations for chemical systems subject to generalized linear constraints using the nasa and stanjan equilibrium programs. *Combustion Theory and Modelling* 1:295
- Bishop DM (1993) Group Theory and Chemistry. Dover Publications
- Bottin B, Abeele DV, Carbonaro M, Degrez G (1999) Thermodynamic and transport properties for inductive plasma modeling. *Journal of Thermophysics and Heat Transfer* 13(3):343–350
- Boulos MI, Fauchais P, Pfender E (1994) Thermal Plasmas: Fundamentals and Applications: Vol 1, vol 1. Plenum Press, New York
- Burm KTAL (2005) The isentropic exponent and relation for monoatomic plasmas. *Physics Letters A* 336(2–3):200–203
- Burm KTAL, Goedheer WJ, Schram DC (1999) The isentropic exponent in plasmas. *Physics of Plasmas* 6(6):2622–2627

- Callen H (1985) Thermodynamics and an Introduction to Themostatistics, 2nd edn. John Wiley & Sons
- Capitelli M, Ferraro G (1976) Cut-off criteria of electronic partition functions: effects on spectroscopic quantities. *Spectrochimica Acta* 31B:323–326
- Capitelli M, Ficocelli E (1970) Frozen properties and cut-off criteria of high temperature gases. *Zeitschrift für Naturforschung A* 25a(6):977–979
- Capitelli M, Ficocelli E (1971) The contribution of electronic excitation to the total specific heat of high temperature gases: a misinterpreted absence. *Journal of Plasma Physics* 5(1):115–121
- Capitelli M, Ficocelli E (1977) Thermodynamic properties of $Ar - H_2$. *Revue Internationale des Hautes Températures et des Refractaires* 14:195–200
- Capitelli M, Giordano D (2002) Demysticizing the Gibbs potential for determination of chemical equilibrium conditions. *Journal of Thermophysics and Heat Transfer* 16(2):283–285
- Capitelli M, Giordano D (2009) Energy levels of atomic hydrogen in a closed box: A natural cutoff criterion of the electronic partition function. *Physical Review A* 80(3):032,113
- Capitelli M, Lamanna UT (1976) Second virial coefficients of oxygen–oxygen and carbon–oxygen interactions in different electronic states. *Chemical Physics* 14:261–266
- Capitelli M, Molinari E (1970) Problems of determination of high temperature thermodynamic properties of rare gases with application to mixtures. *Journal of Plasma Physics* 4(2):335–355
- Capitelli M, Cramarossa F, Provenzano G, Molinari E (1968) A FORTRAN IV programme for the computation of equilibrium compositions of gas mixtures at high temperature. *La Ricerca Scientifica* 38(7–8):695–701
- Capitelli M, Ficocelli E, Molinari E (1970a) Equilibrium composition and thermodynamic properties of mixed plasmas. II argon–oxygen plasmas at 10^{-2} – 10 atmospheres, between 2000 K and 35000 K. *Adriatica Editrice*, Bari, Italy
- Capitelli M, Ficocelli E, Molinari E (1970b) Equilibrium properties of helium–nitrogen, argon–nitrogen, and xenon–nitrogen plasmas at atmospheric pressure, between 5000 K and 35000 K. *Revue Internationale des Hautes Températures et des Refractaires* 7:153–163
- Capitelli M, Ficocelli E, Molinari E (1971) Electronic excitation and thermodynamic properties of high temperature gases. *Zeitschrift für Naturforschung A* 26a(4):672–683
- Capitelli M, Ficocelli E, Molinari E (1972) Equilibrium composition and thermodynamic properties of mixed plasmas. III $Ar - H_2$ plasmas at 10^{-2} – 10 atmospheres, between 2000K and 35000 K. *Adriatica Editrice*, Bari, Italy
- Capitelli M, Guidotti C, Lamanna U (1974) Potential energy curves and excitation transfer cross sections of excited hydrogen atoms. *Journal of Physics B (Atomic and Molecular Physics)* 7:1683–1691
- Capitelli M, Colonna G, Gorse C, Giordano D (1994) Survey of methods of calculating high-temperature thermodynamic properties of air species. Tech. Rep. STR-236, European Space Agency
- Capitelli M, Colonna G, Gorse C, Minelli P, Pagano D, Giordano D (2001) Thermodynamic and transport properties of two-temperature H_2 plasmas. AIAA 2001–3018
- Capitelli M, Colonna G, Gorse C, Minelli P, Pagano D, Giordano D (2002) Two-temperature Saha equations: Effects on thermophysical properties of H_2 plasmas. *Journal of Thermophysics and Heat Transfer* 16(3):469–472
- Capitelli M, Colonna G, Giordano D, Marraffa L, Casavola A, Minnelli D P ad Pagano, Pietanza LD, Taccogna F (2005a) Tables of internal partition functions and thermodynamic properties of high-temperature Mars-atmosphere species from 50 K to 50000 K. Tech. Rep. STR-246, European Space Agency
- Capitelli M, Longo S, Petrella G, Giordano D (2005b) Equivalent potential functions to calculate thermodynamic equilibria. *Plasma Chemistry and Plasma Processing* 25(6):659–675
- Capitelli M, Giordano D, Colonna G (2008) The role of Debye–Hückel electronic energy levels on the thermodynamic properties of hydrogen plasmas including isentropic coefficients. *Physics of Plasmas* 15:082,115

- Capitelli M, Bruno D, Colonna G, Catalfamo C, Laricchiuta A (2009) Thermodynamics and transport properties of thermal plasmas: the role of electronic excitation. *J Phys D: Appl Phys* 42:1–19
- Capitelli M, Celiberto R, Longo S (2010) Fondamenti di Chimica. Termodinamica e Cinetica Chimica. Adriatica Divisione Arte
- Capitelli M, Bruno D, Colonna G, D'Ammando G, D'Angola A, Giordano D, Gorse C, Laricchiuta A, Longo S (2011a) Thermodynamic properties of gases behind shock waves. In: Brun R (ed) Encyclopaedia of Shock Waves, vol 7, Springer
- Capitelli M, Celiberto R, Gorse C, Longo S (2011b) Fondamenti di Chimica. Legame Chimico. Adriatica Divisione Arte
- Celiberto R, Lamanna UT, Capitelli M (1998) Elastic, diffusion, and viscosity cross sections for collisions involving excited atomic hydrogen. *Physical Review A* 58:2106–2114
- Chase Jr MW (1998) NIST-JANAF Thermochemical Tables, vol 1–2. American Institute of Physics, Woodbury, New York
- Chen K, Eddy T (1998) A thermodynamic analysis of nonequilibrium argon plasma torches. *Plasma Chemistry and Plasma Processing* 18(1):29–52
- Chen X, Han P (1999) On the thermodynamic derivation of the Saha equation modified to a two-temperature plasma. *Journal of Physics D: Applied Physics* 32(14):1711–1718
- Cliteur G, Suzuki K, Tanaka Y, Sakuta T, Matsubara T, Yokomizu Y, Matsumura T (1999) On the determination of the multi-temperature SF_6 plasma composition. *Journal of Physics D: Applied Physics* 32(15):1851–1856
- Colonna G (2007) Improvements of hierarchical algorithm for equilibrium calculation. *Computer Physics Communications* 177:493–499
- Colonna G, Capitelli M (2001a) The influence of atomic and molecular metastable states in high enthalpy nozzle expansion nitrogen flows. *Journal of Physics D: Applied Physics* 34:1812–1818
- Colonna G, Capitelli M (2001b) Self-consistent model of chemical, vibrational, electron kinetics in nozzle expansion. *Journal of Thermophysics and Heat Transfer* 15:308–316
- Colonna G, Capitelli M (2009) A few level approach for the electronic partition function of atomic systems. *Spectrochimica Acta Part B: Atomic Spectroscopy* 64(9):863–873
- Colonna G, D'Angola A (2004) A hierarchical approach for fast and accurate equilibrium calculation. *Computer Physics Communications* 163:177–190
- D'Ammando G, Colonna G, Pietanza LD, Capitelli M (2010) Computation of thermodynamic plasma properties: a simplified approach. *Spectrochimica Acta Part B–Atomic Spectroscopy* 65:603–615
- D'Angola A, Colonna G, Gorse C, Capitelli M (2008) Thermodynamic and transport properties in equilibrium air plasmas in a wide pressure and temperature range. *European Physical Journal D* 46:129–150
- De Palma F, Casavola A, Capitelli M (2006) The influence of electronic excitation on the thermodynamic properties of hydrogen plasmas. *Journal of Thermophysics and Heat Transfer* 20(4):921–952
- Drellishak KS, Knopp CF, Cambel AB (1963a) Partition functions and thermodynamic properties of argon plasma. *Physics of Fluids* 6(9):1280–1288
- Drellishak KS, Knopp CF, Cambel AB (1963b) Partition functions and thermodynamic properties of argon plasmas. AEDC–TDR–63–146
- Drellishak KS, Aeschliman DP, Cambel AB (1964) Tables of thermodynamic properties of argon, nitrogen and oxygen plasmas. AEDC–TDR–64–12
- Drellishak KS, Aeschliman DP, Cambel AB (1965) Partition functions and thermodynamic properties of nitrogen and oxygen plasmas. *Physics of Fluids* 8(9):1590–1600
- Ebeling W, Kraeft WD, Kremp D (1976) Theory of Bound States and Ionization Equilibrium in Plasmas and Solids. Akademie-Verlag, Mir, Berlin, Moscow
- Ecker G, Weizel W (1956) Zustandssumme und effektive Ionisierungsspannung eines atoms im innern des plasmas. *Annalen der Physik* 17(2–3):126–140

- Ecker G, Weizel W (1957) Zustandssumme und effektive Ionisierungsspannung im innern des plasmas. Zeitschrift für Naturforschung 12(10):859–860
- Esposito F (1999) Dinamica quasiclassica di processi collisionali inelastici e reattivi in sistemi $H + H_2$ e $N + N_2$ rotovibrazionalmente risolti. PhD thesis, Dottorato di Ricerca in Scienze Chimiche XI Ciclo, Dipartimento di Chimica, Università di Bari
- Fermi E (1936) Termodynamics. Prentice-Hall, New York
- Fisher BB (1966) Calculation of the thermal properties of hydrogen. Tech. Rep. LA-3364, Los Alamos Scientific Laboratory
- Fortov V, Khrapak IIA (2006) Physics of Strongly Coupled Plasma. Oxford University Press
- Frenkel D, Smit B (2002) Understanding molecular simulation : from algorithms to applications, 2nd edn. Academic Press
- Ghorui S, Heberlein JVR, Pfender E (2008) Thermodynamic and transport properties of two-temperature nitrogen-oxygen plasma. Plasma Chemistry and Plasma Processing 28(4):553–582
- Giordano D (1998) Equivalence of energy, entropy, and thermodynamic potentials in relation to the thermodynamic equilibrium of multitemperature gas mixtures. Physical Review E - Statistical, Nonlinear, and Soft Matter Physics 58(3, Part A):3098–3112
- Giordano D, Capitelli M (1995) Two-temperature Saha equation: a misunderstood problem. Journal of Thermophysics and Heat Transfer 9(4):803–804
- Giordano D, Capitelli M (2002) Nonuniqueness of the two-temperature Saha equation and related considerations. Physical Review E - Statistical, Nonlinear, and Soft Matter Physics 65(1):016,401/1–7
- Giordano D, Capitelli M, Colonna G, Gorse C (1994) Tables of internal partition functions and thermodynamic properties of high-temperature air species from 50 K to 10000 K. Tech. Rep. STR-237, European Space Agency
- Girard R, Belhaouari J, Gonzalez J, Gleizes A (1999) A two-temperature kinetic model of SF_6 plasma. Journal of Physics D: Applied Physics 32(22):2890–2901
- Gleizes A, Chervy B, Gonzalez J (1999) Calculation of a two-temperature plasma composition: bases and application to SF_6 . Journal of Physics D: Applied Physics 32(16):2060–2067
- Gordon S, McBride B (1994) Computer program for calculation of complex chemical equilibrium compositions and applications. NASA Reference Publication 1311, NASA
- Griem HR (1962) High-density corrections in plasma spectroscopy. Physical Review 128: 997–1003
- Griem HR (1997) Principles of Plasma Spectroscopy. Cambridge University Press, Cambridge
- Guidotti C, Arrighini G, Capitelli M, Lamanna UT (1976) Second virial coefficients of ground state nitrogen atom. Zeitschrift für Naturforschung 31a:1722–1724
- Gurvich L, Veys I (1989) Thermodynamic Properties of Individual Substances, vol 1–4. Hemisphere Publishing Corporation
- Henderson SJ, Menart JA (2008) Equilibrium properties of high-temperature air for a number of pressures. Journal of Thermophysics and Heat Transfer 22(4):718–726
- Herzberg G (1963) Molecular Spectra and Molecular Structure, I. Spectra of Diatomic Molecules. D. Van Nostrand, Inc., New York
- Herzberg G (1966) Electronic Spectra of Polyatomic Molecules. D. Van Nostrand, Inc., New York
- Hill TL (1955) Molecular clusters in imperfect gases. Journal Chemical Physics 23(4):617–623
- Hilsenrath J, Klein M (1965) Tables of thermodynamic properties of air in chemical equilibrium including second virial corrections from 1500 K to 15000 K. Tech. Rep. AEDC-TR-65-58, AEDC
- Hirschfelder JO, Curtiss CF, Bird RB (1966) Molecular Theory of Gases and Liquids, 2nd edn. Structure of Matter Series, John Wiley & Sons
- Huang K (1987) Statistical Mechanics. John Wiley & Sons
- Hummer D, Mihalas D (1988) The equation of state for stellar envelopes. i. an occupation probability formalism for the truncation of internal partition functions. The Astrophysical Journal 331:794–814
- Johnson JH, Panagiotopoulos AZ, Gubbins KE (1994) Reactive canonical Monte Carlo - a new simulation technique for reacting or associating fluids. Molecular Physics 81(3):717–733

- Koalaga Z (2002) Influence of the choice of internal temperatures on the composition of $C_xH_yO_zN_t$ plasmas out of thermodynamic equilibrium: application to CH_2 plasma. *Physics of Plasmas* 9(11):4776–4787
- Koalaga Z, Zougmore F (2002) Composition of $C_xH_yO_zN_t$ plasmas out of thermal equilibrium using quite different modified forms of Saha and Guldberg–Waage equations. *Physics of Plasmas* 9(11):4776–4787
- Kremp D, Schlange M, Kraeft WD (2005) Quantum Statistics of Nonideal Plasmas. Atomic, Optical and Plasma Physics, Springer
- Landau D, Lifshitz E (1981) Quantum Mechanics: Non–Relativistic Theory. Butterworth–Heinemann
- Landau D, Lifshitz E (1986) Statistical Physics. Pergamon Press, Oxford
- Leonardi E, Petrongolo C (1997) Ab initio study of NO_2 . VI. vibrational and vibronic coupling in the $\tilde{X}^2A_1/\tilde{A}^2B_2$ conical intersection up to 16 000 cm⁻¹. *Journal of Chemical Physics* 106(24):10,066–10,071
- Leonardi E, Petrongolo C, Hirsch G, Buerker RJ (1996) Ab initio study of NO_2 . V. nonadiabatic vibronic states and levels of the $\tilde{X}^2A_1/\tilde{A}^2B_2$ conical intersection. *Journal of Chemical Physics* 105(20):9051–9067
- Lisal M, Smith W, Nezbeda I (2000) Computer simulation of the thermodynamic properties of high-temperature chemically-reacting plasmas. *Journal of Chemical Physics* 113(12): 4885–4895
- Lisal M, Smith W, Bures M, Vacek V, Navratil J (2002) REMC computer simulations of the thermodynamic properties of argon and air plasmas. *Molecular Physics* 100:2487–2497
- Maczek A (1998) Statistical Thermodynamics. Oxford University Press
- Margenau H, Lewis M (1959) Structure of spectral lines from plasmas. *Reviews of Modern Physics* 31(3):569–615
- McDonald CM, Floudas CA (1997) Glopeq: A new computational tool for the phase and chemical equilibrium problem. *Computers & Chemical Engineering* 21:1
- Meintjes K, Morgan AP (1985) Performance of algorithms for calculating the equilibrium composition of a mixture of gases. *Journal of Computational Physics* 60:219
- Miller SA, MartinezSanchez M (1996) Two-fluid nonequilibrium simulation of hydrogen arcjet thrusters. *Journal of Propulsion and Power* 12(1):112–119
- Mioshi RN, do Lago CL (1996) An equilibrium simulator for multiphase equilibria based on the extent of reaction and Newton–Raphson method with globally convergent strategy (seqex2). *Analitica Chimica Acta* 334:271
- Moelwin-Hughes EA (1947) Physical Chemistry. MacMillan Company
- Moore CE (1949) Selected tables of atomic spectra. Nbs-467, National Bureau of Standards
- Mostaghimi J, Proulx P, Boulou MI (1987) A two-temperature model of the inductively coupled rf plasma. *Journal of Applied Physics* 61(45):1753–1760
- NIST (2009) URL <http://www.nist.gov/srd/index.htm>
- Pagano D, Casavola A, Pietanza LD, Colonna G, Giordano D, Capitelli M (2008) Thermodynamic properties of high-temperature jupiter-atmosphere components. *Journal of Thermophysics and Heat Transfer* 22(3):8
- Pagano D, Casavola A, Pietanza LD, Capitelli M, Colonna G, Giordano D, Marraffa L (2009) Internal partition functions and thermodynamic properties of high-temperature jupiter-atmosphere species from 50 K to 50,000 K. *Tech. Rep. STR-257*
- Patch RW (1969) Components of a hydrogen plasma. including minor species. NASA Reference Publication TN-D-4993, NASA
- Patch RW, McBride BJ (1969) Partition functions and thermodynamic properties to high temperatures for H_3^+ and H_2^+ . NASA Reference Publication TN-D-4523, NASA
- Pauling L (1988) General Chemistry. Dover Publication Inc., New York
- Pauling L, Wilson EB (1985) Introduction to Quantum Mechanics with Applications to Chemistry. Dover Publications

- Phoenix AV, Heidemann RA (1998) A non-ideal multiphase chemical equilibrium algorithm. *Fluid Phase Equilibria* 150–151:255
- Pierce FJ (1968) Microscopic Thermodynamics: The Kinetic Theory and Statistical Thermodynamics of Dilute Gas Systems. International Textbook Co. (Scranton)
- Pirani F, Albertí M, Castro A, Teixidor MM, Cappelletti D (2004) Atom–bond pairwise additive representation for intermolecular potential energy surfaces. *Chemical Physics Letters* 394 (1–3):37–44
- Pirani F, Maciel GS, Cappelletti D, Aquilanti V (2006) Experimental benchmarks and phenomenology of interatomic forces: open-shell and electronic anisotropy effects. *International Reviews in Physical Chemistry* 25(1–2):165–199
- Potapov AV (1966) Chemical equilibrium of multitemperature systems. *High Temperature* 4(1):48–55
- Prigogine I (1955) Thermodynamics of Irreversible Processes. John Wiley & Sons
- Rainwater JC (1984) On the phase space subdivision of the second virial coefficient and its consequences on kinetic theory. *Journal of Chemical Physics* 81(1):495–510
- Rat V, Murphy A, Aubreton J, Elchinger M, Fauchais P (2008) Treatment of non-equilibrium phenomena in thermal plasma flows. *Journal of Physics D: Applied Physics* 41:183,001
- Ree FH (1983) Solubility of hydrogen-helium mixtures in fluid phases to 1 GPa. *The Journal of Physical Chemistry* 87(15):2846–2852
- Reynolds W (1986.) The element potential method for chemical equilibrium analysis: implementation in the interactive program stajan. Stanford University Report ME 270 HO 7, Stanford University, Stanford
- Roussel KM, O'Connell RF (1974) Variational solution of Schrödinger equation for the static screened Coulomb potential. *Physical Review A* 9:52–56
- Sharp TE (1970) Potential-energy curves for molecular hydrogen and its ions. *Atomic Data and Nuclear Data Tables* 2:119–169
- Singh K, Singh G, Sharma R (2010) Role of electronic excitation on thermodynamic and transport properties of argon and argon–hydrogen plasma. *Physics of Plasmas* 17(7):072,309
- Smith CR (1964) Bound states in a Debye–Hückel potential. *Physical Review* 134(5A): A1235–A1237
- Smith W, Lisal M, Nezbeda I (2006) Molecular-level Monte Carlo simulation at fixed entropy. *Chemical Physics Letters* 426(4–6):436–440
- Smith WR, Lísal M (2002) Direct Monte Carlo simulation methods for nonreacting and reacting systems at fixed total internal energy or enthalpy. *Phys Rev E* 66(1):011,104
- Smith WR, Missen RW (1982) Chemical Reaction Equilibrium Analysis: Theory and Algorithms. John Wiley and Sons, New York
- Smith WR, Triska B (1994) The reaction ensemble method for the computer simulation of chemical and phase equilibria. i. theory and basic examples. *The Journal of Chemical Physics* 100(4):3019–3027
- Sofyan Y, Ghajar AJ, Gasem KAM (2003) Multiphase equilibrium calculations using gibbs minimization techniques. *Industrial & Engineering Chemistry Research* 42:3786
- Stancil PC (1994) Partition functions and dissociation equilibrium constants for H_2^+ and He_2^+ . *Journal of Quantitative Spectroscopy and Radiative Transfer* 51(4):655–658
- Stupochenko EV, Stakhenov IP, Samuilov EV, Pleshakov AS, Rozhdestvenskii IB (1960) Thermo-dynamic properties of air in the temperature interval from 1000 K to 12000 K and pressure interval from 10^{-3} to 10^3 atmospheres. *American Rocket Society Journal Supplement* 30:98
- Szabo A, Ostlund N (1996) Modern Quantum Chemistry: Introduction to Advanced Electronic Structure Theory. Dover Publications
- Tanaka Y, Yokomizu Y, Ishikawa M, Matsumura T (1997) Particle composition of high-pressure SF_6 plasma with electron temperature greater than gas temperature. *IEEE transactions on plasma science* 25(5):991–995
- Tournier JMP, El-Genk MS (2008) Properties of helium, nitrogen, and $He - N_2$ binary gas mixture. *Journal of Thermophysics and Heat Transfer* 22(3):442–456

- Turner H, Brennan J, Lisal M, Smith W, Johnson J, Gubbins K (2008) Simulation of chemical reaction equilibria by the reaction ensemble Monte Carlo method: a review. *Molecular Simulation* 34:119–146
- Van De Sanden M, Schram P, Peeters A, Van Der Mullen J, Kroesen G (1989) Thermodynamic generalization of the saha equation for a two-temperature plasma. *Physical Review A* 40(9):5273–5276
- Villars DS (1959) A method of successive approximations for computing combustion equilibria on high speed digital computer. *Journal of Chemical Physics* 60:521
- Villars DS (1960) Computation of complicated combustion equilibria on a high-speed digital computer. In: Bahn G, Zuckowsky E (eds) *Proceedings of the First Conference on the Kinetics Equilibria and Performance of High Temperature Systems*, Western States Section of the Combustion Institute, Butterworths Scientific Publications, Washington D.C., p 18
- Vorob'ev V, Mulenko I, Khomkin A (2000) The importance of excited states in the thermodynamics of partially ionized plasma. *High Temperature* 38(4):509–514
- Wannier GH (1966) Statistical Physics. John Wiley & Sons, New York
- Yos J (1967) Revised transport properties of high temperature air and its components. Avco rad-63-7
- Zaghoul MR (2004) Reduced formulation and efficient algorithm for the determination of equilibrium composition and partition functions of ideal and nonideal complex plasma mixtures. *Physical Review E* 69:026,702
- Zaghoul MR (2005) Efficient and consistent methodology for the calculation of population densities, partition functions, and thermodynamic properties of ideal and weakly non-ideal multicomponent plasma mixtures in the p-t phase space. *IEEE transactions on plasma science* 33(6):1973–1983
- Zaghoul MR (2010) On the ionization equilibrium of the hot hydrogen plasma and thermodynamic consistency of formulating finite internal partition functions. *Physics of Plasmas* 17:062,701
- Živný O (2009) Composition and thermodynamic functions of non-ideal plasma. *European Physical Journal D* 54:(349–367)

Index

A

advancement degree, 4, 6, 9
air
plasma, 110–112, 127, 129, 137, 181, 184, 199
anharmonic oscillator, 79
anharmonicity, 92
argon
plasma, 137, 154
auto-ionizing states, 240

B

Bose/Einstein distribution, 117

C

chemical potential, 3, 4, 56, 57, 67, 69, 70, 74, 107, 108, 120, 133, 165, 168, 171, 172
atomic -, 74
electrons -, 115
ideal -, 115
internal -, 69, 168
minimization, 163
species -, 5, 108, 114
standard variation, 5
translational -, 168
Clausius inequality, 2
cutoff
criterion, 71, 76, 87, 139, 141, 142, 144, 146, 148–158, 160, 161, 181, 231
criterion -, 251

D

de Broglie length, 64, 122

Debye

energy levels, 161, 162
length, 102, 104, 107, 143, 146, 147, 161, 183
mixture, 101
potential, 103, 141, 146, 147, 161
Debye–Hückel
corrections, 139
Debye–Hückel
approximations, 138, 139, 199
corrections, 10, 69, 103, 109, 110, 114, 115, 129, 181
chemical potential, 107, 108, 115
enthalpy, 110, 111
Helmholtz, 104
internal energy, 104
pressure, 110
volume, 107
cutoff, 71, 142, 175
theory, 73, 101, 108, 113, 115, 127, 133, 134, 168, 182
dissociation, 9, 10, 13, 20–22, 25–28, 87, 151, 172, 178
degree, 6–8, 10, 19, 27, 32
limit, 86, 89, 90, 175
multi-temperature -, 172
process, 5, 10, 14, 24, 27, 28, 31, 75, 76, 81, 151
reaction, 19, 27, 28, 131, 172, 176
regime, 1, 13, 29, 127, 153, 176–178

E

energy, 2, 14, 17, 23, 56, 58, 62, 63, 65, 72, 86, 89, 97, 118, 119, 133–135, 146, 147, 156, 184, 233, 245
bias, 21

- energy (*cont.*)
 class, 51
 configuration -, 135, 136
 core -, 240
 dissociation -, 8, 72, 81, 82, 87, 88
 eigenvalue, 144
 electron -, 165
 electronic -, 1, 39, 71, 72, 93, 94
 electrostatic -, 101, 102, 109
 equipartition, 18
 formation -, 65, 68, 69, 109, 164
 functions, 68
 group, 51
 hydrogenic level -, 239
 interaction -, 126
 internal -, 1, 17, 23, 24, 40, 42, 44, 46, 62,
 68, 69, 72, 79, 81, 91, 93, 101, 103,
 104, 133, 176, 182
 ionization -, 10, 30, 70, 109, 242
 level -, 41, 42, 45, 49, 55, 56, 65, 70, 80,
 81, 86–88, 90, 93, 97, 131, 141–143,
 145, 146, 148, 159, 161, 233,
 238–243
 levels, 17, 58, 62, 65, 70, 80, 86, 91, 95,
 141, 144, 146, 161, 231, 237, 238,
 241, 242
 mean -, 41, 121, 181
 molar -, 17, 23, 42
 nuclear -, 79
 particle -, 51
 potential -, 18, 81, 86–90, 121, 134, 144,
 245
 reaction -, 23, 109, 167
 reference, 17, 23, 65
 reference -, 58, 81, 96
 ro-vibrational -, 91, 93
 rotational -, 81, 86, 87, 89, 95, 96
 system -, 51, 54, 119, 120
 thermal -, 102
 total -, 51
 translational -, 17, 46, 65, 66, 72, 181
 unit -, 87
 variance, 58
 vibrational -, 18, 81, 86, 87, 89
 ensemble
 canonical, 119, 123, 125
 grand-canonical, 119, 120, 125, 133, 159
 micro-canonical, 118–120
 enthalpy, 1, 2, 14, 18, 19, 21–23, 35, 39, 55, 66,
 106, 111, 133, 163, 175, 176
 air, 184, 185, 188, 189, 197, 198
 electronic -, 17, 19
 formation -, 17, 19, 58
 internal -, 17, 23, 68
 ionization -, 9, 149
 jupiter, 184, 218, 223
 mars, 184, 206, 214
 molar -, 14, 16, 17, 19, 20, 22, 137, 138,
 199
 reaction -, 5, 23, 76, 150
 species -, 15, 16
 standard -, 8
 entropy, 1, 2, 35, 52, 53, 56, 59, 62, 106, 121,
 127, 129, 133, 150, 152, 155, 164,
 165
 air, 129, 184, 186, 188, 190, 196, 199
 equation, 2
 internal -, 69
 jupiter, 184, 186, 218, 219, 224
 mars, 184, 206, 207, 214
 maximization, 52, 165, 167, 171, 172, 175
 ionization, 171
 molar -
 O^{+2} , 153
 O^+ , 152
 oxygen, 151
 reaction -, 5
 standard -, 8
 translational -, 66, 67
 of free electrons, 67
 variation
 ionization, 9
 equilibrium, 2, 3, 6, 9, 54, 57, 146, 163, 183
 air, 184
 chemical -, 3
 coefficient, 166, 171, 173
 composition, 13, 19, 61, 141, 175, 179, 183,
 184
 computer program, 181
 concentration, 133
 condition, 2, 4–6, 9, 27, 74, 163, 165, 168,
 171–173, 176
 constant, 5, 6, 8, 9, 20, 27, 75, 81, 108, 110,
 112, 129, 131, 136, 139, 147
 dissociation -, 11
 distribution, 56
 equation, 11, 12, 74, 183
 flow, 27
 global -, 22
 internal -, 163
 ionization -, 11, 76
 Jupiter atmosphere, 217
 Mars atmosphere, 202
 mixture -, 24
 multi-temperature -, 114, 163, 166, 168,
 171, 172, 176, 177
 one-temperature -, 167
 plasma, 176, 181

- position, 88
- reaction -, 4
- state, 52
- equipartition theorem, 1, 17–19, 29, 81, 97

- F**
- Fermi
 - criterion, 142–144, 147, 148, 152, 154
 - cutoff, 76, 146, 148–155, 182
- Fermi/Dirac distribution, 117
- few-level approach, 39, 47

- G**
- Gibbs
 - free energy, 2, 3, 35, 56, 58, 66, 68, 79, 106, 121, 133, 166, 172
 - minimization, 166, 168, 172, 173, 175, 177, 184
 - paradox, 56
- Griem
 - approach, 159
 - criterion, 147, 148, 154
 - cutoff, 71, 142, 143, 148–155, 182
 - method, 154
- ground state, 39–42, 45, 65, 70, 81, 87, 88, 93, 94, 99, 142, 148, 149, 155, 156, 158, 231, 233, 240, 242, 244, 246, 247
- approach, 149
- configuration, 45, 234, 241
- contribution, 83, 96
- degeneracy, 71, 160
- helium -, 239
- hydrogen -, 244
- method, 92, 141, 142, 147, 150, 152, 154, 156, 161
- model, 150
- nitrogen -, 246, 249
- nitrogen ion -, 249
- nobel gas -, 234
- nuclear -, 62
- oxygen atom, 131
- potential curve, 91, 175
- structure, 241
- values, 154
- vibrational -, 81, 82

- H**
- harmonic oscillator, 79–82, 86, 88, 91, 95, 99
- heat
 - capacity, 15, 16, 55, 69, 106, 107
 - constant volume, 23

- I**
- ideal gas, 1, 4, 8, 13, 14, 16, 17, 23, 26, 32, 35, 51, 55, 58, 64, 69, 101, 108, 115, 120, 122
 - state law, 23, 122, 123
- ionization, 13, 26, 149
 - atomic -, 27, 28, 172
 - degree, 9–11, 21, 32, 75, 76
 - equation, 179
 - lowering, 109, 136
 - peak, 153
 - potential, 10, 40–42, 45, 71, 108–110, 112, 134, 142, 149, 156, 159, 160, 168, 238, 240, 242
- process, 8, 9, 22, 31, 150, 151, 171
- reaction, 21, 27–29, 32, 74, 76, 137, 149, 150, 153, 168, 176, 178
- regime, 1, 13, 31, 32, 127, 153, 154, 176–178
- isentropic coefficient, 26, 29–32, 155, 202
 - equilibrium -, 193, 200, 206, 210, 215, 227
 - frozen -, 27–29, 31, 32, 188, 194, 200, 202, 206, 211, 216, 225, 226

- L**
- Lagrange multipliers, 53
- levels
 - electronic -, 70, 79, 95, 139, 142, 148, 156, 158, 161, 231, 237, 241

levels (*cont.*)

- ro-vibrational -, 86, 90–93, 182
- rotational -, 81, 91, 97
- vibrational -, 81, 88, 92, 175

M

Margenau and Lewis, 143

- cutoff, 142, 146

- results, 146

- method, 143

- theory, 143

multiplicity

- electronically excited state -, 41
- nuclear -, 83
- spin -, 233, 243, 245, 247
- total -, 93, 233

N

nitrogen

- plasma, 247

non-rigid rotor, 89

O

occupation

- numbers, 160

- probability, 158–161

ortho-

- configuration, 84, 86

- contribution, 85

- hydrogen, 84–86

- molecule, 83, 117

- state, 83

- system, 84

oxygen

- plasma, 141, 147, 151, 152, 154, 155

P

para-

- configuration, 84, 86

- contribution, 85

- hydrogen, 85, 86

- molecule, 83, 117

- state, 83

- system, 84

partition function, 40, 43, 48, 54–56, 58, 62, 74, 80, 85, 86, 91, 95, 118, 120, 141, 143, 146, 147, 164, 165, 168, 169, 184

- atomic -, 110, 148

atomic hydrogen -, 160

canonical -, 119, 121–123

closed form, 86

divergence, 87, 146

electronic -, 32, 49, 71–74, 79, 80, 91, 93,

110, 141–144, 148, 150, 153, 155,

156, 158–161, 167, 231, 237, 244,

245, 247

grand-canonical -, 120, 121, 123, 133, 136

helium -, 139

hydrogen -, 49, 85, 175

internal -, 61, 64, 65, 70, 75, 86, 91, 97, 109,

131, 134, 142, 143, 147, 167, 169,

170, 173, 175, 181, 182, 251

micro-canonical -, 119

molecular -, 181

nitrogen -, 49

nuclear -, 62, 75, 164

ortho-para -, 85

oxygen -, 49

particle -, 58

ro-vibrational -, 91, 176

rotational -, 62, 79, 82, 84, 96, 97

self-consistent -, 141, 251

system -, 56

translational -, 61, 63–65, 85, 87, 181

vibrational -, 79–81

Pauli exclusion principle, 117, 234, 245

Plank–Larkin

- partition function, 158, 161

- results, 160

plasma, 32, 101–103, 108, 109, 114, 133, 137,

141, 161, 163, 178

- atmospheric -, 160, 175

- atomic -, 29, 32

- bulk, 103

- composition, 69, 107, 110, 151, 182

- dense -, 161

- flowing -, 163

- high pressure -, 158

- ideal -, 101, 113, 158

- kinetics, 244

- mixture, 61, 141, 152

- multi-temperature -, 163, 177

- multicomponent -, 31, 133

- non degenerate -, 117

- non ideal, 134

- physics, 158

- planetary, 181, 184

- potential, 182

- properties, 110, 115, 133

- thermal -, 141, 154, 156, 242

Q

quantum number, 63
 angular -, 146, 231
 azimuthal -, 144, 146, 242
 magnetic -, 231
 orbital -, 234
 orbital angular -, 232, 238, 243
 principal -, 41, 45, 47, 70, 143, 145, 146, 231, 234, 236–238, 241, 242
 rotational -, 82, 86, 90, 182
 maximum -, 90, 91
 spin -, 231, 232, 238, 243
 total angular -, 243
 vibrational -, 80, 86, 88, 90, 182
 quasi-bound states, 86, 90, 91, 94, 95, 131

R

real gas, 32, 120, 123, 182, 245
 state law, 123
 rigid rotor, 79, 81, 82, 91, 99

S

Sackur-Tetrode equation, 67
 Saha equation, 61, 74, 108, 134, 146, 163, 169, 170, 173, 175, 178
 Schrödinger Equation, 144
 Schrödinger equation, 61, 62, 80, 81, 86, 87, 91–93, 141, 144–147, 161, 231
 specific heat, 1, 14, 16, 22, 32, 39, 48, 57, 62, 73, 76, 79, 81, 91, 93–95, 97, 111, 112, 148, 149, 152–154, 161, 162, 176, 178, 179
 air, 184, 188, 192, 197, 199
 constant pressure -, 20, 21, 37, 156, 157, 176, 178, 180
 constant volume -, 42, 49, 81
 electronic -, 73, 93
 frozen -, 22, 24, 25, 77, 78, 127, 152–154, 161, 162
 internal -, 18, 40, 42, 44, 47, 73, 74, 76–78, 91–94, 97, 99, 148
 Jupiter, 218, 222, 224
 jupiter, 184
 Mars, 206, 209, 215
 mars, 184
 molar -, 16, 38, 43, 46
 reactive -, 20, 24, 25, 76, 77, 86, 153, 162
 rotational -, 85
 single species -, 16
 translational -, 66
 vibrational -, 81

statistical

distribution, 13
 mean, 57
 mechanics, 51, 66
 physics, 113, 117
 probability, 51
 thermodynamics, 1, 13, 17, 39, 51, 61, 76, 147, 164
 weight, 40, 41, 45, 55, 65, 71, 80, 82, 83, 85, 86, 95, 117, 131, 142, 161, 182, 231, 233, 237–240, 242, 245

Stirling formula, 52, 56

T

thermodynamic, 179
 classical -, 120
 equation, 105, 179
 functions, 1, 14–16, 34, 35, 39, 47, 51, 54, 57–59, 69, 79, 93, 101, 106, 134
 model, 101
 potentials, 22, 58, 66, 121, 163
 principles, 122
 properties, 39, 51, 58, 61, 76, 79, 85, 86, 101, 103, 109, 110, 115, 117, 126, 129, 133, 139, 141, 151, 152, 154, 156, 161, 164, 175, 181, 184, 199, 202, 217, 242
 state, 54
 system, 118
 thermodynamics, 244
 classical -, 1, 13, 57, 119
 equilibrium -, 1
 first law, 1, 54
 ideal gas -, 13
 irreversible -, 163, 164
 mixture -, 19, 22
 multi-temperature -, 163
 plasma -, 76, 181
 reacting system -, 13
 real gas -, 32
 second law, 1, 54
 single species -, 65, 141
 statistical -, 139
 three-level
 approach, 48
 approximation, 49
 system, 39, 42, 45
 two-level
 approach, 73
 approximation, 42, 48
 system, 39–41, 43

V

Van der Waals equation, 1, 32, 33, 37, 130
Van der Waals equation, 34
virial
 coefficients, 32, 33, 37, 38, 125–127, 130,
 245
 phenomenological -, 130
 second -, 34, 125, 126, 130–132
 third -, 127, 130
corrections, 34, 35, 37, 117, 127, 129, 184

enthalpy, 127
entropy, 106, 129
equilibrium constant, 129
heat capacity, 36
internal energy, 35
pressure, 34, 128
specific heat, 128
specific heat -, 36
expansion, 1, 32, 34, 120, 125, 126,
 133